Advances in Clinical and Experimental Medicine

MONTHLY ISSN 1899-5276 (PRINT) ISSN 2451-2680 (ONLINE) www.advances.umw.edu.pl

2021, Vol. 30, No. 12 (December)

Impact Factor (IF) – 1.727
Ministry of Science and Higher Education – 70 pts
Index Copernicus (ICV) – 166.39 pts

Wroclaw Medical University

Advances
in Clinical and Experimental
Medicine

Advances
in Clinical and Experimental Medicine

ISSN 1899-5276 (PRINT) ISSN 2451-2680 (ONLINE) www.advances.umw.edu.pl

MONTHLY 2021
Vol. 30, No. 12
(December)

Advances in Clinical and Experimental Medicine (*Adv Clin Exp Med*) publishes high quality original articles, research-in-progress, research letters and systematic reviews and meta-analyses of recognized scientists that deal with all clinical and experimental medicine.

Editorial Office
ul. Marcinkowskiego 2–6
50-368 Wrocław, Poland
Tel.: +48 71 784 11 36
E-mail: redakcja@umw.edu.pl

Publisher
Wroclaw Medical University
Wybrzeże L. Pasteura 1
50-367 Wrocław, Poland

Online edition is the original version of the journal

Editorial Policy

Advances in Clinical and Experimental Medicine (Adv Clin Exp Med) is an independent multidisciplinary forum for exchange of scientific and clinical information, publishing original research and news encompassing all aspects of medicine, including molecular biology, biochemistry, genetics, biotechnology and other areas. During the review process, the Editorial Board conforms to the "Uniform Requirements for Manuscripts Submitted to Biomedical Journals: Writing and Editing for Biomedical Publication" approved by the International Committee of Medical Journal Editors (www.ICMJE.org/). The journal publishes (in English only) original papers and reviews. Short works considered original, novel and significant are given priority. Experimental studies must include a statement that the experimental protocol and informed consent procedure were in compliance with the Helsinki Convention and were approved by an ethics committee.

For all subscription-related queries please contact our Editorial Office:
redakcja@umw.edu.pl

For more information visit the journal's website:
www.advances.umw.edu.pl

Pursuant to the ordinance No. 134/XV R/2017 of the Rector of Wroclaw Medical University (as of December 28, 2017) from January 1, 2018 authors are required to pay a fee amounting to 700 euros for each manuscript accepted for publication in the journal Advances in Clinical and Experimental Medicine.

Indexed in: MEDLINE, Science Citation Index Expanded, Journal Citation Reports/Science Edition, Scopus, EMBASE/Excerpta Medica, Ulrich's™ International Periodicals Directory, Index Copernicus

Typographic design: Piotr Gil, Monika Kolęda
DTP: Wydawnictwo UMW
Cover: Monika Kolęda
Printing and binding: Soft Vision Mariusz Rajski

Advances
in Clinical and Experimental Medicine

MONTHLY 2021, Vol. 30, No. 12 (December)

ISSN 1899-5276 (PRINT)
ISSN 2451-2680 (ONLINE)
www.advances.umw.edu.pl

Contents

Acknowledgements

We would like to express our gratitude to all reviewers who devoted their time and expertise to evaluate manuscripts in Advances in Clinical and Experimental Medicine. We sincerely appreciate all your hard work and dedication. It is due to your contribution that we can achieve the standard of excellence.

Editors

Reviewers in 2021:

Dawud Abawi, Abdelrahman I. Abushouk, Marcin Adamczak, Anil Ahsan, Sinan Akıncı, Alessio Alogna, Durdu Altuner, Artur Anisiewicz, Mabel Aoun, Muhammad Sohaib Asghar, Jan Azarov, Karolis Azukaitis, Teresa Bachanek, Dagmara Baczyńska, Christopher Baines, Waldemar Balcerzak, Agata Bałdys-Waligórska, Julia Bar, Simge Bardak, Srikanth Barkeer, Tomasz Baron, Rafał Bartoszewski, Grzegorz Bartoszewski, Sandip Basu, Simone Battaglia, Ewelina Bąk, Ilona Bednarek, Wojciech Bednarz, Evgeny Belyavskiy, Joanna Bereta, Marta Berghausen-Mazur, Sebastjan Bevc, Sonu Bhaskar, Maciej Biały, Mariusz Bidziński, Monika Bielecka, Tomasz Bielecki, Beata Bieniaś, Marta Bižić, Anna Bizoń, Krzysztof Błaszyk, Vladimir Bobek, Sylwia Bobis-Wozowicz, Joanna Bogusławska, Andrzej Bohatyrewicz, Romuald Bohatyrewicz, Agnieszka Bojarska-Junak, Dariusz Boroń, Rafael Boscolo-Berto, Sergey Brodsky, Mariusz Bromke, Anna Brzecka, Natalia Buda, Grzegorz Bukato, Paweł Burchardt, Marco Capuzzo, Alessandra Cassoni, Nidia Castro, Ersin Çelik, Magdalena Celińska-Lowenhoff, Yubo Chai, Andrzej Chamienia, Andrzej Chciałowski, Chong Chen, Min Chen, Magdalena Chmielewska, Liyan Chu, Jerzy Chudek, Halina Cichoż-Lach, Joanna Cieślińska-Swider, Lidia Ciszak, Erica Costantini, Alessandro Crestani, Sifu Cui, Monika Czerwińska, Mirosław Czuczwar, Małgorzata Daczewska, Zofia Danilczuk, Jacek Daroszewski, Alicja Dąbrowska-Kugacka, Alessandro De Cassai, Beatriz De Lucas, Carolina D'Elia, Urszula Demkow, Andrzej Deptała, Katarzyna Derwich, Engin Deveci, Rosanna di Paola, Dimitrios Dimitroulis, Łukasz Dobrek, Piotr Domagała, Erwan Donal, Adrian Doroszko, Ines Drenjančević, Anna Dubaniewicz, Magdalena Dubińska-Magiera, Murat Dursun, Fazilet Duygu, Jadwiga Dwilewicz-Trojaczek, Dariusz Dziedzic, Piotr Dzięgiel, Gabriella Emri, Angela Faga, Kenneth Faulkner, Izabela Fecka, Julia Fedotova, Anna Filipowicz-Sosnowska, Martin Floer, Marcin Frączek, Mónica Furlano, Tomasz Gabryelewicz, Jacek Gajek, Agata Gajos, Andrea Galassi, Piotr Gałecki, Maria Ganeva, Eugenia Gatiatulina, Dariusz Gawryluk, Zbigniew Gąsior, Adam Gesing, Ashraf Ghulam, Maciej Głyda, Justyna Gołębiewska, Andrzej Gołębiewski, Maciej Gonciarz, Monika Gos, Jolanta Gozdowska, Waldemar Goździk, Stuart Grossman, Grzegorz Grześk, Andrzej Grzybowski, Jakob Gubenšek, Cecilia Guiot, Katarzyna Gustaw-Rothenberg, Maciej Guziński, Katarzyna Haczkiewicz-Leśniak, Piotr Harbut, Marek Hartleb, Zehra Hatipoğlu, Olga Haus, Kai He, Weiwei He, Lynne Hinterbuchner, András Hrabák, Jian Hu, Rong Hu, Qiang Huang, Hongxia Hui, Quan Huynh, Irena Ilić, Stanislav Isayenkov, Arda Işık, Zbigniew Jabłonowski, Anna Janas-Naze, Dominika Janiszewska, Ewa Jankowska, Alina Jankowska-Konsur, Barbara Jarząb, Monika Jasek, Marek Jasiński, Aleksandra Jezela-Stanek, Marcin Jędryka, Zhang Jingfa, James John, Krystian Josiak, Piotr Kałmucki, Marta Kałużna-Oleksy, Grzegorz Kamiński, Karol Kamiński, Paweł Karpiński, Martyna Kasper-Jędrzejewska, Beata Kasztelan-Szczerbińska, Theodora Katopodi, Karolina Kędzierska, Ehsan Khalili, Jarosław Kierkuś, Yoji Kishi, Mariusz Klencki, Maria Kłopocka, Aureliusz Kolonko, Parastou Kordestani-Moghadam, Wojciech Korlacki, Magdalena Koszewicz, Euphrosyni Koutsouraki, Jerzy Kowalczyk, Marcin Kozakiewicz, Katarzyna Koziak, Magdalena Krajewska, Iwona Krela-Kaźmierczak, Soňa Křížková, Tadeusz Krzemiński, Paweł Kubasiewicz-Ross, Eliza Kubicka, Adriana Kubis-Kubiak, Paweł Kuca, Ernest Kuchar, Piotr Kuczera, Tamara Kujawska, Julita Kulbacka, Wiktor Kuliczkowski, Sonam Kumari, Paweł Kunicki, Markku Kurkinen, Ilona Kurnatowska, Jacek Kusa, Damian Kusz, Michał Kuszewski, Halyna Kuznietsova, Katarzyna Kwiatkowska, Paweł Lampe, Małgorzata Latocha, Anna Lebedeva, Aleksandra Lesiak, Damian Lewandowski, Łukasz Lewandowski, Ewa Lewicka, Fang Li, Fuyang Li, Piotr Lipiec, Mariusz Lipski, Xuejian Liu, Kamila Ludwikowska, Izabela Łaczmańska, Łukasz Łaczmański, Tadeusz Łapiński, Joanna Maj, Jennifer Majer, Przemysław Majewski, Preeti Malik, Grzegorz Małek, Małgorzata Małodobra-Mazur, Hina Manzoor, Wojciech Marlicz, Andrzej Marszałek, Helena Martynowicz, Marcin Masalski, Maria Maślińska, Ivan Matia, Rafał Matkowski, Małgorzata Matusiewicz, Jacek Matys, Grzegorz Mazur, Richard Merrill, Frederic Meyer, Krystyna Michalak, Michał Michalak, Marta Migocka-Patrzałek, Przemysław Mikołajczak, Wioletta Mikulakova, Joanna Miłkowska-Dymanowska, Małgorzata Mizerska-Wasiak, Agnieszka Młynarska, Gustavo Molina, Piotr Morasiewicz, Daniel Morris, Janusz Moryś, Bożena Mroczek, Tomoyuki Mukai, Agata Mulak, Sameh Naguib, Karol Nartowski, Anna Nasierowska-Guttmejer, Joseph Nassif, Kazuaki Negishi, Jadwiga Nessler, Piotr Niewiński, Przemysław Niewiński, Marita Nittner-Marszalska, Beata Nowak, Krzysztof Nowak, Michał Nowak, Marta Nowakowska-Kotas, Antonio Núñez, Mateusz Olbromski, Paweł Olczyk, Robert Olszewski, Hanna Osadnik, Abdulkadir Özgür, Olga Pakhomova, Dorota Paluszyńska, Lijian Pan, Anatol Panasiuk, Małgorzata Pańczyk-Tomaszewska, Mark Parker, Tomasz Pawiński, Edyta Pawlak, Guido Pelletti, Joanna Peredzyńska, Cristian Persu, Mariya Petrosyan, Adriano Piattelli, Grzegorz Piecha, Aleksandra Piechota-Polańczyk, Jadwiga Pietkiewicz, Anna Pietrzak, Jakub Piotrkowski, Elżbieta Płuciennik, Adam Płużański, Indrani Poddar, Monika Podhorecka, Ilona Pokora, Renata Polaniak, Katarzyna Połtyn-Zaradna, Michał Pomorski, Raluca Pop, Daniela Popescu, Tanja Popp, Tomasz Porażko, Małgorzata Poręba, Rafał Poręba, Francesco Prattichizzo,

Monika Przewłocka-Kosmala, Tadeusz Przybyłowski, Anna Raciborska, Elżbieta Radzikowska, Reza Rahbarghazi, Dariusz Rakus, Wafaa Rashed, Sanjay Rastogi, Mariusz Z. Ratajczak, Laura Reed, Bożena Regulska-Ilow, Paweł Reichert, Rafi Romano, Michał Romanski, Umberto Romeo, Christine Rondanino, Joanna Rossowska, Piotr Rozentryt, Monika Rucińska, Lidia Rutkowska-Sak, Przemysław Rutkowski, Justyna Rybka, Józef Ryżko, Makoto Saito, Ioanna Sakellari, Javier Santabarbara, Elżbieta Sarnowska, Naila Sattar, Ewa Sawicka, Ana Scocate, Agata Sebastian, Silvia Secco, James Sharman, Aboubacar Sidibé, Paweł Siekierski, Halina Sienkiewicz-Jarosz, Jerzy Sieńko, Piotr Sieroszewski, Santhi Silambanan, Scott Sills, Krzysztof Simon, Maciej Siński, Rosalba Siracusa, Joanna Siuda, Magdalena Skarżyńska, Andrzej Skorek, Kajetan Słomka, Krzysztof Słowiński, Jacek Smereka, Maciej Sobczyński, Magdalena Sobieska, Grzegorz Sobota, Joanna Socha, Marta Sochocka, Francisco Solano, Roman Sosnowski, Eleonora Spekker, Zbigniew Sroka, Agata Stanek, Ivan Starchenko, Anna Starzyńska, Ewelina Stelcer, Elena Stocco, Rostyslav Stoika, Tomasz Stompór, Jan Styczyński, Pan Su, Lina Suarez, Halis Suleyman, Andrei Surguchov, Edyta Sutkowska, Krzysztof Szczałuba, Tomasz Szczapa, Aleksandra Szczepankiewicz, Jolanta Szelachowska, Grzegorz Szewczyk, Milena Ściskalska, Agnieszka Świdnicka-Siergiejko, Aisha Tahir, Özgür Tan, Hui Tang, Onur Telli, Luca Testarelli, Thavaree Thilavech, Liza Thomas, Dariusz Timler, Michał Tkaczyszyn, Andrzej Torbé, Jonel Trebicka, Krzysztof Tupikowski, Maciej Ugorski, Tomasz Urbaniak, Wiktor Urbański, Marek Ussowicz, Juha Väyrynen, András Végh, Karolina Walewicz, Marta Waliszewska-Prosół, Changqian Wang, Guodong Wang, Lidong Wang, Wenan Wang, Yichao Wang, Peter Ward, Dorota Waśko-Czopnik, Adam Whitley, Wojciech Widuchowski, Bartosz Wielgomas, Karina Wierzbowska-Drabik, Anna Witkowska, Tomasz Witkowski, Kamil Wojnicki, Beata Wojtczak, Dariusz Wołowiec, Olga Wysocka, Yong Xia, Liuling Xiao, Huan-Yu Xiong, Zhihao Xu, Kazumi Yagasaki, Ulyana Yanyshyn, Yongjie Yin, Xiaojun Yu, Agnieszka Zabłocka, Katarzyna Zabłocka-Słowińska, Maria Paz Zafra, Edyta Zagórowicz, Jan Zaucha, Renata Zaucha, Zygmunt Zdrojewicz, Bin-Fei Zhang, Yijian Zhang, Shixi Zhao, Sławomir Zmonarski, Agnieszka Zubkiewicz-Kucharska, Anna Zubrzycka-Sienkiewicz, Istvan Zupko, Małgorzata Zwolińska-Wcisło, Robert Zymliński, Dorota Zyśko, Maciej Żarow

High-quality medical research requires that equipment has been validated for accuracy

James E. Sharman[1,D], Wojciech Kosmala[2,E]

[1] Menzies Institute for Medical Research, University of Tasmania, Hobart, Australia
[2] Department of Cardiovascular Imaging, Institute of Heart Diseases, Wroclaw Medical University, Poland

A – research concept and design; B – collection and/or assembly of data; C – data analysis and interpretation;
D – writing the article; E – critical revision of the article; F – final approval of the article

Advances in Clinical and Experimental Medicine, ISSN 1899–5276 (print), ISSN 2451–2680 (online) *Adv Clin Exp Med*. 2021;30(12):1221–1223

Address for correspondence
James E. Sharman
E-mail: james.sharman@utas.edu.au

Funding sources
None declared

Conflict of interest
None declared

Received on November 10, 2021
Accepted on December 2, 2021

Published online on December 13, 2021

Abstract

It is not always appreciated that medical equipment may be cleared by regulatory authorities to sell within a country, without ever having been tested for accuracy performance according to scientific validation standards. Instead, manufacturers can undertake in-house accuracy testing, using variable methods and without any requirement for test results to be made publicly available. This lack of full transparency together with potential for industry bias can place doubt over the quality of validation results provided to regulatory authorities. Currently, this situation affects the field of hypertension research, where most blood pressure devices have not been independently validated for accuracy according to international scientific standards, nor as expected in clinical practice guidelines. More attention should be paid to such practices in order to improve the quality of research and to optimize further translation of scientific findings to clinical practice. The clinical implications of inaccurate measurements in research can be far-reaching, ultimately impacting on a patient's health. Well-planned validating studies should be more widely considered for new devices that are candidates to be used in research protocols. The awareness of the lack or uncertain validation of equipment used for verifying research hypotheses should prompt all investigators to revisit the idea of conducting the study or, at least, to acknowledge this issue as a relevant study limitation. One of the ways in which authors submitting research findings for publication can add to the quality of the reporting of their work is to ensure reference to the accuracy validation of their research equipment.

Key words: medical devices, equipment and supplies, standards, performance

Cite as
Sharman JE, Kosmala W. High-quality medical research requires that equipment has been validated for accuracy. *Adv Clin Exp Med*. 2021;30(12):1221–1223. doi:10.17219/acem/144440

DOI
10.17219/acem/144440

The international community and funders of research expect the study to be conducted ethically and with high quality, such that it is rigorous, transparent, reproducible, and avoids waste.[1] These expectations are not only essential for the translation of research knowledge to the benefit of the wider community, but also help to promote trust in research findings and deliver the highest value for the money that is invested in research.[2] The failure of many research discoveries to be reproduced by independent investigators is a symptom of rigorous research methods not always being applied, and indicates that more training to improve the understanding of high-quality research methods, particularly for research apprentices, is needed.[1,3]

Resources to aid the rigor and accountability of research practice, from the design to conduct and reporting of research outcomes, have been developed for researchers (e.g., Enhancing the QUAlity and Transparency Of health Research (EQUATOR) network, Cochrane Collaboration).[4,5] Working towards similar intent to improve the quality of research publications, the International Committee of Medical Journal Editors (ICMJE) publishes "Recommendations for the Conduct, Reporting, Editing and Publication of Scholarly Work in Medical Journals".[6] These recommendations align with best practice standards to assist all those involved in publishing medical research to present unbiased findings clearly and accurately. The journal "Advances in Clinical and Experimental Medicine" is an ICMJE member journal that requires authors of all submitted papers to adhere to the ICMJE recommendations.

The ICMJE Recommendations rightly state that, in order to allow others to reproduce the results of research, there should be sufficient detail provided on the methods, equipment and procedures of the research.[6] However, a factor that is not considered within the ICMJE recommendations, but can have a marked influence on the results of research, is providing confirmation that the research equipment is accurate, preferably through testing it in accordance with established scientific validation standards. Without such confirmation, there is little to assure that the equipment can measure what it purports to measure, nor whether its use may critically undermine the quality of research outputs. This concept of confirming the quality of all data to increase the confidence in research results is familiar to researchers across disciplines.[7–9]

It is not always appreciated that medical equipment may be cleared by regulatory authorities to sell within a country, without ever having been tested for accuracy performance according to scientific validation standards. Instead, manufacturers can undertake in-house accuracy testing, using variable methods and without any requirement for test results to be made publicly available. This lack of full transparency together with potential for industry bias can place doubt over the quality of validation results provided to regulatory authorities. Currently, this situation affects the field of hypertension research,[10,11] where most blood pressure devices have not been independently validated for accuracy according to international scientific standards, nor as expected in clinical practice guidelines.[12–14] Global estimates indicate that less than 20% of blood pressure devices from among thousands of separate models available for purchase have been independently validated.[15,16]

As may be anticipated, the untested, non-validated devices are more likely to be inaccurate when compared with established reference standards,[17–19] which in addition to the impact on research quality has obvious implications for appropriate clinical diagnosis and management. Compared with validated devices, those whose accuracy has not been tested also have a greater dispersion of measurement values (higher variance),[20] which will influence estimation of sample size for research projects. Higher variance in the measurement of a primary outcome variable means that more research study participants will be needed to answer the research question and demonstrate statistical between-group differences.[21] This places extra burden on research resources and also has ethical implications in higher-risk study protocols by needlessly exposing more research participants to otherwise avoidable risk.

Regulatory loopholes that enable widespread availability of blood pressure devices with uncertain quality assurance[10] may also apply to other medical equipment used in research, such as blood glucose monitors and pulse oximeters,[22–24] although the breadth of the problem more generally across equipment being used in research is not known. This being the case, the onus of responsibility to determine the worthiness of medical equipment to be used in research falls to the shoulders of individual researchers in the planning and conduct of their research projects. What can researchers do in relation to this?

Researchers can check that all research equipment has been assessed, and passed validation testing, or the performance can be verified (including where participants of the study use personal monitoring equipment to collect research data).[17] Ideally, the values derived from the equipment have been compared using an established, standardized protocol with a recognized reference standard, for example, blood glucose measured with a point-of-care device compared with an automated procedure from an accredited laboratory with known accuracy and precision. Researchers can also seek information from relevant professional societies,[25] web-based resources,[5] other sources of published guidance,[26] or ask the equipment distributor to provide published material as proof of accuracy. Where available, they should cite the published validation material within the methods of research manuscripts when referencing the equipment used. It is important to note that validation testing is only relevant to the device under scrutiny and the results cannot be extrapolated to other models or devices made by different manufacturers.

In the hypertension field, international efforts are being undertaken to redress the problem of non-validated equipment used in research, clinical practice and population

level interventions.[27–30] This requires ongoing, multisectoral lobbying for regulatory change, as well as widespread education and advocacy for exclusive use of validated equipment. Whether such activities are needed in other research areas is something for the wider research community to be alert for.

Indeed, the scale of the problem being discussed is increasing, and more attention should be paid to it in order to improve the quality of research and to optimize further translation of scientific findings to clinical practice. The clinical implications of inaccurate measurements in research can be far-reaching, ultimately impacting on a patient's health. Well-planned validating studies should be more widely considered for new devices that are candidates to be used in research protocols. The awareness of the lack or uncertain validation of equipment used for verifying research hypotheses should prompt all investigators to revisit the idea of conducting the study or, at least, to acknowledge this issue as a relevant study limitation. One of the ways that authors submitting research findings for publication can add to the quality of the reporting of their work is to ensure reference to the accuracy validation of their research equipment.

ORCID iDs

James E. Sharman https://orcid.org/0000-0003-2792-0811
Wojciech Kosmala https://orcid.org/0000-0003-3807-8201

References

1. Chalmers I, Glasziou P. Avoidable waste in the production and reporting of research evidence. *Lancet.* 2009;374(9683):86–89. doi:10.1016/S0140-6736(09)60329-9
2. National Health and Medical Research Council. NHMRC's Research Quality Strategy. https://www.nhmrc.gov.au/file/16823/download?token=ha80bBhZ. Accessed November 25, 2021.
3. Begley CG, Ioannidis JPA. Reproducibility in science: Improving the standard for basic and preclinical research. *Circ Res.* 2015;116(1):116–126. doi:10.1161/CIRCRESAHA.114.303819
4. Green S, Mcdonald S. Cochrane Collaboration: More than systematic reviews? *Intern Med J.* 2005;35(1):3–4. doi:10.1111/j.1445-5994.2004.00747.x
5. Simera I, Moher D, Hirst A, Hoey J, Schulz KF, Altman DG. Transparent and accurate reporting increases reliability, utility, and impact of your research: Reporting guidelines and the EQUATOR Network. *BMC Med.* 2010;8:24. doi:10.1186/1741-7015-8-24
6. International Committee of Medical Journal Editors. Recommendations for the Conduct, Reporting, Editing and Publication of Scholarly Work in Medical Journals – updated December 2018. http://www.ICMJE.org. Accessed August 17, 2019.
7. Ehrenstein V, Petersen I, Smeeth L, et al. Helping everyone do better: A call for validation studies of routinely recorded health data. *Clin Epidemiol.* 2016;8:49–51. doi:10.2147/clep.S104448
8. Lash TL, Olshan AF. EPIDEMIOLOGY announces the "Validation Study" submission category. *Epidemiology.* 2016;27(5):613–614. doi:10.1097/ede.0000000000000532
9. Coecke S, Bernasconi C, Bowe G, et al. Practical aspects of designing and conducting validation studies involving multi-study trials. *Adv Exp Med Biol.* 2016;856:133–163. doi:10.1007/978-3-319-33826-2_5
10. Alpert BS. Can 'FDA-cleared' blood pressure devices be trusted? A call to action. *Blood Press Monit.* 2017;22(4):179–181. doi:10.1097/mbp.0000000000000279
11. Sharman JE, Padwal R, Campbell NRC. Global marketing and sale of accurate cuff blood pressure measurement devices. *Circulation.* 2020;142(4):321–323. doi:10.1161/circulationaha.120.046205
12. Campbell NR, Gelfer M, Stergiou GS, et al. A call to regulate manufacture and marketing of blood pressure devices and cuffs: A position statement from the World Hypertension League, International Society of Hypertension and supporting hypertension organizations. *J Clin Hypertens (Greenwich).* 2016;18(5):378–380. doi:10.1111/jch.12782
13. Muntner P, Einhorn PT, Cushman WC, et al. Blood pressure assessment in adults in clinical practice and clinic-based research: JACC Scientific Expert Panel. *J Am Coll Cardiol.* 2019;73(3):317–335. doi:10.1016/j.jacc.2018.10.069
14. Whelton PK, Carey RM, Aronow WS, et al. 2017 ACC/AHA/AAPA/ABC/ACPM/AGS/APhA/ASH/ASPC/NMA/PCNA guideline for the prevention, detection, evaluation, and management of high blood pressure in adults: A report of the American College Of Cardiology/American Heart Association task force on clinical practice guidelines. *J Am Coll Cardiol.* 2018;71(19):e127–e248. doi:10.1016/j.jacc.2017.11.006
15. Medaval. Blood pressure monitors. https://medaval.ie/blood-pressure-monitors. Accessed October 26, 2021.
16. Picone DS, Deshpande RA, Schultz MG, et al. Nonvalidated home blood pressure devices dominate the online marketplace in Australia: Major implications for cardiovascular risk management. *Hypertension.* 2020;75(6):1593–1599. doi:10.1161/HYPERTENSIONAHA.120.14719
17. Jung MH, Kim GH, Kim JH, et al. Reliability of home blood pressure monitoring: In the context of validation and accuracy. *Blood Press Monit.* 2015;20(4):215–220. doi:10.1097/mbp.0000000000000121
18. Akpolat T, Dilek M, Aydogdu T, et al. Home sphygmomanometers: Validation versus accuracy. *Blood Press Monit.* 2009;14(1):26–31. doi:10.1097/MBP.0b013e3283262f31
19. Dilek M, Adibelli Z, Aydogdu T, Koksal AR, Cakar B, Akpolat T. Self-measurement of blood pressure at home: Is it reliable? *Blood Press.* 2008;17(1):34–41. doi:10.1080/08037050701758018
20. Ringrose JS, Polley G, McLean D, Thompson A, Morales F, Padwal R. An assessment of the accuracy of home blood pressure monitors when used in device owners. *Am J Hypertens.* 2017;30(7):683–689. doi:10.1093/ajh/hpx041
21. Jones B, Jarvis P, Lewis JA, Ebbutt AF. Trials to assess equivalence: The importance of rigorous methods. *BMJ.* 1996;313(7048):36–39. doi:10.1136/bmj.313.7048.36
22. Medaval. Pulse oximeters. https://medaval.ie/mv-pulse-oximeters. Accessed November 2, 2021.
23. Medaval. Blood glucose meters. https://medaval.ie/mv-blood-glucose-meters. Accessed November 2, 2021.
24. Ward JR, Clarkson PJ. An analysis of medical device-related errors: Prevalence and possible solutions. *J Med Eng Technol.* 2004;28(1):2–21. doi:10.1080/0309190031000123747
25. Stergiou GS, Alpert B, Mieke S, et al. A universal standard for the validation of blood pressure measuring devices: Association for the Advancement of Medical Instrumentation/European Society of Hypertension/International Organization for Standardization (AAMI/ESH/ISO) collaboration statement. *Hypertension.* 2018;71(3):368–374. doi:10.1161/hypertensionaha.117.10237
26. Picone DS, Padwal R, Campbell NRC, et al. How to check whether a blood pressure monitor has been properly validated for accuracy. *J Clin Hypertens (Greenwich).* 2020;22(12):2167–2174. doi:10.1111/jch.14065
27. Olsen MH, Angell SY, Asma S, et al. A call to action and a lifecourse strategy to address the global burden of raised blood pressure on current and future generations: The Lancet Commission on Hypertension. *Lancet.* 2016;388(10060):2665–2712. doi:10.1016/s0140-6736(16)31134-5
28. Sharman JE, O'Brien E, Alpert B, et al. Declaración de posición del Grupo de la Comisión Lancet de Hipertensión con respecto a la mejora mundial de las normas de exactitud para los dispositivos de medición de la presión arterial. *Pan American Journal of Public Health.* 2020;44(e21). https://iris.paho.org/bitstream/handle/10665.2/51862/v44e212020.pdf?sequence=1&isAllowed=y. Accessed November 25, 2021.
29. Sharman JE, O'Brien E, Alpert B, et al. Lancet Commission on Hypertension group position statement on the global improvement of accuracy standards for devices that measure blood pressure. *J Hypertens.* 2020;38(1):21–29. doi:10.1097/hjh.0000000000002246
30. Lombardi C, Sharman JE, Padwal R, et al. Weak and fragmented regulatory frameworks on the accuracy of blood pressure-measuring devices pose a major impediment for the implementation of HEARTS in the Americas. *J Clin Hypertens (Greenwich).* 2020;22(12):2184–2191. doi:10.1111/jch.14058

Kynurenic acid and kynurenine aminotransferase are potential biomarkers of early neurological improvement after thrombolytic therapy: A pilot study

Ádám Annus[1,B–D], Ferenc Tömösi[2,B,D], Ferenc Rárosi[3,C], Evelin Fehér[4,B], Tamás Janáky[2,B,E], Gábor Kecskeméti[2,B], József Toldi[4,E], Péter Klivényi[1,A], László Sztriha[5,E,F], László Vécsei[1,6,7,A,E,F]

[1] Department of Neurology, Albert Szent-Györgyi Health Centre, University of Szeged, Hungary
[2] Department of Medical Chemistry, University of Szeged, Hungary
[3] Department of Medical Physics and Informatics, University of Szeged, Hungary
[4] Department of Physiology, Anatomy and Neuroscience, University of Szeged, Hungary
[5] Department of Neurology, King's College Hospital, London, UK
[6] MTA-SZTE Neuroscience Research Group, Szeged, Hungary
[7] Interdisciplinary Excellence Centre, University of Szeged, Hungary

A – research concept and design; B – collection and/or assembly of data; C – data analysis and interpretation; D – writing the article; E – critical revision of the article; F – final approval of the article

Advances in Clinical and Experimental Medicine, ISSN 1899–5276 (print), ISSN 2451–2680 (online) *Adv Clin Exp Med*. 2021;30(12):1225–1232

Address for correspondence
László Vécsei
E-mail: vecsei.laszlo@med.u-szeged.hu

Funding sources
Grants No. GINOP 2.3.2-15-2016-00048; EFOP-3.6.1-16-2016-00008; TUDFO/47138-1/2019-ITM; 20391-3/2018/FEKUSTRAT.

Conflict of interest
None declared

Acknowledgements
We are grateful for the dedicated work of the nurses of the Stroke Unit at Department of Neurology, Albert Szent-Györgyi Clinical Centre, University of Szeged. We also appreciate the help of our co-workers in our Biobank facility, who handled and stored the blood samples.

Received on March 16, 2021
Reviewed on June 25, 2021
Accepted on August 27, 2021

Published online on October 12, 2021

DOI
10.17219/acem/141646

Abstract

Background. Biomarkers for predicting treatment response to thrombolysis in acute ischemic stroke are currently lacking. Both, animal models and clinical studies have provided evidence that the kynurenine (KYN) pathway is activated in ischemic stroke.

Objectives. In our pilot study, we aimed to investigate whether KYN pathway enzymes and metabolites could serve as potential biomarkers for treatment response in the hyperacute phase of ischemic stroke.

Materials and methods. We included 48 acute ischemic stroke patients who received thrombolysis. Blood samples were taken both before and 12 h after treatment. Concentrations of 11 KYN metabolites were determined using ultra-high-performance liquid chromatography-mass spectrometry. To assess the treatment response, we used early neurological improvement (ENI), calculated as the difference between the admission and discharge National Institutes of Health Stroke Scale (NIHSS) scores. We performed receiver operating characteristic (ROC) analysis for KYN pathway metabolites and enzymes that showed a correlation with ENI.

Results. In the samples taken before thrombolysis, significantly lower concentrations of kynurenic acid (KYNA) and kynurenine aminotransferase (KAT) activity were found in patients who had ENI ($p = 0.01$ and $p = 0.002$, respectively). According to the ROC analysis, the optimal cut-off value to predict ENI for KYNA was 37.80 nM (sensitivity (SN) 69.2%, specificity (SP) 68.4%) and 0.0127 for KAT activity (SN 92.3%, SP 73.7%).

Conclusions. Our research is the first clinical pilot study to analyze changes in the KYN pathway in ischemic stroke patients who received thrombolytic treatment. Based on our results, baseline KYNA concentration and KAT activity could serve as potential biomarkers to predict early treatment response to thrombolysis.

Key words: kynurenine, biomarker, ischemic stroke, acute stroke, thrombolysis

Cite as
Annus Á, Tömösi F, Rárosi F, et al. Kynurenic acid and kynurenine aminotransferase are potential biomarkers of early neurological improvement after thrombolytic therapy: A pilot study. *Adv Clin Exp Med*. 2021;30(12):1225–1232. doi:10.17219/acem/141646

Introduction

Biomarkers are objective indicators of physiological or pathological processes and have valuable applications in predicting and monitoring clinical response to therapeutic interventions.[1] At present, biomarkers aiding in prediction of response to intravenous thrombolysis treatment and prognosis in acute ischemic stroke are lacking in routine clinical practice.[2] However, a few blood biomarkers have shown promise: copeptin, a fragment of vasopressin produced in the hypothalamus, was shown to increase the prognostic accuracy of the National Institutes of Health Stroke Scale (NIHSS) in predicting functional outcome and mortality.[3] Matrix metalloproteinase-9 (MMP-9) levels correlated with hemorrhagic transformation after thrombolytic therapy, and S100B was elevated in patients with malignant middle cerebral artery syndrome.[4,5] Higher activated/inactivated thrombin-activatable fibrinolysis inhibitor levels correlated with higher NIHSS scores 2 days after treatment, and with poor outcome on the modified Rankin Scale (mRS) score at day 90.[6] Faille et al. reported that low admission levels of soluble thrombomodulin and soluble endothelial protein C receptor in patients with arterial occlusion were associated with higher recanalization rates after thrombolytic therapy.[7] In another study, low endogenous thrombin potential before thrombolysis was found to be an independent predictor of both short- and long-term mortality following treatment.[8]

The kynurenine (KYN) pathway is the main route of tryptophan (TRP) metabolism. Animal models and clinical studies have unequivocally proven that the KYN pathway is activated in acute ischemic stroke.[9–15] The first step of the pathway is the metabolism of TRP to KYN by indoleamine-2,3-dioxygenase (IDO). Inflammatory cytokines (e.g., interleukin 1β (IL-1β), tumor necrosis factor α (TNF-α) and interferon γ (INF-γ)) were shown to increase the expression of IDO.[16,17] Therefore, the activation of the KYN pathway following ischemic brain injury is likely part of a secondary inflammatory reaction.[18,19] The most well-studied metabolites of the pathway are kynurenic acid (KYNA), 3-hydroxykynurenine (3-HK) and quinolinic acid (QUIN). Kynurenic acid is metabolized by kynurenine aminotransferase (KAT) from KYN. It is a known endogenous, competitive inhibitor of the N-methyl-D-aspartate receptor (NMDAR) and is therefore thought to have neuroprotective properties.[20] In contrast, 3-HK and QUIN are neurotoxic compounds that produce free radicals and cause oxidative stress. Further metabolites and enzymes of the KYN pathway that were analyzed in our study are highlighted in Fig. 1.

The KYN pathway is linked to a number of traditional cerebrovascular risk factors that could influence serum levels of KYN metabolites.[21] It has been demonstrated that IDO expression regulates blood pressure in mouse models of systemic inflammation.[22] Administration of KYNA into the rostral ventrolateral medulla of spontaneously hypertensive rats, decreased mean arterial blood pressure by approx. 40 mm Hg.[23] Median blood KYN levels of patients with stable angina pectoris were higher in hypertensive patients compared to normotensive individuals.[24]

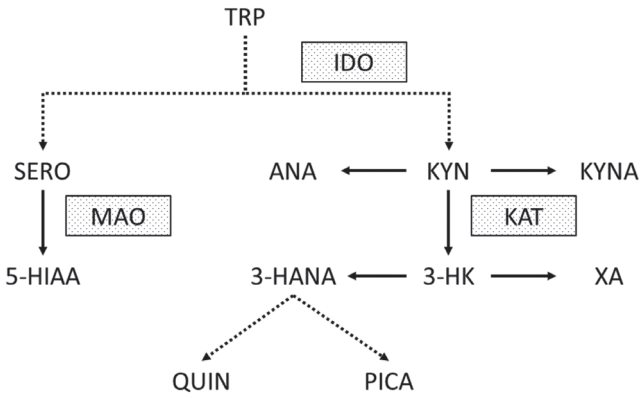

Fig. 1. Kynurenine pathway and other tryptophan metabolites measured in our pilot study. Dotted lines indicate more than 1 enzymatic step. Dotted boxes highlight the most relevant enzymes of the pathway

3-HANA – 3-hydroxyanthranilic acid; 3-HK – 3-hydroxy-kynurenine; 5-HIAA – 5-hydroxy-3-indoleacetic acid; ANA – anthranilic acid; IDO – indoleamine 2,3-dioxygenase; KAT – kynurenine aminotransferase; KYN – kynurenine; KYNA – kynurenic acid; MAO – monoamine oxidase; PICA – picolinic acid; QUIN – quinolinic acid; SERO – serotonin; TRP – tryptophan; XA – xanthurenic acid.

Elevated xanthurenic acid (XA) levels have been found in diabetic patients.[25] Xanthurenic acid forms a complex with insulin that does not activate insulin receptors.[26] Therefore, elevated XA levels contribute to insulin resistance.[27]

Aging, the most relevant non-modifiable risk factor for cerebrovascular diseases, showed a significant association in a multivariate linear regression analysis with serum concentrations of KYN, TRP, and IDO activity.[28] In the Hordaland Health Study, an inverse association was found between heavy smoking and anthranilic acid (AA), TRP, KYN, KYNA, XA, and 3-hydroxyanthranilic acid (3-HANA).[29]

Objectives

Our aim in this single-center pilot study was to investigate whether metabolites of the KYN pathway and activity of relevant enzymes measured before and 12 h after thrombolytic therapy in ischemic stroke could serve as potential biomarkers for predicting treatment response and prognosis.

Patients and methods

Patients and outcomes

Our inclusion criteria were patients with a diagnosis of acute ischemic stroke who underwent intravenous thrombolysis with alteplase between January and December 2018. We excluded patients who received thrombectomy and those who had a baseline mRS score >2. The pilot study

was conducted in accordance with the revised Declaration of Helsinki, and the protocol was approved by the Ethics Committee of the University of Szeged, Albert Szent-Györgyi Clinical Centre (Project GINOP 2.3.2-15-2016-00048). All patients or their relatives gave informed consent for inclusion before the participation in the study.

C-reactive protein (CRP) and white cell count were measured from blood samples taken upon arrival in the emergency department. The time when the alteplase bolus was administered is referred to as "needle time". All patients underwent repeat imaging approx. 24 h after treatment. The NIHSS and mRS scores were established by a certified expert. The NIHSS scores were calculated on admission before thrombolysis, and at discharge from the stroke unit.

Efficacy endpoints were early neurological improvement (ENI) and good functional outcome at 30 and 90 days after the stroke. We defined ENI as a ≥4 point decrease in the NIHSS score from admission to discharge. The criterion for good functional outcome was an mRS score ≤2.

Sampling

Peripheral venous blood samples were taken just before thrombolysis and 12 h after the initiation of treatment (samples A and B, respectively). Blood samples were centrifuged at 3000/min for 13 min, and sera were then stored at –80°C until further analysis. Due to restricted opening times of our biobank facility, samples were only processed on weekdays.

Measurement of kynurenines by ultra-high-performance liquid chromatography (UHPLC) coupled to tandem mass spectrometry (MS/MS)

Reagents and chemicals

All reagents and chemicals were of analytical or liquid chromatography-mass spectrometry (LC-MS) grade. Tryptophan and its metabolites and d4-picolinic acid (PICA) were purchased from Sigma-Aldrich (St. Louis, USA). The d3-3-HK was obtained from Buchem BV (Apeldoorn, the Netherlands). The other deuterated internal standards (ISs; d4-serotonin (SERO), d4-KYN, d3-3-3-HANA, d5-TRP, d5-5-hydroxy-3-indoleacetic acid (5-HIAA), d5-KYNA, d4-XA and d3-QUIN) were purchased from Toronto Research Chemicals (Toronto, Canada). Acetone, methanol (MeOH) and water were obtained from VWR Chemicals (Monroeville, USA). Formic acid (FA) was purchased from Thermo Fisher Scientific (Portsmouth, USA).

Preparation of standard, IS and quality control solutions

Stock solutions, calibration standards and quality control (QC) samples were prepared as described previously.[30] Calibration standards consisted of 100 µL of "blank" serum, 10 µL of standard solution mix (156.25–5000 nM SERO, 312.5–10,000 nM KYN, 7.8–250 nM 3-HANA, 6.25–200 µM TRP, 7.8–250 nM 5-HIAA, 6.25–200 nM ANA, 4.7–150 nM KYNA, 6.25–200 nM 3-HK, 1.5–50 nM XA, 3.125–100 nM PICA, and 62.5–2000 nM QUIN in 0.1% (v/v) aqueous FA), were treated with 370 µL of ice-cold acetone: MeOH (1:1, (v/v)) containing 10 µL of the SIL-IS mix (1500 nM d4-SERO, 1000 nM d4-KYN, 65 nM d3-3-HANA, 5250 nM d5-TRP, 200 nM d5-5-HIAA, 50 nM d5-KYNA, 90 nM d3-3-HK, 25 nM d4-XA, 80 nM d4-PICA, and 300 nM d3-QUIN) to precipitate proteins. After centrifugation, 400 µL of supernatant were transferred to a new tube, spun for 15 s and split into 2 equal parts. After concentration under a vacuum (Savant SC 110 A Speed Vac Plus; Savant, Holbrook, USA), half of the sample was treated with 70 µL of derivatizing reagent (n-butanol-acetyl chloride, 9:1, (v/v)) and was incubated for 1 h at 60°C. The mixture was dried under nitrogen before reconstitution. Both parts of the sample were dissolved in 100–100 µL of the starting eluent, vortexed, centrifuged, and combined.

Preparation of human serum samples for analysis

The human serum samples were prepared as described previously.[30] Briefly, to 100 µL of each serum sample, 10 µL 0.1% (v/v) of aqueous FA and 370 µL of ice-cold acetone–MeOH (1:1, (v/v)) containing 10 µL of the SIL-IS mix (the same as used in the preparation of the calibration standards) were added, and 400 µL of supernatant was treated as above.

Instrumentation and UHPLC-MS/MS analysis

The UHPLC separation of TRP and its metabolites was performed on a pentafluorophenyl (PFP) column (100 Å, 100 mm × 2.1 mm, particle size 2.6 µm; Phenomenex, Torrance, USA) connected to an ACQUITY I-Class UPLC™ liquid chromatography system (Waters, Manchester, UK) using 0.1% (v/v) aqueous FA as solvent A and MeOH containing 0.1% (v/v) FA as solvent B. All mass spectrometric measurements were carried out on an online connected Q Exactive™ Plus Hybrid Quadrupole-Orbitrap Mass Spectrometer (Thermo Fisher Scientific, San Jose, USA), operating in the positive electrospray ionization mode. For quantitative mass spectrometric analysis through MS/MS, the parallel reaction monitoring (PRM) data acquisition mode was chosen. The optimization of parameters and the validation of the UHPLC-MS/MS analysis for human serum were carried out previously.[30]

Statistical analyses

Our outcome measures were categorical variables (ENI, good outcome at 30 and 90 days). Based on the Shapiro–Wilk test, some KYN metabolites and enzymatic activities

did not show normal distribution (namely, 3-HANA, TRP, ANA, 3-HK, PICA, XA, monoamine oxidase (MAO), and KAT). Therefore, based on the distribution, continuous variables were either expressed as mean ± standard deviation (SD) or median and interquartile range (IQR). Kynurenine metabolite concentrations and enzymatic activities measured at the 2 timepoints were compared with either paired sample t-test (if the distribution was normal), or Wilcoxon matched-pairs signed-ranks test (when data was nonparametric) for cases where both samples were taken. To compare means of concentrations and enzymatic activities between groups with and without ENI or good functional outcome, we used the independent sample t-test or Mann–Whitney U test (depending on the distribution of the data). Boxplots were drawn to allow for better visualization of statistically significant findings. Furthermore, if statistical significance was met, we performed receiver operating characteristic (ROC) analysis. We calculated area under the curve (AUC), as well as sensitivity (SN) and specificity (SP) for different cut-off values. Due to the small sample size of our pilot study, logistic regression was not performed. A p-value of <0.05 was regarded statistically significant. Confidence intervals (CI) of 95% were presented where appropriate. Analyses were carried out with IBM SPSS v. 24 (IBM Corp., Armonk, USA) statistical software.

Results

Our pilot study included 48 patients. Thirty-nine were known to be within the 4.5 h thrombolysis time window. In the remaining 9 patients with unknown stroke onset time, intravenous alteplase was administered on the basis of a diffusion-weighted imaging (DWI)-fluid-attenuated inversion recovery (FLAIR) mismatch demonstrated on an acute brain magnetic resonance imaging (MRI), as per the WAKE-UP trial.[31] The flowchart of patient selection is shown in Fig. 2. The clinical characteristics of our study population are highlighted in Table 1. Seventeen patients had large vessel occlusion (LVO), but mechanical thrombectomy was not performed due to limited availability of this service in our center at the time. We collected 32 blood samples before thrombolysis and 36 samples 12 h after treatment. Twenty-three patients had samples taken at both timepoints. The UHPLC-MS/MS method provided simultaneous quantification of TRP and its 10 most important metabolites (SERO, KYN, 3-HANA, 5-HIAA, ANA, KYNA, 3-HK, XA, PICA, and QUIN).[30] Concentrations of the measured KYN metabolites of the 23 patients who had sampling at both timepoints are shown in Table 2. Significant changes in paired serum levels were observed for KYN, ANA, KYNA, XA, PICA, and QUIN. Enzymatic activity of IDO, MAO and KAT were calculated by the following ratios: KYN/TRP, 5-HIAA/SERO and KYNA/KYN, respectively. Enzymatic activities are also demonstrated in Table 2. The activity of IDO and MAO decreased significantly after 12 h.

Table 1. Clinical data of our study population (n = 48). Some data were not available for all patients. These are highlighted after each criteria accordingly

Patient characteristics	Value
Mean age ±SD [years]	67.33 ±12.04
Female	24 (50%)
Male	24 (50%)
Hypertension	41 (85.42%)
Diabetes mellitus	13 (27.08%)
Hyperlipidemia	39 (81.25%)
Smoking	14 (29.17%)
Atrial fibrillation	7 (14.58%)
Coronary artery disease	10 (20.83%)
Mean baseline NIHSS score ±SD	8.81 ±4.29
Mean baseline mRS score ±SD	0.79 ±0.77
Large vessel occlusion	17 (35.42%)
Mean SOtN time ±SD (min, n = 39)	136.59 ±53.9
Mean DtN time ±SD (min, n = 47)	57.45 ±35.72
Length of stay in stroke unit [days]	4.91 ±2.05
Intracerebral hemorrhage after treatment	4 (8.33%)
Mean C-reactive protein ±SD [mg/L], n = 47)	10.44 ±18.78
Mean white cell count ±SD [g/L]	8.07 ±2.31
Mean discharge NIHSS score ±SD	6.71 ±7.89
Early neurological improvement	19 (39.58%)
Mean mRS score at 30 days ±SD (n = 45)	2.47 ±1.84
Mean mRS score at 90 days ±SD (n = 40)	2.38 ±1.9
Good functional outcome at day 30 (n = 45)	27 (60%)
Good functional outcome at day 90 (n = 40)	24 (60%)

DtN – door to needle; mRS – modified Rankin Scale; NIHSS – National Institutes of Health Stroke Scale; SD – standard deviation; SOtN – stroke onset to needle.

Patients with ENI had significantly lower concentrations of KYNA and lower KAT activity in sample A (independent sample t-test, p = 0.01, df = 30, t = –2.722; and Mann–Whitney U test, p = 0.002, z = –3.050, respectively, Fig. 3). There was no statistically significant difference in sample B. Regarding the presence or absence of good outcome at 30 and 90 days, concentrations and enzymatic activities did not statistically significantly differ in samples A or B. Receiver operating characteristic analysis for ENI was performed using KYNA levels and KAT activity measured before treatment (Fig. 4). The AUC for KYNA concentrations was 0.74, 95% CI = 0.57–0.91, p = 0.02. The optimal cut-off value to predict ENI was 37.8 nM (SN 69.2%, SP 68.4%). Similarly, the AUC for KAT activity was 0.82, 95% CI = 0.67–0.98, p = 0.002. The optimal cut-off activity was 0.0127 (SN 92.3%, SP 73.7%).

Discussion

To our knowledge, this is the first study to analyze the changes in KYN metabolite serum levels and enzymatic

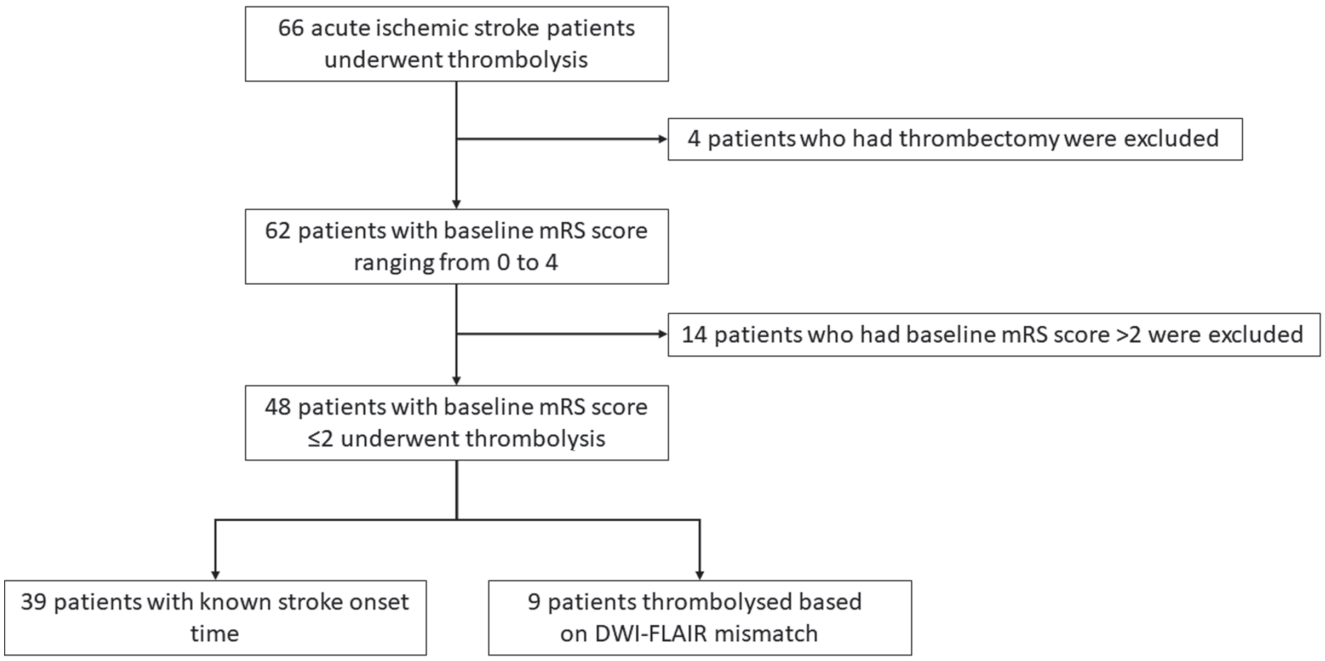

Fig. 2. Flowchart showing patient enrollment in our pilot study

DWI – diffusion weighted imaging; FLAIR – fluid attenuated inversion recovery; mRS – modified Rankin Scale.

Table 2. Mean and median concentrations of KYN metabolites taken before thrombolysis (sample A) and 12 hours after (sample B) alteplase treatment. Only the results of 23 patients who had sampling at both timepoints are presented. The unit of measurement for all metabolites is nanomoles (nM). Enzymatic activities are also shown (these ratios do not have units of measurement). Concentrations are expressed as mean ±SD if the distribution was normal or median and interquartile range when data was nonparametric. Concentrations and enzymatic activities were compared with either paired sample t-test (if the distribution was normal) or Wilcoxon matched-pairs signed-ranks test (when data was nonparametric)

Metabolites and enzymes	Sample A (nM) (n = 23)	Sample B (nM) (n = 23)	p-value
SERO	655.34 ±301.3	680.97 ±263.54	0.44
KYN	3669.52 ±1044.79	3413.1 ±1114.47	0.03
3-HANA	53.07 (40.9–79.74)	43.33 (35.58–62.01)	0.05
TRP	46,371.75 (41,588.69–54,644.26)	50,599.91 (41,798.89–53,961.54)	0.56
5-HIAA	96.58 ±35.47	88.15 ±36.29	0.18
ANA	53.75 (38.73–68.44)	43.8 (27.07–60.2)	0.01
KYNA	45.44 ±20.02	37.69 ±14.55	0.004
XA	11.27 (5.8–16.51)	4.58 (2.56–7.93)	0.001
3-HK	125.68 (79.33–175.98)	115.73 (87.04–161.72)	0.26
PICA	43.33 (34.09–52.22)	29.47 (24.12–39.6)	<0.001
QUIN	673.69 ±230.82	620.26 ±236.66	0.001
IDO	0.08 ±0.02	0.07 ±0.02	0.02
MAO	0.16 (0.11–0.21)	0.12 (0.08–0.2)	0.02
KAT	0.01 (0.01–0.02)	0.01 (0.01–0.01)	0.14

3-HANA – 3-hydroxyanthranilic acid; 3-HK – 3-hydroxykynurenine; 5-HIAA – 5-hydroxy-3-indoleacetic acid; ANA – anthranilic acid; IDO – indoleamine 2,3-dioxygenase; KAT – kynurenine aminotransferase; KYN – kynurenine; KYNA – kynurenic acid; MAO – monoamine oxidase; PICA – picolinic acid; QUIN – quinolinic acid; SD – standard deviation; SERO – serotonin; TRP – tryptophan; XA – xanthurenic acid.

activity in acute ischemic stroke patients who received thrombolytic treatment.

The main finding of our pilot study is that ischemic stroke patients with ENI after thrombolysis have significantly lower concentrations of KYNA and lower KAT activity at baseline. Therefore, we propose that pre-thrombolysis KYNA levels and KAT activity are potential biomarkers of ENI. It should be highlighted that ENI was defined as the difference between the admission and discharge NIHSS scores, although we are aware that ENI is usually calculated with the NIHSS score taken 24 h after symptom onset or treatment.[32] The mean time difference between

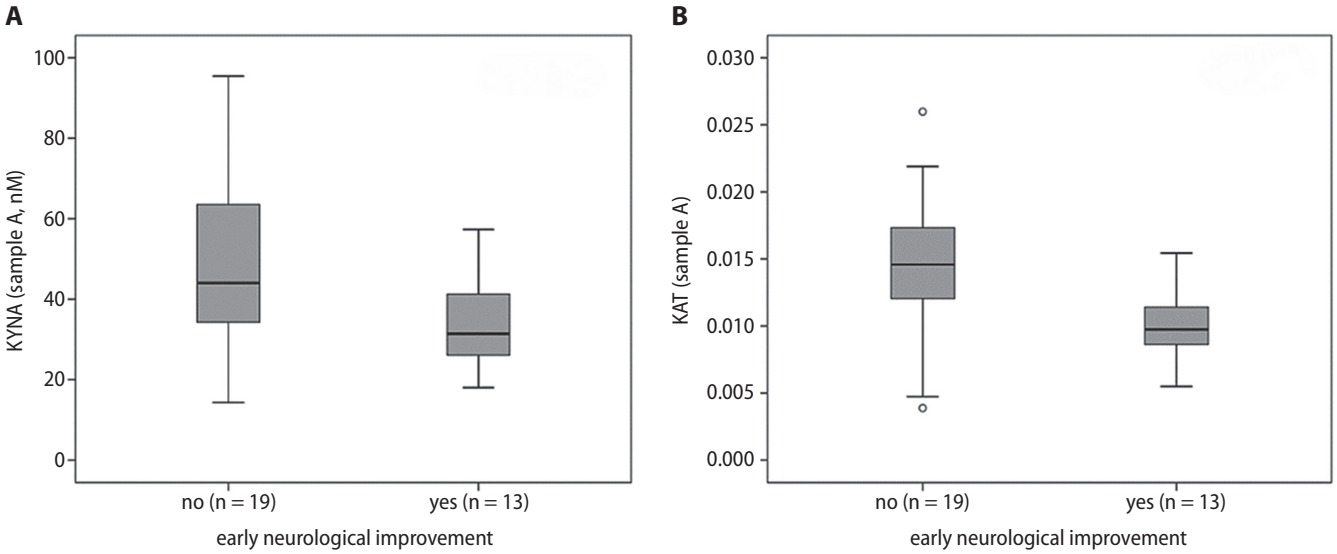

Fig. 3. Boxplots highlighting the significant difference of KYNA levels (A) and KAT activity (B) between patients with and without early neurological improvement. Measurements were made from samples taken before alteplase treatment. For each box, the horizontal line inside the box shows the median. The ends of the boxes represent the 1st and 3rd quartiles. The whiskers extend to the highest and lowest values not considered outliers (defined as 1.5 times the interquartile range (IQR)). Outliers are shown as circles

KAT – kynurenine aminotransferase; KYNA – kynurenic acid.

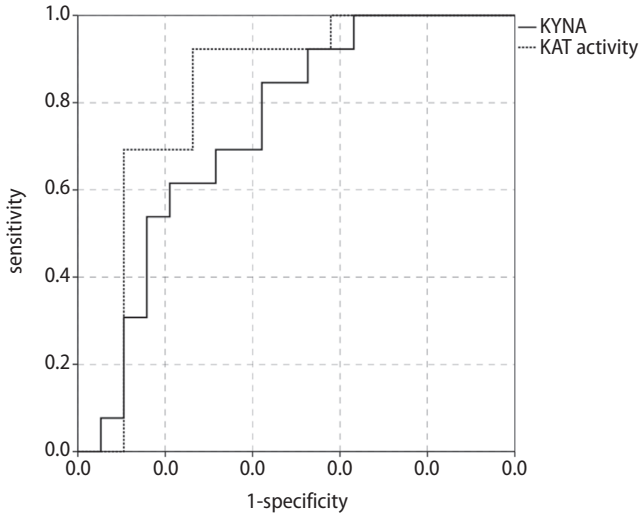

Fig. 4. Receiver operating characteristic (ROC) curve showing the accuracy of KYNA concentration and KAT activity (measured before thrombolysis) in predicting early neurological improvement

KAT – kynurenine aminotransferase; KYNA – kynurenic acid.

the admission and discharge date in our population was 4.91 days. We believe that this five-day difference does not confound the treatment effect size of intravenous alteplase. Our view is that the true effect of thrombolysis is better reflected in the short-term NIHSS change than in the 30 and 90 day mRS scores, which are more dependent on a number of additional factors, such as the pre-stroke condition of patients, comorbidities, polypharmacy, the availability and quality of rehabilitation, and support provided by family.

Based on our previous research in animal stroke models, we had hypothesized that levels of neuroprotective KYNA would be higher in patients with better outcomes.[13,33] However, lower concentrations of KYNA and lower KAT activity were found to predict good treatment response, with good sensitivity and specificity. Our findings support previous observations by Darlington et al. of higher KYNA levels being detected in patients who died within 21 days after ischemic stroke compared to those who survived.[11] It is unclear why increased levels of KYNA are associated with worse clinical outcome in ischemic stroke. One possible explanation is that KYNA is an endogenous NMDAR antagonist; therefore, it could further decrease synaptic activity in brain ischemia and, consequently, worsen brain function.[11,34] It has also been reported that KYNA can interfere with mitochondrial respiration, resulting in reduced ATP synthesis and increased levels of oxidative stress.[35]

We did not find any correlation between KYN metabolites or enzymes and good functional outcome measured 30 and 90 days after the stroke. This finding was somewhat surprising, given the results of the ROC analysis. Brouns et al. reported that the KYN/TRP ratio correlated with the mRS score 3 months after the ischemic stroke.[10] Possible explanations behind the lack of correlation in our study are the small sample size and the effect of thrombolytic treatment.

Limitations

The main limitations of our pilot study are the small sample size and the absence of a control group. An ideal control group would have been acute ischemic stroke patients who did not receive alteplase treatment. However, this would have been unethical, given the evidence supporting thrombolytic treatment.[36]

We could not obtain blood samples from every patient at both timepoints due to occasional limited availability of our biobank facility, and the loss of several patients before follow-up. Due to the small number of individuals included in our study, logistic regression analysis was not applicable.

Also, it is important to note that KYN metabolites were measured from the serum of patients. Therefore, our findings do not necessarily reflect the intracerebral changes in KYN metabolites and enzymes in the setting of acute ischemic stroke. It has been previously reported that approx. 40% of KYN is produced locally in the central nervous system and the remaining 60% is taken up from circulation.[37] Metabolites that can cross the blood-brain barrier (BBB) via large neutral amino acid transporters are TRP, KYN and 3-HK.[20,38] Kynurenic acid only has a limited ability to traverse across the BBB.

Conclusions

In conclusion, our pilot study provides further evidence that the KYN pathway is already activated within the first few hours after symptom onset in acute ischemic stroke. We propose that baseline serum KYNA concentration and KAT activity are potential biomarkers predicting early treatment response to thrombolytic therapy in stroke. Consequently, genetic polymorphisms of KAT could also hold promise as a further research target. Future studies with larger samples, well-chosen control groups and rigorous methodology are needed.

ORCID iDs

Ádám Annus https://orcid.org/0000-0003-0498-6578
Ferenc Tömösi https://orcid.org/0000-0002-6657-5777
Ferenc Rárosi https://orcid.org/0000-0002-1014-9242
Evelin Fehér https://orcid.org/0000-0003-2564-3937
Tamás Janáky https://orcid.org/0000-0002-6466-8283
Gábor Kecskeméti https://orcid.org/0000-0002-5584-6869
József Toldi https://orcid.org/0000-0001-7355-0503
Péter Klivényi https://orcid.org/0000-0002-5389-3266
László Sztriha https://orcid.org/0000-0003-4639-3180
László Vécsei https://orcid.org/0000-0001-8037-3672

References

1. Biomarkers Definitions Working Group. Biomarkers and surrogate endpoints: Preferred definitions and conceptual framework. *Clin Pharmacol Ther*. 2001;69(3):89–95. doi:10.1067/mcp.2001.113989
2. Kim SJ, Moon GJ, Bang OY. Biomarkers for stroke. *J Stroke*. 2013;15(1):27–37. doi:10.5853/jos.2013.15.1.27
3. Katan M, Fluri F, Morgenthaler NG, et al. Copeptin: A novel, independent prognostic marker in patients with ischemic stroke. *Ann Neurol*. 2009;66(6):799–808. doi:10.1002/ana.21783
4. Castellanos M, Sobrino T, Millan M, et al. Serum cellular fibronectin and matrix metalloproteinase-9 as screening biomarkers for the prediction of parenchymal hematoma after thrombolytic therapy in acute ischemic stroke: A multicenter confirmatory study. *Stroke*. 2007;38(6):1855–1859. doi:10.1161/STROKEAHA.106.481556
5. Foerch C, Otto B, Singer OC, et al. Serum S100B predicts a malignant course of infarction in patients with acute middle cerebral artery occlusion. *Stroke*. 2004;35(9):2160–2164. doi:10.1161/01.STR.0000138730.03264.ac
6. Alessi MC, Gaudin C, Grosjean P, et al. Changes in activated thrombin-activatable fibrinolysis inhibitor levels following thrombolytic therapy in ischemic stroke patients correlate with clinical outcome. *Cerebrovasc Dis*. 2016;42(5–6):404–414. doi:10.1159/000447722
7. Faille D, Labreuche J, Meseguer E, Huisse MG, Ajzenberg N, Mazighi M. Endothelial markers are associated with thrombolysis resistance in acute stroke patients. *Eur J Neurol*. 2014;21(4):643–647. doi:10.1111/ene.12369
8. Hudak R, Szekely EG, Kovacs KR, et al. Low thrombin generation predicts poor prognosis in ischemic stroke patients after thrombolysis. *PloS One*. 2017;12(7):e0180477. doi:10.1371/journal.pone.0180477
9. Hertelendy P, Toldi J, Fulop F, Vecsei L. Ischemic stroke and kynurenines: Medicinal chemistry aspects. *Curr Med Chem*. 2018;25(42):5945–5957. doi:10.2174/0929867325666180313113411
10. Brouns R, Verkerk R, Aerts T, et al. The role of tryptophan catabolism along the kynurenine pathway in acute ischemic stroke. *Neurochem Res*. 2010;35(9):1315–1322. doi:10.1007/s11064-010-0187-2
11. Darlington LG, Mackay GM, Forrest CM, Stoy N, George C, Stone TW. Altered kynurenine metabolism correlates with infarct volume in stroke. *Eur J Neurosci*. 2007;26(8):2211–2221. doi:10.1111/j.1460-9568.2007.05838.x
12. Mo X, Pi L, Yang J, Xiang Z, Tang A. Serum indoleamine 2,3-dioxygenase and kynurenine aminotransferase enzyme activity in patients with ischemic stroke. *J Clin Neurosci*. 2014;21(3):482–486. doi:10.1016/j.jocn.2013.08.020
13. Robotka H, Sas K, Agoston M, et al. Neuroprotection achieved in the ischaemic rat cortex with L-kynurenine sulphate. *Life Sci*. 2008;82(17–18):915–919. doi:10.1016/j.lfs.2008.02.014
14. Colpo GD, Venna VR, McCullough LD, Teixeira AL. Systematic review on the involvement of the kynurenine pathway in stroke: Pre-clinical and clinical evidence. *Front Neurol*. 2019;10:778. doi:10.3389/fneur.2019.00778
15. Ormstad H, Verkerk R, Aass HC, Amthor KF, Sandvik L. Inflammation-induced catabolism of tryptophan and tyrosine in acute ischemic stroke. *J Mol Neurosci*. 2013;51(3):893–902. doi:10.1007/s12031-013-0097-2
16. Maes M, Leonard BE, Myint AM, Kubera M, Verkerk R. The new '5-HT' hypothesis of depression: Cell-mediated immune activation induces indoleamine 2,3-dioxygenase, which leads to lower plasma tryptophan and an increased synthesis of detrimental tryptophan catabolites (TRYCATs), both of which contribute to the onset of depression. *Prog Neuropsychopharmacol Biol Psychiatry*. 2011;35(3):702–721. doi:10.1016/j.pnpbp.2010.12.017
17. Oxenkrug GF. Genetic and hormonal regulation of tryptophan kynurenine metabolism: Implications for vascular cognitive impairment, major depressive disorder, and aging. *Ann N Y Acad Sci*. 2007;1122:35–49. doi:10.1196/annals.1403.003
18. Eltzschig HK, Eckle T. Ischemia and reperfusion: From mechanism to translation. *Nat Med*. 2011;17(11):1391–1401. doi:10.1038/nm.2507
19. Schroeter M, Jander S, Witte OW, Stoll G. Local immune responses in the rat cerebral cortex after middle cerebral artery occlusion. *J Neuroimmunol*. 1994;55(2):195–203. doi:10.1016/0165-5728(94)90010-8
20. Vecsei L, Szalardy L, Fulop F, Toldi J. Kynurenines in the CNS: Recent advances and new questions. *Nat Rev Drug Discov*. 2013;12(1):64–82. doi:10.1038/nrd3793
21. Song P, Ramprasath T, Wang H, Zou MH. Abnormal kynurenine pathway of tryptophan catabolism in cardiovascular diseases. *Cell Mol Life Sci*. 2017;74(16):2899–2916. doi:10.1007/s00018-017-2504-2
22. Wang Y, Liu H, McKenzie G, et al. Kynurenine is an endothelium-derived relaxing factor produced during inflammation. *Nat Med*. 2010;16(3):279–285. Erratum in: *Nat Med*. 2010;16(5):607. doi:10.1038/nm.2092
23. Ito S, Komatsu K, Tsukamoto K, Sved AF. Excitatory amino acids in the rostral ventrolateral medulla support blood pressure in spontaneously hypertensive rats. *Hypertension*. 2000;35(1 Pt 2):413–417. doi:10.1161/01.hyp.35.1.413
24. Pedersen ER, Tuseth N, Eussen SJ, et al. Associations of plasma kynurenines with risk of acute myocardial infarction in patients with stable angina pectoris. *Arterioscler Thromb Vasc Biol*. 2015;35(2):455–462. doi:10.1161/ATVBAHA.114.304674
25. Hattori M, Kotake Y, Kotake Y. Studies on the urinary excretion of xanthurenic acid in diabetics. *Acta Vitaminol Enzymol*. 1984;6(3):221–228. PMID:6524581

26. Kotake Y, Ueda T, Mori T, Igaki S, Hattori M. Abnormal tryptophan metabolism and experimental diabetes by xanthurenic acid (XA). *Acta Vitaminol Enzymol.* 1975;29(1–6):236–239. PMID:1244098
27. Stone TW, Darlington LG. Endogenous kynurenines as targets for drug discovery and development. *Nat Rev Drug Discov.* 2002;1(8): 609–620. doi:10.1038/nrd870
28. Capuron L, Schroecksnadel S, Féart C, et al. Chronic low-grade inflammation in elderly persons is associated with altered tryptophan and tyrosine metabolism: Role in neuropsychiatric symptoms. *Biol Psychiatry.* 2011;70(2):175–182. doi:10.1016/j.biopsych.2010.12.006
29. Theofylaktopoulou D, Midttun Ø, Ulvik A, et al. A community-based study on determinants of circulating markers of cellular immune activation and kynurenines: The Hordaland Health Study. *Clin Exp Immunol.* 2013;173(1):121–130. doi:10.1111/cei.12092
30. Tomosi F, Kecskemeti G, Cseh EK, et al. A validated UHPLC-MS method for tryptophan metabolites: Application in the diagnosis of multiple sclerosis. *J Pharm Biomed Anal.* 2020;185:113246. doi:10.1016/j.jpba.2020.113246
31. Thomalla G, Simonsen CZ, Boutitie F, et al. MRI-guided thrombolysis for stroke with unknown time of onset. *N Engl J Med.* 2018;379(7): 611–622. doi:10.1056/NEJMoa1804355
32. Agarwal S, Cutting S, Grory BM, et al. Redefining early neurological improvement after reperfusion therapy in stroke. *J Stroke Cerebrovasc Dis.* 2020;29(2):104526. doi:10.1016/j.jstrokecerebrovasdis.2019.104526
33. Gigler G, Szenasi G, Simo A, et al. Neuroprotective effect of L-kynurenine sulfate administered before focal cerebral ischemia in mice and global cerebral ischemia in gerbils. *Eur J Pharmacol.* 2007;564(1–3): 116–122. doi:10.1016/j.ejphar.2007.02.029
34. Kessler M, Terramani T, Lynch G, Baudry M. A glycine site associated with N-methyl-D-aspartic acid receptors: Characterization and identification of a new class of antagonists. *J Neurochem.* 1989;52(4):1319–1328. doi:10.1111/j.1471-4159.1989.tb01881.x
35. Baran H, Kepplinger B, Herrera-Marschitz M, Stolze K, Lubec G, Nohl H. Increased kynurenic acid in the brain after neonatal asphyxia. *Life Sci.* 2001;69(11):1249–1256. doi:10.1016/s0024-3205(01)01215-2
36. Powers WJ, Rabinstein AA, Ackerson T, et al. Guidelines for the early management of patients with acute ischemic stroke. 2019 update to the 2018 guidelines for the early management of acute ischemic stroke: A guideline for healthcare professionals from the American Heart Association/American Stroke Association. *Stroke.* 2019;50(12): e344–e418. doi:10.1161/STR.0000000000000211
37. Gal EM, Sherman AD. Synthesis and metabolism of L-kynurenine in rat brain. *J Neurochem.* 1978;30(3):607–613. doi:10.1111/j.1471-4159.1978.tb07815.x
38. Pardridge WM. Blood-brain barrier carrier-mediated transport and brain metabolism of amino acids. *Neurochem Res.* 1998;23(5):635–644. doi:10.1023/a:1022482604276

Severe cases of osteogenesis imperfecta type VIII due to a homozygous mutation in *P3H1* (LEPRE1) and review of the literature

Mehmet Murat Bala[1,A–F], Keziban Aslı Bala[2,B]

[1] Department of Orthopaedics and Traumatology, Health Sciences University, Trabzon Kanuni Training and Research Hospital, Turkey
[2] Department of Pediatric Endocrinology, Faculty Of Medicine, Health Sciences University, Trabzon Kanuni Training and Research Hospital, Turkey

A – research concept and design; B – collection and/or assembly of data; C – data analysis and interpretation;
D – writing the article; E – critical revision of the article; F – final approval of the article

Advances in Clinical and Experimental Medicine, ISSN 1899–5276 (print), ISSN 2451–2680 (online) *Adv Clin Exp Med*. 2021;30(12):1233–1238

Address for correspondence
Mehmet Murat Bala
E-mail: muratbala@hotmail.com

Funding sources
None declared

Conflict of interest
None declared

Acknowledgements
We would like to thank the patients and their parents for participating in this study. We would like to also thank Prof. Dr. Hüseyin Yüce for his contribution to the genetic analysis in the study.

Received on June 16, 2021
Reviewed on August 8, 2021
Accepted on August 18, 2021

Published online on October 12, 2021

Abstract

Background. Osteogenesis imperfecta (OI) is a genetic disorder that causes skeletal fragility, multiple fractures and several extraskeletal disorders. Most cases of OI are caused by mutations in COL1A1/A2. Osteogenesis imperfecta type VIII typically causes a severe and fatal phenotype that presents at birth with severe osteopenia, congenital fractures and other clinical manifestations.

Objectives. We describe the cases of an 11-year-old female and a 9-year-old male with homozygous truncating mutations in *P3H1*. Both cases were born with intrauterine fractures and suffered multiple fractures shortly after birth, requiring multiple operations to correct both fractures and severe scoliosis. The patients have been treated with pamidronate since the age of 2.

Materials and methods. Whole exome sequencing (WES) was performed by Gene by Gene using Twist Bioscience technology. Initially, ~36.5 Mb of consensus coding sequences (targeting >98% of RefSeq and Gencode v. 28 regions obtained from the human genome) was replicated from fragmented genomic DNA using the Twist Human Core Exome Plus kit. The subsequent library was sequenced on the Illumina Novaseq Next Generation Sequencing platform to achieve at least ×20 reading depth for >98% of the targeted bases. Variant annotations and filtering was performed using Ingenuity Variant Analysis software.

Results. We identified a homozygous mutation in the 3rd exon of *P3H1* (c.628C>T/p.Arg210 Ter). Our cases broaden the phenotypic spectrum of OI type VIII as, to the best of our knowledge, these are the first postnatal cases with *P3H1* (c.628C>T/p.Arg210 Ter) mutations published in the literature.

Conclusions. We present the first recorded postnatal cases from unrelated families of OI type VIII, broadening our understanding of the severe, but nonfatal spectrum of clinical phenotype of this recessive form of OI.

Key words: osteogenesis imperfecta, severe, homozygous mutation, *P3H1*, LEPRE1

Cite as
Bala MM, Bala KA. Severe cases of osteogenesis imperfecta type VIII due to a homozygous mutation in P3H1 (LEPRE1) and review of the literature. *Adv Clin Exp Med*. 2021;30(12):1233–1238. doi:10.17219/acem/141367

DOI
10.17219/acem/141367

Background

Osteogenesis imperfecta (OI) is a clinically and genetically heterogeneous skeletal dysplasia that occurs in approx. 1 in 10,000–20,000 births.[1] It is characterized by multiple fractures caused by skeletal fragility and extra-skeletal findings, such as blue sclera, dentinogenesis imperfecta, hearing loss, joint hypermobility, and hyperlaxity.[1] Most OI cases (type I–IV) are associated with heterozygous mutations in *COL1A1* (MIM 120150) or *COL1A2* (MIM 120160), which encode the type I procollagen alpha chain to proalpha1 and proalpha2.[1] Osteogenesis imperfecta type V is caused by heterozygous mutations in *IFITM5* (MIM 614757).[2]

Osteogenesis imperfecta types VI–XV are inherited in a recessive manner.[3] Homozygous truncating mutations in *P3H1* (LEPRE 1) (NM_022356) are responsible for OI type VIII and were first reported in 2007.[4] The *P3H1* encodes prolyl 3-hydroxylase 1, which forms a molecular complex with cyclophilin B, encoded by the cartilage-associated protein (CRTAP) and peptidyl prolyl isomerase B (PPIB). The *P3H1* is involved in the post-translational modification of collagen in the endoplasmic reticulum and prolyl 3-hydroxylation of specific proline residues (especially a1 (I) Pro986).[5,6] So far, 48 different mutant *P3H1* alleles have been reported in patients with OI.[7]

Objectives

We describe 2 cases – of an 11-year-old female and a 9-year-old male – with a clinical presentation of severe OI, and identify a homozygous mutation in the 3rd exon of *P3H1* (c.628C>T/p.Arg210 Ter). Our cases broaden the phenotypic spectrum of OI type VIII as, to the best of our knowledge, these are the first postnatal cases with *P3H1* (c.628C>T/p.Arg210 Ter) mutations published in the literature.

Case reports

Case 1

The female patient was 11 years and 7 months of age at the time of the study. She was born from the first pregnancy of a 21-year-old mother. The mother and 27-year-old father of the child were first cousins, Turkish in origin, and had a height of 150 cm and 180 cm, respectively. Neither of the parents had a history of chronic illness or fracture. The patient was an only child, and the mother had no history of stillbirth or miscarriage. Moreover, there was no known familial history of OI or any other bone dysplasia.

The mother's pregnancy was followed up every 4–8 weeks starting from the 8th gestational week, and no maternal medical problems affecting pregnancy were found. She took prenatal vitamins regularly. The ultrasound performed during the 12th gestational week revealed the fetus had curved and short legs. The amniotic fluid level was normal. The patient was born in the 39th gestational week via normal vaginal delivery without intervention. Her birth weight was 3020 g and height was 47 cm.

Her right upper arm was swollen, and leg movements were reduced on the 1st postnatal day. The patient was evaluated by orthopedic surgeons, and direct radiographic examination was performed. Fractures were detected in the right humeral diaphysis, right clavicle, distal aspect of both the femurs, right proximal tibia, right distal fibula, and left distal tibia. Spinal body fracture was not detected. Chronic changes were detected in the symmetrical, curved and weakened femurs and ribs, suggesting intrauterine fractures.

Pamidronate treatment at a dose of 9.0 mg/kg/year was initiated when the patient was 2 years of age. She underwent a total of 6 operations, 5 of which were for the fractures and 1 for scoliosis, and she has been followed up for the last 3 years, over which she did not sustain any new fractures. The latest bone mineral density (BMD) of the patient was –2.2 SDS (standard deviation score). During follow-up, her calcium, phosphorus and alkaline phosphatase levels were normal, and she was given vitamin D supplements to ensure that her 25-hydroxy vitamin D (25(OH)D) levels were within the normal range.

On physical examination, her height was –7 SDS and weight was –4.7 SDS, according to her age and sex. The patient had normal results for echocardiographic, urinary, hearing and dental examinations, and did not have blue sclera (Table 1). Both femurs had anterolateral curvatures. The patient was able to walk with the help of a walker. Radiographic examinations of the patient demonstrated severe osteopenia, thoracolumbar scoliosis, diaphyseal expansion in the distal humerus and proximal radioulnar metaphyses, trabeculae in the bones, and popcorn-like concentric concentrations (Fig. 1, 1a–f).

No mutation was found in *COL1A1*, *COL1A2*, *CRTAP*, and *SERPINH1* in the initial genetic analyses of the patient. Following the initial investigations, whole exome sequencing (WES) was performed using peripheral blood in the Microgen Genetic Diseases Diagnosis Center, Ankara, Turkey, and a homozygous nonsense mutation (c.628C>T/p.Arg210 Ter) was detected in the 3rd exon of *P3H1*. Mutations in *CRTAP*, *PPIB*, *FKBP10*, *SERPINF1*, *PLOD2*, *SERPINH1*, *SP7*, or *ALPL* were excluded using WES. The patient's mother and father were found to be heterozygous for the same mutation, based on the targeted mutation analyses.

Case 2

The male patient was 9 years and 3 months of age at the time of evaluation. He was born from the 2nd pregnancy of a 30-year-old mother, whose 1st child was a 10-year-old, healthy female at the time of the investigation.

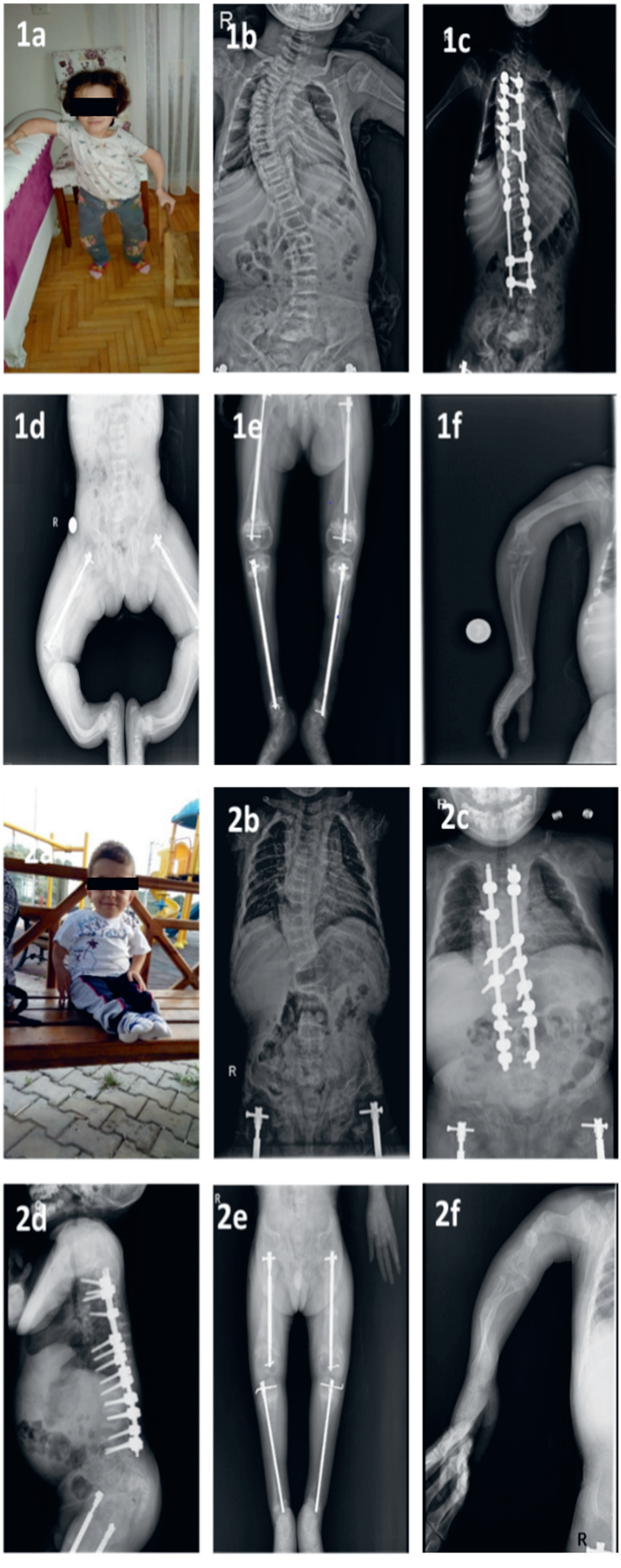

Fig. 1. Autosomal recessive osteogenesis imperfecta (OI) phenotype due to P3H1 mutations (clinical presentation and skeletal graphs). Severe scoliosis, asymmetry of the lower limbs, thin bones, and severe deformities in the femurs, tibias and fibulas were observed. 1a. Clinical pictures of case 1 (11 years and 7 months of age: walks and stands with assistance); 2a. Clinical pictures of case 2 (9 years and 3 months of age: walks and stands with assistance); 1b and 2b. Anteroposterior (AP) view of the thoracolumbar spine on radiography; 1c and 2c. The AP view of thoracolumbar scoliosis on a radiograph taken postoperatively; 1d. Bilateral tibia and fibula showing anterolateral curvatures; 2d. Lateral view of thoracolumbar scoliosis on a radiograph taken postoperatively; 1e and 2e. Postoperative radiographic images showing nailing and healing of the fracture; 1f and 2f. Severe deformities of the upper limbs. Informed consent was obtained from the patients prior to publishing these images

Table 1. Clinical features of the presented cases

Parameter	Case 1	Case 2
P3H1 (LEPRE1) mutation	(c.628C>T/p.Arg210 Ter)	(c.628C>T/p.Arg210 Ter)
Growth data birth current age [years] weight (SDS) length (SDS)	 term, 3.2 kg 11 –4.7 –7	 term, 2.8 kg 9 –9 –6.6
Facial features facial shape scleral hue dentiogenesis imperfecta	 triangular white no	 triangular white no
Hearing loss	no	yes
Phenotype	severe OI, type B progressive	severe OI, type B progressive
Pulmonary functions	normal	moderate restrictive
Echocardiography	normal	normal
Spinal abnormalities	scoliosis, multiple T-L vertebral compression	scoliosis, multiple T-L vertebral compression
Rhizomelia	yes	yes
Bone mineral density score (pre- and post-biphosphonate therapy) (SDS)	–8.1 (pre-therapy) –2.2 (post-therapy)	–9.3 (pre-therapy) –3.7 (post-therapy)

OI – osteogenesis imperfecta; SDS – standard deviation score; T-L – thoracolumbar.

The mother and 35-year-old father were of Turkish origin, not related, and had a height of 157 cm and 175 cm, respectively. Neither of them had a history of chronic illness or fracture. Moreover, the mother had no history of stillbirth or miscarriage, nor any known familial history of OI or other bone dysplasia.

The pregnancy was followed up every 4–8 weeks starting from the 6th gestational week, and no maternal medical problems that may affect the pregnancy were found. The mother took prenatal vitamins regularly. The fetus was found to have short legs during an ultrasound in the 12th gestational week. The amniotic fluid level was normal. The child was delivered via cesarean section in the 38th gestational week. His birth weight was 2850 g and height was 48 cm.

The patient had swollen arms and legs on the 1st postnatal day. Orthopedic surgeons evaluated the patient and direct radiographic examination was conducted. Fractures were detected in both, the distal femurs and humeri. Spinal body fractures were not detected.

Pamidronate treatment at a dose of 9.0 mg/kg/year was initiated when the patient was 2 years old. He underwent a total of 11 operations, 10 of which were for fractures and 1 was for scoliosis, and the patient has been followed up for the last 2.5 years, over which time he did not sustain any new fractures. The latest BMD of the patient was –3.7 SDS. During follow-up, the patient's calcium, phosphorus and alkaline phosphatase levels were normal, and vitamin D supplements were administered to ensure that his 25(OH)D levels were within the normal range.

On physical examination, the patient's height was –6.6 SDS and weight was –9 SDS, according to his age and sex. His echocardiographic and dental examinations were normal. However, conductive deafness in the right ear and bilateral nephrolithiasis were detected on the audiological and urinary examination, respectively. He did not have blue sclera, but had frequent pulmonary infections due to restrictive lung disease (Table 1). The patient was unable to walk because of his almost immobile legs. Severe osteopenia, thinning of long bones, marked appearance of epiphysis, and curvatures caused by multiple fractures were observed on radiographic examinations. The ribs were extremely thin and thoracolumbar scoliosis was also observed (Fig. 1,2a–f).

The *COL1A1*, *COL1A2*, *CRTAP*, and *SERPINH1* genes were excluded in the initial patient's 1st genetic analysis. Subsequent WES analyses of the patient demonstrated a homozygous pathogenic variant (c.628C>T/p.Arg210 Ter) in the 3rd exon of the *P3H1* gene (performed at the Microgen Genetic Diseases Diagnosis Center). Mutations in other genes, including *CRTAP*, *PPIB*, *FKBP10*, *SERPINF1*, *PLOD2*, *SERPINH1*, *SP7*, and *ALPL*, were excluded using WES. Sanger sequencing of parental DNA samples revealed that both parents were heterozygous for c.628C>T.

Method of genetic analyses

Whole exome sequencing was performed by Gene by Gene using Twist Bioscience technology (Microgen Genetic Diseases Diagnosis Center). Initially, ~36.5 Mb of consensus coding sequences (targeting >98% of RefSeq and Gencode

v. 28 regions obtained from the human genome) were replicated from fragmented genomic DNA using the Twist Human Core Exome Plus kit (Twist Bioscience, South San Francisco, USA). The subsequent library was then sequenced on the Illumina Novaseq NGS (Illumina, San Diego, USA) platform to achieve at least a ×20 reading depth for >98% of the targeted bases. Variant annotations and filtering was performed using the Ingenuity Variant Analysis software (Qiagen, Hilden, Germany).

Discussion

The *P3H1* (c.628C>T/p.Arg210 Ter) was first reported by Willaert et al. in a consanguineous Turkish family.[8] The mother had 2 pregnancies in which the fetuses were found to have genetic mutations, and elective termination was performed at the 20th and 18th gestational week, respectively. To the best of our knowledge, our cases are the first recorded postnatal cases of OI type VIII carrying homozygous *P3H1* (c.628C>T/p.Arg210 Ter) mutation.

The *P3H1* mutations typically have a clinical presentation of severe or fatal OI, and are characterized by rhizomelic short limb, white sclera, severe demineralization of bones, excessive growth retardation, intrauterine fractures, and bulbous expansion of metaphyses.[4] Similar to typical *P3H1* mutations in literature, our cases also had considerably short stature, severe demineralization, white sclera, and fractures detected at birth. According to the Van Dijk and Sillence criteria, the 2 patients were classified into OI type B group with progressive deformation and severe OI group.[9] Currently, Willaert et al. is the only publication to present cases with the same mutation.[8] Their study reported a case of siblings who were electively aborted, and hence there was no data on postnatal physical examination findings. In addition, similar to their findings, intrauterine skeletal dysplasia-associated findings were detected in both of our cases.

Literature on pamidronate treatment in OI type VIII is limited. In a case published by Santana et al., pamidronate treatment was initiated at 7 weeks of age. Although the measurements were made using different equipment in different centers, a good response was obtained with >300% improvement.[10] Takagi et al. also reported an OI type VIII case in which pamidronate treatment was started at 2 months of age. The patient developed very few fractures and presented a good response.[5] In both of our cases, pamidronate treatment was started at ~2 years of age at a dose of 9.0 mg/kg/year. These patients, who were followed up in different clinics until they presented to our center, had a history of many fractures because of starting the treatment later than the previous cases. In their study, Willaert et al. reported a significant improvement in BMD Z-score (from –11.0 to –6.8) in an OI type VIII case of a six-year-old patient treated with pamidronate.[8] When our patients presented to our center, their BMD Z-scores were –2.2 SDS and –3.7 SDS for case 1 and case 2, respectively. This indicated that they responded well to the treatment. They were followed up and did not sustain any new fractures over the last 3 years.

The c.628C>T mutation in *P3H1* was identified as pathogenic.[8] A significant decrease in *P3H1* mRNA was observed on evaluation of fibroblast samples from fetuses with this mutation, using quantitative polymerase chain reaction (qPCR), as expected with the degradation of mutant transcripts by the nonsense-mediated decay pathway. They found that mRNA expression in the patients' parents, who were heterozygous carriers of these nonsense *P3H1* mutations, was similar to that of the control group. The western blot analysis of fibroblast cell lysates probed with anti-*P3H1* antibody showed that *P3H1* was completely absent in patients and slightly decreased in their parents.

Interestingly, in the review from 2010, Marini et al. reported 17 mutant P3H1 alleles occuring throughout the gene.[6] Most of these mutations showed a loss of *P3H1* expression in real-time reverse transcription PCR (RT-PCR) with RNA isolated from the patients' fibroblasts.[4] Mrosk et al., in their study on genotype–phenotype correlation, found 5 novel pathogenic variants in *P3H1* in 5 cases in an Indian OI cohort. Moreover, they observed a variant that was predicted to affect a donor splice site, resulting in a splicing alteration in another patient.[11] Scollo et al. reported a retinal tear in a 9-year-old OI type VIII case with a c.1914 + 1G>A (NM_001243246.1) homozygous mutation in *P3H1*.[12] Furthermore, de Souza et al. reported retinal detachment in a 28-year-old OI type VIII case with a similar mutation (c.1914 + 1G>C (NM_001243246.1)).[13] However, fundoscopic examinations of our cases were found to be normal.

Fratzl-Zelman et al. performed the first study in the literature on the effect of null mutations in *P3H1* on the patient's bone tissue. They evaluated bone histology and histomorphometry, bone mineralization density distribution, and procollagen 3-hydroxylation measurements in bone and skin tissue in non-lethal OI type VIII.[14] Although the bones sampled from these OI type VIII children resembled those of OI type VII, its distinctive features were bone matrix hypermineralization, extremely thin trabeculae, focal osteoid deposition, and an increase in the proportion of bone with low mineral density.

Li et al. found that *P3H1* mutations had a prevalence of 4.05% in an autosomal recessive OI Chinese cohort, and they reported 3 mutations, including 2 new mutations (c.652G>T; c.1948G>C, c.652G>T; c.2164C>T), and 1 previously reported mutation (c.1466T>C; c.1915-1G>A). The most common clinical manifestations were reported to be gait problems, scoliosis and frequent fractures (fractures ≥2/year) in this autosomal recessive OI cohort, which was similar to our cases.[15] Madhuri et al. found 2 new homozygous duplications in *P3H1* in an Indian OI cohort of 52 patients (c.2131dup (p.Leu711Profs*19) (SCV000987189) and c.1980dup (p.Val661Serfs*33) (SCV000987190)).[16]

Progressive deformities, blue sclera, recurrent long bone fractures, rhizomelia, scoliosis/kyphosis, vertebral compression fractures, and wormian bones have been reported in these children, which are similar to the findings in our cases. The researchers have also observed a previously reported variant (c.1346-1G>C) in 5 of their patients, and considered it a recurrent *P3H1* variant in India.

Pepin et al. examined 200 samples from an African population and a neonatal death record of a hospital in Tobago, and they found the prevalence of carriers of the c.1080 + 1G>T mutation in *P3H1* was approx. 1 in 200.[17] During sequence analysis, they found a surprisingly high LEPRE1 allelic diversity in the DNA samples from Tobago. These findings suggested that the milder end of the clinical spectrum may be due to the as yet unidentified missense mutations in *P3H1*. Caudevilla Lafuente et al. reported 1 (fatal) homozygous case in which both parents were heterozygous carriers of the most common variant (c.1080 + 1G>T/IVS5 + 1G>T) in *P3H1* in West African populations.[18] They also reported a case having a previously reported pathogenic heterozygous variant (c.1080 + 1G>T (i5) with c.35T>G (p.Leu12Arg) exon 1, *P3H1*-VUS and c.969C>T (p.Gly323Gly) exon 7, *SERPINF1* gene-VUS). However, this case exhibited a very severe, although nonfatal clinical course. Finally, Tonelli et al. found that the defective chaperone role of the 3-hydroxylation complex was the primary cause of the skeletal phenotype.[19] However, Cabral et al. observed that the functions of the modification complex as a collagen chaperone are distinct from its role as prolyl 3-hydroxylase.[20]

Limitations

Our study has several limitations. First, we only have 2 cases, although our findings may be useful in clinical practice. Second, we could not study in vivo or in vitro models, and hence, there is a need for further studies in this field.

Conclusions

In conclusion, we reported cases of OI type VIII from 2 unrelated families that are the first postnatal cases in which this mutation was detected, and they presented a more severe, but nonfatal spectrum of the clinical phenotype of this recessive form of OI.

ORCID iDs

Mehmet Murat Bala https://orcid.org/0000-0002-7213-5647
Keziban Aslı Bala https://orcid.org/0000-0001-8755-7714

References

1. Forlino A, Marini JC. Osteogenesis imperfecta. *Lancet*. 2016;387(10028):1657–1671. doi:10.1016/S0140-6736(15)00728-X
2. Semler O, Garbes L, Keupp K, et al. A mutation in the 5'-UTR of IFITM5 creates an in-frame start codon and causes autosomal-dominant osteogenesis imperfecta type V with hyperplastic callus. *Am J Hum Genet*. 2012;91(2):349–357. doi:10.1016/j.ajhg.2012.06.011
3. Byers PH, Pyott SM. Recessively inherited forms of osteogenesis imperfecta. *Annu Rev Genet*. 2012;46:475–497. doi:10.1146/annurev-genet-110711-155608
4. Cabral WA, Chang W, Barnes AM, et al. Prolyl 3-hydroxylase 1 deficiency causes a recessive metabolic bone disorder resembling lethal/severe osteogenesis imperfecta. *Nat Genet*. 2007;39(3):359–365. doi:10.1038/ng1968
5. Takagi M, Ishii T, Barnes AM, et al. A novel mutation in LEPRE1 that eliminates only the KDEL ER-retrieval sequence causes non-lethal osteogenesis imperfecta. *PLoS One*. 2012;7(5):e36809. doi:10.1371/journal.pone.0036809
6. Marini JC, Cabral WA, Barnes AM. Null mutations in LEPRE1 and CRTAP cause severe recessive osteogenesis imperfecta. *Cell Tissue Res*. 2010;339(1):59–70. doi:10.1007/s00441-009-0872-0
7. Cabral WA, Barnes AM, Adeyemo A, et al. A founder mutation in LEPRE1 carried by 1.5% of West Africans and 0.4% of African Americans causes lethal recessive osteogenesis imperfecta. *Genet Med*. 2012;14(5):543–551. doi:10.1038/gim.2011.44
8. Willaert A, Malfait F, Symoens S, et al. Recessive osteogenesis imperfecta caused by LEPRE1 mutations: Clinical documentation and identification of the splice form responsible for prolyl 3-hydroxylation. *J Med Genet*. 2009;46(4):233–241. doi:10.1136/jmg.2008.062729
9. Van Dijk FS, Sillence DO. Osteogenesis imperfecta: Clinical diagnosis, nomenclature and severity assessment. *Am J Med Genet A*. 2014;164A(6):1470–1481. doi:10.1002/ajmg.a.36545
10. Santana A, Franzone JM, McGreal CM, Kruse RW, Bober MB. A moderate form of osteogenesis imperfecta caused by compound heterozygous LEPRE1 mutations. *Bone Reports*. 2018;9:132–135. doi:10.1016/j.bonr.2018.09.002
11. Mrosk J, Bhavani GS, Shah H, et al. Diagnostic strategies and genotype–phenotype correlation in a large Indian cohort of osteogenesis imperfecta. *Bone*. 2018;110:368–377. doi:10.1016/j.bone.2018.02.029
12. Scollo P, Snead MP, Richards AJ, Pollitt R, DeVile C. Bilateral giant retinal tears in osteogenesis imperfecta. *BMC Med Genet*. 2018;19(1):8. doi:10.1186/s12881-018-0521-0
13. de Souza LT, Nunes RR, de Azevedo Magalhães O, Maria Félix T. A new case of osteogenesis imperfecta type VIII and retinal detachment. *Am J Med Genet Part A*. 2021;185(1):238–241. doi:10.1002/ajmg.a.61934
14. Fratzl-Zelman N, Barnes AM, Weis MA, et al. Non-lethal type VIII osteogenesis imperfecta has elevated bone matrix mineralization. *J Clin Endocrinol Metab*. 2016;101(9):3516–3525. doi:10.1210/jc.2016-1334
15. Li S, Cao Y, Wang H, et al. Genotypic and phenotypic analysis in Chinese cohort with autosomal recessive osteogenesis imperfecta. *Front Genet*. 2020;11:984. doi:10.3389/fgene.2020.00984
16. Madhuri V, Selina A, Loganathan L, et al. Osteogenesis imperfecta: Novel genetic variants and clinical observations from a clinical exome study of 54 Indian patients. *Ann Hum Genet*. 2021;85(1):37–46. doi:10.1111/ahg.12403
17. Pepin MG, Schwarze U, Singh V, Romana M, Jones-Lecointe A, Byers PH. Allelic background of LEPRE1 mutations that cause recessive forms of osteogenesis imperfecta in different populations. *Mol Genet Genomic Med*. 2013;1(4):194–205. doi:10.1002/mgg3.21
18. Caudevilla Lafuente P, Izquierdo-Álvarez S, Labarta Aizpún JI. Osteogenesis imperfecta caused by COL1A1, CRTAP and LEPRE1 mutations: Report of 2 cases. *Med Clin (Barc)*. 2019;153(8):336–337. doi:10.1016/j.medcli.2018.08.017
19. Tonelli F, Cotti S, Leoni L, et al. Crtap and p3h1 knock out zebrafish support defective collagen chaperoning as the cause of their osteogenesis imperfecta phenotype. *Matrix Biol*. 2020;90:40–60. doi:10.1016/j.matbio.2020.03.004
20. Cabral WA, Fratzl-Zelman N, Weis M, et al. Substitution of murine type I collagen A1 3-hydroxylation site alters matrix structure but does not recapitulate osteogenesis imperfecta bone dysplasia. *Matrix Biol*. 2020;90:20–39. doi:10.1016/j.matbio.2020.02.003

Characteristics of idiopathic inflammatory myopathies with novel myositis-specific autoantibodies

Anna Rams[1,A–D], Joanna Kosałka-Węgiel[2,B], Piotr Kuszmiersz[2,B], Aleksandra Matyja-Bednarczyk[3,B], Stanisław Polański[3,B], Lech Zaręba[3,C], Stanisława Bazan-Socha[3,A,D–F]

[1] Department of Pulmonology and Allergology, University Hospital, Kraków, Poland
[2] Department of Rheumatology and Immunology, University Hospital, Kraków, Poland
[3] Faculty of Medicine, Jagiellonian University, Medical College, Kraków, Poland

A – research concept and design; B – collection and/or assembly of data; C – data analysis and interpretation; D – writing the article; E – critical revision of the article; F – final approval of the article

Advances in Clinical and Experimental Medicine, ISSN 1899–5276 (print), ISSN 2451–2680 (online) *Adv Clin Exp Med*. 2021;30(12):1239–1248

Address for correspondence
Stanisława Bazan-Socha
E-mail: stanislawa.bazan-socha@uj.edu.pl

Funding sources
Research grant of Jagiellonian University Medical College No. N41/DBS/000687.

Conflict of interest
None declared

Received on May 28, 2021
Reviewed on July 6, 2021
Accepted on August 10, 2021

Published online on October 5, 2021

Abstract

Background. In recent years, many novel myositis-specific autoantibodies (MSAs) have been identified. However, their links with the pathogenesis and clinical manifestations of inflammatory myopathies remain uncertain.

Objectives. To characterize the population of adult dermatomyositis (DM) and polymyositis (PM) patients treated at our center for autoimmune diseases using clinical and laboratory measures.

Materials and methods. According to the Bohan and Peter criteria, we retrospectively analyzed patients who fulfilled diagnostic criteria for DM or PM. Myositis-specific autoantibodies and myositis-associated autoantibodies (MAAs) were identified using immunoblot assays.

Results. Fifty-one PM (71% women) and 36 DM (67% women) Caucasian patients with a median age of 58 (range: 21–88) years who met the definite or probable diagnostic criteria for myositis were included in the study. Myositis-specific autoantibodies were identified in 63 (72%) patients, whereas MAAs were observed in 43 (49%) of them. Interstitial lung disease (ILD) was characteristic of PM patients (67%, χ^2 with Yates's correction (χ_c^2) = 13.8078, df = 1, p = 0.0002), being associated with anti-Jo-1 or anti-PL-12 antibodies (fraction comparison test (FCT) 6.4878, p < 0.0001, 6.8354, p = 0.0003, respectively). Interestingly, among patients with anti-MDA5 antibodies (n = 8, 9.2%), all but one had an amyopathic form, with more frequent ILD, skin changes and arthralgias than observed in other patients (FCT 4.7029, p = 0.0228 and p = 7.7986, p = 0.0357, p = 4.7029 and p = 0.0228, respectively). Anti-signal recognition particle (SRP) was strongly associated with the Raynaud's phenomenon (FCT 4.1144, p = 0.0289) and the highest muscle injury markers (Mann–Whitney U test, z = 2.5293, p = 0.0114). Malignancy was recorded in 14 (16%) patients and was equally common in those with PM and DM. The anti-TIF-1γ was the most frequently related to cancer χ^2 = 14.7691, df = 1, p < 0.0001). The anti-Mi-2α, similarly prevalent in DM and PM, was typically accompanied by skin changes (FCT 7.7986, p = 0.0357) but not ILD (FCT 8.7339, p = 0.0026).

Conclusions. Identification of MSAs might help to predict the clinical course of the autoimmune myopathy and malignancy risk. However, these antibodies were absent in about 30% of patients with typical PM or DM manifestations, which encourages further research in this area.

Keywords: myositis-specific antibodies, polymyositis, dermatomyositis, idiopathic inflammatory myopathies

Cite as
Rams A, Kosałka-Węgiel J, Kuszmiersz P, et al. Characteristics of idiopathic inflammatory myopathies with novel myositis-specific autoantibodies. *Adv Clin Exp Med*. 2021;30(12):1239–1248. doi:10.17219/acem/141181

DOI
10.17219/acem/141181

Background

Dermatomyositis (DM) and polymyositis (PM) belong to the heterogeneous group of rare inflammatory myopathies. The prevalence of these disorders ranges from 5 to 22 per 100,000. Interestingly, in Europe, morbidity significantly increases from the north to the south, likely due to the environmental or genetic factors.[1]

Multiple epidemiological studies have reported an association between inflammatory myopathies and cancer, strongly linked with DM.[2–4] It has been demonstrated that even 1/3 of patients with DM may present malignancy in the 3 years after DM diagnosis. An exact explanation for this relationship remains unknown, although it may be related to altered cellular and humoral immunity.[5,6] Interestingly, the type of associated neoplasm varies between races. In the Asian population, the most frequent is nasopharyngeal and lung cancer, while in Europe and North America, it is ovarian cancer.[7]

Few reports have described the clinical manifestations of inflammatory myopathies over the world. However, the clinical presentation seems to be similar and independent of race. Both diseases are characterized by proximal skeletal muscle weakness and evidence of immune-mediated muscle injury. On the other hand, skin changes are more common in DM and may not be accompanied by laboratory confirmed or clinically diagnosed muscle injury. In turn, interstitial lung disease (ILD), dysphagia and polyarthritis occur with the same frequency in both disorders, together with constitutional symptoms and the Raynaud's phenomenon.[8]

The exact pathogenesis of inflammatory myopathies remains unknown. However, autoantibodies in peripheral blood and T cell muscle infiltrations suggest an autoimmune background with unidentified or heterogenic antigens. It has been postulated that capillary, myofiber and keratinocyte injury in DM might be related to the interferons[9–11] and antigen-antibody complexes.[12,13] On the other hand, common PM findings include the endomysial T cells surrounding and invading myofibers,[14,15] and muscle infiltration of macrophages,[15,16] myeloid dendritic cells[17] and plasma cells.[18]

The PM and DM are diagnosed based on clinical presentations and laboratory findings, including the presence of myositis-specific autoantibodies (MSAs) and myositis-associated autoantibodies (MAAs). Myositis-specific autoantibodies are considered relatively specific for DM/PM, whereas MAAs may also be found in other autoimmune diseases.

The MSA group consists of antibodies directed against aminoacyl-transfer RNA synthetases, such as anti-Jo-1, anti-PL-7, anti-PL-12, anti-OJ, and anti-EJ. The other identified antigens for MSAs include a signal recognition particle (anti-SRP antibody), nuclear helicase Mi-2 (anti-Mi-2 antibody), 155-kD nuclear protein transcriptional intermediary factor 1 gamma (anti-TIF-1γ antibody), RNA helicase encoded by the melanoma differentiation-associated gene 5 (anti-MDA5 antibody), nuclear matrix protein 2 (anti-NXP-2 antibody), and small ubiquitin-like modifier activating enzyme (anti-SAE1 antibody). To date, a few publications have suggested that the type of detected MSA may indicate PM and DM specificity, and thus may help to predict clinical prognosis, including cancer risk.[19–21] However, there is a deficiency of large-scale studies characterizing patients with inflammatory myopathies in the Caucasian population.

Objectives

This study aimed to analyze the population of adult DM and PM patients with particular MSAs and MAAs treated at our large center for autoimmune diseases in southern Poland to determine whether the presence of specific antibodies is associated with certain clinical and laboratory features.

Materials and methods

Study design

A retrospective analysis of clinical and laboratory data was carried out.

Setting

This study was conducted in the Department of Allergy and Clinical Immunology, University Hospital, Kraków, Poland, from October 1, 2014 to September 30, 2019.

Participants

All included patients fulfilled the diagnostic criteria for DM or PM. The diagnosis of myositis was established according to the Bohan and Peter criteria, which include: 1) symmetrical, progressing muscle weakness of the limb-girdle muscles; 2) muscle biopsy evidence of myositis; 3) increased serum levels of muscle-associated enzymes (creatine kinase (CK), aldolase, lactate dehydrogenase (LDH), transaminases); 4) electromyographic features of primary muscle damage; and 5) skin rashes, typical for DM. If the patient fulfilled the first 4 criteria, "definite PM" was diagnosed. If they met 3 of the first 4 criteria then "probable PM" was diagnosed, while in the case of 2, "possible PM" was established. On the other hand, "definite DM" was diagnosed if the patient had a rash and 3 of the elective criteria listed above, "probable DM" was diagnosed in those with a rash and 2 elective criteria, and "possible DM" was established when rash and any myositis criterion were observed. Only those who met "definite" or "probable" myositis criteria were included in the study.

Variables

The complete medical history of patients, results of laboratory tests, spirometry and echocardiographic investigations, and high resolution computed tomography (HRCT) of the chest scans were recorded. Potential confounders such as obesity, smoking, hypertension, hypercholesterolemia, diabetes mellitus, heart failure, coronary artery disease, kidney disease, liver failure and other autoimmune diseases were taken into account in the statistical analysis.

Data sources/measurement

Antinuclear antibodies (ANAs) were detected with an indirect immunofluorescence assay using Hep-2 cell lines. The MSAs and MAAs were identified with immunoblotting (Euroline, Lübeck, Germany). The MSAs analyzed included anti-Jo-1, anti-PL-7, anti-PL-12, anti-EJ, anti-OJ, anti-SRP, anti-Mi-2α, anti-Mi-2β, anti-TIF-1γ, anti-MDA5, anti-NXP-2, and anti-SAE1. The MAAs were also identified, including anti-PM-Scl 75, anti-PM-Scl 100, anti-Ku, anti-SSB/La, anti-SSA/Ro, and anti-Ro-52 kDa.

Interstitial lung disease was diagnosed by a radiologist based on interstitial lung infiltration (ground glass and reticular opacities, or honeycombing) demonstrated on HRCT scans. Constitutional symptoms included fever, weight loss and fatigue. The high probability of pulmonary hypertension (PH) was assessed based on echocardiography when pulmonary artery systolic pressure was above 45 mm Hg. This approach has a 95% specificity compared to right heart catheterization, which is considered the gold standard for PH diagnosis.

Quantitative variables

Laboratory features of muscle injury were defined as creatine kinase, myoglobin high-sensitive (hs) I troponin levels above the upper limit of the normal range (>180 U/L, ≥110 μg/L and ≥47.3 μg/L, respectively). An ANA titer higher than 1:160 was considered positive.

Bias

Two researchers checked the accuracy and relevance of the database.

Study size

In order to obtain the appropriate number of patients with rare diseases such as DM and PM treated at 1 center, the enrollment of patients into the study lasted for 5 years.

Statistical methods

Statistical analyses were performed using STATISTICA Tibco v. 13.3 software (StatSoft, Tulsa, USA). The Shapiro–Wilk test was used to evaluate the data distribution. According to the data distribution, continuous variables are shown as the mean and standard deviation (SD) or median and interquartile range (IQR), as appropriate. Categorical variables are given as numbers and percentages. In comparison to other MSA types, patient subsets were compared using the χ^2 test with the Yates's correction. The Mann–Whitney U test and the fraction comparison test (FCT; i.e., standard z-test comparing proportions or its equivalent) were also applied depending on the number of elements. The considered proportions were obtained from conditional probability distributions. A value of $p < 0.05$ was considered statistically significant.

Results

A total of 87 patients were identified, with 51 (58.6%) meeting the PM criteria and 36 (41.4%) meeting the DM criteria. All patients were of the white Caucasian race. The demographic, clinical and laboratory characteristics of these patients are provided in Table 1. Women (n = 60) constituted a group more than twice as large as men (n = 27). The median age of the analyzed individuals was 58 (range: 21–88) years, while the median disease duration since the onset was 3.5 (range: 0.7–8) years. Statistical analysis did not confirm the influence of potential confounders such as obesity, smoking, hypertension, hypercholesterolemia, diabetes, heart failure, coronary artery disease, kidney disease, liver failure and other autoimmune diseases on the observed relationships.

As expected, ILD was significantly more common in patients with PM (n = 34, 66.7% of PM patients) than DM (n = 9, 25% of DM patients, $\chi_c^2 = 13.8078$, df = 1, p = 0.0002). Cancer was diagnosed in 14 (16%) subjects with 7 cases in each subgroup. The majority of patients were treated with corticosteroids (n = 83, 95.4%). Thirty (34.4%) individuals also received methotrexate, 29 (33.3%) azathioprine, while mycophenolate mofetil was used by 13 (14.9%) subjects. Patients with a more severe disease received cyclophosphamide and/or rituximab (n = 32 (36.8%) and n = 8 (9.2%) for PM and DM, respectively).

Immunological characteristics of PM and DM patients

Detectable ANAs were reported in 73 (83.9%) patients, MSAs in 63 (72.4%) and MAAs in 43 (49.4%) of them. The most frequent was anti-Ro-52 (n = 32, 36.8%) followed by anti-Jo-1 (n = 17, 19.5%), and both of these antibodies often coexisted ($\chi_c^2 = 5.0633$, df = 1, p = 0.0244). Figure 1 depicts the MSA frequency in the cohort.

Associations of MSAs with clinical and laboratory presentations

Table 2 presents the leading associations between MSAs and clinical symptoms, as well as imaging and laboratory investigations. These associations are also briefly described in the following paragraphs.

Table 1. Clinical characteristics of subjects studied

Variable	Polymyositis (PM) n = 51	Dermatomyositis (DM) n = 36	PM compared to DM p-value
Age, mean (range) [years]	59 (30–88)	59 (21–79)	Mann–Whitney U test, z = 0.4047 p = 0.9624
Females, n (%)	36 (71)	24 (67)	χ_c^2 = 0.0238, df = 1 p = 0.8775
Constitutional symptoms, n (%)	20 (39)	12 (33)	χ_c^2 = 0.0565, df = 1 p = 0.8122
Elevated muscle injury markers, n (%)	36 (71)	24 (67)	χ_c^2 = 0.0328, df = 1 p = 0.8564
Shoulder/pelvic girdle weakness, n (%)	36 (71)	30 (83)	χ_c^2 = 1.2407, df = 1 p = 0.2653
Interstitial lung disease, n (%)	34 (67)	9 (25)	χ_c^2 = 13.8078, df = 1 p = 0.0002
Pulmonary artery systolic pressure >45 mm Hg, n (%)	6 (12)	2 (6)	χ_c^2 = 0.0620, df = 1 p = 0.8033
Pulmonary artery systolic pressure 31–45 mm Hg, n (%)	22 (43)	8 (22)	χ_c^2 = 0.5313, df = 1 p = 0.4661
Cutaneous involvement, n (%)	14 (27)	34 (94)	χ_c^2 = 38.0997, df = 1 p = 0.0000
Mechanic's hands, n (%)	10 (20)	5 (14)	χ_c^2 = 0.1223, df = 1 p = 0.7265
Gottron's sign, n (%)	1 (2)	9 (25)	χ_c^2 = 9.2023, df = 1 p = 0.0024
Heliotrope rash, n (%)	4 (8)	19 (53)	χ_c^2 = 20.5417, df = 1 p < 0.0001
Shawl sign, n (%)	1 (2)	11 (31)	χ_c^2 = 12.6573, df = 1 p = 0.0004
Thigh rash, n (%)	0 (0)	4 (11)	χ_c^2 = 3.8075, df = 1 p = 0.0510
Raynaud's phenomenon, n (%)	14 (27)	4 (11)	χ_c^2 = 2.3243, df = 1 p = 0.1274
Heart involvement, n (%)	2 (4)	2 (6)	χ_c^2 = 0.0244, df = 1 p = 0.8758
Dysphagia, n (%)	3 (6)	8 (22)	χ_c^2 = 3.8043, df = 1 p = 0.0511
Malignancy, n (%)	7 (14)	7 (19)	χ_c^2 = 1.2350, df = 1 p = 0.539
Treatment used			
Glucocorticoids, n (%)	47 (92)	36 (100)	χ_c^2 = 1.4416, df = 1 p = 0.2299
Cyclophosphamide, n (%)	22 (43)	10 (28)	χ_c^2 = 1.5315, df = 1 p = 0.2159
Azathioprine, n (%)	18 (35)	11 (31)	χ_c^2 = 0.0533, df = 1 p = 0.8174
Methotrexate, n (%)	14 (27)	16 (44)	χ_c^2 = 1.9977, df = 1 p = 0.1575
Mycophenolate mofetil, n (%)	8 (16)	5 (14)	χ_c^2 = 0.0054, df = 1 p = 0.941
Rituximab, n (%)	7 (14)	1 (3)	χ_c^2 = 1.8599, df = 1 p = 0.1726

df – degrees of freedom; χ_c^2 – χ^2 with Yates's correction.

Anti-Jo-1 antibody

Anti-Jo-1 antibodies were detected in 17 (19.5%) patients, 76.5% of whom were female. As expected, these antibodies were detected more frequently in PM than in DM cases (15 compared to 2 cases, χ_c^2 = 6.8971, df = 1, p = 0.0086). All but 1 had radiological signs of ILD (FCT 6.4878, p < 0.0001). These patients were also characterized

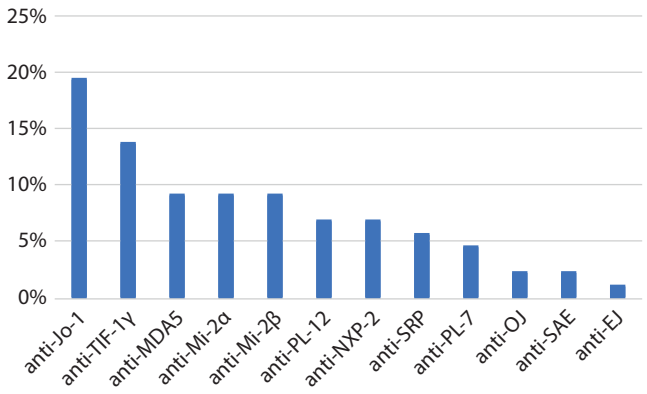

Fig. 1. Prevalence of specific autoantibodies in idiopathic inflammatory myopathies

by severe constitutional symptoms, including fever and weight loss reported in 9 (53%) anti-Jo-1-positive patients, and arthralgia or arthritis documented in 12 (71%) of them. Six (35%) individuals in this group had mechanic's hands as a unique skin manifestation of the disease. Laboratory features of muscle injury were recorded in 11 (65%) of anti-Jo-1-positive patients, while proximal muscle weakness was observed in 15 (88%) of them.

Anti-PL-12 antibody

Six patients (6.9% of all individuals) had circulating anti-PL-12 antibodies. Five of these patients were diagnosed with PM and 1 with DM. All had ILD (FCT 6.8354, p = 0.0003) and 5 (83% of anti-PL-12-positive patients) had severe constitutional symptoms, including recurrent fever (FCT 7.8243, p = 0.0105). Three (50%) patients in this group complained of arthralgia and arthritis, and the same number had laboratory features of muscle injury.

Anti-PL-7 antibody

Anti-PL-7 antibodies were detected in 4 cases (4.6% of all patients), of which 50% were female. Three of these patients were diagnosed with PM, and 1 had systemic lupus erythematosus (SLE)/myositis overlap syndrome. All but 1 had ILD and 1 had pericarditis. Only 1 patient presented laboratory features of muscle injury.

Anti-OJ and anti-EJ antibodies

Anti-OJ antibodies were reported in 2 female patients (2.3% of all patients). In 1 subject, these antibodies coexisted with anti-Jo-1 and were associated with a very severe PM manifestation. The 2nd anti-OJ patient had an amyopathic form of PM. Both patients had ILD and a heliotrope rash. An amyopathic form of PM with ILD and arthritis also characterized the only individual with anti-EJ antibodies.

Anti-TIF-1γ antibody

Twelve patients (13.8%, 9 DM, 2 PM and 1 SLE/myositis overlap syndrome) were positive for anti-TIF-1γ antibodies. The majority of these patients reported proximal muscle weakness and all but 2 had elevated markers of muscle injury. In this subgroup, skin changes were also common, predominantly shawl sign and/or a heliotrope rash (n = 9, 75%, FCT 6.1568, p = 0.007). On the other hand, ILD and joint involvement were rare (i.e., in 1 (8%) and 4 (33%) of anti-TIF-1γ-positive patients, respectively). Interestingly, more than half of these subjects were diagnosed with malignancy (χ_c^2 = 19.3782, df = 1, p < 0.0001).

Anti-MDA5 antibody

Five DM and 3 PM patients (9.2%) had anti-MDA5 antibodies. Interestingly, all of them complained of severe proximal muscle weakness, although all but 1 had an amyopathic form of the disease (χ_c^2 = 10.7787, df = 1, p = 0.001). The only individual who exhibited laboratory features of muscle injury was characterized by a coexistence of anti-TIF-1γ and various MAAs, such as anti-Ku and anti-PM-Scl 100. Interstitial lung disease was detected in 3/4 of these patients, similar to joint involvement (FCT 6.5504, p = 0.0228). Half of these patients complained of severe constitutional symptoms, whereas skin involvement, such as Gottron's and shawl signs, and heliotrope rash was demonstrated in 5 of anti-MDA5-positive patients (62.5%, FCT 7.798, p = 0.0357). Three (37.5%) patients in this group died during the follow-up due to severe ILD, lymphoma and cancer.

Anti-Mi-2α and anti-Mi-2β antibodies

Eight patients (18.4% of all individuals) had anti-Mi-2α and anti-Mi-2β antibodies each. These patients were alike in PM and DM. All of them reported proximal muscle weakness and all but 2 (88%) had laboratory signs of muscle injury. Interstitial lung disease was reported only in 1 (12.5%) of anti-Mi-2α and in 2 (25%) of anti-Mi-2β-positive patients (FCT 6.1456, p = 0.0026, 3.3763, p = 0.0392, respectively; Table 2). Skin lesions occurred in 5 (62.5%) anti-Mi-2α and 4 (50%) of anti-Mi-2β-positive subjects. One woman with anti-Mi-2α antibodies accompanied by Ro-52 had heart involvement in the form of heart failure with preserved ejection fraction.

Anti-NXP-2 antibody

Anti-NXP-2 antibodies were observed in 6 patients (6.9%; 4 DM and 2 PM). All complained of proximal muscle weakness and half of them had general muscle weakness. In 1 case, heart involvement was recorded, in 2 dysphagia (33%) and 3 (50%) of anti-NXP-2-positive subjects had typical DM skin changes.

Table 2. Clinical features of patients with myositis-specific antibodies

Number of patients (n)	Anti-Jo-1 n = 17 n (%)	Anti-PL-12 n = 6 n (%)	Anti-PL-7 n = 4 n (%)	Anti-OJ n = 2 n (%)	Anti-SRP n = 5 n (%)	Anti-Mi-2α n = 8 n (%)	Anti-Mi-2β n = 8 n (%)	Anti-TIF-1γ n = 12 n (%)	Anti-MDA5 n = 8 n (%)	Anti-NXP-2 n = 6 n (%)	Anti-SAE n = 2 n (%)
Interstitial lung disease	16 (94)	6 (100)	3 (75)	2 (100)	3 (60)	1 (13)	2 (25)	1 (8)	6 (75)	1 (17)	0 (0)
Pulmonary artery systolic pressure >45 mm Hg	2 (12)	0 (0)	1 (25)	0 (0)	1 (20)	1 (13)	0 (0)	1 (8)	1 (13)	0 (0)	0 (0)
Pulmonary artery systolic pressure 31–45 mm Hg	5 (29)	2 (33)	2 (50)	1 (50)	2 (40)	0 (0)	5 (63)	3 (25)	4 (50)	3 (50)	0 (0)
Arthritis/arthralgia	12 (71)	3 (50)	2 (50)	0 (0)	1 (20)	3 (38)	3 (38)	4 (33)	6 (75)	1 (17)	2 (100)
Elevated muscle injury markers	11 (65)	2 (33)	1 (25)	1 (50)	4 (80)	7 (88)	7 (88)	10 (83)	1 (13)	5 (83)	2 (100)
Shoulder/pelvic girdle	15 (88)	4 (67)	3 (75)	1 (50)	4 (80)	8 (100)	8 (100)	11 (92)	8 (100)	6 (100)	2 (100)
Dysphagia	2 (12)	0 (0)	0 (0)	0 (0)	1 (20)	1 (13)	1 (13)	1 (8)	2 (25)	2 (33)	0 (0)
Heart involvement	0 (0)	0 (0)	1 (25)	0 (0)	0 (0)	1 (13)	0 (0)	0 (0)	0 (0)	1 (17)	0 (0)
Skin lesions	7 (41)	1 (17)	1 (25)	2 (100)	2 (40)	5 (63)	4 (50)	9 (75)	5 (63)	3 (50)	0 (0)
Gottron's sign	1 (6)	0 (0)	0 (0)	1 (50)	1 (20)	1 (13)	1 (13)	2 (17)	2 (25)	1 (17)	0 (0)
Heliotrope rash	1 (6)	1 (17)	0 (0)	2 (100)	0 (0)	4 (50)	2 (25)	4 (33)	5 (63)	1 (17)	0 (0)
Shawl sign	0 (0)	0 (0)	0 (0)	0 (0)	1 (20)	1 (13)	0 (0)	5 (42)	2 (25)	1 (17)	0 (0)
Thigh rash	0 (0)	0 (0)	0 (0)	0 (0)	1 (20)	1 (13)	0 (0)	3 (25)	0 (0)	0 (0)	0 (0)
Mechanic's hands	6 (35)	1 (17)	1 (25)	1 (50)	1 (20)	2 (25)	1 (13)	1 (8)	0 (0)	0 (0)	0 (0)
Raynaud's phenomenon	2 (12)	3 (50)	0 (0)	0 (0)	4 (80)	2 (25)	2 (25)	1 (8)	1 (13)	1 (17)	0 (0)
Constitutional symptoms	9 (53)	5 (83)	0 (0)	1 (50)	0 (0)	1 (13)	4 (50)	3 (25)	4 (50)	1 (17)	0 (0)
Malignancy	2 (12)	1 (17)	1 (25)	0 (0)	1 (20)	0 (0)	1 (13)	7 (58)	2 (25)	1 (17)	0 (0)

Anti-SRP antibody

Five females (5.7% of all patients) were anti-SRP-positive. Four of these patients were diagnosed with PM and 1 with DM. One patient was characterized by the coexistence of other antibodies and had clinical signs of systemic sclerosis, rheumatoid arthritis, antiphospholipid syndrome, and PM.

Interstitial lung disease was present in 3 (60%) of anti-SRP-positive patients and Raynaud's phenomenon in 4 of them (80%, FCT 4.1144, p = 0.0289). Furthermore, all but 1 complained of severe proximal muscle weakness and had the highest muscle injury markers among all PM patients (Mann–Whitney U test, z = 2.5293, p = 0.0114). Interestingly, in our data, the anti-SRP antibody was also recorded in non-myositis patients, such as in muscular dystrophy, undifferentiated connective tissue disease and cold agglutinin disease.

Anti-SAE antibody

Anti-SAE was reported in only 2 (2.3%) subjects (both PM) who were characterized by arthritis/arthralgia and proximal muscle weakness with elevated creatine kinase levels. No ILD or skin lesions were observed.

Coexistence of MSAs and MAAs

Myositis-specific autoantibodies coexisted with MAAs in 35.6% of cases. The most common coexisting antibody was anti-Ro-52, which was detected, for example, in 11 patients with anti-Jo-1 antibodies (64.7% of all anti-Jo-1-positive patients, $\chi_c^2 = 5.0633$, df = 1, p = 0.0244) and in 3 patients with anti-PL-7 antibodies. Anti-Ro-52 also accompanied anti-SRP in 3 PM patients who, interestingly, all had ILD. A 55-year-old woman had anti-Jo-1, anti-PL-7, anti-MDA5, anti-NXP-2, and anti-TIF-1γ antibodies. In this patient, we also identified anti-dsDNA, anti-SSA, anti-SSB, anti-centromere B, anti-nucleosomes, anti-histones, and anti-Ro52 antibodies, with a very high ANA titer (higher than 1:20,480). This patient was diagnosed with SLE/myositis overlap syndrome with no laboratory signs of muscle injury but proximal muscle weakness, ILD and arthritis. Furthermore, 1 interesting case was observed with coexisting anti-Jo-1 and anti-OJ related to severe PM with ILD, rhabdomyolysis, mechanic's hands, Gottron's sign, and heliotrope rash. To our knowledge, this case with the coexistence of those antibodies is only the 2nd one described in the literature. In both cases, ILD was the prominent manifestation.[22]

In 1 typical DM patient, anti-SRP coexisted with anti-Mi-2α antibodies, whereas in 1 PM case, anti-SRP was accompanied by anti-NXP-2. The latter is the 1st such case described in the literature with severe muscle injury and

dysphagia. Interestingly, this female patient was also diagnosed with papillary thyroid cancer and endometrial adenocarcinoma 13 and 5 years before autoimmune disease onset, respectively.

Among the 12 anti-TIF-1γ-positive patients, 3 also had anti-MDA5 antibodies. One of these patients fulfilled the criteria for DM and the other one for PM. Interestingly, both had a neoplastic disease in anamnesis. The 3rd patient had SLE/myositis overlap syndrome without malignancy.

Myositis-specific autoantibodies and myositis-associated autoantibodies-negative patients

Nine patients (5 DM and 4 PM, 10.3% of all patients) had no detectable MSAs or MAAs. Neoplasm and ILD were found in 1 (11%) of these patients, whereas skin changes and arthralgia were observed in 7 (77.8%) of these cases (FCT 5.4177, p = 0.0091, both).

Myositis-specific autoantibodies and their associations with malignancy

As expected, neoplastic diseases were frequent in this cohort. Fourteen (16% of all patients) cancer or lymphoma cases were documented, equally common in DM and PM. In half of the cases, the neoplasm was diagnosed before myositis. Malignancy was strongly associated with anti-TIF-1γ antibodies (χ_c^2 = 19.3782, df = 1, p < 0.0001). Neoplasms occurred in 7 (58.3%) of anti-TIF-1γ-positive patients, 6 (85.7%) of them were diagnosed with DM and 1 with PM.

Two of these patients had lung cancer and the others presented with urethral, endometrial and renal cell carcinoma, diffuse large B-cell lymphoma, or carcinoma of unknown primary. Two of the anti-TIF-1γ-positive malignancy patients had coexisting anti-MDA5 antibodies. Bladder cancer and cervical cancer in patients with anti-Jo-1 antibodies were also observed, and ovarian cancer and prostate cancer in those with anti-PL-7 and anti-PL-12 coexisting with anti-Mi-2β antibodies were documented. No tumors were recorded in anti-Mi-2α-positive patients.

Discussion

In this study, we characterized 87 adult Caucasian patients with autoimmune inflammatory myopathies using clinical and laboratory measures. The majority of these patients presented with MSAs or MAAs, indicating that both of these antibody groups are valuable biomarkers for determining disease course and malignancy risk. However, the presence or absence of these antibodies cannot be used to differentiate DM from PM. Furthermore, a specific MSA may accompany other MSAs or MAAs and be associated with different clinical presentations, such as those seen in SLE or systemic scleroderma in the current data. Some of these antibodies may also be seen in other immune or nonimmune disorders. For example, an anti-SRP antibody has been documented in association with muscular dystrophy or cold agglutinin disease at our center.

The role of MSAs in the pathogenesis of inflammatory myopathies is not entirely understood. These antibodies likely sustain inflammatory processes, although their pathological links with muscle injury remain unknown.[23] The anti-Jo-1 antibody is the most common MSA, as confirmed by the current data.[8] However, this antibody was detected in only 19.5% of patients, thus indicating the immunologic heterogeneity of autoimmune myopathies. Typically, this type of antibody is linked with the presence of ILD, the Raynaud's phenomenon, arthritis, and mechanic's hands,[24,25] findings confirmed by the present study. Furthermore, similar to our data, anti-Jo-1 often accompanies anti-Ro-52 antibodies. According to the literature, such a coincidence may be a risk factor for a more severe disease course and cancer.[26,27] Interestingly, 1 of our 2 anti-Jo-1-positive cancer patients had coexisting anti-Ro-52, and in both cases anti-PM-Scl-75 was also detected.

Anti-Jo-1, anti-PL-12, anti-PL-7, anti-EJ, and anti-OJ antibodies are associated with the common anti-synthetase syndrome. However, several recent studies have suggested a clinical heterogeneity, particularly regarding ILD or muscle injury signs.[28] Some authors documented that antibodies other than anti-Jo-1 may be related to a poorer clinical prognosis and more aggressive ILD.[29,30] On the other hand, Hamaguchi et al. reported that muscle injury was closely associated with anti-Jo-1, anti-EJ and anti-PL-7 antibodies.[31] At the same time, ILD might have been observed in all of these patients, while skin changes, such as heliotrope rash and Gottron's sign, were less common but also frequent.[31] The anti-OJ has also been shown to be associated with ILD, often being the sole manifestation of idiopathic inflammatory myopathy. However, if recorded, myositis seems to be more severe than with other anti-synthetase antibodies.[25,32] The anti-PL-12 antibodies were also documented in linkage with ILD and, to a lesser extent, with muscle injury and arthritis.[28,33–35] In turn, pericardial effusion may be a characteristic of anti-PL-7-positive patients.[25] Our data are in line with the presented reports, indicating that all anti-synthetase antibodies have a strong relationship with ILD and PM, but not with the typical DM skin changes. Also, 1 patient with heart involvement in the current cohort had an anti-PL-7 antibody.

The another interesting antibody that relates to PM and DM is anti-SRP. Targoff et al. reported a classical PM manifestation with a low prevalence of ILD, arthritis and Raynaud's phenomenon in these subjects.[36] However, some of these cases were severe and/or rapid in onset.[28,36] The current results do not entirely confirm these findings. Although most of anti-SRP-positive patients in this study complained of proximal muscle weakness and had

very high creatine kinase, more than half of them had ILD or Raynaud's phenomenon. Recent studies have reported a histologically unique necrotizing myopathy, which might explain the particularly high levels of muscle injury biomarkers in anti-SRP-positive patients.[37–39]

In contrast to anti-SRP antibodies, anti-MDA5 is likely related to the amyopathic PM/DM form but with rapidly progressive ILD, acute respiratory failure and poor clinical prognosis.[40,41] Indeed, most of our anti-MDA5 patients had aggressive ILD leading to rapid and severe lung fibrosis, and even to a related death in 1 case.

In the literature, anti-Mi-2 and anti-NXP-2 antibodies have mainly been associated with DM.[42,43] Anti-Mi-2 was shown to be associated with Gottron's sign or papules, and heliotrope rash, lung-sparing and an excellent clinical response to corticosteroids.[43] Surprisingly, in the current study, the PM and DM distribution among anti-Mi-2-positive patients was almost equal. However, ILD was rare.

Anti-NXP-2 autoantibodies are associated with a young-onset DM with subcutaneous edema, skin calcinosis and severe muscle involvement with dysphagia.[42,44,45] Moreover, these antibodies may be linked with malignancy.[46,47] Our data partially mirror these reports, including the typical skin changes reported in half of the current patients.

One of the rarest antibody types in the current cohort was anti-SAE1, identified in only 2 individuals. Previous reports demonstrated that these patients may have severe skin changes, mild muscle involvement and ILD.[48,49] Surprisingly, our anti-SAE-1 subjects had no skin lesions or ILD, but proximal muscle weakness, laboratory signs of muscle injury and arthritis. This observation points to the heterogeneity of autoimmune myopathies and the need for further research on this subject.

The last issue that merits comment is the relation of PM, DM, and MSAs to malignancy. Surprisingly, in the current data, a strong association was demonstrated only with anti-TIF-1γ, which is in line with the data in the literature.[28,50,51] In this subgroup of patients, 58% had documented malignancy. Moreover, patients with anti-TIF-1γ antibodies had a lower prevalence of fever, Raynaud's phenomenon, arthritis, ILD, and mechanic's hands. At the same time, these patients have more frequent DM-typical skin changes, particularly shawl sign rash.[28,52] The current study confirms these observations. The presence of anti-TIF-1γ antibodies was highly associated with malignancy, while typical skin rash was reported in 3/4 of these patients. Only 1 patient had ILD, while joint involvement was demonstrated in 1/3 of them.

Among patients with no detectable MSAs or MAAs, ILD was rarely observed, in contrast to skin changes and arthralgia. One patient in this group was diagnosed with cancer. There are limited data on the clinical course of these patients in the available literature.

Limitations

The current study has several limitations. First, it was retrospective in nature. In addition, the number of subjects studied was relatively small, especially with regard to some MSA types, such as anti-OJ, anti-EJ and anti-SAE antibodies. Therefore, future multicenter studies characterizing patients with DM and PM are needed.

Conclusions

The MSA type cannot differentiate DM from PM, although some antibodies may be more prevalent in PM (e.g., anti-Jo1) and others in DM (e.g., anti-TIF-1γ). Interstitial lung disease was common in patients with anti-synthetase antibodies, particularly anti-Jo-1 and anti-PL-12, but also in those with anti-MDA5 antibodies. The majority of ILD patients fulfilled PM criteria. Patients with anti-SRP were characterized by the presence of the Raynaud's phenomenon and the highest serum concentration of muscle injury markers. In turn, an amyopathic form characterized anti-MDA5-positive individuals. Malignancy was highly associated with anti-TIF-1γ antibodies, but also with anti-Jo-1, anti-PL-7, anti-PL-12, anti-SRP, anti-MDA-5, anti-NXP-2, and anti-Mi-2β antibodies.

ORCID iDs

Anna Rams https://orcid.org/0000-0001-7590-7318
Joanna Kosałka-Węgiel https://orcid.org/0000-0003-1013-2253
Piotr Kuszmiersz https://orcid.org/0000-0002-2031-6657
Aleksandra Matyja-Bednarczyk https://orcid.org/0000-0003-4038-5016
Stanisław Polański https://orcid.org/0000-0002-4638-3823
Lech Zaręba https://orcid.org/0000-0002-2221-614X
Stanisława Bazan-Socha https://orcid.org/0000-0001-9634-0963

References

1. Cheeti A, Brent LH, Panginikkod S. Autoimmune myopathies. In: StatPearls [Internet]. Treasure Island: StatPearls Publishing; 2021. PMID:30422455
2. Ungprasert P, Bethina NK, Jones CH. Malignancy and idiopathic inflammatory myopathies. *N Am J Med Sci*. 2013;5(10):569–572. doi:10.4103/1947-2714.120788
3. Fayyaz B, Rehman HJ, Uqdah H. Cancer-associated myositis: An elusive entity. *J Community Hosp Intern Med Perspect*. 2019;9(1):45–49. doi:10.1080/20009666.2019.1571880
4. Tiniakou E, Mammen AL. Idiopathic Inflammatory myopathies and malignancy: A comprehensive review. *Clin Rev Allergy Immunol*. 2017;52(1):20–33. doi:10.1007/s12016-015-8511-x
5. Casciola-Rosen L, Nagaraju K, Plotz P, et al. Enhanced autoantigen expression in regenerating muscle cells in idiopathic inflammatory myopathy. *J Exp Med*. 2005;201(4):591–601. doi:10.1084/jem.20041367
6. Jakubaszek M, Kwiatkowska B, Maślińska M. Polymyositis and dermatomyositis as a risk of developing cancer. *Reumatologia*. 2015;53(2):101–105. doi:10.5114/reum.2015.51510
7. Ungprasert P, Leeaphorn N, Hosiriluck N, Chaiwatcharayut W, Ammannagari N, Raddatz DA. Clinical features of inflammatory myopathies and their association with malignancy: A systematic review in Asian population. *ISRN Rheumatol*. 2013;2013:509354. doi:10.1155/2013/509354
8. Miller M, Vleugels R, Amato AA. Clinical manifestations of dermatomyositis and polymyositis in adults. https://www.uptodate.com/contents/clinical-manifestations-of-dermatomyositis-and-polymyositis-in-adults. Accessed March 17, 2020.

9. Greenberg SA. Type 1 interferons and myositis. *Arthritis Res Ther*. 2010;12(Suppl 1):S4. doi:10.1186/ar2885
10. Greenberg SA. Proposed immunologic models of the inflammatory myopathies and potential therapeutic implications. *Neurology*. 2007;69(21):2008–2019. doi:10.1212/01.WNL.0000291619.17160.b8
11. Greenberg SA. Dermatomyositis and type 1 interferons. *Curr Rheumatol Rep*. 2010;12(3):198–203. doi:10.1007/s11926-010-0101-6
12. Dalakas MC. Inflammatory disorders of muscle: Progress in polymyositis, dermatomyositis and inclusion body myositis. *Curr Opin Neurol*. 2004;17(5):561–567. doi:10.1097/00019052-200410000-00006
13. Dalakas MC, Hohlfeld R. Polymyositis and dermatomyositis. *Lancet*. 2003;362(9388):971–982. doi:10.1016/S0140-6736(03)14368-1
14. Arahata K, Engel AG. Monoclonal antibody analysis of mononuclear cells in myopathies. IV: Cell-mediated cytotoxicity and muscle fiber necrosis. *Ann Neurol*. 1988;23(2):168–173. doi:10.1002/ana.410230210
15. Engel AG, Arahata K. Monoclonal antibody analysis of mononuclear cells in myopathies. II: Phenotypes of autoinvasive cells in polymyositis and inclusion body myositis. *Ann Neurol*. 1984;16(2):209–215. doi:10.1002/ana.410160207
16. Arahata K, Engel AG. Monoclonal antibody analysis of mononuclear cells in myopathies. I: Quantitation of subsets according to diagnosis and sites of accumulation and demonstration and counts of muscle fibers invaded by T cells. *Ann Neurol*. 1984;16(2):193–208. doi:10.1002/ana.410160206
17. Greenberg SA, Pinkus GS, Amato AA, Pinkus JL. Myeloid dendritic cells in inclusion-body myositis and polymyositis. *Muscle Nerve*. 2007;35(1):17–23. doi:10.1002/mus.20649
18. Greenberg SA, Bradshaw EM, Pinkus JL, et al. Plasma cells in muscle in inclusion body myositis and polymyositis. *Neurology*. 2005;65(11):1782–1787. doi:10.1212/01.wnl.0000187124.92826.20
19. Hirakata M. Autoantibodies and their clinical significance in idiopathic inflammatory myopathies: Polymyositis/dermatomyositis and related conditions. *Japanese J Clin Immunol*. 2007;30(6):444–454. doi:10.2177/jsci.30.444
20. Yang H, Peng Q, Yin L, et al. Identification of multiple cancer-associated myositis-specific autoantibodies in idiopathic inflammatory myopathies: A large longitudinal cohort study. *Arthritis Res Ther*. 2017;19(1):259. doi:10.1186/s13075-017-1469-8
21. Ceribelli A, Isailovic N, De Santis M, et al. Myositis-specific autoantibodies and their association with malignancy in Italian patients with polymyositis and dermatomyositis. *Clin Rheumatol*. 2017;36(2):469–475. doi:10.1007/s10067-016-3453-0
22. Gelpí C, Kanterewicz E, Gratacos J, Targoff IN, Rodriguez-Sanchez JL. Coexistence of two antisynthetases in a patient with the antisynthetase syndrome. *Arthritis Rheum*. 1996;39(4):692–697. doi:10.1002/art.1780390424
23. Miller FW, Waite KA, Biswas T, Plotz PH. The role of an autoantigen, histidyl-tRNA synthetase, in the induction and maintenance of autoimmunity. *Proc Natl Acad Sci U S A*. 1990;87(24):9933–9937. doi:10.1073/pnas.87.24.9933
24. Love LA, Leff RL, Fraser DD, et al. A new approach to the classification of idiopathic inflammatory myopathy: Myositis-specific autoantibodies define useful homogeneous patient groups. *Medicine (Baltimore)*. 1991;70(6):360–374. doi:10.1097/00005792-199111000-00002
25. Labirua-Iturburu A, Selva-O'Callaghan A, Vincze M, et al. Anti-PL-7 (anti-threonyl-tRNA synthetase) antisynthetase syndrome: Clinical manifestations in a series of patients from a European multicenter study (EUMYONET) and review of the literature. *Medicine (Baltimore)*. 2012;91(4):206–211. doi:10.1097/MD.0b013e318260977c
26. La Corte R, Lo Mo Naco A, Locaputo A, Dolzani F, Trotta F. In patients with antisynthetase syndrome the occurrence of anti-Ro/SSA antibodies causes a more severe interstitial lung disease. *Autoimmunity*. 2006;39(3):249–253. doi:10.1080/08916930600623791
27. Marie I, Hatron PY, Dominique S, et al. Short-term and long-term outcome of anti-Jo1-positive patients with anti-Ro52 antibody. *Semin Arthritis Rheum*. 2012;41(6):890–899. doi:10.1016/j.semarthrit.2011.09.008
28. Satoh M, Tanaka S, Ceribelli A, Calise SJ, Chan EKL. A comprehensive overview on myositis-specific antibodies: New and old biomarkers in idiopathic inflammatory myopathy. *Clin Rev Allergy Immunol*. 2017;52(1):1–19. doi:10.1007/s12016-015-8510-y
29. Pinal-Fernandez I, Casal-Dominguez M, Huapaya JA, et al. A longitudinal cohort study of the anti-synthetase syndrome: Increased severity of interstitial lung disease in black patients and patients with anti-PL7 and anti-PL12 autoantibodies. *Rheumatology (Oxford)*. 2017;56(6):999–1007. doi:10.1093/rheumatology/kex021
30. Mejía M, Herrera-Bringas D, Pérez-Román DI, et al. Interstitial lung disease and myositis-specific and associated autoantibodies: Clinical manifestations, survival and the performance of the new ATS/ERS criteria for interstitial pneumonia with autoimmune features (IPAF). *Respir Med*. 2017;123:79–86. doi:10.1016/j.rmed.2016.12.014
31. Hamaguchi Y, Fujimoto M, Matsushita T, et al. Common and distinct clinical features in adult patients with anti-aminoacyl-tRNA synthetase antibodies: Heterogeneity within the syndrome. *PLoS One*. 2013;8(4):e60442. doi:10.1371/journal.pone.0060442
32. Vulsteke JB, Satoh M, Malyavantham K, Bossuyt X, De Langhe E, Mahler M. Anti-OJ autoantibodies: Rare or underdetected? *Autoimmun Rev*. 2019;18(7):658–664. doi:10.1016/j.autrev.2019.05.002
33. Targoff IN, Arnett FC. Clinical manifestations in patients with antibody to PL-12 antigen (alanyl-tRNA synthetase). *Am J Med*. 1990;88(3):241–251. doi:10.1016/0002-9343(90)90149-8
34. Hirakata M, Suwa A, Nagai S, et al. Anti-KS: Identification of autoantibodies to asparaginyl-transfer RNA synthetase associated with interstitial lung disease. *J Immunol*. 1999;162(4):2315–2320. PMID: 9973509
35. Friedman AW, Targoff IN, Arnett FC. Interstitial lung disease with autoantibodies against aminoacyl-tRNA synthetases in the absence of clinically apparent myositis. *Semin Arthritis Rheum*. 1996;26(1):459–467. doi:10.1016/S0049-0172(96)80026-6
36. Targoff IN, Johnson AE, Miller FW. Antibody to signal recognition particle in polymyositis. *Arthritis Rheum*. 1990;33(9):1361–1370. doi:10.1002/art.1780330908
37. Hengstman GJD, Ter Laak HJ, Vree Egberts WTM, et al. Anti-signal recognition particle autoantibodies: Marker of a necrotising myopathy. *Ann Rheum Dis*. 2006;65(12):1635–1638. doi:10.1136/ard.2006.052191
38. Aggarwal R, Oddis CV, Goudeau D, et al. Anti-signal recognition particle autoantibody ELISA validation and clinical associations. *Rheumatology (Oxford)*. 2015;54(7):1194–1199. doi:10.1093/rheumatology/keu436
39. Suzuki S, Nishikawa A, Kuwana M, et al. Inflammatory myopathy with anti-signal recognition particle antibodies: Case series of 100 patients. *Orphanet J Rare Dis*. 2015;10:61. doi:10.1186/s13023-015-0277-y
40. Ichiyasu H, Sakamoto Y, Yoshida C, et al. Rapidly progressive interstitial lung disease due to anti-MDA-5 antibody-positive clinically amyopathic dermatomyositis complicated with cervical cancer: Successful treatment with direct hemoperfusion using polymyxin B-immobilized fiber column therapy. *Respir Med Case Rep*. 2017;20:51–54. doi:10.1016/j.rmcr.2016.11.015
41. Tansley SL, Betteridge ZE, McHugh NJ. The diagnostic utility of autoantibodies in adult and juvenile myositis. *Curr Opin Rheumatol*. 2013;25(6):772–777. doi:10.1097/01.bor.0000434664.37880.ac
42. Ceribelli A, Fredi M, Taraborelli M, et al. Anti-MJ/NXP-2 autoantibody specificity in a cohort of adult Italian patients with polymyositis/dermatomyositis. *Arthritis Res Ther*. 2012;14(2):R97. doi:10.1186/ar3822
43. Ghirardello A, Borella E, Beggio M, Franceschini F, Fredi M, Doria A. Myositis autoantibodies and clinical phenotypes. *Auto Immun Highlights*. 2014;5(3):69–75. doi:10.1007/s13317-014-0060-4
44. Valenzuela A, Chung L, Casciola-Rosen L, Fiorentino D. Identification of clinical features and autoantibodies associated with calcinosis in dermatomyositis. *JAMA Dermatol*. 2014;150(7):724–729. doi:10.1001/jamadermatol.2013.10416
45. Albayda J, Pinal-Fernandez I, Huang W, et al. Antinuclear matrix protein 2 autoantibodies and edema, muscle disease, and malignancy risk in dermatomyositis patients. *Arthritis Care Res (Hoboken)*. 2017;69(11):1771–1776. doi:10.1002/acr.23188
46. Ichimura Y, Matsushita T, Hamaguchi Y, et al. Anti-NXP2 autoantibodies in adult patients with idiopathic inflammatory myopathies: Possible association with malignancy. *Ann Rheum Dis*. 2012;71(5):710–713. doi:10.1136/annrheumdis-2011-200697
47. Fiorentino DF, Chung LS, Christopher-Stine L, et al. Most patients with cancer-associated dermatomyositis have antibodies to nuclear matrix protein NXP-2 or transcription intermediary factor 1γ. *Arthritis Rheum*. 2013;65(11):2954–2962. doi:10.1002/art.38093

48. Fujimoto M, Matsushita T, Hamaguchi Y, et al. Autoantibodies to small ubiquitin-like modifier activating enzymes in Japanese patients with dermatomyositis: Comparison with a UK Caucasian cohort. *Ann Rheum Dis*. 2013;72(1):151–153. doi:10.1136/annrheumdis-2012-201736
49. Betteridge ZE, Gunawardena H, Chinoy H, et al. Clinical and human leucocyte antigen class II haplotype associations of autoantibodies to small ubiquitin-like modifier enzyme, a dermatomyositis-specific autoantigen target, in UK Caucasian adult-onset myositis. *Ann Rheum Dis*. 2009;68(10):1621–1625. doi:10.1136/ard.2008.097162
50. Targoff IN, Mamyrova G, Trieu EP, et al. A novel autoantibody to a 155-kd protein is associated with dermatomyositis. *Arthritis Rheum*. 2006; 54(11):3682–3689. doi:10.1002/art.22164
51. Kang EH, Nakashima R, Mimori T, et al. Myositis autoantibodies in Korean patients with inflammatory myositis: Anti-140-kDa polypeptide antibody is primarily associated with rapidly progressive interstitial lung disease independent of clinically amyopathic dermatomyositis. *BMC Musculoskelet Disord*. 2010;11:223. doi:10.1186/1471-2474-11-223
52. Targoff IN, Trieu E, Levy-Neto M, Prasertsuntarasai T, Miller FW. Autoantibodies to transcriptional intermediary factor 1-gamma (TIF1-g) in dermatomyositis. *Arthritis Rheum*. 2007;54:S518.

Effect of the COVID-19 pandemic on foot surgeries

Patryk Kuliński[1,A–F], Łukasz Tomczyk[2,B–D], Piotr Morasiewicz[3,A,C–F]

[1] Department of Trauma and Orthopaedic Surgery, T. Marciniak Lower Silesia Specialist Hospital – Emergency Medicine Center, Wrocław, Poland
[2] Department of Food Safety and Quality Management, Poznan University of Life Sciences, Poland
[3] Department of Orthopaedic and Trauma Surgery, University Hospital in Opole, Institute of Medical Sciences, University of Opole, Poland

A – research concept and design; B – collection and/or assembly of data; C – data analysis and interpretation;
D – writing the article; E – critical revision of the article; F – final approval of the article

Advances in Clinical and Experimental Medicine, ISSN 1899–5276 (print), ISSN 2451–2680 (online) *Adv Clin Exp Med*. 2021;30(12):1249–1253

Address for correspondence
Piotr Morasiewicz
E-mail: morasp@poczta.onet.pl

Funding sources
None declared

Conflict of interest
None declared

Received on April 8, 2021
Reviewed on May 28, 2021
Accepted on July 28, 2021

Published online on October 5, 2021

Abstract

Background. Musculoskeletal dysfunction due to deformities and injuries of the foot is a common orthopedic problem.

Objectives. To analyze the effect of the COVID-19 pandemic on both elective and emergency foot surgeries.

Materials and methods. This study analyzed the effect of the COVID-19 pandemic on elective and emergency foot surgeries. The comparison included data collected in 2019 (March 15–October 15, when the epidemic did not influence the Polish healthcare system or patient demographics) and in a corresponding period in 2020. This study was conducted in the trauma and orthopedic surgery wards and the emergency departments of 2 regional Polish hospitals.

Results. The analysis of the data from the orthopedic wards showed a reduction in the total number of admissions in 2020 by 55%. The number of elective and emergency interventions was differently related to the pandemic, with elective interventions declining by 72% and emergency interventions increasing by 27% in 2020 compared to 2019. The total number of elective foot surgeries in children decreased by 59% in 2020. The mean duration of hospital stay was approx. 2.5 days shorter in adults and 1.7 days shorter in children during the 2nd evaluation period. The emergency department data showed a decline of 32% in the number of patients presenting with injuries during the pandemic. Nonetheless, the pandemic did not affect the mean age of patients and the female-to-male ratio.

Conclusions. The global COVID-19 pandemic affected the epidemiology of foot injuries as well as the prevalence of foot surgeries in children and adults.

Key words: COVID-19, pandemic, epidemiology, foot surgery, lockdown

Cite as
Kuliński P, Tomczyk Ł, Morasiewicz P. Effect of the COVID-19 pandemic on foot surgeries. *Adv Clin Exp Med.* 2021;30(12):1249–1253. doi:10.17219/acem/140610

DOI
10.17219/acem/140610

Background

Musculoskeletal dysfunction due to deformities and injuries of the foot is a common orthopedic problem.[1,2] According to the Illinois Podiatric Medical Association, approx. 6% of the USA population are affected by foot injuries, forefoot deformities or flat feet (pes planus). The global spread of severe acute respiratory syndrome coronavirus type 2 (SARS-CoV-2) infections has had an impact on many aspects of everyday life, including changes in people's habits, lifestyles and fears regarding their health and the health of their loved ones.[2–19]

The COVID-19 pandemic unquestionably affected the functioning of national healthcare systems.[2–19] This included changes in the character of hospitals, including conversions of surgical wards into infectious wards, limiting the number of elective admissions and reducing the number of medical staff. The latter was due to temporary quarantines placed on those who had a contact with patients suspected of having COVID-19 infections and the furloughing of elderly or chronic disease-burdened staff.[3–5,10]

The available literature has a limited number of reports on the effects the COVID-19 pandemic has had on foot surgeries in adults and children.[2,4,5] The available reports assess the number of surgeries for foot injuries during the pandemic to a limited extent[2] or estimate elective foot surgery restrictions based on surveys conducted among orthopedic surgeons.[4,5]

Objectives

The purpose of this study was to analyze the effect of the COVID-19 pandemic on foot surgery in both elective and emergency settings.

Materials and methods

Study design and patients

The study was conducted in the trauma and orthopedic surgery departments and the emergency departments of 2 Polish regional hospitals. Adult and pediatric patients were included in this study. The compared periods were March 15–October 15, 2019, when the (at that time nonexistent) COVID-19 epidemic did not influence the Polish healthcare system or patient demographics, and the corresponding period in 2020 (March 15–October 15, 2020). Informed consent was obtained for experimentation with human subjects. The study was approved by the local ethics committee (approval No. 4/PNDR/2021).

Evaluation of epidemiological parameters

This study analyzed the number of elective foot surgeries most commonly performed in the surgical wards, i.e., correction of forefoot deformities, including bunions (hallux valgus) and hammertoes. A large group of patients presented with multiple forefoot deformities, which were corrected simultaneously during a single procedure. Other elective procedures included arthrodesis, planovalgus foot surgery and removal of implants. The total number of elective foot surgeries in children was assessed. The procedures performed on children were divided into those most frequently performed in our departments (correction of the planovalgus foot, correction of clubfoot).

Injury interventions were divided into 2 groups. The 1st group comprised interventions for foot fractures, defined as fractures involving any bone in the foot from the talus to the phalanges. The 2nd group comprised interventions for injuries such as wounds, dislocations and sprains within the foot (excluding those of the ankle joint).

The groups were analyzed in terms of the number of surgeries, distribution of the sexes, age distribution, and mean duration of hospital stay. The data from 2019 were compared with the data collected in 2020.

Statistical analyses

Statistical analyses were performed using Statistica v. 13.1 software (StatSoft Inc., Tulsa, USA). The Shapiro–Wilk test was used to assess distribution normality. The variables did not follow a normal distribution; therefore, Pearson's χ^2 test and Mann–Whitney test was used. The level of significance was set at $\alpha = 0.05$.

Results

All results have been compiled in Table 1 and Table 2. The analysis of the orthopedic ward data showed a reduction in the total number of adult admissions by 55% in 2020.

The number of elective and emergency interventions was differently affected by the pandemic, with elective interventions declining by 72% and emergency interventions increasing by 27% in 2020 compared to 2019. These changes were statistically significant ($p = 0.01770$; $p = 0.01922$). In adults, arthrodesis and planovalgus foot surgeries decreased by 50% in 2020, implant removal surgeries decreased by 63% and hallux valgus and hammertoe surgeries decreased by 82%.

The total number of elective foot surgeries performed in children decreased by 59% in 2020 compared to 2019. This difference was statistically significant ($p = 0.0487$). In children, the number of planovalgus foot surgeries decreased by 61% and clubfoot surgeries decreased by 56% in 2020.

Table 1. Comparison totals, means and ratios of epidemiology of foot trauma and surgery (p-value for Mann–Whitney U test)

Variables	N		Difference between the year 2020 and 2019 [%]	df	p-value
	2019	2020			
Orthopedic surgery department – surgically					
Total number of patients	86	39	–54.65	–	–
Total number of elective surgery	67	19	–71.64	–	–
Arthrodesis	6	3	–50.00	–	–
Planovalgus foot surgery	4	2	–50.00	–	–
Removal of implants	19	7	–63.15	–	–
Total number of trauma surgery	11	14	27.27	–	–
Total number of patients treated conservatively	8	6	–25.00	–	–
Mean duration of hospital stay [days]	6.77	4.28	36.77	124	0.02737
Female-to-male ratio	2.74	2.00	–26.98	–	–
Mean age of all patients	56.06	56.05	–0.01	123	0.9981
Total number of elective foot surgery in children	27	11	–59.25	–	–
Mean duration of hospital stay in children [days]	5.44	3.72	–31.61	126	0.0046
Emergency ward – conservatively					
Total number of patients	145	99	–31.72	–	–
Total number of patients treated conservatively	130	85	–34.61	–	–
Total number of patients transferred to the orthopedic ward	15	14	–6.66	–	–
Female-to-male ratio	0.59	0.57	–3.7	–	–
Mean age of all patients	41.26	45.05	9.13	242	0.0722

Table 2. Change in composition of epidemiology of foot trauma and surgery (p-value for Pearson's χ^2 test)

Variables	N		Difference between the year 2020 and 2019 [%]	df	p-value
	2019	2020			
Orthopedic surgery department – surgical treatment					
Elective surgery halux valgus and hammertoe surgery other surgeries	 38 29	 7 12	 –81.57 –58.62	1	0.0177
Trauma surgery fractures other injuries	 8 3	 7 7	 –12.5 133.33	1	0.01922
Gender women men	 63 23	 26 13	 –58.73 –43.47	1	0.451
Surgery in children					
Trauma surgery planovalgus foot surgery in children clubfoot surgery in children	 18 9	 7 4	 –61.11 –55.55	1	0.0487
Emergency ward – conservative treatment					
Type of injuries fractures injuries	 95 50	 56 43	 –41.05 –14.00	1	0.1574
Gender women men	 54 91	 36 63	 –33.33 –30.76	1	0.889

The mean duration of hospital stay for adults was approx. 2.5 days shorter in the 2nd evaluated period, which was statistically significant (Fig. 1, p = 0.02737). The mean duration of hospital stay for children decreased in 2020 by 1.7 days compared to 2019. This difference was statistically significant (p = 0.0046).

There was not a significant decrease in the proportion of females and males admitted to the hospital (with a female-to-male ratio of 2.74 in 2019 compared to 2.00 in 2020, p = 0.541). In addition, the mean age of patients undergoing surgery remained unchanged (p = 0.9981).

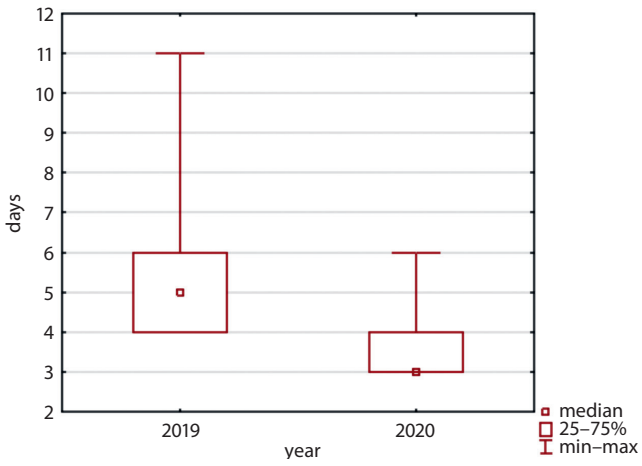

Fig. 1. Mean duration of hospital stay in days

The greatest rise in emergency procedures (133%) was observed in interventions performed due to other foot injuries (mostly soft-tissue injuries) (p = 0.01922). The emergency department data showed 32% fewer patients presenting with injuries during the evaluated pandemic period. These changes were statistically significant (p = 0.0153). Moreover, the number of patients with fractures showed a greater decline (41%) in 2020 compared with pre-pandemic figures than the number of patients with soft-tissue injuries (14% decline), although these differences did not reach statistical significance (p = 0.1574).

The mean patient age in the emergency ward increased from 41 years in 2019 to 45 years in 2020, but the difference was not statistically significant (p = 0.0722). The proportion of patients seen in the emergency departments who required surgical treatment or more diagnostic tests on the orthopedic ward did not change between the evaluated periods (with only a single case fewer in the 2nd period).

Discussion

Key results and generalizability

The COVID-19 pandemic considerably altered the organization of healthcare services across the world.[2–19] Elective admissions were halted or limited, medical personnel numbers decreased and patients' fears associated with hospitalization increased.[3–5,10] However, the impact of the COVID-19 pandemic on elective and emergency treatment of foot injuries has not been fully evaluated.

Our study confirms the impact of the pandemic in the form of lower numbers of elective procedures in children and adults, and shorter hospital stays to minimize the amount of contact between patients and medical staff, who are the potential vectors in coronavirus transmission. Similarly, other authors have reported decreases in the number of elective procedures during the pandemic by 23–100%.[3–5,10] An estimated 26.6–75.2% of centers cancelled or rescheduled (postponed) foot surgeries during the COVID-19 pandemic.[4,5] We observed a decrease in all types of elective surgeries performed in both, adults and children. The reduction in the number of elective admissions of children during the COVID-19 pandemic, observed in our study, may have negative effects in the form of increasing the severity of deformities in patients awaiting surgery. The postponing of any musculoskeletal surgery in a growing child is particularly dangerous, and can have irreversible consequences and a significant impact on their health.

No statistically significant reduction was seen in the ratio of female-to-male patients admitted to orthopedic surgery departments in 2020, largely due to the fact that females are generally more prone to develop forefoot deformities.[20,21]

During the pandemic, the introduction of travel restrictions and remote work led to fewer patients presenting with pain, which undoubtedly resulted in a reduction of patients admitted for elective forefoot procedures. In many cases, patients decided to postpone their treatment due to less severe pain, and – particularly among the elderly – out of fear of the coronavirus.

In contrast to the pronounced change in sex distribution among orthopedic ward patients, the change in sex distribution among emergency room patients was negligible. Males presented nearly 2 times more frequently than females in both evaluated periods (the female-to-male ratio was 0.59 in 2019 and 0.57 in 2020), which indicates a higher incidence of foot injuries in males.

The increased number of foot injury patients transferred to the orthopedic ward from the emergency room to undergo surgical treatment was due to several factors. These include the increasingly stringent restrictions imposed by the Polish government during the period of national lockdown, which directly affected the etiology of injuries, with lower numbers of high-energy injuries and only slightly lower numbers of soft-tissue injuries. These changes were a result of travel restrictions and the consequent decline in the number of traffic accidents.[13,15,18] Conversely, the amount of work around the house increased due to no restrictions being imposed on hardware and DIY stores. This, combined with increased alcohol consumption, resulted in a higher incidence of injuries at home.[13,15,18] Moreover, heavy industry did not experience any direct lockdown measures, which was associated with undiminished injuries in this field.

Limitations

The limitation in the assessment of the impact of the COVID-19 pandemic on foot surgery is that it was only conducted at 2 centers and on a limited group of patients. This allowed the authors to quickly assess and present the important research results. However, in the future, we plan to conduct a multicenter study on a larger group of patients.

In light of the uncertain future and lack of reliable estimates as to the duration of this pandemic, orthopedic wards and surgery scheduling must develop protocols to increase their availability and ensure the safety of patients and staff.

Conclusions

Our analysis of the collected data showed the effects of the global COVID-19 pandemic on the types of patients, availability of elective foot surgeries in children and adults, and epidemiology of foot injuries. This study highlights the need to make elective surgeries more available, while simultaneously improving the safety for both hospital staff and patients by minimizing the risk of possible SARS CoV-2 transmission. The COVID-19 pandemic saw a reduction in the number of all types of elective foot surgeries in children and adults, an increase in the number of trauma-related foot surgeries, and shortening of hospital stays. Nonetheless, the pandemic had no effect on mean patient age and female-to-male ratio.

ORCID iDs

Patryk Kuliński https://orcid.org/0000-0002-1048-7460
Łukasz Tomczyk https://orcid.org/0000-0002-4644-0111
Piotr Morasiewicz https://orcid.org/0000-0002-7587-666X

References

1. Cichero MJ. Elective foot and ankle surgery: Activity and perioperative complications in Queensland public hospitals, Australia. *Foot (Edinb)*. 2009;19(3):139–144. doi:10.1016/j.foot.2009.02.003
2. Vosoughi AR, Borazjani R. COVID-19 effect on foot & ankle surgery in Shiraz, south Iran. *J Foot Ankle Surg*. 2020;59(5):887. doi:10.1053/j.jfas.2020.06.013
3. Thaler M, Khosravi I, Hirschmann MT, et al. Disruption of joint arthroplasty services in Europe during the COVID-19 pandemic: An online survey within the European Hip Society (EHS) and the European Knee Associates (EKA). *Knee Surg Sports Traumatol Arthrosc*. 2020;28(6):1712–1719. doi:10.1007/s00167-020-06033-1
4. Liebensteiner MC, Khosravi I, Hirschmann MT, Heuberer PR, Thaler M; Board of the AGA – Society of Arthroscopy and Joint-Surgery. Massive cutback in orthopaedic healthcare services due to the COVID-19 pandemic. *Knee Surg Sports Traumatol Arthrosc*. 2020;28(6):1705–1711. doi:10.1007/s00167-020-06032-2
5. Liebensteiner MC, Khosravi I, Hirschmann MT, Saffarini M, Thaler M; The Board of the AGA – Society of Arthroscopy and Joint-Surgery. It is not 'business as usual' for orthopaedic surgeons in May 2020: The Austrian-German-Swiss experience. *J Exp Orthop*. 2020;7:61. doi:10.1186/s40634-020-00272-4
6. Kort NP, Gomez Barrena E, Bédard M, et al. Resuming elective hip and knee arthroplasty after the first phase of the SARS-CoV-2 pandemic: The European Hip Society and European Knee Associates recommendations. *Knee Surg Sports Traumatol Arthrosc*. 2020;28(9):2730–2746. doi:10.1007/s00167-020-06233-9
7. Kort NP, Gomez Barrena E, Bédard M. Recommendations for resuming elective hip and knee arthroplasty in the setting of the SARS-CoV-2 pandemic: The European Hip Society and European Knee Associates Survey of Members. *Knee Surg Sports Traumatol Arthrosc*. 2020;28(9):2723–2729. doi:10.1007/s00167-020-06212-0
8. Kort NP, Zagra L, Gomez Barrena E. Resuming hip and knee arthroplasty after COVID-19: Ethical implications for wellbeing, safety and the economy. *Hip Int*. 2020;30(5):492–499. doi:10.1177/1120700020941232
9. Athey AG, Cao L, Okazaki K. Survey of AAHKS International Members on the impact of COVID-19 on hip and knee arthroplasty practices. *J Arthroplasty*. 2020;35(7S):S89–S94. doi:10.1016/j.arth.2020.04.053
10. D'Apolito R, Faraldi M, Ottaiano I, Zagra L. Disruption of arthroplasty practice in an orthopedic center in northern Italy during the coronavirus disease 2019 pandemic. *J Arthroplasty*. 2020;35(7S):S6–S9. doi:10.1016/j.arth.2020.04.057
11. Verde F, D'Ambrosi R, Biazzo A, Masia F, Perazzo P. Guidelines for resuming elective hip and knee surgical activity following the COVID-19 pandemic: An Italian perspective [Epub ahead of print]. *HSS J*. 2020;13:1–6. doi:10.1007/s11420-020-09809-w
12. Donell ST, Thaler M, Budhiparama NC, et al. Preparation for the next COVID-19 wave: The European Hip Society and European Knee Associates recommendations. *Knee Surg Sports Traumatol Arthrosc*. 2020;28(9):2747–2755. doi:10.1007/s00167-020-06213-z
13. Upadhyaya GK, Iyengar K, Jain VK, Vaishya R. Challenges and strategies in management of osteoporosis and fragility fracture care during COVID-19 pandemic. *J Orthop*. 2020;21:287–290. doi:10.1016/j.jor.2020.06.001
14. Hashmi P, Fahad S, Khan HN, Zahid M, Sadruddin A, Noordina S. Covid-19 pandemic: Economic burden on patients with musculoskeletal injuries in a tertiary care hospital of LMIC. Retrospective cross sectional study. *Ann Med Surg (Lond)*. 2020;60:5–8. doi:10.1016/j.amsu.2020.09.049
15. Yu P, Wu C, Zhuang C, et al. The patterns and management of fracture patients under COVID-19 outbreak in China. *Ann Transl Med*. 2020;8(15):932. doi:10.21037/atm-20-4174
16. Maryada VR, Mulpur P, Guravareddy AV, Pedamallu SK, Bhasker BV. Impact of COVID-19 pandemic on orthopaedic trauma volumes: A multi-centre perspective from the state of Telangana. *Indian J Orthop*. 2020;54(Suppl 2):1–6. doi:10.1007/s43465-020-00226-z
17. Mitkovic MM, Bumbasirevic M, Milenkovic S, Gajdobranski D, Bumbasirevic V, Mitkovic MB. Influence of coronavirus disease 2019 pandemic state of emergency in orthopaedic fracture surgical treatment. *Int Orthop*. 2021;45(4):815–820. doi:10.1007/s00264-020-04750-3
18. Murphy T, Akehurst H, Mutimer J. Impact of the 2020 COVID-19 pandemic on the workload of the orthopaedic service in a busy UK district general hospital. *Injury*. 2020;51(10):2142–2147. doi:10.1016/j.injury.2020.07.001
19. Lv H, Zhang Q, Yin Y, et al. Epidemiologic characteristics of traumatic fractures during the outbreak of coronavirus disease 2019 (COVID-19) in China: A retrospective & comparative multi-center study. *Injury*. 2020;51(8):1698–1704. doi:10.1016/j.injury.2020.06.022
20. Roddy E, Zhang W, Doherty M. Prevalence and associations of hallux valgus in a primary care population. *Arthritis Rheum*. 2008;59:857–862. doi:10.1002/art.23709
21. Nix S, Smith M, Vicenzino B. Prevalence of hallux valgus in the general population: A systematic review and meta-analysis. *J Foot Ankle Res*. 2010;3:21. doi:10.1186/1757-1146-3-21

Effects of nano-sized titanium dioxide powder and ultraviolet light on superficial veins in a rabbit model

Fatih Ada[1,A–D], Ferit Kasimzade[2,C–E], Ali Sefa Mendil[3,B,C], Hasan Gocmez[4,E,F]

[1] Department of Cardiovascular Surgery, School of Medicine, Sivas Cumhuriyet University,
[2] Department of Cardiovascular Surgery, Ministry of Health Ankara City Hospital, Turkey
[3] Faculty of Veterinary Medicine, Erciyes University, Kayseri, Turkey
[4] Faculty of Engineering, Kütahya Dumlupınar University, Turkey

A – research concept and design; B – collection and/or assembly of data; C – data analysis and interpretation; D – writing the article; E – critical revision of the article; F – final approval of the article

Advances in Clinical and Experimental Medicine, ISSN 1899–5276 (print), ISSN 2451–2680 (online) *Adv Clin Exp Med*. 2021;30(12):1255–1262

Address for correspondence
Fatih Ada
E-mail: drfatihada@gmail.com

Funding sources
None declared

Conflict of interest
None declared

Received on April 22, 2021
Reviewed on July 1, 2021
Accepted on August 21, 2021

Published online on October 12, 2021

Abstract

Background. Titanium dioxide (TiO_2) is widely used in many fields such as food, cosmetics, and paper industries. Studies on the photocatalytic properties of TiO_2 on living tissue are limited.

Objectives. To examine the histopathological effects of TiO_2 solution on the marginal veins of rabbit ears under ultraviolet (UV) light.

Materials and methods. In this study, 4 groups of rabbits (8 rabbits per group) were used: the 1st group was the control group, the 2nd group received 20% of nano-TiO_2 only, the 3rd group received UV light only, and the 4th group received nano-TiO_2 and UV light, simultaneously. The study lasted for 14 days and samples were taken from the marginal ear vein on the 15th day.

Results. The ear tissues of rabbits in the control and TiO_2 groups showed a normal histological appearance. In the UV group, the results showed severe chronic inflammation due to mononuclear cells around the hair follicles and perivascular areas. However, these findings decreased in the UV/nano-TiO_2 group.

Conclusions. The method applied in this study can be used in the treatment of telangiectasia in the future. However, this study investigating the effects of nano-TiO_2 on vascular structures under UV light had a predominantly histological and observational nature. Further studies involving genetic, cytogenetic, biochemical, histochemical, and immunohistochemical analyses need to be performed to test the theories we proposed.

Key words: animal model, titanium dioxide, vein, nano-TiO_2, ultraviolet light

Cite as
Ada F, Kasimzade F, Mendil AS, Gocmez H. Effects of nano-sized titanium dioxide powder and ultraviolet light on superficial veins in a rabbit model. *Adv Clin Exp Med*. 2021;30(12):1255–1262. doi:10.17219/acem/141501

DOI
10.17219/acem/141501

Background

Titanium dioxide (TiO_2), also known as titania, is widely used in many fields such as paints, cosmetics, food products, and pharmaceuticals. With the discovery of the photocatalytic activity of TiO_2, the use of this material has expanded.[1] Titanium dioxide can be found in many crystalline structures in nature, but it has 2 basic structures: the rutile and anatase polymorphic phases. Titania also has many favorable properties such as semiconductivity, non-toxicity, white color, low cost, chemical stability, and photocatalytic activity.

The nano-TiO_2 electron band gap is higher than 3 eV and has a high absorption in the ultraviolet (UV) region. However, due to its strong optical and biological properties, it can be used in UV light protection applications. Many studies have been conducted to examine the photocatalytic activity of TiO_2.

Photocatalysts can be defined as semiconductors that become active when interacting with light, forming strongly oxidized or reductive active surfaces. Sunlight promotes the purification of water systems in nature, such as rivers, streams, lakes, and pools. The sunrays initiate the breakdown of large organic molecules into smaller, simpler molecules. This breakdown reaction eventually results in the formation of carbon dioxide, water and other molecular products. The results of laboratory studies in the early 1980s indicated that semiconductors accelerated this natural purification process induced by sunlight.[2]

High-efficiency photocatalysts under UV light also have high efficiency under visible light when various methods are applied. The S-doped TiO_2 has high photocatalytic activity under visible light.[3] For example, S-doped TiO_2 has high efficiency at a 500 nm wavelength, while Ru-doped TiO_2 has high photocatalytic activity at a 440 nm wavelength.[3]

Studies on the photocatalytic properties of TiO_2 on living tissue are limited. To address this research gap, this study investigated the histopathological effects of TiO_2 on the superficial veins of rabbit ears under UV light by utilizing its photocatalytic properties.

Objectives

Photocatalysts, which are commonly used for cleaning the environment, water and air, are now being used in different fields. Watanabe et al. evaluated the photocatalytic activity of nano-sized TiO_2 in an artificial skin model.[4] They sequentially measured the CO_2 levels on artificial skin with the addition of nano-sized TiO_2, and found an increase in ambient CO_2 level with photocatalytic activity. Shen et al. encapsulated TiO_2 with zeolite to increase its photocatalytic activity in sunscreens, and found that the harmful effects of UV light were minimized.[5]

The present study aimed to investigate the effects of nano-sized TiO_2 on superficial veins under UV light with a 368 nm wavelength in a rabbit model.

Materials and methods

This study was approved by the Local Ethics Committee of Sivas Cumhuriyet University (Sivas, Turkey; approval No. 65202830-050.04.04-62). All procedures were carried out at Sivas Cumhuriyet University Laboratory of Experimental Animals in accordance with the local rules of care and use of experimental animals.

The study was conducted as a controlled randomized animal experiment. This study employed a total of 8 male and female New Zealand white rabbits from 6 to 8 months of age. The rabbits weighed between 3.2 kg and 3.5 kg for males and between 2.75 kg and 3 kg for females. All animals were fed a standard laboratory diet with free access to water. The rabbits were housed with 1 animal in each cage. Rabbits that were able to perform their normal activities in the cages were kept in rooms with a temperature of 22 ±2°C, a humidity level between 50% and 70%, and a 12 h day/12 h night cycle. All animals were kept under observation for 1 day to determine whether they were healthy before the experiments. Healthy animals without any problems were included in the study.

The rabbits were divided into the following 4 groups (8 rabbits per group; Table 1):

– group 1 – control group: no treatment was performed;

– group 2 – 20% nano-TiO_2 group: 0.2 mL of nano-sized 20% TiO_2 solution was topically applied to the visible marginal vein of the right ears of the rabbits every day. No other procedure was performed;

– group 3 – UV group: rabbits were exposed to ultraviolet A (UVA) light at a wavelength range of 368 nm for 12 h a day, at a distance of approx. 150 cm. No other procedure was performed;

Table 1. Experimental groups and their characteristics

Groups	Procedure	Method of procedure	Procedure modality and duration	Procedure features
Group 1	control group	–	–	–
Group 2	20% nano-TiO_2	topical	daily	0.2 mL solution
Group 3	UV	12 h	12 h a day, at a distance of 150 cm	at a wavelength of 368 nm UV
Group 4	20% nano-TiO_2 + UV	topical + UV	12 h a day, at a distance of 150 cm	0.2 mL of solution also at a wavelength of 368 nm UV

UV – ultraviolet light; TiO_2 – titanium dioxide.

Fig. 1. Ultraviolet light was applied at a distance of 150 cm. Each rabbit was kept in a single cage

– group 4 – 20% nano-TiO_2 and UV light group: 0.2 mL of nano-sized 20% TiO_2 solution was topically applied to the visible marginal vein of the right ears of the rabbits every day. Simultaneously, UVA at a wavelength of 368 nm at a distance of 150 cm was applied for 12 h a day.

The procedures were performed for 14 days (Fig. 1). On the 15th day, punch biopsies were taken from the marginal vein under local anesthesia from all groups. The samples were then examined histologically.

For the nano-TiO_2, 20 nm TiO_2 powder with the tradename Degussa p25 (Nanoshel LLC, Wilmington, USA) was used. The UVA light sources were Sylvania brand UV lamps (Erlangen, Germany), measuring 40W/4FT/T12/BL368 with a wavelength of 368 nm. No treatment or euthanasia was performed on the animals at the end of the study.

Histopathological examination

The ear tissue samples from the rabbits were placed in 10% buffered formalin solution. The samples were then subjected to routine follow-up procedures and embedded in paraffin blocks. Next, the 5-µm sections taken from the blocks were stained with hematoxylin and eosin (H&E) to assess histopathological changes. Sections were examined under a light microscope and semi-quantitatively scored as negative (–), mild (+), moderate (++), or severe (+++) for chronic inflammation. The increase in macrophage and lymphocyte density in the tissue was used as a chronic inflammation marker. We evaluated the vascular samples and scored them according to the histopathological scale described by Kuwahara et al.[6]

Statistical analyses

Microsoft Excel 2010 (Microsoft Corp., Redmond, USA) and SPSS v. 16.0 (SPSS Inc., Chicago, USA) were used to perform the statistical analysis. Based on an α of 0.05, β of 0.20 and 1-β of 0.80, we decided to include 8 rabbits in each group (32 rabbits in total) and the power was calculated to be 0.8345. Since the distribution of the data was not normal, the Kruskal–Wallis H test was conducted to assess significant differences between groups. For post hoc tests of differences between groups, Dunn's post hoc test was used, because it preserves the pooled variance for the tests implied by the Kruskal–Wallis null hypothesis (Table 2). When the data violated the normality assumption (Table 3), we decided to use the nonparametric

Table 2. Statistical significance of differences between groups according to Dunn's post hoc test

Sample 1 compared to sample 2	Test statistic	SD error	SD test statistic	p-value
20% nano-TiO_2 group compared to control group	1.063	4.464	0.238	0.812
20% nano-TiO_2-group compared to 20% nano-TiO_2 and UV group	–12.687	4.464	–2.842	0.004
20% nano-TiO_2 -group compared to UV group	–20.000	4.464	–4.480	0.000
Control group compared to 20% nano-TiO_2 and UV group	–11.625	4.464	–2.604	0.009
Control group compared to UV group	–18.937	4.464	–4.242	0.000
20% nano-TiO_2 and UV group compared to UV group	7.313	4.464	1.638	0.101

UV – ultraviolet light; SD – standard deviation; TiO_2 – titanium dioxide.

Table 3. Descriptive statistics of the treatment groups

Groups	Mean (SD)	Median	Maximum	Minimum
Control group	0.25 (0.463)	0.00	1	0
20% nano-TiO_2 group	0.13 (0.354)	0.00	1	0
UV group	2.88 (0.354)	3.00	3	2
20% nano-TiO_2 and UV group	1.88 (0.354)	2.00	2	1

UV – ultraviolet light; SD – standard deviation; TiO_2 – titanium dioxide.

Kruskal–Wallis H test to compare the mean rank scores of the groups. The effect size for the test was calculated as 4.92.

Results

Four female and 4 male rabbits were included in each experimental group; thus, there were no statistically significant differences between the groups in terms of gender ($p > 0.05$). The results showed that the ear tissues of the rabbits in the control and nano-TiO_2 groups had a normal histological appearance (Fig. 2). However, we observed the formation of severe chronic inflammation of mononuclear cells in the perivascular areas and around the hair follicles in the UV group (Table 4).

The results of the Kruskal–Wallis H test indicated significant differences between groups subjected to different treatment methods ($\chi^2(3) = 27.835$, $p < 0.001$), with mean rank scores of 9.12 for the control group, 8.06 for the 20% nano-TiO_2 group, 28.06 for the UV group, and 20.75 for the group administered both 20% nano-TiO_2 and UV. Dunn's pairwise post hoc test indicated significant differences between the control group and the UV group ($p < 0.001$), between the 20% nano-TiO_2 group and the UV group ($p < 0.001$), between the 20% nano-TiO_2 group and the group administered both 20% nano-TiO_2 and UV light ($p = 0.004$), and between the control group and the group administered both 20% nano-TiO_2 and UV light ($p = 0.009$). There were no other significant differences (Table 5). The histopathological changes decreased in the group that received both UV and nano-TiO_2. Macroscopically, the results indicated that the visibility of rabbit ear veins decreased in the 20% nano-TiO_2 and UV light group (Fig. 3).

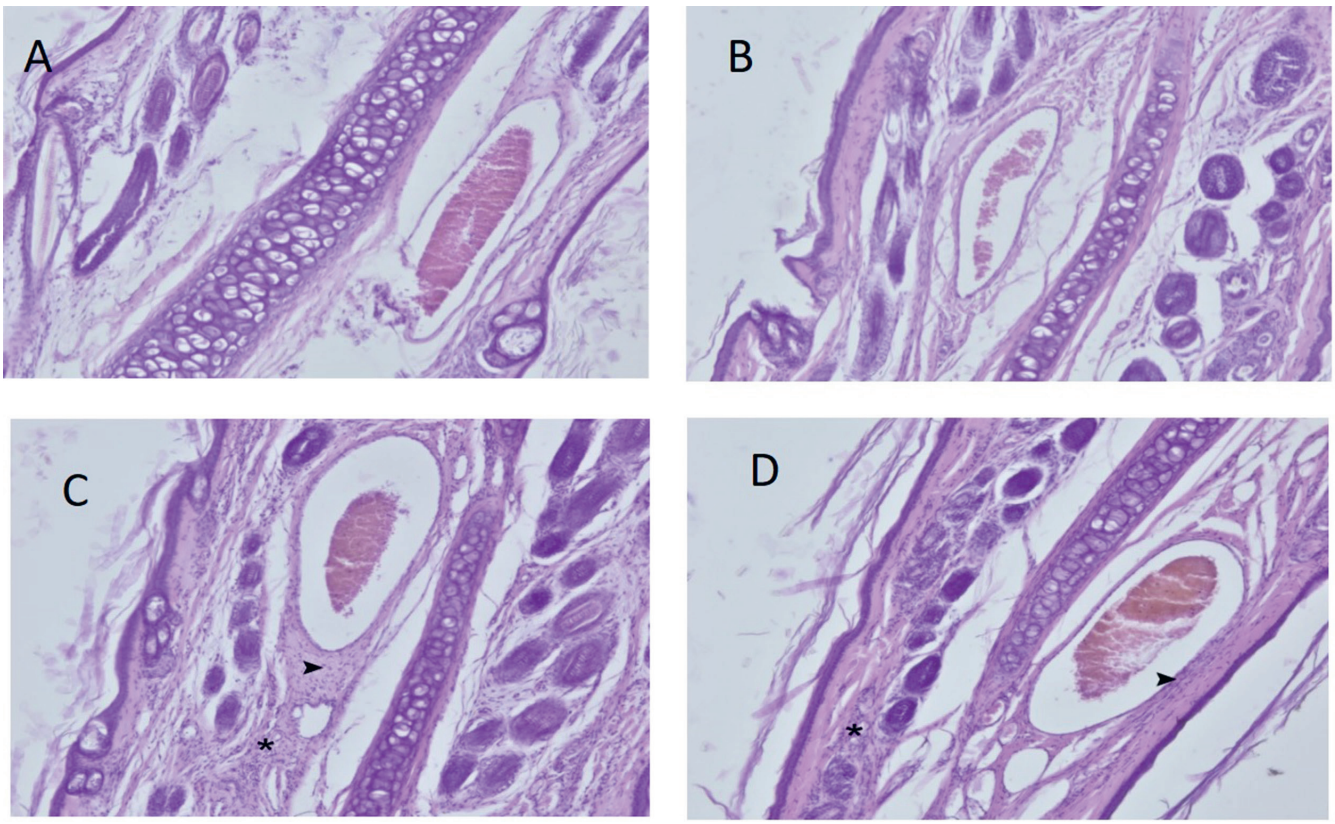

Fig. 2. A. Control group. Normal histological appearance. ×40 magnification, hematoxylin and eosin (H&E) staining; B. Titanium dioxide (TiO_2) group. Normal histological appearance. ×40 magnification, H&E staining; C. Ultraviolet (UV) group. Severe mononuclear cell infiltration is present around the vein (arrowhead) and near the hair follicles (*). ×40 magnification, H&E staining; D. Ultraviolet light + TiO_2 group. Moderate mononuclear cell infiltration is present around the vessel (arrowhead) and near the hair follicles (*). ×40 magnification, H&E staining

Table 4. Inflammation degrees of the groups

Inflammation	Group 1 (n = 8)	Group 2 (n = 8)	Group 3 (n = 8)	Group 4 (n = 8)
Negative [%]	75	87.5	0	0
Mild [%]	25	12.5	0	12.5
Moderate [%]	0	0	12.5	87.5
Severe [%]	0	0	87.5	0

Table 5. Kruskal–Wallis H test analysis table for all treatment groups

Groups	Mean rank	χ^2	df	p-value
Control group	9.12	27.835	3	0.000
20% nano-TiO_2 group	8.06	–	–	–
UV light group	28.06	–	–	–
20% nano-TiO_2 and UV light group	20.75	–	–	–

UV – ultraviolet light; TiO_2 – titanium dioxide; df – degrees of freedom.

Discussion

At present, TiO_2 is widely used in many industries such as pharmaceuticals, cosmetics (especially in sunscreens), food, biomedical products, etc. Given its wide use, it is necessary to investigate the toxicological and histological effects of nano-TiO_2, as well as its effects on the immune system. Fabian et al. administered titanium dioxide nanoparticles intravenously to rats and found that they did not cause any toxic effects at a 5 mg/kg dose and could be used safely at this dose.[7] Warheit et al. administered 300 nm of titanium dioxide via inhalation in rabbits and showed that short-term exposure did not cause any lung problems.[8] In the same study, they reported that TiO_2 of this size had no genotoxic effect and did not cause any irritation of the skin, but reversible conjunctival redness in the eyes of rabbits was observed. In a review of the effects of nano-sized TiO_2 on the lung, size, exposure time, and the amount of nano-titanium were identified as the most important risk factors.[9]

Fig. 3. On the 14th day of the study, titanium dioxide (TiO_2) and ultraviolet (UV) light were applied to the rabbits. Titanium dioxide was applied to the upper ear, but not lower ear. Note the difference between venous structures

In a wide-ranging review, Iavicoli et al. investigated the effects of nano-TiO_2 on mammals organ by organ and system by system.[10] Although they discussed the effects of nano-TiO_2 on many systems, they emphasized that their effects on vascular structures were not clear. However, they stated that the effects of TiO_2 were directly related to the way it was administered, its dose, duration, and particle size. Tang et al. examined the relationship between administration routes and doses of TiO_2.[11] They found that TiO_2 with a size of 5 nm could be passed to the blood intratracheally; when it reached a dose of 0.8 mg/kg, it could reach the lungs and kidneys and it changed liver and kidney function. However, they observed that these effects were reversible after 1 week without permanent damage.

There is a limited number of studies on the effects of TiO_2 on vascular structures in the literature. In a study using porcine pulmonary artery endothelial culture, Han et al. reported that nano-TiO_2 increased the inflammatory response in endothelial cells.[12] They concluded that the increased inflammation response occurred via the redox-sensitive cell signaling pathway.

Montiel-Dávalos et al. conducted a study on human umbilical vein endothelial cell culture (HUVEC) and found that TiO_2 inhibited the proliferation of endothelial cells and accelerated apoptotic and necrotic death.[13] Alinovi et al. also conducted a study using HUVEC and found that TiO_2 nanoparticles increased inflammation in endothelial cells.[14] Park et al. conducted a study using a mouse endothelial cell culture line and evaluated whether the size of the nanotube affected the endothelial adhesion and apoptosis rates of TiO_2 nanotubes.[15] They observed more endothelial adhesion, less apoptosis, and less inflammation in 15 nm nanotubes. Furthermore, their results indicated an increase in inflammation and apoptosis as the size of the nanotubes increased. These findings demonstrate the importance of size in terms of the effectiveness of nano-TiO_2 to be used in vascular implants.

Ge et al. conducted a study using HUVEC and their results indicated that thin film nano-TiO_2 provided laminin immobilization and an increase in endothelial adhesion.[16]

Ultraviolet light has been used in the treatment of skin diseases since the beginning of the 20th century. Although the mechanism of UV light action is not clear, hypotheses that it increases cell proliferation, epidermal thickness and blood flow in cutaneous capillaries have been proposed.[17] In a study that applied UV light to patients with venous ulcers, Dodd et al. concluded that UV light had no benefit in the treatment of venous ulcers.[18] However, they observed that UV light increased skin oxygen permeability and inhibited normal vasoconstrictor response.

When light treatment is required in medicine, the preferred UV light wavelength is in the 300–320 nm range. In dermatology, psoralen ultraviolet A (PUVA) treatment for psoriasis, eczema, vitiligo, and cutaneous lymphoma is widely used.[19] Although UV light has positive results when applied to appropriate patients for a certain period of time, dose and treatment, excessive exposure can lead to many adverse conditions such as skin cancer, T cell damage, immune depression, sunburn, and premature skin aging.[20]

Telangiectasias are enlarged venous vessels with a diameter of 0.5–1 mm near the skin surface. Telangiectasias are enlarged postcapillary venules located in the papillary and superficial reticular dermis with histologically complete meaning.[21]

Engel et al. conducted a field study with a large population in the USA and found that the rate of telangiectasia in the legs was 29–41% in women and 6–15% in men.[22] Facial telangiectasia affects tens of millions of people around the world.[23] Sclerotherapy is the standard approach for the treatment of telangiectasias. Sclerosis of the telangiectatic vein is the main target in sclerotherapy. In order to achieve sclerosis, various chemical sclerosing agents are administered directly into the enlarged telangiectatic vein, resulting in the formation of a thrombosis and endothelial damage within the vein.[24]

Apart from sclerotherapy, many different laser treatments, such as argon ion lasers, diode lasers and intense pulsed light sources, are applied.[25,26] Laser treatment was first performed in the treatment of telangiectasias in 1960 using light at a 694 nm wavelength, followed by different systems and wavelengths.[27] The underlying logic of laser treatment in telangiectasia is to cause the loss of veins close to the skin surface by creating thermal damage to the vascular structures through the heat generated by UV light. Hemoglobin in the vessel absorbs light best at 418 nm, 542 nm and 577 nm wavelengths.[28] However, the wavelengths used in the treatment of vascular lesions are usually 488 nm and 600 nm.[28]

Photocatalysts can be described as semiconductors that create a strongly oxidized environment on the surface through the effect of UV light. Therefore, photocatalysts can cause degradation in organic tissues close to the region where they are applied. Among the known semiconductor photocatalysts, TiO_2 is widely used due to its high activity, high stability under lighting, nontoxic nature, and low price. Titanium dioxide performs its photocatalytic effect best under 340 nm wavelength light, but a wavelength range of 320–380 nm is also good for photocatalyst activity.[29]

In general, studies have demonstrated that organic cell degradation increases as the wavelength decreases. This means that at a wavelength of 280 nm or less, TiO_2 has its maximum photocatalytic effect, leading to the degradation of DNA and RNA.[30,31] Therefore, the light wavelength selected in our study was in the range of 320–380 nm. The same ultraviolet light wavelength and application methods used in previous animal experiments, as well as the dose, concentration, and routes of TiO_2 administration were applied in the current study.[32,33] What distinguishes this study from the other studies is that we investigated the effects of TiO_2 and UV light on vascular structures simultaneously.

Photodynamic therapy, especially in dermatology and plastic surgery, is used effectively and widely for the treatment of many dermatological diseases in the form of a combination of light and various creams applied to the skin. The main principle of creams with methyl aminolevulinate as the active ingredient is to be absorbed by the skin and subcutaneous tissue, and to provide local apoptosis with the effect of light. In fact, Galvão found that telangiectasias on the face were not visible after photodynamic therapy in a patient with facial actinic keratosis.[34]

Photodynamic therapy consists of 3 main elements: a photosensitive material, a light source and oxygen. When these 3 factors are combined effectively, they can be applied for the successful treatment of many skin lesions. In photodynamic therapy, the therapeutic effect is achieved by a slight activation of a light-sensitive substance, and reactive oxygen intermediates are formed in the presence of oxygen. These intermediates irreversibly oxidize the essential cellular components that cause apoptosis and necrosis, thereby providing the treatment of lesions on the skin.[35] Essentially, our study has shown similar results to photodynamic therapy. In this sense, the study demonstrated that substances with photocatalytic activation may be an appropriate choice for this treatment.

Limitations

The method applied in the present study could be used in the treatment of telangiectasia in the future. However, our study has a predominantly histological and observational nature. Further studies involving genetic, cytogenetic, biochemical, histochemical, and immunohistochemical analyses are needed to test the theories described above.

Conclusion

The results of this study revealed that nano-TiO_2 protected the skin and the main vascular structures close to the skin from the harmful effects of UV light.

Furthermore, this study determined that telangiectatic structures close to the skin were not observed in the UV and nano-TiO_2 group.

Several theories were put forward regarding the absence of telangiectatic structures in the rabbit ear on macroscopic observation. The 1st is that nano-TiO_2 and UV light induced apoptosis in telangiectatic structures, just as in photodynamic therapy. The 2nd is that thermal damage was caused by heating during the photocatalytic activation of nano-TiO_2. The 3rd theory is that collagen tissue deposited under the epidermis compressed the telangiectatic veins or precipitated them towards the dermis. The 4th is damage of hemoglobin in the telangiectatic vein. The 5th is selective photothermolysis that led to panendothelial obliteration. Any combination of these theories, or some other mechanism of action, may have led to these results.

ORCID iDs

Fatih Ada https://orcid.org/0000-0002-6953-5906
Ferit Kasimzade https://orcid.org/0000-0003-3646-3181
Ali Sefa Mendil https://orcid.org/0000-0003-2722-3290
Hasan Gocmez https://orcid.org/0000-0003-3748-0311

References

1. Şam ED, Ürgen M, Tepehan FZ. TiO_2 fotokatalistleri. *İTÜ Dergisi/D Mühendislik*. 2007;6(5–6):81–92. http://itudergi.itu.edu.tr/index.php/itudergisi_d/article/viewFile/395/337. Accessed November 1, 2020.
2. Ochiai T, Fujishima A. Design and optimization of photocatalytic water purification reactors. In: Pichat P, ed. *Photocatalysis Water Purification: From Fundamentals to Recent Applications*. Weinheim, Germany: Wiley-VCH; 2013:361. doi:10.1002/9783527645404.ch14
3. Ohno T, Akiyoshi M, Umebayashi T, et al. Preparation of S-doped TiO_2 photocatalysts and their photocatalytic activities under visible light. *Appl Catal A Gen.* 2004;265(1):115–121. doi:10.1016/j.apcata.2004.01.007
4. Watanabe E, Fukaya M, Nishizawa K, Miki T, Taoda H. Test method for skin damage of titania photocatalyst nanoparticles in vitro. *Mater Sci Forum.* 2008;569:9–12. doi:10.4028/www.scientific.net/MSF.569.9
5. Shen B, Scaiano JC, English AM. Zeolite encapsulation decreases TiO_2-photosensitized ROS generation in cultured human skin fibroblasts. *Photochem Photobiol*. 2006;82(1):5–12. doi:10.1562/2005-05-29-RA-551
6. Kuwahara T, Asanami S, Kubo S. Experimental infusion phlebitis: Tolerance osmolality of peripheral venous endothelial cells. *Nutrition*. 1998;14(6):496–501. doi:10.1016/s0899-9007(98)00037-9
7. Fabian E, Landsiedel R, Ma-Hock L, Wiench K, Wohlleben W, van Ravenzwaay B. Tissue distribution and toxicity of intravenously administered titanium dioxide nanoparticles in rats. *Arch Toxicol.* 2008;82(3):151–157. doi:10.1007/s00204-007-0253-y
8. Warheit DB, Hoke RA, Finlay C, Donner EM, Reed KL, Sayes CM. Development of a base set of toxicity tests using ultrafine TiO_2 particles as a component of nanoparticle risk management. *Toxicol Lett.* 2007;171(3):99–110. doi:10.1016/j.toxlet.2007.04.008
9. Warheit DB. How to measure hazards/risks following exposures to nanoscale or pigment-grade titanium dioxide particles. *Toxicol Lett.* 2013;220(2):193–204. doi:10.1016/j.toxlet.2013.04.002
10. Iavicoli I, Leso V, Fontana L, Bergamaschi A. Toxicological effects of titanium dioxide nanoparticles: A review of in vitro mammalian studies. *Eur Rev Med Pharmacol Sci.* 2011;15(5):481–508. doi:10.1155/2012/964381
11. Tang M, Zhang T, Xue Y, et al. Dose dependent in vivo metabolic characteristics of titanium dioxide nanoparticles. *J Nanosci Nanotechnol.* 2010;10(12):8575–8583. doi:10.1166/jnn.2010.2482
12. Han SG, Newsome B, Hennig B. Titanium dioxide nanoparticles increase inflammatory responses in vascular endothelial cells. *Toxicology.* 2013;306:1–8. doi:10.1016/j.tox.2013.01.014
13. Montiel-Dávalos A, Ventura-Gallegos JL, Alfaro-Moreno E, et al. TiO_2 nanoparticles induce dysfunction and activation of human endothelial cells. *Chem Res Toxicol.* 2012;25(4):920–930. doi:10.1021/tx200551u
14. Alinovi R, Goldoni M, Pinelli S, et al. Oxidative and pro-inflammatory effects of cobalt and titanium oxide nanoparticles on aortic and venous endothelial cells. *Toxicol In Vitro.* 2015;29(3):426–437. doi:10.1016/j.tiv.2014.12.007
15. Park J, Bauer S, Schmuki P, von der Mark K. Narrow window in nanoscale dependent activation of endothelial cell growth and differentiation on TiO_2 nanotube surfaces. *Nano Lett.* 2009;9(9):3157–3164. doi:10.1021/nl9013502
16. Ge SN, Chen JY, Leng YX, Huang N. Laminin immobilized on titanium oxide films for enhanced human umbilical vein endothelial cell adhesion and growth. *Key Eng Mater.* 2007;342:305–308. doi:10.4028/www.scientific.net/KEM.342-343.305
17. Thai TP, Houghton PE, Keast DH, Woodbury MG. Ultraviolet C in the treatment of chronic wounds with MRSA: A case study. *Ostomy Wound Manage.* 2002;48(11):52–60. PMID:12426452
18. Dodd HJ, Sarkany I, Gaylarde PM. The short-term benefit and long-term failure of ultraviolet light in the treatment of venous leg ulcers. *Br J Dermatol.* 1989;120(6):809–818. doi:10.1111/j.1365-2133.1989.tb01379.x
19. Hönigsmann H, Szeimies RM, Knobler R, et al. Photochemotherapy and photodynamic therapy. In: Goldsmith LA, Katz SI, Gilchrest BA, Paller AS, Leffell DJ, Wolff K. *Dermatology in General Medicine.* New York, USA: McGraw-Hill; 1999:2477–2493.
20. Elmets CA, Bergstresser PR, Tigelaar RE, Wood PJ, Streilein JW. Analysis of the mechanism of unresponsiveness produced by haptens painted on skin exposed to low dose ultraviolet radiation. *J Exp Med.* 1983;158:781–794. doi:10.1084/jem.158.3.781
21. Walker JG, Stirling J, Beroukas D, et al. Histopathological and ultrastructural features of dermal telangiectasias in systemic sclerosis. *Pathology.* 2005;37(3):220–225. doi:10.1080/00313020500033262
22. Engel A, Johnson ML, Hynes SG. Health effects of sunlight exposure in the United States: Results from the first National Health and Nutrition Examination Survey 1971–1974. *Arch Dermatol.* 1988;124:72–79. doi:10.1001/archderm.1988.01670010036018
23. Cassuto DA, Ancona, DM, Emanuelli G. Treatment of facial telangiectasias with a diode-pumped Nd: YAG laser at 532 nm. *J Cutan Laser Ther.* 2000;2(3):141–146. doi:10.1080/14628830050516399
24. Rabe E, Breu FX, Cavezzi A, et al. European guidelines for sclerotherapy in chronic venous disorders. *Phlebology.* 2014;29(6):338–354. doi:10.1177/0268355513483280
25. Landthaler M, Hohenleutner U. Laser therapy of vascular lesions. *Photodermatol Photoimmunol Photomed.* 2006;22(6):324–332. doi:10.1111/j.1600-0781.2006.00254
26. Goldman MP, Martin DE, Fitzpatrick RE, Ruiz-Esparza J. Pulsed dye laser treatment of telangiectases with and without subtherapeutic sclerotherapy: Clinical and histologic examination in the rabbit ear vein model. *J Am Acad Dermatol.* 1990;23(1):23–30. doi:10.1016/0190-9622(90)70180-p
27. Apfelberg DB, Maser MR, Lash H, White DN, Flores JT. Use of the argon and carbon dioxide lasers for the treatment of superficial venous varicosities of the lower extremity. *Lasers Surg Med.* 1984;4:221–232. doi:10.1002/lsm.1900040302
28. Spendel S, Prandl EC, Schintler MV, et al. Treatment of spider leg veins with the KTP (532 nm) laser: A prospective study. *Lasers Surg Med.* 2002;31(3):194–201. doi:10.1002/lsm.10088
29. Thiruvenkatachari R, Vigneswaran S, Moon IS. A review on UV/TiO_2 photocatalytic oxidation process. *Korean J Chem Eng.* 2008;25(1):64–72. doi:10.1007/s11814-008-0011-8
30. Matthews RW, McEvoy SR. Photocatalytic degradation of phenol in the presence of near-UV illuminated titanium dioxide. *J Photochem Photobiol.* 1992;64(2):231–246. doi:10.1016/1010-6030(92)85110-G
31. Li PG, Yue PL. Photocatalytic oxidation of chlorophenols in single component and multicomponent systems. *Ind Eng Chem Res.* 1999;38(9):3238–3245. doi:10.1021/ie9807598
32. Emerson JA, Whittington JK, Allender MC, Mitchell MA. Effects of ultraviolet radiation produced from artificial lights on serum 25-hydroxyvitamin D concentration in captive domestic rabbits (Oryctolaguscuniculi). *Am J Vet Res.* 2014;75(4):380–384. doi:10.2460/ajvr.75.4.380

33. Lansdown ABG, Taylor A. Zinc and titanium oxides: Promising UV-absorbers but what influence do they have on the intact skin? *Int J Cosmet Sci.* 1997;19(4):167–172. doi:10.1111/j.1467-2494.1997.tb00180.x
34. Galvão LEG. Terapia fotodinâmica com luz do dia: benefício clínico e estético com sessões repetidas para ceratoses actínicas faciais. *Surg Cosmet Dermatol.* 2016;8(4):40–42. doi:10.5935/scd1984-8773.201683103
35. Wan MT, Lin JY. Current evidence and applications of photodynamic therapy in dermatology. *Clin Cosmet Investig Dermatol.* 2014;7:145–163. doi:10.2147/CCID.S35334

MicroRNA-221 inhibits the transition of endothelial progenitor cells to mesenchymal cells via the PTEN/FoxO3a signaling pathway

*En Zhou[1,C–E], *Yinghua Zou[2,C–E], *Chengyu Mao[1,C–E], *Dongjiu Li[1,C–E], Changqian Wang[1,A,F], Zongqi Zhang[1,A,E,F]

[1] Department of Cardiology, Shanghai Ninth People's Hospital, School of Medicine, Shanghai Jiao Tong University, China
[2] Department of Anesthesiology, Shuguang Hospital, Shanghai University of Traditional Chinese Medicine, China

A – research concept and design; B – collection and/or assembly of data; C – data analysis and interpretation;
D – writing the article; E – critical revision of the article; F – final approval of the article

Advances in Clinical and Experimental Medicine, ISSN 1899–5276 (print), ISSN 2451–2680 (online) *Adv Clin Exp Med*. 2021;30(12):1263–1270

Address for correspondence
Zongqi Zhang
E-mail: zqzhangdoctor@126.com

Funding sources
National Natural Science Foundation of China (grant No. 81200206 to ZQ Zhang); Scientific Research and Innovation Project of Shanghai Education Commission (grant No. 12YZ045 to ZQ Zhang); Shanghai Committee of Science and Technology, China (grant No. 18411950500); National Natural Science Foundation of China (grant No. 81870264).

Conflict of interest
None declared

*En Zhou, Yinghua Zou, Chengyu Mao and Dongjiu Li contributed equally to this study.

Received on March 9, 2021
Reviewed on May 16, 2021
Accepted on August 19, 2021

Published online on October 5, 2021

Abstract

Background. Coronary heart disease is one of the most common cardiovascular diseases worldwide and is often associated with vascular endothelial injury. Endothelial–mesenchymal transition (EndMT) is an important process in vascular endothelial injury.

Objectives. This study investigated the function of miR-221 in the EndMT process of endothelial progenitor cells (EPCs).

Materials and methods. Transforming growth factor beta (TGF-β1) was used to induce EndMT in EPCs, and SM22α expression was detected using immunocytochemistry. Western blot was used to detect alpha smooth muscle actin (αSMA) expression, and miR-221 function was evaluated using inhibitors or mimics of the miR-221 sequences that were transfected into EPCs. Reverse transcription polymerase chain reaction (RT-PCR) was used to detect the expression of miR-221 and western blot was used to detect the expression of αSMA, myocardin, phosphatase and tensin homolog (PTEN), p-FoxO3a, and FoxO3a in EPCs. Finally, the expression of the miR-221 target genes was determined using RT-PCR.

Results. The expression of SM22α and αSMA increased in EPCs treated with TGF-β1, while the expression of miR-221 was decreased in EPCs on the 5th day, when compared with the control. The expression of SM22α increased after inhibiting miR-221 in EPCs treated with TGF-β1 and this was reversed by the overexpression of miR-221. The expression of αSMA and myocardin was significantly increased after inhibiting miR-221 in EPCs treated with TGF-β1 and decreased in EPCs overexpressing miR-221. Conversely, PTEN was increased in TGF-β1-treated EPCs and decreased following the overexpression of miR-221. The decrease in phosphorylated-FoxO3a expression in EPCs was accompanied by an increase in αSMA expression, which was reversed in the presence of miR-221 mimics. This effect was nearly abolished following the addition of PTEN cDNA.

Conclusions. The overexpression of miR-221 inhibits EndMT in EPCs, possibly by interacting with PTEN to regulate FoxO3a signaling, to facilitate the repair of the endothelium by EPCs.

Key words: EPC, miR-221, EndMT, PTEN/FoxO3a

Cite as
Zhou E, Zou Y, Mao C, Li D, Wang C, Zhang Z. MicroRNA-221 inhibits the transition of endothelial progenitor cells to mesenchymal cells via the PTEN/FoxO3a signaling pathway. *Adv Clin Exp Med*. 2021;30(12):1263–1270. doi:10.17219/acem/141446

DOI
10.17219/acem/141446

Background

Coronary heart disease is one of the most common cardiovascular diseases worldwide and is caused by vascular endothelial injury. It has been demonstrated that once the vascular endothelium is damaged, the endothelial progenitor cells (EPCs) migrate from the bone marrow (BM) to the ischemic tissue and differentiate into mature vascular endothelial cells in an attempt to repair the injured site.[1] However, accumulating evidence suggests that EPCs contribute to intimal hyperplasia during this process. For example, BM-derived EPCs have been shown to augment intimal hyperplasia by migrating into the intima of balloon-injured carotid arteries,[2] and our previous study showed that BM-derived EPCs can transdifferentiate into smooth muscle lineage cells that are positive for alpha smooth muscle actin (αSMA), producing an endothelial-to-mesenchymal transition (EndMT).[3] These results suggest that the EndMT capacity of EPCs may contribute to intimal hyperplasia. This is further supported by evidence that EndMT increases the thickness of the intimal layer in pulmonary arteries.[4] However, the mechanisms underlying the EndMT process in EPCs have not yet been fully elucidated.

MicroRNAs (miRs) are short (only 21–23 nucleotides), highly conserved, non-coding RNA sequences that bind to the 3'-untranslated region of a variety of mRNA targets and function to regulate gene expression at the post-transcriptional level by inhibiting the translation or promoting mRNA degradation.[5,6] Previous microarray-based expression profiles have shown that several miRs are expressed in EPCs, including miR-126, miR-21, miR-27a, and miR-221.[7,8] Furthermore, some studies have shown that both miR-21 and miR-127 are involved in mature endothelial cell EndMT that can be induced by TGF-β1 and TGF-β2.[8,9] In addition, miR-221, an endothelial-specific miR, has been shown to exert anti-angiogenic, anti-inflammatory and pro-apoptotic effects by targeting both ZEB2 and Ets-1.[10,11] Finally, miR-221 maintains the angiogenic capacity of EPCs by inhibiting p27 expression.[12] However, few studies have described the role of miR-221 in the EndMT process of EPCs.

Previous investigations have confirmed that phosphatase and tensin homolog (PTEN) is a direct target of miR-221.[13] In vascular endothelial cells, downregulation of miR-221 decreased cell viability, migration and invasion, while all of these effects were reversed in response to the overexpression of PTEN.[13] Furthermore, recent studies have shown that a decrease in PTEN activates the phosphorylation of FoxO3a.[14,15] In our previous study, we showed that phosphorylated FoxO3a plays an inhibitory role in EndMT by inactivating the Smad3/4 pathway in the nucleus of EPCs.[16] Given this, we hypothesized that the activation of the miR-221/PTEN/FoxO3a pathway may inhibit EndMT in EPCs.

Objectives

This study was designed to determine the function of miR-221 in the EndMT process of EPCs and to explore the potential signaling pathways underlying these functions.

Materials and methods

Ethical approval

All animal experiments were approved by the Animal Research Ethics Committee of the No. 9 People's Hospital affiliated with the Shanghai Jiao Tong University School of Medicine, Shanghai, China. All animals were sacrificed using bilateral thoracotomy during anesthesia.

Cell isolation and culture

Bone marrow-derived EPCs were isolated from male Sprague Dawley rats, as described previously.[2] Ficoll-Isopaque Plus (Histopaque-1077; Sigma-Aldrich, St. Louis, USA) density gradient centrifugation was used to isolate mononuclear cells from rat bone marrow. The cells were cultured in endothelial cell growth medium (EGM2; Lonza, Basel, Switzerland) consisting of endothelial cell basal medium-2 (EBM-2), supplemented with 20% fetal bovine serum (FBS). Cells were then cultured on a fibronectin-coated dish at 37°C in a 5% CO_2 incubator. The medium was removed after 4–7 days, and cells were gently washed with phosphate-buffered solution (PBS). The attached cells were then used for further experiments. The CD31 fluorescence staining was then performed as previously described[7] to identify vascular endothelial cells.

Inducing EndMT in EPCs

Endothelial progenitor cell EndMT was induced as previously described.[17] Briefly, the cells were seeded on culture plates in Ham's F-12 media containing 5% FBS, and then treated with TGF-β1 (5 ng/mL) for 7 days.

Immunocytochemistry

The EPCs were cultured on cell slides and then rinsed with PBS, before being fixed with 4% paraformaldehyde phosphate buffer for 15 min at room temperature. Slides were then blocked for 2 h in PBS containing 5% normal goat serum and 2% bovine serum albumin (BSA), and incubated with monoclonal antibodies (diluted 1:500) against SM22α (Cat. No. SAB1400272; Sigma-Aldrich) overnight at 4°C. Cells were washed 5 times in PBS and incubated with AlexaFluor® 594-conjugated goat anti-mouse/rabbit antibody diluted 1:500 (Santa Cruz Biotechnology, Dallas, USA) for 1 h at room temperature. The mean fluorescence intensity of SM22α was

evaluated using ImageJ software (RRID:SCR_003070; National Institutes of Health (NIH), Bethesda, USA).

Real-time PCR

Total RNA was isolated from EPCs using TRIzol reagent (Cat. No. 10296028, Lot No. 79348502; Life Technologies, Carlsbad, USA), as described in the manufacturer's instructions. Extracted RNA was then reverse transcribed to cDNA using a Thermo Cycler (Applied Biosystems, Waltham, USA) and real-time polymerase chain reaction (RT-PCR) was performed using a real-time PVR machine (LightCycler 480 II; Roche, Basel, Switzerland). The mRNA was quantified using a TaKaRa reverse transcription assay (Cat. No. R0037A; TaKaRa, Tokyo, Japan) and SYGRII (Cat. No. RR820A; TaKaRa). Gene-specific primers were synthesized by Sangon Biotech (Shanghai, China) and mRNA levels were quantified using the $2^{-\Delta\Delta ct}$ method (Table 1).

Transfection

The miR-221 mimics and inhibitors were synthesized using the Qiagen (Hilden, Germany) reagents and the miR-221 mimic sequence was set as 5'-AGCUACAUUGUCUGCUGGGUUUC-3'. The gene ID of PTEN in National Center for Biotechnology Information (NCBI) was NM_000314 and both, the PTEN cDNA and siRNAs, were synthesized by Sangon Biotech. Cells were seeded in six-well plates and transfected with the miR-221 mimic, miR-221 inhibitor or their negative controls using Lipofectamine 3000 transfection reagent (Cat. No. 11668019; Invitrogen, Carlsbad, USA) according to the manufacturer's instructions. Transfections were performed on days 4 and 7. All subsequent experiments were performed 24 h after the final transfection.

Western blot

Total protein from the EPCs was extracted using radioimmunoprecipitation assay (RIPA) buffer and then separated using 10% sodium dodecyl sulfate polyacrylamide gel electrophoresis (SDS-PAGE) before being transferred to polyvinylidene fluoride (PVDF) membranes using electrophoresis, and probed with primary antibodies against αSMA (Cat. No. CBL171; Merck Millipore, Billerica, USA), myocardin (Cat. No. 14760S; Cell Signaling Technology, Danvers, USA), PTEN (Cat. No. sc-7974; Santa Cruz Biotechnology, Dallas, USA), p-FoxO3a (Cat. No. sc-101683; Santa Cruz Biotechnology), FoxO3a (Cat. No. 2497s, Cell Signaling Technology), and β-actin (Cat. No. 3700; Cell Signaling Technology). Appropriate horseradish peroxidase (HRP)-conjugated secondary antibodies were then used to facilitate visualization, and protein bands were detected using an electrochemiluminescence (ECL) system (Fusion FX7; Vilber, Lemont, USA).

Statistical analyses

All data were initially tested using the one-sample Kolmogorov–Smirnov normality test and F-test. This highlighted that not all data were normally distributed and that some data variance was uneven. All experiments were repeated 5 times and therefore we used the more reliable nonparametric tests. The data were expressed as maximum, minimum, median, percentiles 25, and percentiles 75, and analyzed with the Kruskal–Wallis H test followed by a Mann–Whitney U test for post hoc comparison, using the SPSS v. 13.0 software (SPSS Inc., Chicago, USA). The values of $p \leq 0.05$ were considered statistically significant.

Results

TGF-β1 induces EndMT in EPCs

Endothelial progenitor cells were identified as described in our previous research.[7] The cells cultured from mononuclear cells showed a cobblestone-like appearance, while EPCs treated with TGF-β1 showed a spindle-shaped appearance (Fig. 1A,B). Immunofluorescent staining showed that EPCs treated with TGF-β1 had a high SM22α expression (Fig. 1C,D) and the expression of αSMA also increased in response to TGF-β1 (Fig. 1E).

miR-221 expression was decreased following EPC EndMT

The miR-221 expression continuously increased in EPCs cultured in medium without TGF-β1. In contrast, when

Table 1. The primer sequences used for this investigation

Gene	Forward 5′ → 3′	Reverse 5′ → 3′
miR-221	CGCGAGCTACATTGTCTGCTG	AGTGCAGGGTCCGAGGTATT
PTEN	TTGAAGACCATAACCCACCACAGC	CATTACACCAGTCCGTCCTTTCCC
PIK3R1	ACTGAAGCAGATGTTGAACAAC	CATCGATCATTTCCAAGTCCAC
FoxO3a	TGGACGCCTGGACCGACTTC	GCTCCGTGCTCGCCAAGATG
ESR1	CTGCTGCTGGAGATGCTGGATG	CTGGCTCTGGCTAGGCTCCTC
MMP-1	TGTTCGCCTTCTACAGAGGAGACC	CTGGTGGGAATGTGTGAGCAAGTC
GAPDH	GACATGCCGCCTGGAGAAAC	AGCCCAGGATGCCCTTTAGT

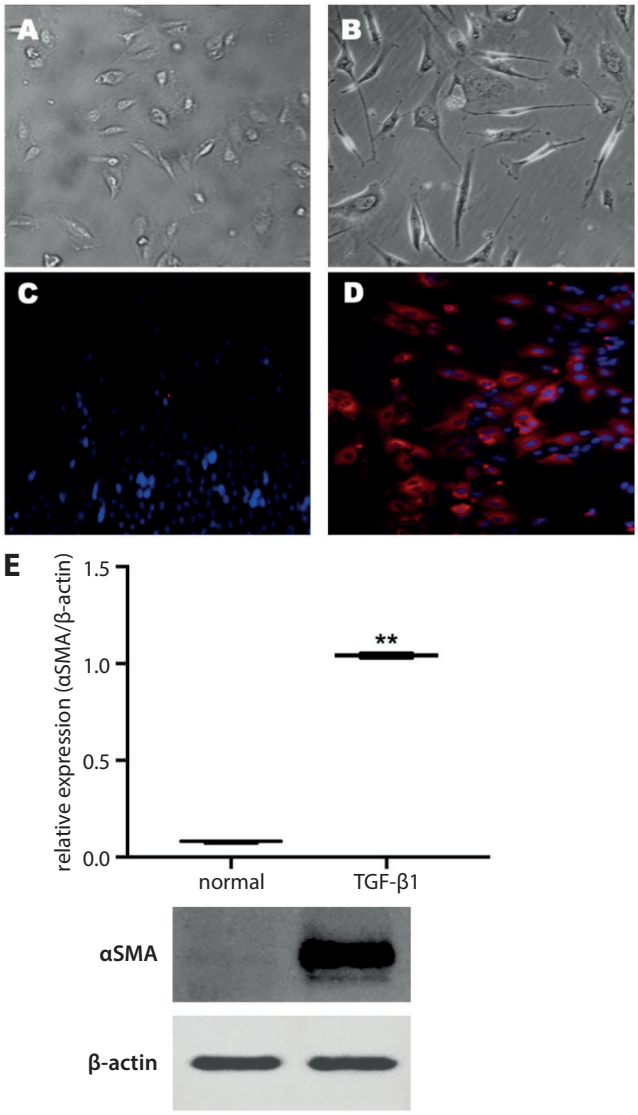

Fig. 1. TGF-β1 induces endothelial–mesenchymal transition (EndMT) in endothelial progenitor cells (EPCs). A and B. Morphology of EPCs under a light microscope; A. EPCs cultured in endothelial cell basal medium-2 (EBM-2) containing 20% fetal bovine serum (FBS); B. The EPCs treated with TGF-β1; C and D. Immunofluorescence staining of SM22α in EPCs (red: SM22α; blue: DAPI); C. The EPCs cultured in EBM-2 containing 20% FBS; D. The EPCs treated with TGF-β1; E. The expression of αSMA in EPCs with or without TGF-β1 was detected with western blot (data expressed as maximum, minimum, median, percentiles 25 and percentiles 75, and analyzed with Kruskal–Wallis H test followed by Mann–Whitney U test for post hoc comparison using the SPSS v. 13.0 software). Normal – EPCs cultured in EBM-2 containing 20% FBS; TGFβ1 – EPCs treated with TGF-β1; **p < 0.01

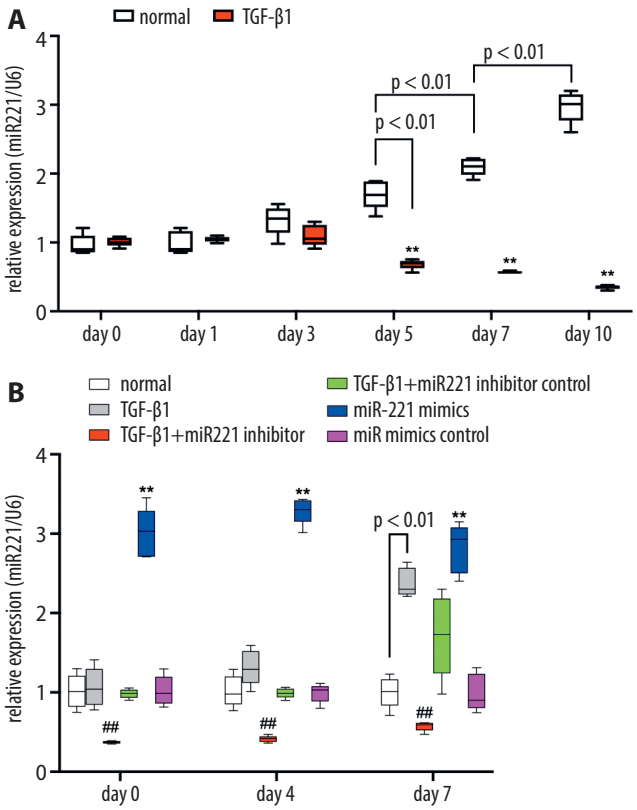

Fig. 2. The expression of miR-221 in endothelial progenitor cells (EPCs) during endothelial–mesenchymal transition (EndMT). A. The expression of miR-211 in EPCs with or without TGF-β1 over 10 days and detected with reverse transcription polymerase chain reaction (RT-PCR). Normal – EPCs cultured in endothelial cell basal medium-2 (EBM-2) containing 20% fetal bovine serum (FBS); TGFβ1 – EPCs treated with TGF-β1; **normal cpmpared to TGF-β1, p < 0.01; B. The expression of miR-221 every 3 days following the treatment with miR-221 mimics and inhibitors as detected with RT-PCR. The data were expressed as maximum, minimum, median, percentiles 25 and percentiles 75, and analyzed with Kruskal–Wallis H test, followed by Mann–Whitney U test for post hoc comparison. Normal – EPCs cultured in EBM-2 containing 20% FBS; TGFβ1 – EPCs treated with TGF-β1; TGFβ1 + miR-221 inhibitor – EPCs transfected with miR-221 inhibitor then treated with TGF-β1; TGFβ1 + miR-221 inhibitor control – EPCs transfected with the negative control of miR-221 inhibitor then treated with TGF-β1; miR-221 mimics – EPCs cultured in EBM-2 containing 20% FBS and transfected with miR-221 mimics; miR-221 mimics control – EPCs cultured in EBM-2 containing 20% FBS and transfected with the negative control of miR-221 mimics; ** normal compared to miR-221 mimics, p < 0.01; ## TGF-β1 compared to TGF-β1 + miR-221 inhibitor, p < 0.01

EPCs were treated with TGF-β1, the miR-221 expression remained comparable over the first 3 days and then began to gradually decrease compared to controls (Fig. 2A).

Overexpression of miR-221 inhibits TGF-β1-induced EndMT of EPCs

To demonstrate the role of miR-221 in EPC EndMT, EPCs were transfected with either a miR-221 inhibitor or miR-221 mimic (Fig. 2B), and then treated with TGF-β1. Endothelial progenitor cells transfected with the miR-221 inhibitor exhibited a spindle-shaped appearance, while EPCs transfected with miR-221 mimics presented with a cobblestone-like appearance (Fig. 3A–C). Immunofluorescent staining revealed that the SM22α expression significantly increased or decreased in response to the miR-221 inhibitor or miR-221 mimic, respectively (Fig. 3D–G). The expression of both αSMA and myocardin was significantly increased in the presence of the miR-221 inhibitor and attenuated in the presence of miR-221 mimics in EPCs treated with TGF-β1 (Fig. 4A,B).

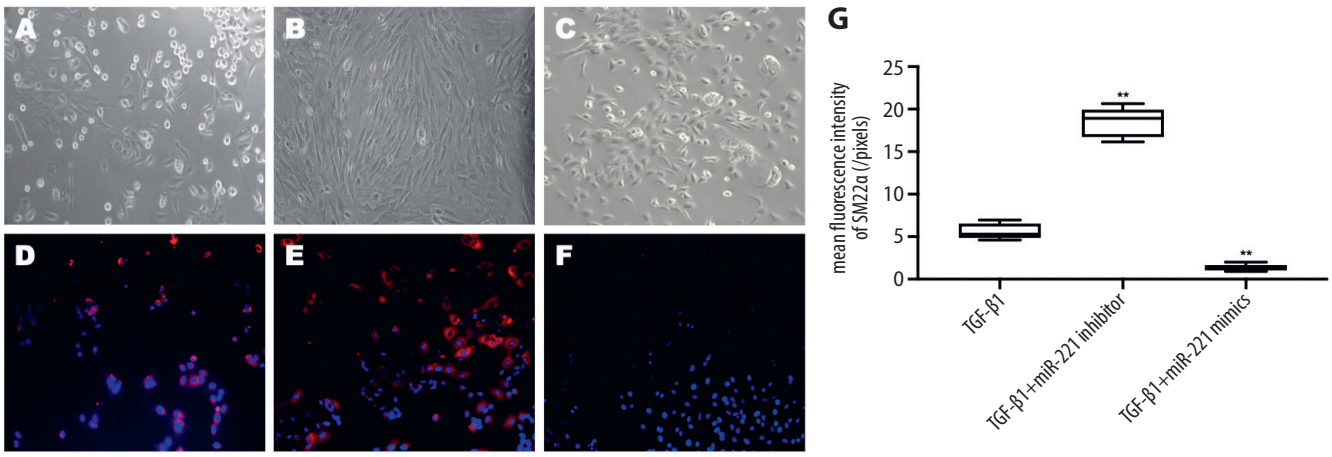

Fig. 3. Morphological and SM22α expression changes in endothelial progenitor cells (EPCs) following miR-221 overexpression or silencing during endothelial–mesenchymal transition (EndMT). A–C. Morphological changes in EPCs evaluated using light microscopy; A. The EPCs treated with TGF-β1; B. The EPCs transfected with miR-221 inhibitors and treated with TGF-β1; C. The EPCs transfected with miR-221 mimics and treated with TGF-β1; D–F. Immunofluorescence staining of SM22α in EPCs. The expression of SM22α in EPCs during EndMT following miR-221 overexpression or silencing; D. The EPCs treated with TGF-β1; E. Silencing of miR-221 in EPCs treated with TGF-β1; F. Overexpression of miR-221 in EPCs treated with TGF-β1; G. Mean fluorescence intensity of SM22α in EPCs following miR-221 overexpression or silencing during EndMT. Data expressed as maximum, minimum, median, percentiles 25 and percentiles 75, and analyzed with Kruskal–Wallis H test followed by Mann–Whitney U test for post hoc comparison. TGFβ1 – EPCs treated with TGF-β1; TGFβ1 + miR-221 inhibitor – EPCs transfected with miR-221 inhibitor and treated with TGF-β1; TGFβ1 + miR-221 mimics – EPCs transfected with miR-221 mimics and treated with TGF-β1; **p < 0.01

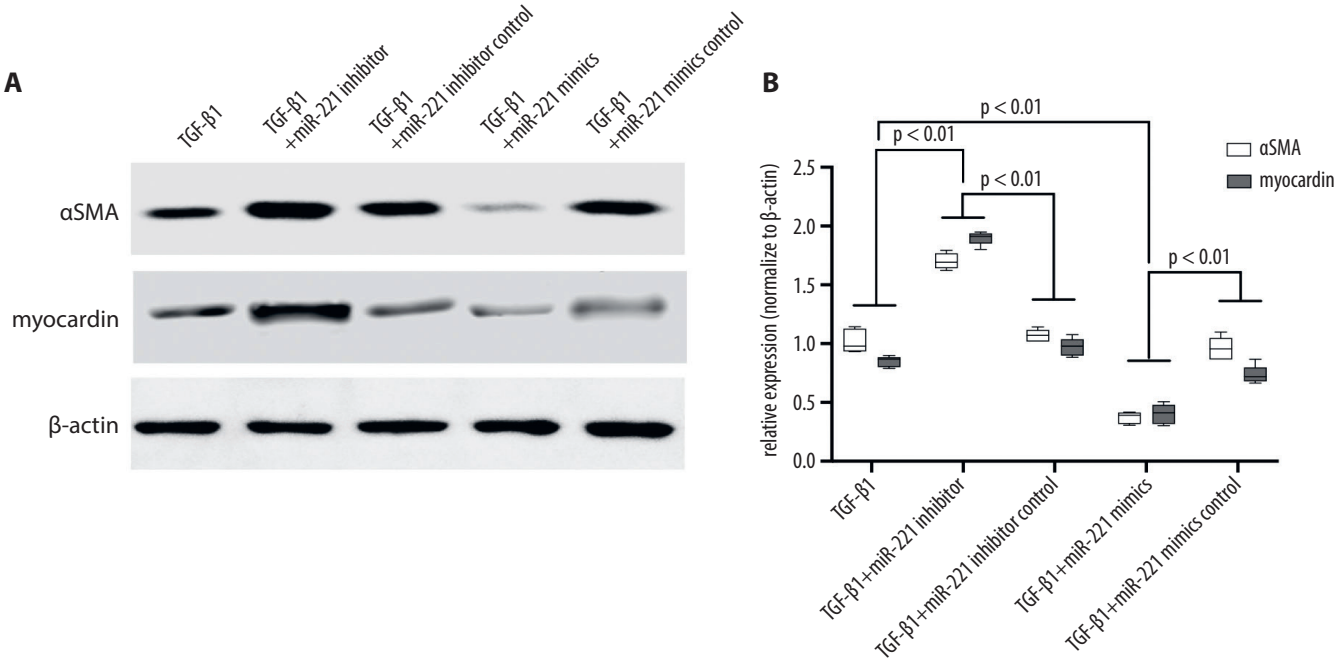

Fig. 4. Expression of αSMA and myocardin in endothelial progenitor cells (EPCs) undergoing endothelial–mesenchymal transition (EndMT). A. Western blot describing αSMA and myocardin expression during EndMT in EPCs; B. The relative expression of αSMA and myocardin under these conditions. Data expressed as maximum, minimum, median, percentiles 25 and percentiles 75, and analyzed with Kruskal–Wallis H test followed by Mann–Whitney U test for post hoc comparison. TGFβ1 – EPCs treated with TGF-β1; TGFβ1 + miR221 inhibitor – EPCs transfected with miR-221 inhibitor then treated with TGF-β1; TGFβ1 + miR221 inhibitor control – EPCs transfected with the negative control of miR-221 inhibitor and treated with TGF-β1; TGFβ1 + miR221 mimics – EPCs transfected with miR-221 mimics and treated with TGF-β1; TGFβ1 + miR221 mimics control – EPCs transfected with the negative control of miR-221 mimics and treated with TGF-β1

miR-221 regulates the PTEN/FoxO3 signaling pathways in TGF-β1-induced EndMT

The expression of several potential targets of miR-221 in EPCs undergoing TGF-β1-dependent EndMT was assessed with RT-PCR. The expression of PTEN was shown to be significantly higher in EPCs treated with TGF-β1, while the expression of PIK3R1, FoxO3a, ESR1, and MMP-1 was comparable between the 2 groups (Fig. 5A). The expression of αSMA was increased in TGF-β1-treated EPCs and was attenuated in response to PTEN siRNA. However,

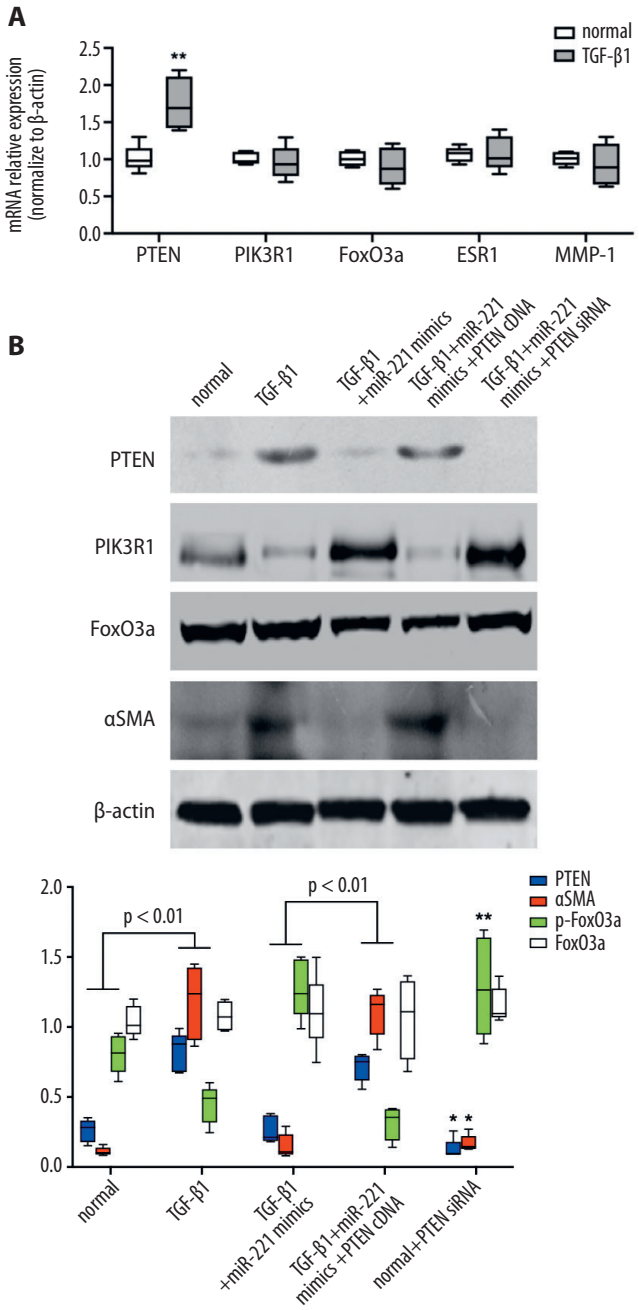

Fig. 5. Expression of miR-221 related genes in endothelial progenitor cells (EPCs) during endothelial–mesenchymal transition (EndMT). A. The expression of phosphatase and tensin homolog (PTEN), PI3KR1, FoxO3a, ESR1, and MMP-1 during EndMT was detected with reverse transcription polymerase chain reaction (RT-PCR). Normal – EPCs cultured in endothelial cell basal medium-2 (EBM-2) containing 20% fetal bovine serum (FBS); TGFβ1 – EPCs treated with TGF-β1, **p < 0.01; B. Western blot evaluating PTEN, p-FoxO3a, FoxO3a, and αSMA expression. Data expressed as maximum, minimum, median, percentiles 25 and percentiles 75, and analyzed with Kruskal–Wallis H test followed by Mann–Whitney U test for post hoc comparison. Normal – EPCs cultured in EBM-2 containing 20% FBS; TGFβ1 – EPCs treated with TGF-β1; TGFβ1 + miR221 mimics – miR-221 overexpressing EPCs treated with TGF-β1; TGFβ1 + miR221 mimics + PTEN cDNA – miR-221 and PTEN overexpressing EPCs treated with TGF-β1; normal + PTEN siRNA – PTEN silenced EPCs cultured in EBM-2 containing 20% FBS; *normal compared to normal + PTEN siRNA 5, p < 0.05; **normal compared to normal + PTEN siRNA, p < 0.01

the increase in αSMA expression was significantly attenuated by the addition of miR-221 mimics in EPCs treated with TGF-β1, which was reversed in response to PTEN cDNA (Fig. 5B). At the same time, the total expression of FoxO3a remained unchanged. However, phosphorylated FoxO3a expression was notably reduced in response to TGF-β1, which was reversed following the addition of the miR-221 mimics. This reversal was nearly completely abolished following the addition of the PTEN cDNA. In addition, the phosphorylation of FoxO3a was significantly augmented in EPCs treated with PTEN siRNA compared to normal cells (Fig. 5B).

Discussion

It has been widely reported that EPCs are beneficial in the treatment of coronary heart disease, as these cells can differentiate into mature vascular endothelial cells. However, accumulating evidence suggests that EPCs can also differentiate into mesenchymal cells, which may aggravate intimal hyperplasia and contribute to atherogenesis.[18,19] Several studies have shown that TGF-β1 induces the EndMT process in EPCs in vitro. However, only half of the EPCs transplanted into the impaired endothelium were transformed into smooth muscle cells (SMCs) following TGF-β1 treatment, while the others acted to enhance intimal hyperplasia in vivo.[2] These results suggest that the EndMT process in EPCs can be regulated. In this study, we found that a deficiency in miR-221 may facilitate TGF-β1-dependent EndMT in EPCs. Furthermore, miR-221 inhibits the EndMT process by interacting with PTEN, which regulates PTEN/FoxO3 signaling.

The SM22α and αSMA are mesenchymal markers used to detect EndMT in EPCs, as described previously.[7] In this study, the expression of SM22α and αSMA significantly increased in EPCs after the treatment with TGF-β1, suggesting that EPCs underwent EndMT.[7] It has also been reported that EPCs derived from rat bone marrow are able to undergo EndMT after treatment with TGF-β1,[2] while human circulating EPCs only differentiated into mesenchymal cells following direct contact with smooth muscle cells,[19] indicating a complex regulatory system in different tissues.

Some studies have reported that miRs are closely associated with cellular transdifferentiation. The miRNA-221 exerts anti-angiogenic, anti-inflammatory and pro-apoptotic effects in EPCs through their interactions with ZEB2 and Ets-1.[10,11] In ectopic endometrial tissues and ectopic endometrial stromal cells, the inhibition of miR-221 expression leads to decreased cellular proliferation.[20] In our study, we found that the expression of miR-221 was markedly decreased for up to 5 days following TGF-β1 treatment, and was accompanied by an increase in αSMA expression. This suggests that miR-221 is involved in the EndMT process of EPCs.

To determine the role of miR-221 in EndMT, miR-221 inhibitor or mimics were repeatedly transfected into EPCs following TGF-β1 treatment on days 1, 4 and 7, to induce either upregulation or downregulation of miR-221. As a result, the expression of SM22α, αSMA and myocardin in EPCs undergoing EndMT was either increased or decreased following transfection with miR-221 inhibitors and miR-221 mimics, respectively. The previous study suggests that myocardin plays a critical role in the development of cardiac myocytes and vascular SMCs. Loss of myocardin results in a synthetic, dedifferentiated phenotype that leads to atherosclerosis.[21] These results suggest that miR-221 inhibits the EndMT process in EPCs by suppressing the expression of αSMA and myocardin.

Previous studies have also reported that the PI3K/Akt/FoxO3 signaling pathway plays an important role in the self-renewal of hematopoietic stem cells.[22] In our previous study, we also found that miR-126 targets PI3KR2 to inhibit EPC EndMT through the PI3K/Akt/FoxO3 pathway.[7] In this study, we evaluated several potential target genes for miR-221, including *PTEN*, *PI3KR1*, *FoxO3a*, *ESR1*, and *MMP-1*, in EPCs undergoing EndMT. We found that the expression of PTEN was increased in EPCs treated with TGF-β1, while its expression was inhibited by overexpression of miR-221. The expression levels of *PI3KR2*, *FoxO3a*, *ESR1*, and *MMP-1* were comparable between the 2 groups. These results suggest that PTEN might be a target of miR-221 and regulate the EndMT process in EPCs. This was supported by the finding that miR-221 overexpression amplified PI3K signaling to promote precursor B-cell retention by targeting PTEN.[23]

In addition, we found that FoxO3a expression was slightly decreased in EPCs treated with TGF-β1. A downstream effector of the PTEN/Akt pathway, FoxO3a, is localized within the nucleus, where it drives transcription. However, when phosphorylated, the protein translocates to the cytoplasm.[24] One example of this kind of regulation can be seen in the differential regulation of onco- and anti-oncogene expression in cells following the nuclear translocation of phosphorylated AKT.[14,25] Interestingly, we found that the expression of phosphorylated FoxO3a (p-FoxO3a) was significantly increased when PTEN was suppressed, while overexpression of PTEN led to the inhibition of p-FoxO3a expression. This further suggests that PTEN decreases the phosphorylation of FoxO3a, thereby suppressing its nuclear translocation in EPCs undergoing TGF-β1-dependent EndMT. Furthermore, we found that miR-221 overexpression led to a decrease in PTEN expression and an increase in αSMA expression, both of which were reversed by PTEN overexpression. Finally, our previous study demonstrated that the phosphorylation of FoxO3a negatively regulates EPC EndMT.[7] Taken together, these findings suggest that miR-221 may lead to PTEN downregulation and the activation of the FoxO3a signaling pathway, thereby inhibiting the EndMT process in EPCs.

Limitations

In the present study, we report that the overexpression of miR-221 inhibits EndMT in EPCs, but as all experiments in this study were conducted in vitro, there should be some focus on validating these findings in vivo. We believe that miR-221 interacts with PTEN to regulate FoxO3a/Smad4 transcription, but we did not evaluate Smad4 expression in this study, as these observations were recorded in our previous paper.[7] Our findings suggest that miR-221 may be a potential target during the treatment of in-stent restenosis in coronary artery disease, and facilitate the inhibition of intimal hyperplasia through EndMT signaling.

Conclusions

In summary, we found that the overexpression of miR-221 inhibited EndMT in EPCs. This phenomenon is likely the result of the interaction between miR-221 and its target gene, *PTEN*, effecting a change in the regulation of FoxO3a phosphorylation.

ORCID iDs

En Zhou https://orcid.org/0000-0002-6073-8037
Yinghua Zou https://orcid.org/0000-0002-6596-8720
Chengyu Mao https://orcid.org/0000-0001-9740-8835
Dongjiu Li https://orcid.org/0000-0003-4372-6613
Changqian Wang https://orcid.org/0000-0002-7611-7761
Zongqi Zhang https://orcid.org/0000-0001-6785-2038

References

1. Toya SP, Malik AB. Role of endothelial injury in disease mechanisms and contribution of progenitor cells in mediating endothelial repair. *Immunobiology*. 2012;217(5):569–580. doi:10.1016/j.imbio.2011.03.006
2. Imamura H, Ohta T, Tsunetoshi K, et al. Transdifferentiation of bone marrow-derived endothelial progenitor cells into the smooth muscle cell lineage mediated by tansforming growth factor-beta1. *Atherosclerosis*. 2010;211(1):114–121. doi:10.1016/j.atherosclerosis.2010.02.040
3. Hong L, Du X, Li W, Mao Y, Sun L, Li X. EndMT: A promising and controversial field. *Eur J Cell Biol*. 2018;97(7):493–500. doi:10.1016/j.ejcb.2018.07.005
4. Peinado VI, Ramírez J, Roca J, Rodriguez-Roisin R, Barberà JA. Identification of vascular progenitor cells in pulmonary arteries of patients with chronic obstructive pulmonary disease. *Am J Respir Cell Mol Biol*. 2006;34(3):257–263. doi:10.1165/rcmb.2005-0255OC
5. Lee Y, Kim M, Han J, et al. MicroRNA genes are transcribed by RNA polymerase II. *EMBO J*. 2004;23(20):4051–4060. doi:10.1038/sj.emboj.7600385
6. Cai X, Hagedorn CH, Cullen BR. Human microRNAs are processed from capped, polyadenylated transcripts that can also function as mRNAs. *RNA*. 2004;10(12):1957–1966. doi:10.1261/rna.7135204
7. Zhang J, Zhang Z, Zhang DY, Zhu J, Zhang T, Wang C. microRNA 126 inhibits the transition of endothelial progenitor cells to mesenchymal cells via the PIK3R2-PI3K/Akt signalling pathway. *PloS One*. 2013;8(12):e83294. doi:10.1371/journal.pone.0083294
8. Kumarswamy R, Volkmann I, Jazbutyte V, Dangwal S, Park DH, Thum T. Transforming growth factor-β-induced endothelial-to-mesenchymal transition is partly mediated by microRNA-21. *Arterioscler Thromb Vasc Biol*. 2012;32(2):361–369. doi:10.1161/atvbaha.111.234286
9. Ghosh AK, Nagpal V, Covington JW, Michaels MA, Vaughan DE. Molecular basis of cardiac endothelial-to-mesenchymal transition (EndMT): Differential expression of microRNAs during EndMT. *Cell Signal*. 2012;24(5):1031–1036. doi:10.1016/j.cellsig.2011.12.024

10. Chen Y, Banda M, Speyer CL, Smith JS, Rabson AB, Gorski DH. Regulation of the expression and activity of the antiangiogenic homeobox gene *GAX/MEOX2* by ZEB2 and microRNA-221. *Mol Cell Biol*. 2010; 30(15):3902–3913. doi:10.1128/mcb.01237-09
11. Zhu N, Zhang D, Chen S, et al. Endothelial enriched microRNAs regulate angiotensin II-induced endothelial inflammation and migration. *Atherosclerosis*. 2011;215(2):286–293. doi:10.1016/j.atherosclerosis.2010.12.024
12. Ni HZ, Liu Z, Sun LL, et al. Metformin inhibits angiogenesis of endothelial progenitor cells via miR-221-mediated p27 expression and autophagy. *Future Med Chem*. 2019;11(17):2263–2272. doi:10.4155/fmc-2019-0017
13. Peng H, Yang H, Xiang X, Li S. MicroRNA-221 participates in cerebral ischemic stroke by modulating endothelial cell function by regulating the PTEN/PI3K/AKT pathway. *Exp Ther Med*. 2020;19(1):443–450. doi:10.3892/etm.2019.8263
14. Zhang Q, Li X, Li Y, et al. Expression of the PTEN/FOXO3a/PLZF signalling pathway in pancreatic cancer and its significance in tumourigenesis and progression. *Invest New Drugs*. 2020;38(2):321–328. doi:10.1007/s10637-019-00791-7
15. Mziaut H, Henniger G, Ganss K, et al. MiR-132 controls pancreatic beta cell proliferation and survival through Pten/Akt/Foxo3 signaling. *Mol Metab*. 2020;31:150–162. doi:10.1016/j.molmet.2019.11.012
16. Zhang Z, Zhang T, Zhou Y, et al. Activated phosphatidylinositol 3-kinase/Akt inhibits the transition of endothelial progenitor cells to mesenchymal cells by regulating the forkhead box subgroup O-3a signaling. *Cell Physiol Biochem*. 2015;35(4):1643–1653. doi:10.1159/000373978
17. Moonen JR, Krenning G, Brinker MG, Koerts JA, van Luyn MJ, Harmsen MC. Endothelial progenitor cells give rise to pro-angiogenic smooth muscle-like progeny. *Cardiovasc Res*. 2010;86(3):506–515. doi:10.1093/cvr/cvq012
18. Rotmans JI, Heyligers JM, Verhagen HJ, et al. In vivo cell seeding with anti-CD34 antibodies successfully accelerates endothelialization but stimulates intimal hyperplasia in porcine arteriovenous expanded polytetrafluoroethylene grafts. *Circulation*. 2005;112(1): 12–18. doi:10.1161/CIRCULATIONAHA.104.504407
19. Diez M, Musri MM, Ferrer E, Barbera JA, Peinado VI. Endothelial progenitor cells undergo an endothelial-to-mesenchymal transition-like process mediated by TGFbetaRI. *Cardiovasc Res*. 2010;88(3):502–511. doi:10.1093/cvr/cvq236
20. Du XH, Shi G, Lü DH, et al. The expression of microRNA-221 in endometriosis and its impact on endometrial stromal cells [in Chinese]. *Sichuan Da Xue Xue Bao Yi Xue Ban*. 2018;49(4):546–550. PMID:30378307
21. Xia XD, Zhou Z, Yu XH, Zheng XL, Tang CK. Myocardin: A novel player in atherosclerosis. *Atherosclerosis*. 2017;257:266–278. doi:10.1016/j.atherosclerosis.2016.12.002
22. Miyamoto K, Araki KY, Naka K, et al. Foxo3a is essential for maintenance of the hematopoietic stem cell pool. *Cell Stem Cell*. 2007;1(1): 101–112. doi:10.1016/j.stem.2007.02.001
23. Petkau G, Kawano Y, Wolf I, Knoll M, Melchers F. MiR221 promotes precursor B-cell retention in the bone marrow by amplifying the PI3K-signaling pathway in mice. *Eur J Immunol*. 2018;48(6):975–989. doi:10.1002/eji.201747354
24. Wang K, Li PF. Foxo3a regulates apoptosis by negatively targeting miR-21. *J Biol Chem*. 2010;285(22):16958–16966. doi:10.1074/jbc.M109.093005
25. Jang H, Lee OH, Lee Y, et al. Melatonin prevents cisplatin-induced primordial follicle loss via suppression of PTEN/AKT/FOXO3a pathway activation in the mouse ovary. *J Pineal Res*. 2016;60(3):336–347. doi:10.1111/jpi.12316

Identification and functional analysis of changes to the ox-LDL-induced microRNA-124-3p/*DLX5* axis in vascular smooth muscle cells

Chunwen Jia[A–D], Feng Gao[A,C–F], Yanan Zhao[B,C], Siyang Ji[C,D], Shidao Cai[B,D]

Department of Cardiology, Zhongshan Hospital affiliated to Xiamen University, China

A – research concept and design; B – collection and/or assembly of data; C – data analysis and interpretation;
D – writing the article; E – critical revision of the article; F – final approval of the article

Advances in Clinical and Experimental Medicine, ISSN 1899–5276 (print), ISSN 2451–2680 (online) *Adv Clin Exp Med*. 2021;30(12):1271–1281

Address for correspondence
Feng Gao
E-mail: fenggao_xmhos@163.com

Funding sources
The study was supported by departmental funds provided by Department of Cardiology, Zhongshan Hospital, affiliated to Xiamen University (grant No. ZSYY-XN-res-201806).

Conflict of interest
None declared

Received on March 25, 2021
Reviewed on August 17, 2021
Accepted on August 25, 2021

Published online on October 27, 2021

Abstract

Background. The microRNA (miR)–mRNA axes involved in oxidized low-density lipoprotein (ox-LDL)-induced vascular smooth muscle cells (VSMCs) proliferation/apoptosis imbalance need to be investigated in more detail.

Objectives. To investigate the function and any relevant changes to miR–mRNA axes in the ox-LDL-induced proliferation/apoptosis imbalance in VSMCs.

Materials and methods. Human VSMCs were cultured and treated with ox-LDL in vitro. The differentially expressed (DE) miRs and mRNAs in VSMCs following 48-h ox-LDL treatment were detected using RNA sequencing. Candidate miRs and mRNAs were further selected, based on comprehensive bioinformatics analysis. Changes in the expression of candidate miRs and mRNAs in ox-LDL-treated VSMCs were confirmed with quantitative real-time polymerase chain reaction (RT-qPCR) and western blot. The inhibitory effect of candidate miRs on mRNAs were demonstrated using a dual luciferase reporter assay. The functional role of candidate miRs and mRNAs on proliferation, cell cycle and apoptosis of VSMCs were estimated using cell couting kit-8 (CCK-8) and flow cytometry assays, respectively.

Results. The RNA sequencing data indicated that 577 mRNAs and 81 miRs were significantly upregulated in VSMCs following ox-LDL treatment. Gene function and pathway enrichment analysis suggested that the DE-mRNAs and miRs participate in the regulation of proliferation, cell cycle and apoptosis. Increased expression of *DLX5* with decreasing miR-124-3p levels were confirmed in ox-LDL-treated VSMCs. The miR-124-3p could inhibit the *DLX5* level by binding the 3′ UTR of *DLX5* mRNA. Functional analysis showed that the alteration of miR-124-3p/*DLX5* expression mediated the effect of ox-LDL on VSMCs proliferation/apoptosis imbalance.

Conclusions. The ox-LDL affects the VSMC proliferation/apoptosis balance via the miR-124-3p/*DLX5* axis, which results in VSMC hyperproliferation. The miR-124-3p/*DLX5* axis might serve as a therapeutic molecular target to reverse the effect of ox-LDL and prevent atherosclerosis (AS) development and progression.

Key words: atherosclerosis, microRNA, vascular smooth muscle cell, oxidized low-density lipoprotein, *DLX5*

Cite as
Jia C, Gao F, Zhao Y, Ji S, Cai S. Identification and functional analysis of changes to the ox-LDL-induced microRNA-124-3p/DLX5 axis in vascular smooth muscle cells. *Adv Clin Exp Med*. 2021;30(12):1271–1281. doi:10.17219/acem/141580

DOI
10.17219/acem/141580

Background

Atherosclerosis (AS) is a vascular disease characterized by stiff, thickened artery walls with reduced elasticity, together with the formation of atherosclerotic plaques within the intimal layer.[1] Its development and progression involves vascular endothelial cell damage and dysfunction, inflammatory cell recruitment, lipid deposition, and thrombosis, in addition to abnormal vascular smooth muscle cell (VSMC) proliferation.[2] Excessive proliferation of VSMCs causes an inflammatory response and thickening of vessel walls, both of which facilitate lipoprotein deposition and fibrous cap formation.[3]

Elevated low-density lipoprotein (LDL) is a major risk factor for AS. Low-density lipoprotein comprises a core (mainly triglycerides and cholesterol lipids) and a surface rich in polyunsaturated fatty acids.[4] Therefore, LDL is easily oxidized and modified by stimulatory factors such as cigarette smoke, hyperglycemia and diabetes.[5] Oxidized LDL (ox-LDL) is even more potent in inducing AS. It is able to damage vascular endothelial cells, causing dysfunction and increased permeability, which initiates AS.[6] Furthermore, ox-LDL intake upregulates the transition of macrophages to foam cells within plaques. Previous studies have reported that ox-LDL promotes excessive proliferation of VSMCs by promoting endothelin-1 secretion and inhibiting prostacyclin synthesis.[7] Some of the ox-LDL-induced cytokines involved in the regulation of VSMC proliferation include platelet-derived growth factor (PDGF), basic fibroblast growth factor (bFGF) and transforming growth factor beta (TGF-β).[8] Reversing ox-LDL-induced VSMC hyperproliferation may represent a new strategy in AS treatment. However, the mechanisms underlying ox-LDL-induced regulation of VSMC proliferation need to be explored prior to the clinical application of this strategy.[9]

Recent studies investigating the regulatory mechanisms of microRNAs (miRs) have shown that miRs play an important regulatory role in ox-LDL-induced VSMC proliferation, and several potential miR therapeutic targets have been identified there. Sun et al. reported that miR-490-3p is associated with increased ox-LDL-induced VSMC proliferation through the regulation of its target gene, *PAPP-A*. The Ox-LDL inhibits miR-490-3p expression, and the upregulated miR-490-3p reduces ox-LDL-induced abnormal VSMC proliferation by inhibiting *PAPP-A*.[10] Furthermore, Wang et al. identified another ox-LDL-induced miR, miR-195. They found that ox-LDL inhibits miR-195 levels in VSMCs and that miR-195 inhibits VSMC proliferation and migration.[11]

Objectives

In this study, we aimed to analyze RNA sequencing data from ox-LDL-treated VSMCs to find novel miR–messenger RNA (mRNA) axes involved in ox-LDL-induced VSMC proliferation. We selected differentially expressed (DE) miRs and mRNAs in ox-LDL-treated cells and conducted functional and bioinformatics analyses on these genes. We selected the miR-124-3p/*DLX5* axis as one potentially related to VSMC proliferation, which was confirmed following ox-LDL treatment. Considering that ox-LDL promotes VSMC proliferation by breaking the cell proliferation/apoptosis balance, we further explored the regulatory function of the miR-124-3p/*DLX5* axis in VSMC proliferation and apoptosis.

Materials and methods

Cell culture and ox-LDL treatment

Human aorta smooth muscle cells (HA-VSMC, product code: CRL-1999) were obtained from the American Type Culture Collection (ATCC, Manassas, USA) and cultured using F-12K media (Thermo Fisher Scientific, Waltham, USA) in a humidified incubator at 5% CO_2 and 37°C. To make the complete growth medium, the following components were provided by Procell Life Science&Technology (Wuhan, China) and added to the base medium: 0.05 mg/mL of ascorbic acid; 0.01 mg/mL of insulin; 0.01 mg/mL of transferrin; 10 ng/mL of sodium selenite; 0.03 mg/mL of Endothelial Cell Growth Supplement (ECGS); fetal bovine serum (FBS; Thermo Fisher Scientific) to a final concentration of 10%, HEPES to a final concentration of 10 mM, and TES to a final concentration of 10 mM. Antibiotics were not added into the medium. The HA-VSMCs in their 5th passage were treated with 100 µg/mL of ox-LDL (Thermo Fisher Scientific) for 24 h before further experiments.

No approval was required from bioethical committee due to the fact that no human or animals were enrolled in the present study.

RNA sequencing and data analysis

After 48 h of exposure to ox-LDL, cells were collected, and samples sent for RNA sequencing (BGI Technology Service, Shenzheng, China). The DE-mRNAs and miRs were analyzed using theDESeq2 package in R software v. 3.4.1 (R Foundation for Statistical Computing, Vienna, Austria). The DE-genes are defined as genes with a fold-change of expression >2.0 and $p < 0.05$.

Bioinformatic analysis

To explore the potential biological function of DE mRNA and miRs, further functional and signaling pathway analyses were performed. Gene Ontology (GO) gene enrichment analysis and Kyoto Encyclopedia of Genes and Genomes (KEGG) signaling pathway enrichment analyses were performed on a set of DE-mRNAs using

data from the Database for Annotation, Visualization and Integrated Discovery (DAVID; https://david.ncifcrf.gov/). Signaling pathway analyses for DE-miRs were conducted using the online tool mirPath v. 3 (http://snf-515788.vm.okeanos.grnet.gr/). The miR-mRNA target relationship was predicted using miRanda-mirSVR tools (http://www.microrna.org/microrna/getMirnaForm.do).

Quantitative real-time polymerase chain reaction

The total RNA, including miRs was isolated from cells using TRIzol reagent (Thermo Fisher Scientific). To evaluate miR-124-3p expression levels, RNA samples were reverse transcribed into cDNA using miScript Reverse Transcription Kit (Qiagen, Shanghai, China) and amplified using miScript SYBR-Green PCR Kits (cat. No. 218073; Qiagen). The expression value of miR-124-3p was normalized to the reference gene *RNU6B*. The primers of miR-124-3p and RNU6B were provided using miScript Primer Assay Kit (cat. No. 218300; Qiagen) and are patent-protected. To detect the level of *DLX5*, cDNA was synthesized using PrimeScript RT reagent Kit (cat. no. RR037A; TaKaRa, Beijing, China) and analyzed using TB Green® Premix Ex Taq™ II Kit (cat. No. RR820A; TaKaRa). The expression value of *DLX5* was normalized to GAPDH. The forward primer of *DLX5* was 5'-TTCCAAGCTCCGTTCCAGAC-3'. The reverse primer of *DLX5* was 5'-GAATCGGTAGCTGAAGACTCG-3'. The forward primer of GAPDH was 5'-GGAGCGAGATCCCTCCAAAAT-3'. The reverse primer of GAPDH was 5'-GGCTGTTGTCATACTTCTCATGG-3'.

Western blot

Treated cells were lysed on ice in radioimmunoprecipitation assay (RIPA) buffer supplemented with a protease and phosphatase inhibitor cocktail (Beyotime, Shanghai, China). The concentration of extracted protein was measured using BCA protein assay kit (Beyotime). Equal amounts of protein samples were loaded and separated with 10% polyacrylamide gel electrophoresis (PAGE) gel. After electrophoresis, samples were transferred to nitrocellulose membranes and membranes were blocked using 5% fat-free milk. Then, membranes were incubated with rabbit monoclonal primary antibodies of *DLX5* (Abcam, Cambridge, UK) and GAPDH (Abcam). Next, goat anti-rabbit IgG H&L (horseradish peroxidase (HRP)-labeled) secondary antibody (Abcam) was used. Protein bands were detected using the electrochemiluminescence (ECL) detection kit (Beyotime).

Cell transfection

The pcDNA3.1-*DLX5* expression vectors were constructed and transfected into HA-VSMC to overexpress *DLX5* expression. An empty pcDNA3.1 vector served as the transfection negative control (NC). To knockdown *DLX5* expression, siRNA-*DLX5* were transfected into cells. To up- or downregulate the expression of miR-124-3p, specific miR-mimics and miR-inhibitors (Qiagen) were used. For siRNA and miR-mimics, the Allstars sequence (cat. No. 1027280; Qiagen) was used as the transfection NC. For miR-inhibitors, miScript Inhibitor Negative Control (cat. No. 1027272; Qiagen) was used as the transfection NC. Lipofectamine 2000 Reagent was used 48 times according to the manufacturer's instructions. Once the transfection was confirmed with qRT-PCR (Fig. 1), cells were used for further experiments.

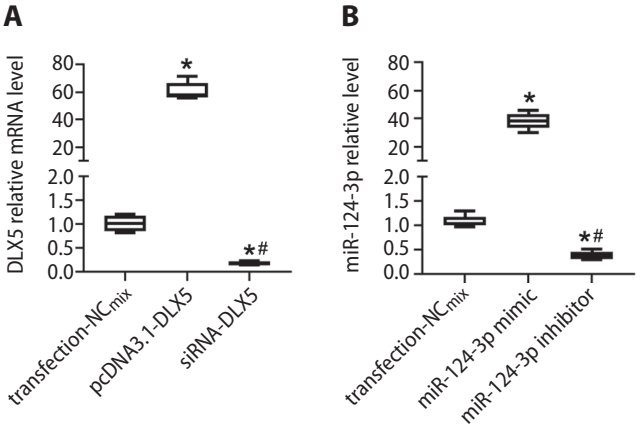

Fig. 1. Transfection effects of human aorta vascular smooth muscle cells (HA-VSMCs) were confirmed using quantitative real-time polymerase chain reaction (RT-qPCR). A. The effect of pcDNA3.1-*DLX5* and siRNA-*DLX5*; B. The effect of miR-124-3p mimic and miR-124-3p inhibitor

* $p < 0.05$ compared with matched transfection negative control (NC) mixture; # $p < 0.05$ compared with pcDNA3.1-*DLX5* or miR-124-3p mimic. Transfection NC_{mix} was a mixture of Allstars sequence and empty pcDNA3.1 in A (n = 5). Transfection NC_{mix} was a mixture of Allstars sequence and miScript Inhibitor Negative Control in B (n = 5).

Proliferation analysis

Treated cells were plated into 96-well plates at 5000 cells/well. At 0 h, 24 h, 48 h and 72 h timepoints, 10 µL Cell Counting Kit-8 reagent (Beyotime) was added into each well (200 µL medium/well) and the cells were incubated at 37°C for 1 h. The absorbance was measured at 450 nm using an automatic microplate reader BioTek Elx800 (BioTek, Winooski, USA) and normalized to the blank well. Relative proliferation = normalized absorbance value at other timepoints/N = normalized absorbance value at 0 h.

Flow cytometry analysis for cell cycle

Treated cells were collected and washed with cold phosphate-buffered saline (PBS). Cell cycle assay was performed using BD Pharmingen BrdU Flow Kit (Becton Dickinson Biosciences, San Diego, USA). In brief, cells were labeled with and fixed/permeabilized using BD Cytofix/Cytoperm Buffer (Becton Dickinson Biosciences). Then, cells were

treated with deoxyribonuclease (DNase) and incubated with fluorescein isothiocyanate (FITC)-conjugated anti-BrdU. After staining with 7-AAD and resuspending, Guava® easyCyte 8HT Benchtop Flow Cytometer (Merck Millipore, Darmstadt, Germany) was used to perform flow cytometry analysis. Data were analyzed using Guava® InCyte and GuavaSuite software v. 3.0 (Merck Millipore).

Apoptosis assay

Cells were plated in 96-well plates and treated with indicated transfection contents and/or ox-LDL. Following 24 h of treatment, cells were incubated with prepared 2× detection reagent from the RealTime-Glo™ Annexin V Apoptosis Assay Kit (Thermo Fisher Scientific). Luminescence was detected using Spark® 10M fluorescence plate reader (Tecan, Männedorf, Switzerland) to indicate apoptosis.

Dual-luciferase reporter assay

The wild-type and mutant *DLX5* 3′-UTR fragment was subcloned into the pMIR REPORT™ miRNA expression firefly luciferase reporter vectors (Ambion, Austin, USA). The pRL-TK reporter control vectors (Ambion) expressing Renilla luciferase were used as the internal control. Luciferase reporter vector (*DLX5* 3′-UTR-WT and *DLX5* 3′-UTR-MUT) or control vectors were co-transfected with miR-124-3p mimic or mimic controls, using Lipofectamine 2000 according to the manufacturer's protocols. After 24 h of co-transfection, firefly luciferase activity was determined using the Dual-Luciferase® Reporter Assay System (Promega, Beijing, China), and normalized to the background Renilla luciferase activity.

Statistical analyses

Statistical analyses were performed using R v. 3.4.1 (R Foundation for Statistical Computing, Vienna, Austria). Results were presented as the means ± standard deviation (SD). Differences in means between 2 groups were determined using Student's t-test. For groups of more than 2, a one-way analysis of variance (ANOVA) with a Bonferroni's post hoc test or Dunnett's multiple comparisons test was performed to determine significance. A p-value of <0.05 was considered statistically significant.

Results

Changes in mRNA and miR expression profiles and functional analysis in ox-LDL-treated VSMCs

High-throughput RNA sequencing showed that 577 mRNAs had significantly altered expression in VSMCs, 24 h after ox-LDL treatment (fold-change (FC) of expression > 2.0; $p < 0.05$), of which 219 genes were upregulated and 258 downregulated (Fig. 2A,C). In addition, a significant change in the expression of 81 miRs following ox-LDL treatment was observed (FC > 2.0; $p < 0.05$), of which 63 were upregulated and 18 downregulated (Fig. 2B,D). We also performed Gene Ontology (GO) gene enrichment analysis of DE-mRNAs (Fig. 3A). The DE-mRNAs were involved in a range of cellular processes, such as "cell proliferation", "cell growth" and "regulation of cell cycle". Kyoto Encyclopedia of Genes and Genomes (KEGG) signaling pathway enrichment analysis of DE-mRNAs (Fig. 3B) demonstrated that the DE-mRNAs are related to cell cycle and apoptosis pathways. Pathway enrichment analysis of DE-miRs, whose expression was significantly altered, showed that the target genes of these miRs are also involved in apoptosis and cell cycle pathways (Fig. 3C). Taken together, the ox-LDL responsive DE-mRNAs and DE-miRs may play a functional role in the regulation of proliferation, cell cycle and apoptosis in VSMCs.

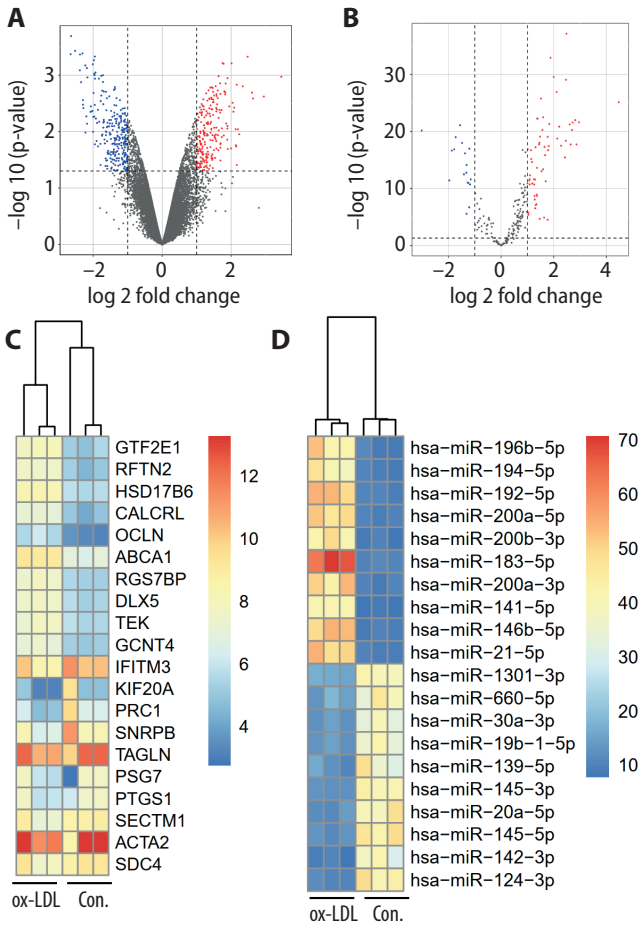

Fig. 2. Differentially expressed mRNAs and microRNAs after 48 h of oxidized low-density lipoprotein (ox-LDL) treatment. A. Volcano plot showing 219 significantly upregulated and 258 downregulated mRNAs in cells after 48 h of ox-LDL treatment; B. The volcano plot showing 63 significantly upregulated and 18 downregulated microRNAs in cells after 48 h of ox-LDL treatment; C. Heatmap showing top 10 upregulated and downregulated mRNAs in cells after 48 h of ox-LDL treatment; D. Heatmap showing top 10 upregulated and downregulated mRNAs in cells after 48 h of ox-LDL treatment

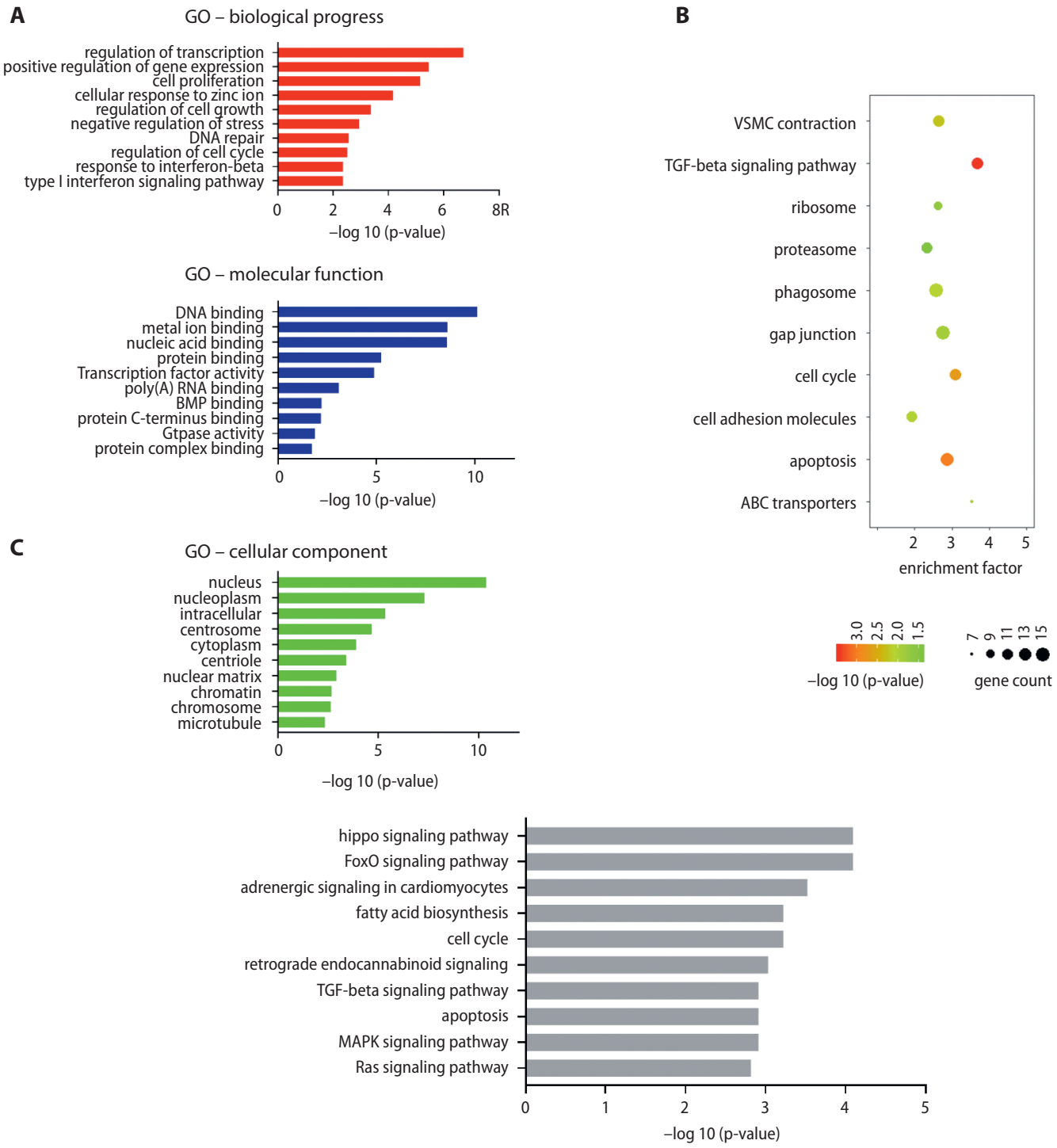

Fig. 3. Functional annotation analysis for differentially expressed mRNAs and microRNAs in human aorta vascular smooth muscle cells (HA-VSMCs) after 48 h of oxidized low-density lipoprotein (ox-LDL) treatment. A. Top 10 Gene Ontology (GO) gene enrichment analysis results for differentially expressed mRNAs showed their potential biological progress, molecular function and cellular component; B. Top 10 Kyoto Encyclopedia of Genes and Genomes (KEGG) signaling pathway enrichment analysis result for differentially expressed (DE) mRNAs; C. Top 10 pathway enrichment analysis results for DE microRNAs

Aberrant changes in the miR-124-3p/*DLX5* axis in ox-LDL-treated VSMCs

Based on GO gene enrichment analysis and KEGG pathway enrichment analysis results, we selected DE-genes related to the proliferation, apoptosis and cell cycle of VSMCs as candidate genes for further analysis. A total of 35 genes were potentially related to proliferation, apoptosis and cell cycle of VSMCs (Fig. 4A). Among these, *DLX5* had the highest upregulation. Next, we predicted miRs that could complementarily bind to *DLX5* mRNA 3'UTR using the miRabda-mirSVR tools and compared

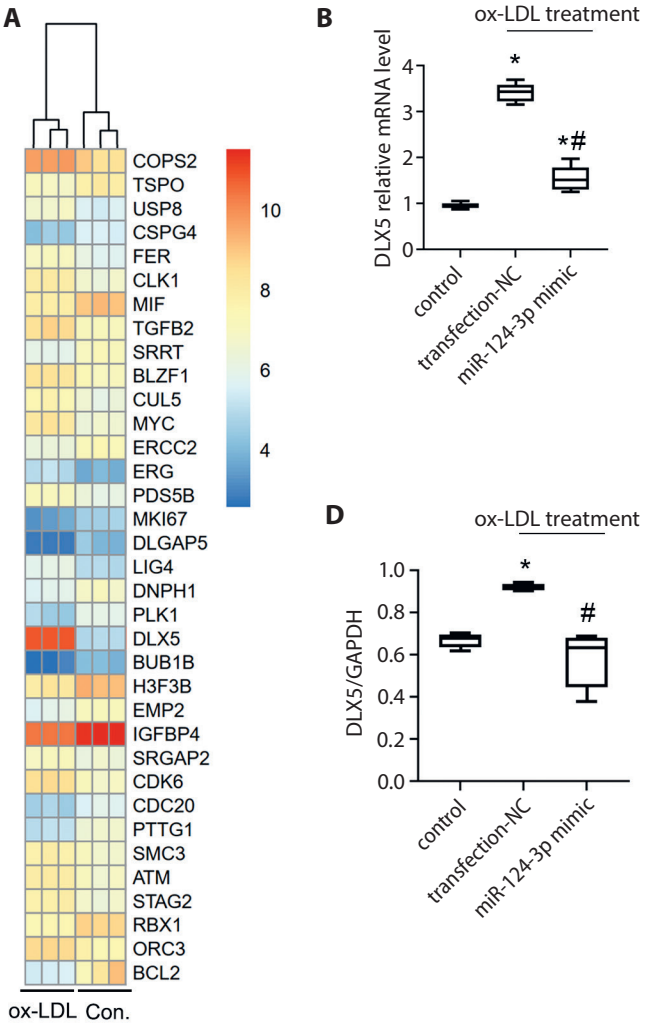

Fig. 4. Oxidized low-density lipoprotein (ox-LDL) increased expression of *DLX5* and reduced miR-124-3p level in human aorta vascular smooth muscle cells (HA-VSMCs). A. Heatmap showing expression alteration of proliferation, cell cycle and apoptosis-related candidate genes induced by ox-LDL in HA-VSMCs; B. Forty-eight hours of ox-LDL treatment increased mRNA level of *DLX5*; C and D. Forty-eight hours of ox-LDL treatment increased protein level of *DLX5*; E. Forty-eight hours of ox-LDL treatment reduced miR-124-3p level in cells

* $p < 0.05$ compared with control; # $p < 0.05$ compared with transfection negative control (NC); n = 5.

these results with the ox-LDL-treated downregulated miR list, finding only miR-124-3p being overlapped. We found that less than 200 μg/mL of ox-LDL induced proliferation and apoptosis at same time, but 200 μg/mL or more inhibited proliferation (Fig. 5A,B). Hence, we selected 100 μg/mL of ox-LDL for further study, which was shown to significantly enhance cell proliferation (Fig. 5C). Furthermore, this dose of ox-LDL also induced significant apoptosis after 12 h of treatment, although there was no further increase to the apoptotic rate with further treatment (Fig. 5D). We suggest that ox-LDL could promote the proliferation of VSMC and induce apoptosis at the same time, but the pro-proliferative effect of ox-LDL is greater than the pro-apoptotic effect, hence the imbalance.

Following the treatment with 100 μg/mL ox-LDL, the DLX5 expression in VSMCs was detected using qRT-PCR and western blotting. These results showed that ox-LDL treatment significantly upregulates *DLX5* at 24 h (Fig 4B–D). Transfection with the miR-124-3p mimic antagonized the effect of ox-LDL on *DLX5*. The qRT-PCR verification showed that ox-LDL treatment significantly decreased miR-124-3p expression after 24 h (Fig. 4E), although the *DLX5* mRNA level did not significantly change following ox-LDL treatment for 12 h (Fig. 5E). Yet, changes of miR-124-3p could be observed after 12 h of ox-LDL treatment (Fig. 5F). The *DLX5* and miR-124-3p did not further change after 48 h of ox-LDL treatment.

Next, we analyzed the inhibitory effect of miR-124-3p on its molecular target, *DLX5*. These data showed that mRNA and protein levels of *DLX5* significantly decreased in response to miR-124-3p upregulation, and significantly increased after downregulating miR-124-3p in VSMCs ($p < 0.05$) (Fig. 6A–C). The dual luciferase reporter assay indicated that miR-124-3p directly binds to the *DLX5* 3'UTR. Overall, these results indicated that ox-LDL can alter the balance of the miR-124-3p/*DLX5* axis in VSMCs.

Oxidized low-density lipoprotein-induced VSMC proliferation/apoptosis imbalance via the miR-124-3p/*DLX5* axis

Next, we analyzed the function of the miR-124-3p/*DLX5* axis in VSMCs. Overexpressed miR-124-3p inhibited VSMC proliferation ($p = 0.03$), while VSMC proliferation was increased ($p = 0.04$) when miR-124-3p was inhibited

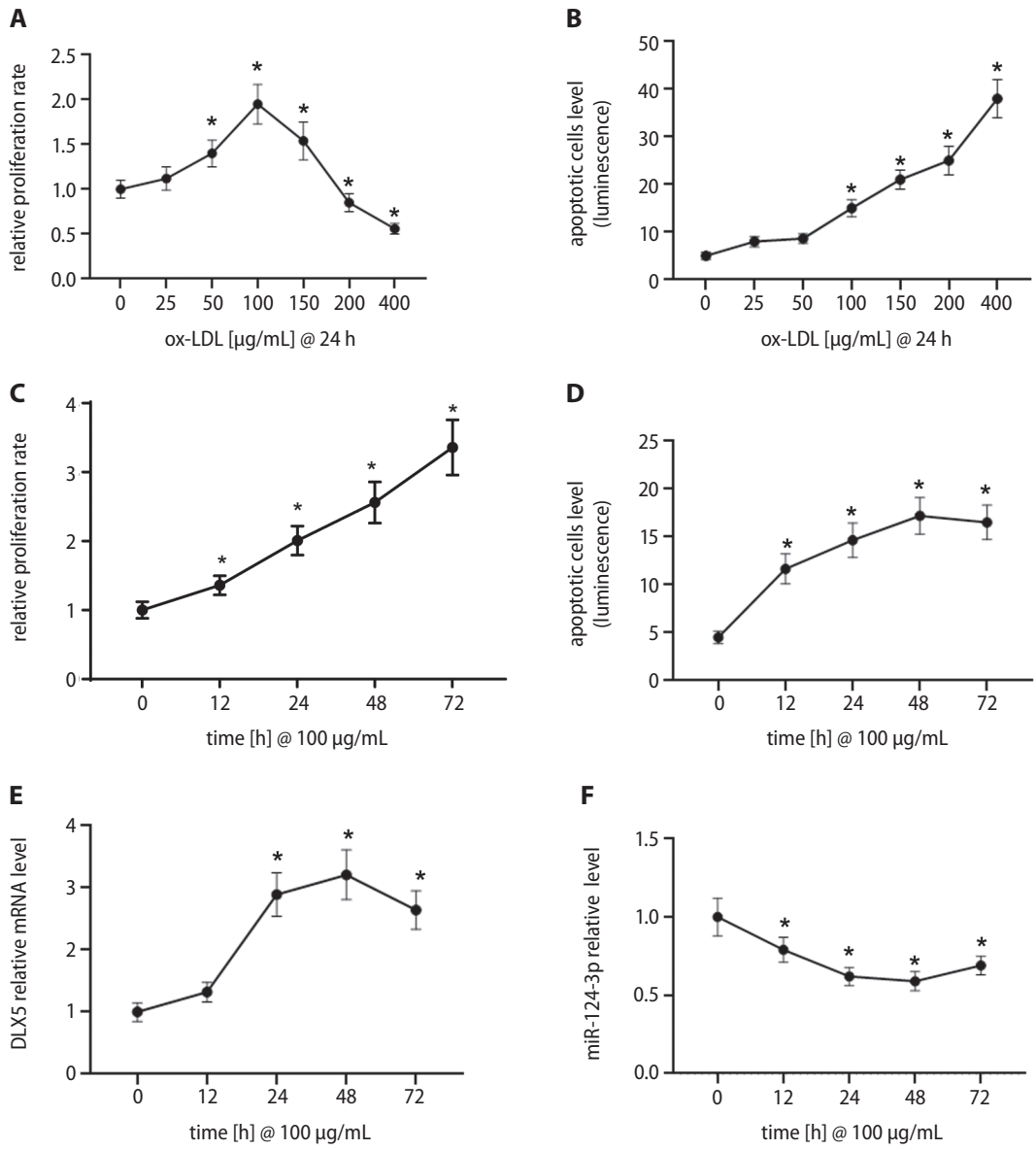

Fig. 5. Dose- and time-dependent effect of oxidized low-density lipoprotein (ox-LDL) on *DLX5*. A and B. The vascular smooth muscle cells (VSMCs) were treated with different concentration of ox-LDL. Proliferation and apoptosis were analyzed; C and D. The VSMCs were treated with 100 μg/mL of ox-LDL for different timepoints. Proliferation and apoptosis were analyzed; E and F. The *DLX5* and miR-124-3p were detected in 100 μg/mL of VSMCs treatment for different timepoints

* $p < 0.05$ compared with control; n = 3; @ – indicated time point or concentration.

(Fig. 7A). The *DLX5* had a stimulatory effect on VSMCs proliferation ($p = 0.003$), while siRNA-*DLX5* inhibited proliferation ($p = 0.016$) (Fig. 7B). According to our flow cytometry results, transfection with miR-124-3p mimics and siRNA-*DLX5* arrested the cell cycle at the G_0/G_1 phase ($p = 0.02$ and 0.03, respectively) (Fig. 7C,D), and induced apoptosis ($p = 0.005$ and 0.008, respectively) (Fig. 7E,F). However, transfection with miR-124-3p inhibitor and pcDNA3.1-*DLX5* increased the proportion of cells in G2/M phases, but with no effect on apoptosis. When investigating proliferation, cell cycle and apoptosis of VSMCs, overexpression of *DLX5* antagonized the effect of miR-124-3p mimics.

Following transfection with miR-124-3p mimics and siRNA-*DLX5* for 48 h, cells were treated with ox-LDL for 24 h. As expected, ox-LDL treatment significantly increased VSMC proliferation ($p < 0.05$) (Fig. 8A) and increased the proportion of cells in S and G_2/M phases ($p = 0.03$) (Fig. 8B). The overexpression of miR-124-3p or inhibition of *DLX5* antagonized the effect of ox-LDL significantly ($p = 0.03$ and $p = 0.004$, respectively). The ox-LDL tended to induce VSMC apoptosis, and this effect was enhanced by upregulation of miR-124-3p or inhibition of *DLX5* (Fig. 8C). Together, ox-LDL regulates the VSMC proliferation/apoptosis balance through the miR-124-3p/*DLX5* axis.

Discussion

Recent studies have shown that ox-LDL may regulate the VSMC proliferation/apoptosis balance through miRs, making ox-LDL-related miR pathways promising therapeutic targets for AS treatment.[12] In this study, we determined mRNA and miR expression in VSMCs 24 h after ox-LDL treatment using high-throughput RNA sequencing. These data demonstrated significant changes to both, mRNA and miR expressions following ox-LDL treatment.

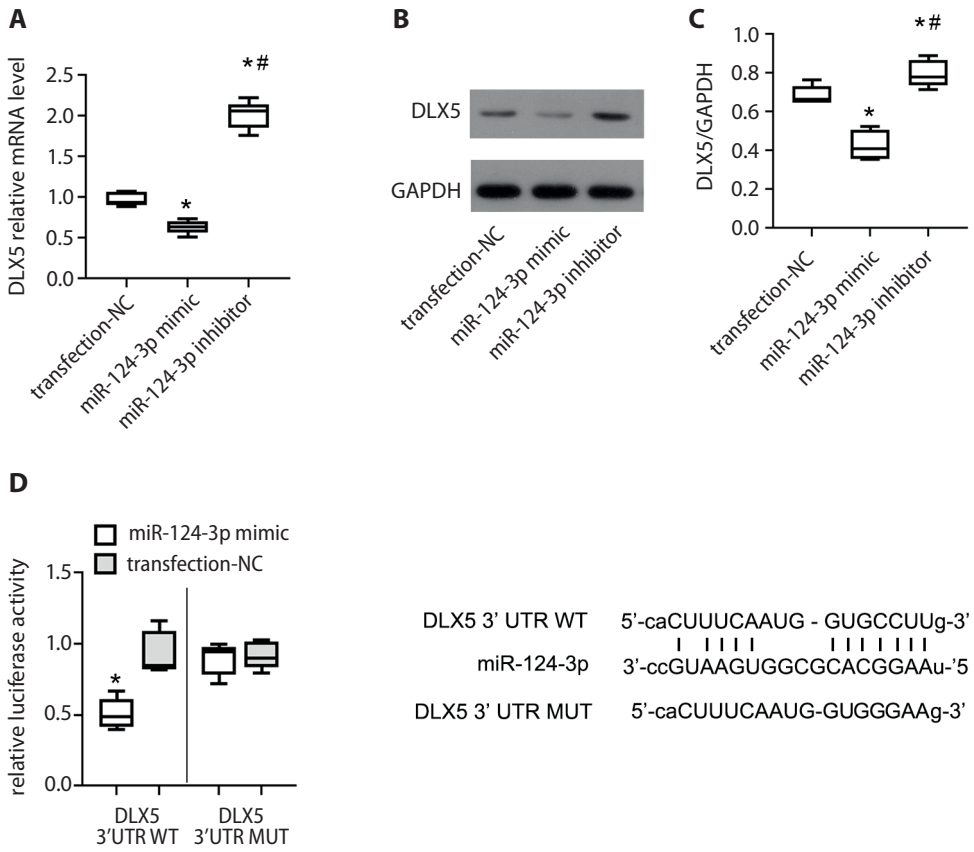

Fig. 6. The miR-124-3p negatively regulated *DLX5* expression. A. Up- or downregulation of miR-124-3p changed the mRNA level of *DLX5*; B and C. Up- or downregulation of miR-124-3p changed the protein level of *DLX5*; D. The miR-124-3p binding to the *DLX5* 3'UTR was indicated using luciferase reporter assay (left). The wild-type and mutant *DLX5* 3'UTR sequence and the predicted binding site to miR-124-3p is shown (right)

* $p < 0.05$ compared with transfection negative control (NC); # $p < 0.05$ compared with miR-124-3p mimic.

Then, to further reveal the biological functions of these mRNAs and miRs, we conducted functional enrichment analysis of these DE-mRNAs using the GO database, finding that some of the DE-mRNAs are related to the proliferation and cell cycle of VSMCs. In addition, KEGG signal pathway enrichment analysis showed that some of the DE-mRNAs are the components of signaling pathways involved in VSMC functions. The DIANA-mirPath (http://snf-515788.vm.okeanos.grnet.gr/) is an online tool that reveals the function of miRs of interest through pathway enrichment analysis of target genes for those miRs. This analysis highlighted that cell cycle, apoptosis and MAPK and RAS signaling pathways are involved after ox-LDL treatment. This evidence indicated that miRs might also participate in ox-LDL-induced VSMC proliferation/apoptosis imbalance.

Because it was not possible for us to verify all these sequencing data, it was necessary to screen out mRNAs of interest and their corresponding miRs for further analysis. With a focus on the regulatory effect of ox-LDL on the VSMC proliferation/apoptosis balance, together with the results of GO gene enrichment analysis, only DE-genes related to the proliferation and cell cycle regulation of VSMCs were selected as candidates for verification. However, we found many such candidates, and we selected the gene with the highest expression of FC, *DLX5*, for further analysis. Next, miRs that can use *DLX5* as the target gene were predicted and compared with previously obtained DE-miRs. These candidate miRs should be expressed at a low level in ox-LDL-treated VSMCs and bound to the 3'UTR of *DLX5*. Finally, we only selected miR-124-3p in this study and assumed that ox-LDL can regulate the VSMC proliferation/apoptosis balance through the miR-124-3p/*DLX5* axis, which was verified in vitro. Quantitative real-time polymerase chain reaction (RT-qPCR) confirmed that miR-124-3p expression decreased in ox-LDL-treated VSMCs. In addition, the expression of mRNA and protein levels of *DLX5* increased in VSMCs after ox-LDL treatment. Furthermore, we confirmed the targeted inhibitory effect of miR-124-3p on *DLX5*. Together, these data indicated the presence of the miR-124-3p/*DLX5* axis that can be regulated by ox-LDL in VSMCs.

Some studies investigating cancer have reported that miR-124-3p inhibits cell proliferation. Xu et al. showed that miR-124-3p inhibits the proliferation of nasopharyngeal carcinoma cells,[13] while Wu et al. reported the inhibitory effect of miR-124-3p on glioma proliferation.[14] The inhibitory effect of miR-124-3p on VSMC proliferation and migration has also been reported previously.[15] However, Cheng et al. showed that miR-124-3p promotes VSMC proliferation, so the role of miR-124-3p in VSMCs remains controversial.[16] The current study showed that the upregulation of miR-124-3p inhibits VSMC proliferation, arrests the cell cycle and increases apoptosis, while its inhibition accelerates VSMC proliferation. Therefore, we believe that miR-124-3p can inhibit VSMC growth. Moreover, we discovered that miR-124-3p overexpression counteracts the stimulatory effect of ox-LDL on VSMC proliferation.

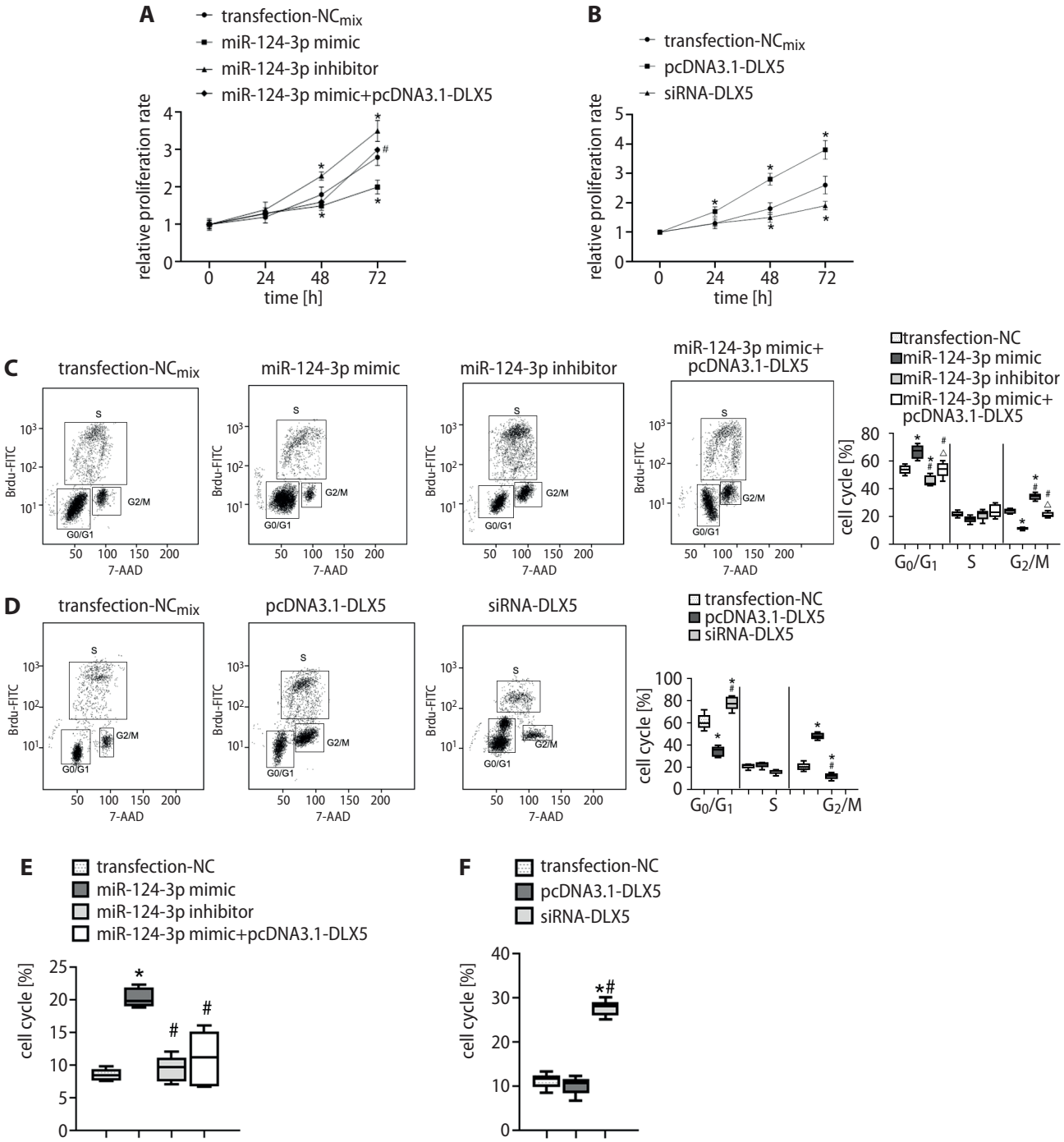

Fig. 7. Functional roles of miR-124-3p and *DLX5* on proliferation, cell cycle and apoptosis in human aorta vascular smooth muscle cells (HA-VSMCs). A and B. The miR-124-3p inhibited proliferation of HA-VSMCs, but *DLX5* promoted cell proliferation; C and D. The miR-124-3p caused G_1/G_0 phase arrest, while *DLX5* increased proportion of G_2/M; E and F. Upregulation of miR-124-3p and knockdown of *DLX5* induced cells apoptosis

* $p < 0.05$ compared with transfection negative control (NC) mixture; # $p < 0.05$ compared with miR-124-3p mimic or pcDNA3.1-*DLX5*; Δ $p < 0.05$ compared with miR-124-3p inhibitor. Transfection NC_{mix} was a mixture of Allstars sequence, miScript Inhibitor Negative Control and empty pcDNA3.1 in A, C and E. Transfection NC^{mix} was a mixture of pcDNA3.1 empty vectors and Allstars sequence in B, D and F (n = 5).

These results show that ox-LDL induces VSMC proliferation partially by regulating miR-124-3p.

One of the target genes of miR-124-3p, *DLX5*, was further investigated to explore its underlying mechanisms. The *DLX5* is a member of the protein family encoded by DLX (Drosophila distal-less) homeobox genes, and a transcription factor.[17] Recent studies have shown that *DLX5* promotes cell proliferation by regulating the MYC and protein kinase B (AKT) pathways.[18] Tan et al. found that *DLX5* knockdown inhibits the proliferation of ovarian cancer cells and arrests the cell cycle at the G_0/G_1 phase.[19] Furthermore, previous results on *DLX5* functions were consistent with our results. Previous evidence, supporting the promoting effect of *DLX5* on cell proliferation,

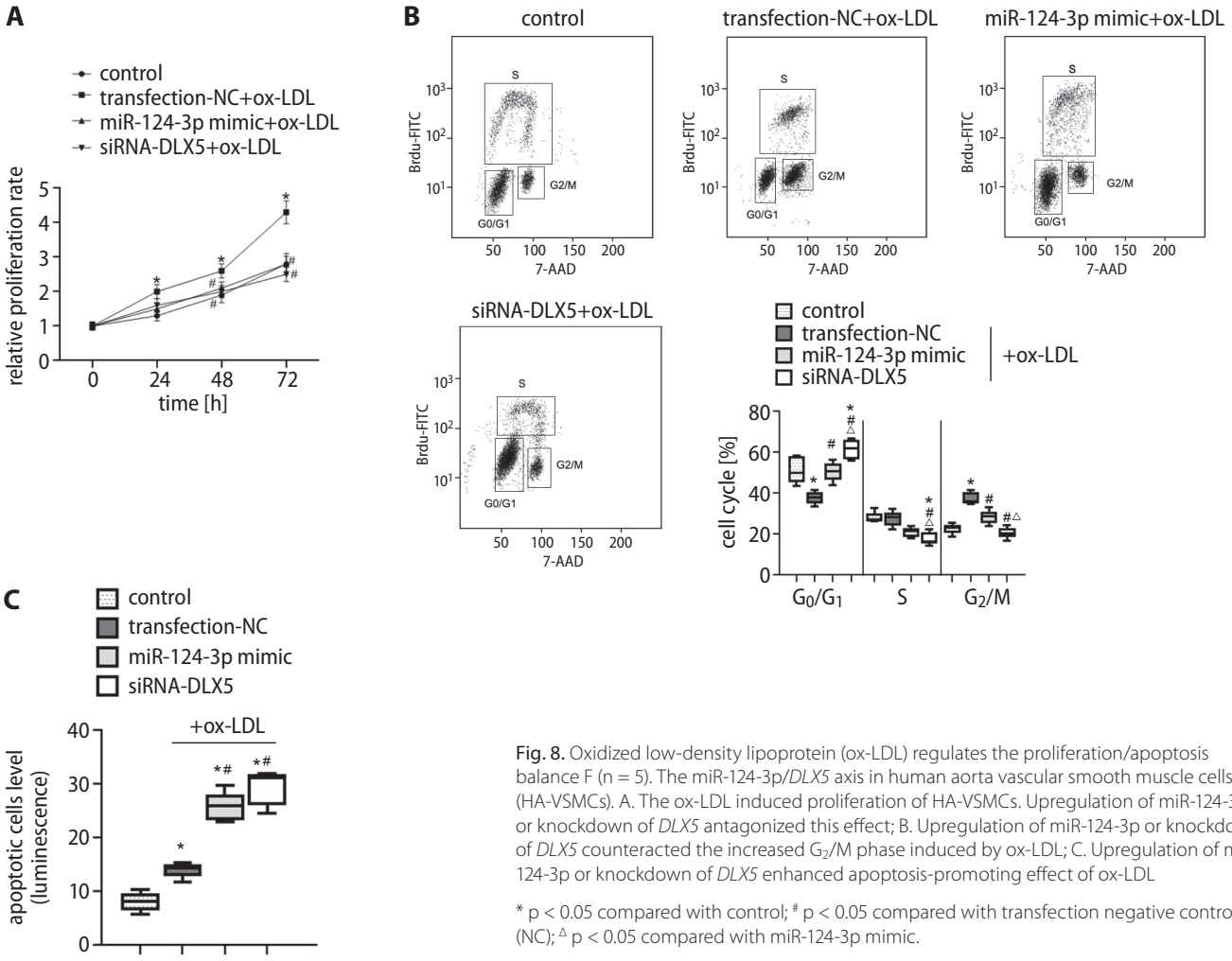

Fig. 8. Oxidized low-density lipoprotein (ox-LDL) regulates the proliferation/apoptosis balance F (n = 5). The miR-124-3p/*DLX5* axis in human aorta vascular smooth muscle cells (HA-VSMCs). A. The ox-LDL induced proliferation of HA-VSMCs. Upregulation of miR-124-3p or knockdown of *DLX5* antagonized this effect; B. Upregulation of miR-124-3p or knockdown of *DLX5* counteracted the increased G_2/M phase induced by ox-LDL; C. Upregulation of miR-124-3p or knockdown of *DLX5* enhanced apoptosis-promoting effect of ox-LDL

* $p < 0.05$ compared with control; # $p < 0.05$ compared with transfection negative control (NC); △ $p < 0.05$ compared with miR-124-3p mimic.

is mainly derived from tumor studies, and the role of *DLX5* in VSMCs has limited literature. Our results showed that *DLX5* overexpression increases VSMC proliferation, while *DLX5* knockdown inhibits this process, arrests the cell cycle and increases apoptosis. Therefore, we believe that the function of *DLX5* in VSMCs is consistent with that in tumor cells (i.e., promotion of cell proliferation). Although we verified the function of the miR-124-3p/*DLX5* axis in VSMCs, we did not explore related mechanisms any further. Future studies may examine the target gene of *DLX5* to shed light on any potential downstream effects. In addition, the miR-124-3p/*DLX5* axis was selected due to the expression FC, and the functions of other miR-mRNA axes that play a role in ox-LDL-treated VSMCs were ignored, which was also a limitation of this study.

Limitations

We did not explain how ox-LDL inhibits miR-124-3p levels. Whether ox-LDL reduces miR-124-3p by affecting transcription or by posttranscriptional regulation needs to be confirmed in subsequent studies.

Conclusion

In summary, ox-LDL affects the VSMC proliferation/apoptosis balance through the miR-124-3p/*DLX5* axis and eventually results in VSMC hyperproliferation. The miR-124-3p/*DLX5* axis might serve as a therapeutic molecular target to reverse the effect of ox-LDL and prevent AS development and progression.

Availability of data and materials

The RNA-seq data generated and analyzed during the current study are available in the Sequence Read Archive (SRA) database in National Center for Biotechnology Information (NCBI). Data can be accessed at https://www.ncbi.nlm.nih.gov/bioproject/PRJNA714763.

ORCID iDs

Chunwen Jia https://orcid.org/0000-0002-6578-9554
Feng Gao https://orcid.org/0000-0002-2695-1280
Yanan Zhao https://orcid.org/0000-0002-4854-5689
Siyang Ji https://orcid.org/0000-0003-2137-5314
Shidao Cai https://orcid.org/0000-0003-3116-5863

References

1. Kobiyama K, Ley K. Atherosclerosis. *Circ Res*. 2018;123(10):1118–1120. doi:10.1161/CIRCRESAHA.118.313816
2. Gimbrone MA, García-Cardeña G. Endothelial cell dysfunction and the pathobiology of atherosclerosis. *Circ Res*. 2016;118(4):620–636. doi:10.1161/CIRCRESAHA.115.306301
3. Dzau VJ, Braun-Dullaeus RC, Sedding DG. Vascular proliferation and atherosclerosis: New perspectives and therapeutic strategies. *Nat Med*. 2002;8(11):1249–1256. doi:10.1038/nm1102-1249
4. Kattoor AJ, Kanuri SH, Mehta JL. Role of Ox-LDL and LOX-1 in atherogenesis. *Curr Med Chem*. 2019;26(9):1693–1700. doi:10.2174/0929867325666180508100950
5. Gao S, Zhao D, Wang M, et al. Association between circulating oxidized LDL and atherosclerotic cardiovascular disease: A meta-analysis of observational studies. *Can J Cardiol*. 2017;33(12):1624–1632. doi:10.1016/j.cjca.2017.07.015
6. Mitra S, Goyal T, Mehta JL. Oxidized LDL, LOX-1 and atherosclerosis. *Cardiovasc Drugs Ther*. 2011;25(5):419–429. doi:10.1007/s10557-011-6341-5
7. Pirillo A, Norata GD, Catapano AL. LOX-1, OxLDL, and atherosclerosis. *Mediators Inflamm*. 2013;2013:152786. doi:10.1155/2013/152786
8. Rhoads JP, Major AS. How oxidized low-density lipoprotein activates inflammatory responses. *Crit Rev Immunol*. 2018;38(4):333–342. doi:10.1615/CritRevImmunol.2018026483
9. Balzan S, Lubrano V. LOX-1 receptor: A potential link in atherosclerosis and cancer. *Life Sci*. 2018;198:79–86. doi:10.1016/j.lfs.2018.02.024
10. Sun Y, Chen D, Cao L, et al. MiR-490-3p modulates the proliferation of vascular smooth muscle cells induced by ox-LDL through targeting PAPP-A. *Cardiovasc Res*. 2013;100(2):272–279. doi:10.1093/cvr/cvt172
11. Wang YS, Wang HYJ, Liao YC, et al. MicroRNA-195 regulates vascular smooth muscle cell phenotype and prevents neointimal formation. *Cardiovasc Res*. 2012;95(4):517–526. doi:10.1093/cvr/cvs223
12. Nilsson J, Nordin Fredrikson G, Schiopu A, Shah PK, Jansson B, Carlsson R. Oxidized LDL antibodies in treatment and risk assessment of atherosclerosis and associated cardiovascular disease. *Curr Pharm Des*. 2007;13(10):1021–1030. doi:10.2174/138161207780487557
13. Xu S, Zhao N, Hui L, Song M, Miao ZW, Jiang XJ. MicroRNA-124-3p inhibits the growth and metastasis of nasopharyngeal carcinoma cells by targeting STAT3. *Oncol Rep*. 2016;35(3):1385–1394. doi:10.3892/or.2015.4524
14. Wu Q, Xu L, Wang C, Fan W, Yan H, Li Q. MicroRNA-124-3p represses cell growth and cell motility by targeting EphA2 in glioma. *Biochem Biophys Res Commun*. 2018;503(4):2436–2442. doi:10.1016/j.bbrc.2018.06.173
15. Afzal TA, Luong LA, Chen D, et al. NCK Associated protein 1 modulated by miRNA-214 determines vascular smooth muscle cell migration, proliferation, and neointima hyperplasia. *J Am Heart Assoc*. 2016;5(12):e004629. doi:10.1161/JAHA.116.004629
16. Cheng C, Xu BL, Sheng JL, He F, Yang T, Shen SC. LncRNA MALAT1 regulates proliferation and apoptosis of vascular smooth muscle cells by targeting miRNA-124-3p/PPARα axis. *Eur Rev Med Pharmacol Sci*. 2019;23(20):9025–9032. doi:10.26355/eurrev_201910_19304
17. Eisenstat DD, Liu JK, Mione M, et al. DLX-1, DLX-2, and DLX-5 expression define distinct stages of basal forebrain differentiation. *J Comp Neurol*. 1999;414(2):217–237. doi:10.1002/(sici)1096-9861(19991115)414:2<217::aid-cne6>3.0.co;2-i
18. Tan Y, Sementino E, Xu J, et al. The homeoprotein *Dlx5* drives murine T-cell lymphomagenesis by directly transactivating Notch and upregulating Akt signaling. *Oncotarget*. 2017;8(9):14941–14956. doi:10.18632/oncotarget.14784
19. Tan Y, Cheung M, Pei J, Menges CW, Godwin AK, Testa JR. Upregulation of *DLX5* promotes ovarian cancer cell proliferation by enhancing IRS-2-AKT signaling. *Cancer Res*. 2010;70(22):9197–9206. doi:10.1158/0008-5472.CAN-10-1568

Possibility of paclitaxel to induce the stemness-related characteristics of prostate cancer cells

Fadime Mutlu Içduygu[1,A–D], Hale Samli[2,A,C,F], Asuman Özgöz[3,C–E], Buse Vatansever[2,B,C], Kuyas Hekimler Oztürk[4,C,E], Egemen Akgün[5,B,C]

[1] Department of Medical Genetics, Faculty of Medicine, Giresun University, Turkey
[2] Department of Genetics, Faculty of Veterinary Medicine, Bursa Uludağ University, Turkey
[3] Department of Medical Genetics, Faculty of Medicine, Kastamonu University, Turkey
[4] Department of Medical Genetics, Faculty of Medicine, Süleyman Demirel University, Isparta, Turkey
[5] Department of Medical Biology, Faculty of Medicine, Giresun University, Turkey

A – research concept and design; B – collection and/or assembly of data; C – data analysis and interpretation; D – writing the article; E – critical revision of the article; F – final approval of the article

Advances in Clinical and Experimental Medicine, ISSN 1899–5276 (print), ISSN 2451–2680 (online) *Adv Clin Exp Med*. 2021;30(12):1283–1291

Address for correspondence
Fadime Mutlu Içduygu
E-mail: fadimemutlu@yahoo.com

Funding sources
Scientific Research Projects Committee of Giresun University, Turkey (Project No. SAĞ-BAP-A-230218-80 and Project No. SAĞ-BAP-A-140316-93).

Conflict of interest
None declared

Received on June 11, 2021
Reviewed on June 29, 2021
Accepted on July 28, 2021

Published online on October 5, 2021

Abstract

Background. Drug resistance poses a crucial problem in the treatment of prostate cancer. Recent studies have shown that chemotherapy agents may cause cancer cells to acquire stem cell-like properties, resulting in drug resistance and, eventually, treatment failure.

Objectives. To evaluate whether long-term paclitaxel exposure causes an increase in the stem cell-like properties of prostate cancer cells.

Materials and methods. Paclitaxel-resistant PC-3 cells were generated from parental PC-3 cells by treating them with increasing concentrations of paclitaxel. The expression levels of the stem cell markers NANOG, C-MYC, CD44, and ABCG2 were evaluated using quantitative real-time polymerase chain reaction (RT-qPCR). A sphere formation assay was performed to test the potential of the cells to behave as stem cells, and a wound healing assay was carried out to evaluate migration ability of the cells.

Results. The expression levels of C-MYC and NANOG were significantly higher in paclitaxel-resistant PC-3 cells compared to the parental PC-3 cells. However, there was no significant increase in the expression of CD44 or ABCG2. In addition, the sphere-forming capacity and migration ability of resistant PC-3 cells were increased.

Conclusions. The results of the current study indicate that paclitaxel exposure may increase the stem cell-like properties of PC-3 prostate cancer cells.

Key words: prostate cancer, cancer stem cell, paclitaxel, taxane resistance

Cite as
Içduygu FM, Samli H, Özgöz A, Vatansever B, Oztürk KH, Akgün E. Possibility of paclitaxel to induce the stemness-related characteristics of prostate cancer cells. *Adv Clin Exp Med*. 2021;30(12):1283–1291. doi:10.17219/acem/140590

DOI
10.17219/acem/140590

Background

Prostate cancer is the 2nd most common cancer and one of the leading causes of cancer death among men worldwide.[1] Generally, the first treatment choice for advanced prostate cancer patients is androgen deprivation therapy (ADT). Although patients tend to respond to ADT at first, treatment resistance develops in the majority of individuals, and the disease is termed castration-resistant prostate cancer (CRPC) at this stage. Taxanes (paclitaxel, abraxane, docetaxel) – a class of microtubule stabilizing agents – causes cell cycle arrest at the G2/M phase and apoptosis.[2] Taxane-based treatment provides a good initial response and an increased survival in CRPC patients. However, almost all patients develop resistance over time, and the clinical use of these drugs is severely limited. Therefore, elucidating the mechanisms of taxane resistance is critical for the development of improved treatment strategies, favorable prognosis and prolonged survival in CRPC patients.[2,3] Despite current data on possible resistance mechanisms (such as increased activation and expression of efflux transporters, reactivation of the androgen receptor pathway, impairment in the apoptotic pathway, cytokine and chemokine induction, changes in the structure and function of microtubules, upregulation of stress survival proteins) and new drugs targeting these mechanisms, CRPC is known to cause death in many patients.[2,4–6] Therefore, other mechanisms causing taxane resistance need to be investigated.

Recent data indicate that tumors are composed of heterogeneous cell populations and most of these cells have a limited self-renewal capacity. On the other hand, a small group of cells within the heterogeneous tumor tissue has been reported to have a high self-renewal capacity, the ability to transform into different cancer cells, and tumor initiation properties. These are known as cancer stem cells (CSCs).[5,7] The CSCs form cellular spheroids in serum-free and non-adherent conditions, and have differential gene expression profiles, as well as enhanced epithelial-to-mesenchymal transformation (EMT) properties. High levels of expression for genes that encode cell surface receptors (such as *CD44* or *CD133*), transcription factors associated with pluripotency and other stemness characteristics (i.e., *NANOG, OCT4, SOX2, C-MYC*), and proteins associated with drug resistance (i.e., ABCG2 and ABCB1) are all the examples of differential gene expression profiles in CSCs.[7,8] An embryonic transcription factor – *NANOG* – is highly expressed in CSCs, and shows a lower expression in differentiated tissues. It plays a key role in CSCs gaining properties such as self-renewal, pluripotency, stemness, metastasis, invasiveness, angiogenesis and drug resistance, with the help of proteins such as WNT, OCT4, SOX2, and Hedgehog.[9]

A transcription factor *C-MYC* plays an important role in processes such as the cell cycle, cell growth, proliferation, differentiation and apoptosis, as well as tumorigenesis, because it regulates the expression of many genes. Recent studies have revealed that *C-MYC* effects the self-renewal capacity of cells and is one of the most important core markers for stem cells.[10,11] The *CD44* is a cell surface receptor. Hyaluronic acid, osteopontin and many other ligands bind to this receptor to mediate processes such as metastasis, invasion and migration. It is one of the most commonly used cell surface receptors in identifying prostate cancer stem cells.[12] The *ABCG2* is one of the ABC family efflux proteins and is responsible for removing drugs and harmful substances from cells. This receptor is responsible for the development of the resistance to many different drugs, and is defined as a stem cell marker for side populations in many types of tumors, including prostate cancer.[13]

Recent studies also suggest that CSCs may be responsible for chemotherapy and radiotherapy resistance in several cancer types, including prostate cancer.[3,14,15] An emerging hypothesis about CSCs and chemotherapy resistance argues that cancer non-stem cells may acquire stemness properties when they are treated with chemotherapy, and that this process may result in chemotherapy resistance.[7,16]

Some studies have reported an increase in the number of chemotherapy- or radiotherapy-resistant cancer cell groups that exhibit stem-like characteristics, as well as features of EMT.[3,17,18] In studies examining the relationship between prostate CSCs and taxane resistance, researchers have isolated CSCs from prostate cancer cell lines and have reported that those cells were resistant to taxanes. However, these studies failed to reveal whether taxanes affected the stem cell-like characteristics of prostate cancer cells. To the best of our knowledge, the present study is the first attempt to investigate whether a long-term exposure to paclitaxel affects the stem cell characteristics of prostate cancer cells.

Objectives

The aim of this study is to evaluate whether there is an increase in the stem cell-like properties of PC-3 prostate cancer cells following treatment with paclitaxel for a prolonged period. Therefore, the expression of the CSC markers *CD44, C-MYC, NANOG,* and *ABCG2,* as well as sphere formation and wound healing capabilities, were compared between parental and paclitaxel-resistant PC-3 cell lines (PC-3-R).

Materials and methods

Cell culture and the establishment of paclitaxel-resistant cell lines

PC-3 androgen-independent cells (CRL-1435™; American Type Culture Collection (ATCC), Manassas, USA) were cultured in RPMI 1640 Media (Biological Industries, Beit HaEmek, Israel), containing 10% heat-inactivated fetal bovine serum (FBS; Biological Industries), 1% L-glutamine

(Biological Industries), penicillin (100 U/mL), and streptomycin (100 µg/mL). Cells were incubated at 37°C in a humidified atmosphere containing 5% CO_2.

PC-3-R cells were generated from parental PC-3 cells by treating them with increasing concentrations of paclitaxel (Sigma–Aldrich, St. Louis, USA). Parental PC-3 cells were incubated for 24 h, and then treated with 5 nM of paclitaxel for 48 h. Then, the culture media was replaced with fresh media without paclitaxel, and the cells were incubated until they reached 80–90% confluency. The same protocol was repeated with gradually increasing concentrations of paclitaxel (5 nM each time) until 100 nM paclitaxel-resistant and viable PC-3 cells (PC-3-R) could be obtained. Cytotoxicity tests were conducted, and the viability of PC-3 and PC-3-R cells was confirmed under an inverted microscope.

Evaluating the viability and the number of the cells

A trypan blue stain was used to determine the number of viable cells. The cell resistance level and cytotoxic effects of paclitaxel in PC-3 and PC-3-R cells were assessed using a MTT assay. Resistant and parental cells were inoculated in 96-well plates at a density of 5×10^3 cells per well (for each dose, triplicate wells were used) and incubated for 24 h. Afterwards, the cells were treated with increasing concentrations of paclitaxel (1.6–600 nM) and incubated for 72 h. After incubation, a MTT test was conducted and the absorbances were measured using a microplate reader at a wavelength of 570 nM.

Quantitative real-time polymerase chain reaction (RT-qPCR)

The total RNA extraction from cells was conducted using a High Pure RNA Isolation Kit (Roche Diagnostics, Basel, Switzerland). A transcriptor First Strand cDNA Synthesis Kit (Roche Diagnostics) was used to obtain cDNA samples from 1 µg of total RNA. The expression levels of genes were quantified using a Lightcycler 480 (Roche Diagnostics). Suitable probes and gene specific primers were designed by the Universal ProbeLibrary (UPL) Assay Design Center. Each sample was quantified in triplicate, and the mean value was used for further calculations. The B-actin was used to normalize the target gene expressions. Relative changes in the amount of mRNA were calculated based on ΔΔCT. The following primers were used for each target gene:

B-ACTIN
- forward 5′- CCCAGCACAATGAAGATCAA -3′
- reverse 5′- CGATCCACACGGAGTACTTG -3′

NANOG
- forward 5′- ACAGGTGAAGACCTGGTTCC -3′
- reverse 5′- TTGCTATTCTTCGGCCAGTT -3′

CD44
- forward 5′- TCCAACACCTCCCAGTATGACA -3′
- reverse 5′- GGCAGGTCTGTGACTGATGTACA -3′

C-MYC
- forward 5′- TCCACCTCCAGCTTGTACCT-3′
- reverse 5′- TGAGAGGGTAGGGGAAGACC-3′

ABCG2
- forward 5′- TGGCTTAGACTCAAGCACAGC-3′
- reverse 5′- TCGTCCCTGCTTAGACATCC-3′

Sphere formation assay

PC-3 and PC-3-R cells were inoculated onto 96-well ultra-low attachment plates at a density of 750 cells per well in serum-free DMEM/F12 (Thermo Fisher Scientific, Waltham, USA), supplemented with 20 ng/mL EGF (Sigma–Aldrich), B27 (1:50; Invitrogen, Waltham, USA), 0.4% bovine serum albumin (BSA; Sigma–Aldrich), and 4 mg/mL insulin (Sigma–Aldrich). Fresh stem cell media was added every 3–4 days. The cultures were incubated at 37°C in a humidified incubator containing 5% CO_2. The sphere growth was monitored for 14 days and the number of spheres was counted on days 7 and 14. Six wells were inoculated for both PC-3 and PC-3-R cells. The assay was conducted in triplicate.

Wound healing assay

PC-3 and PC-3-R cells were inoculated in six-well plates at a density of 5×10^3 cells per well and incubated in order to reach a confluency of 90% in a complete medium. The complete medium was removed, and cells were starved in a serum-free medium for 24 h. Following the formation of cell monolayers, an artificial wound on the monolayer was scratched with a sterile 200 µL pipette tip. The cells were then washed with phosphate-buffered saline (PBS) and cultured in complete media. The assay was conducted in triplicate. Cells migrating into the wound were photographed at 0 h, 8 h, and 24 h using a camera attached to an inverted microscope.

Statistical analysis

Statistical analyses were conducted using SPSS v. 15.0 (SPSS Inc., Chicago, USA). The data are expressed as the mean ± standard error (SE) and were analyzed using the Mann–Whitney U test. The statistical significance of mRNA expression levels was analyzed using REST 2009 v. 2.0.13 (Qiagen, Hilden, Germany). The values of $p < 0.05$ were deemed statistically significant.

Results

Development of paclitaxel resistance

The PC-3-R cells were obtained by treating the parental cells with increasing concentrations of paclitaxel over a period of several months. The proliferation performance

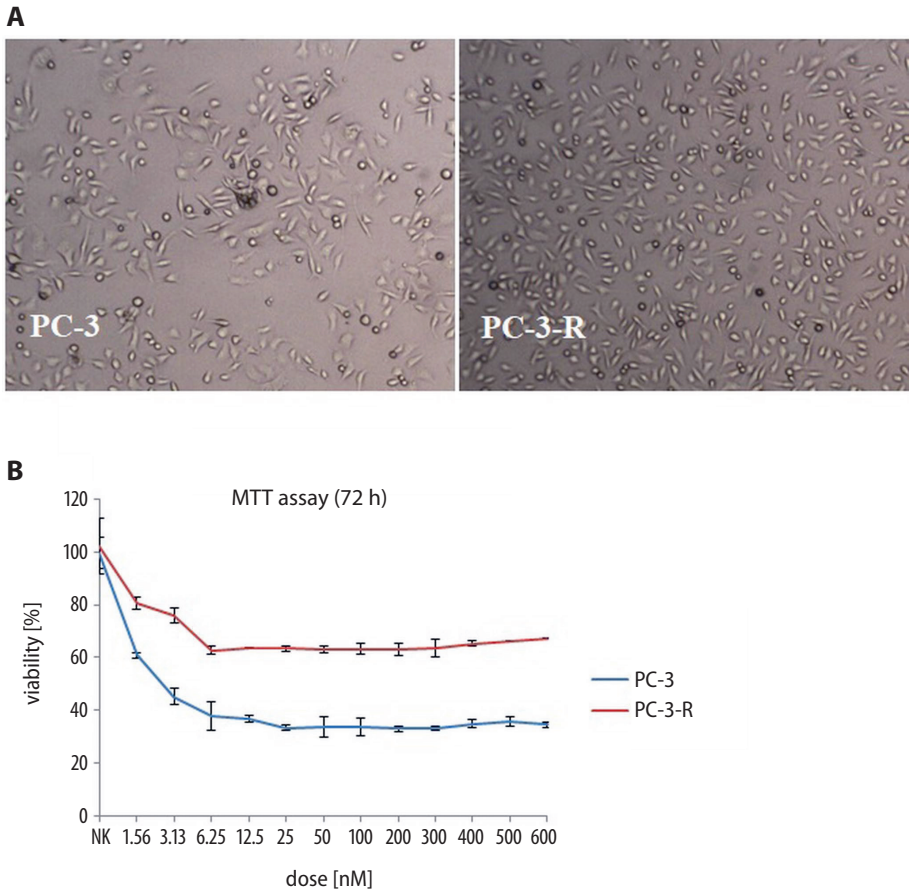

Fig. 1. A. Images of PC-3 and PC-3-R cells at 100 nM paclitaxel concentration (at ×40 total magnification); B. Cytotoxic effect of paclitaxel against PC-3 and PC-3-R cells in MTT assay. The MTT test was conducted in triplicate. Data are shown as mean ± standard error (SE)

of PC-3-R cells at the 100 nM paclitaxel level was higher than the PC-3 cells (Fig. 1A). A MTT test was conducted to assess the cytotoxic effect of paclitaxel in the PC-3 and PC-3-R cells. The IC_{50} dose of PC-3-R cells was higher (>600 nM) than the PC-3 cells (2.65 nM; Fig. 1B).

Expression of stem cell markers in the PC-3 and PC-3-R cells

The expressions of several stem cell markers, including *CD44*, *C-MYC*, *NANOG*, and *ABCG2* in PC-3 and PC-3-R cells were analyzed. The expression levels of *NANOG* and *C-MYC* genes significantly increased with fold changes of 15.5 (p = 0.0130, 95% confidence interval (95% CI) = 12.930–18.259) and 3.28 (p = 0.0400, 95% CI = 2.802–3.909) in PC-3-R cells, respectively, when compared to PC-3 cells. There was no significant difference in the expression levels of *ABCG2* (fold change 1.69, p = 0.0650, 95% CI = 1.647–1.727) and *CD44* (fold change 1.12, p = 0.0630, 95% CI = 1.051–1.226), between resistant and parental cell lines (Fig. 2; Table 1).

Sphere-forming capacity of PC-3 and PC-3-R cells

The sphere formation assay was applied to PC-3 and PC-3-R cells in order to find out whether there was an increase in the stem-like cell population with high sphere forming ability in the PC-3-R cell line (compared to parental PC-3 cells). The results showed that the number of spheres was higher in the PC-3-R cells than in the PC-3 cells, and the difference between the groups was statistically significant both on day 7 (p = 0.0130, z = –2.4810), and day 14 (p = 0.0450, z = –2.0010; Fig. 3; Table 1).

Wound healing assay

The ability of cell migration to serve as an indicator of the stemness-like phenotype was assessed using a wound healing assay. The PC-3-R cells healed wounds better than the PC-3 cells. The rate of wound closure at 8 h for PC-3R cells was 65%, whereas it was only 35.4% for PC-3 cells. At 24 h, the wound had closed at the rate of 100% in PC-3R cells and at 54.5% in the PC-3 cells. The differences in wound closure rates between both groups at 8 h (p = 0.0500, z = –1.964) and 24 h (p = 0.0370, z = –2.0870) were statistically significant (Fig. 4; Table 1).

Discussion

Recent studies have suggested that chemotherapeutics may cause cancer cells to gain stem cell properties, resulting in drug resistance.[19,20] An increased expression in several genes has been reported in CSCs. These genes

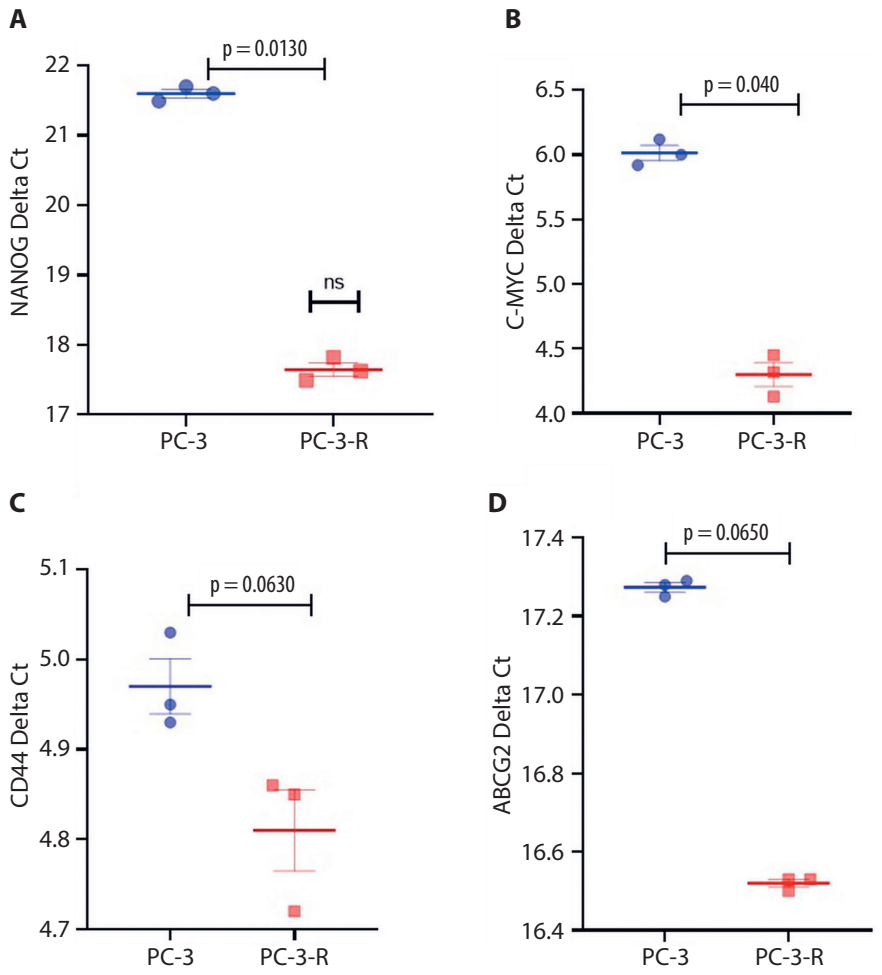

Fig. 2. Expressions of stem cell markers in PC-3 and PC-3-R cells. The expression analysis was conducted in triplicate. A. The NANOG ΔCT values in PC-3 and PC-3-R cells; B. The C-MYC ΔCT values in PC-3 and PC-3-R cells; C. The CD44 ΔCT values in PC-3 and PC-3-R cells; D. The ABCG2 ΔCT values in PC-3 and PC-3-R cells. Statistical significance of mRNA expression levels were analyzed using REST 2009 v. 2.0.13 (Qiagen, Hilden, Germany)

Table 1. Sphere numbers, wound healing rates and relative expression of genes observed in PC-3 and PC-3-R cells

Compared parameters	PC-3 n = 3	PC-3-R n = 3	p-value	z-value or 95% CI
Sphere number on day 7	4.3 ±0.48	9.60 ±1.83	0.0130	–2.4810
Sphere number on day 14	2 ±0.45	3.4 ±0.46	0,0450	–2.0010
Wound healing at 8 h [%]	35.4 ±5.6	54.5 ±3.2	0.0500	–1.964
Wound healing at 24 h [%]	65 ±2.8	100 ±0	0.0370	–2.0870
C-MYC ΔCt	6.02 ±0.06	4.3 ±0.09	0.0400	2.802–3.909
NANOG ΔCt	21.60 ±0.06	17.64 ±0.1	0.0130	12.930–18.259
CD44 ΔCt	4.97 ±0.03	4.81 ±0.04	0.0630	1.051–1.226
ABCG2 ΔCt	17.27 ±0.01	16.52 ±0.01	0.0650	1.647–1.727

Relative expression of genes is expressed as ΔCT, where ΔCT – Ct target gene – Ct B-actin for each sample. The lower the ΔCT values, the higher the gene expression. Data are shown as mean ± standard error (SE). Mann–Whitney U test was used to analyze the data between the groups. The statistical significance of mRNA expression levels was analyzed using REST 2009 v. 2.0.13 (Qiagen, Hilden, Germany). All experiments were conducted triplicate.

encode pluripotency-related proteins, cell surface markers and transporter proteins. In addition, CSCs have increased EMT and migration capabilities.[15,21–23] Another characteristic of these cells is the capability to form spheres in serum-free medium.[24] The aim of this study was to evaluate whether repeated paclitaxel treatment increased the stem cell-like properties of prostate cancer cells. To this end, the expression of genes related to stem cell properties (*NANOG, C-MYC, CD44, ABCG2*), as well as sphere formation and migration capabilities, were compared between PC-3 and PC-3-R cells.

The NANOG protein is encoded by the *NANOG1* gene localized to chromosome 12, spanning 4 exons and 3 introns.[25] Embryonic stem cells have complexes or gene regulation networks containing various transcription factors (*NANOG, Oct4, SOX2, KLF4, C-MYC, SLUG, ESRRB, UTF1, TET2*, and *GLIS1*) that help maintain self-renewal and pluripotency. These complexes regulate the expression

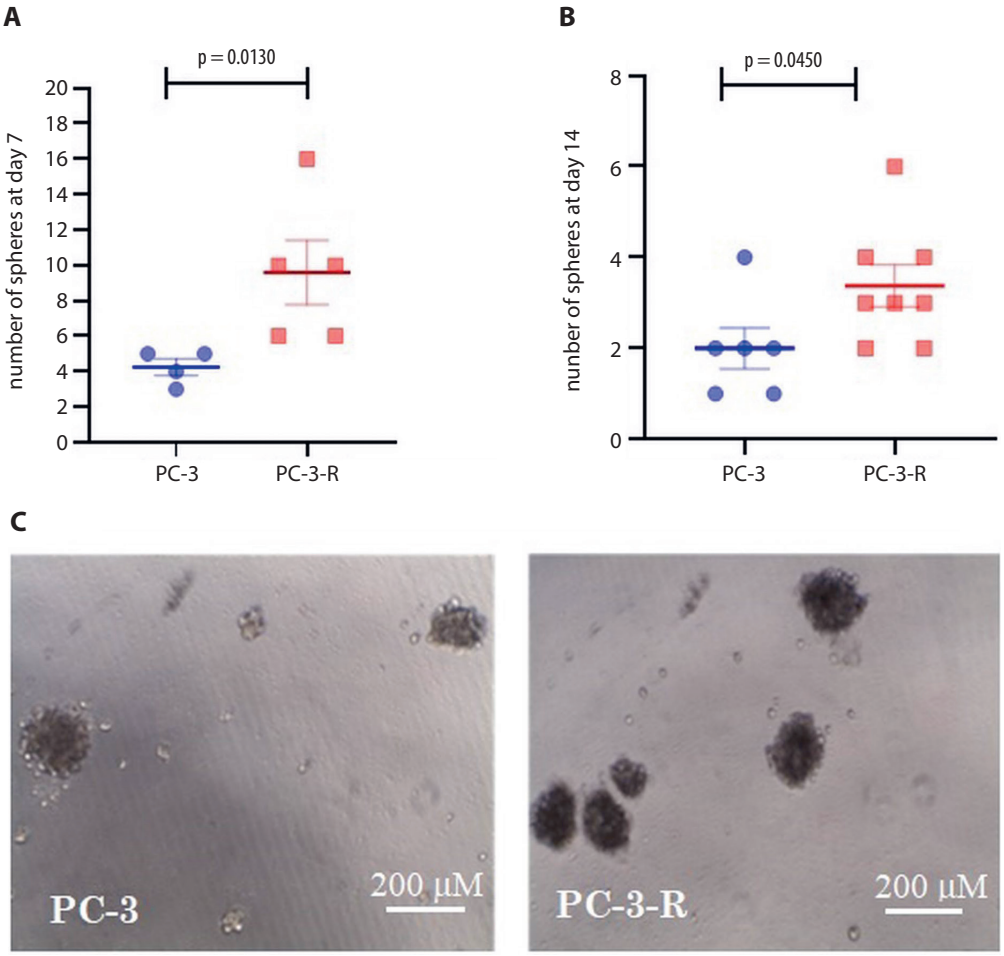

Fig. 3. A. The number of spheres in PC-3 and PC-3-R cells on day 7; B. The number of spheres in PC-3 and PC-3-R cells on day 14; C. Representative micrographs of spheres formed by PC-3 and PC-3-R cells (at ×100 total magnification). Sphere formation assay was conducted in triplicate. Mann–Whitney U test was used to analyze the data between the groups

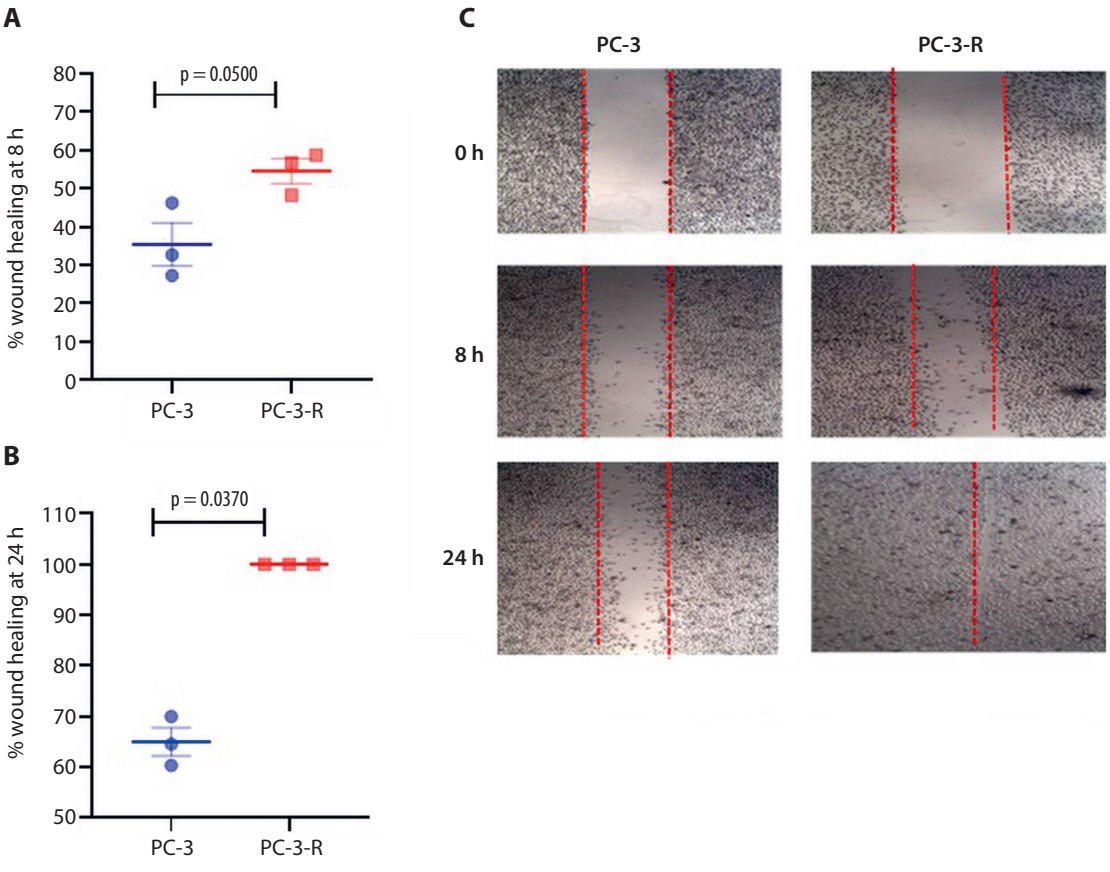

Fig. 4. A. Wound healing rates of PC-3 and PC-3-R cells at 8 h; B. Wound healing rates of PC-3 and PC-3-R cells at 24 h; C. Representative images of wound healing experiments (at ×40 total magnification). Mann–Whitney U test was used to analyze the data between the groups. The wound healing test was conducted in triplicate

of proteins in signaling pathways, such as Wnt, BMP4 and TGF-β, to maintain pluripotency and self-renewal. On the other hand, these complexes interact with various repressors, such as the NuRD complex, REST and coREST, to inhibit differentiation. NANOG plays a key role in these complexes. It activates 2 other crucial proteins, SOX2 and OCT4, and regulates the expression of many downstream proteins.[26] Data from various studies suggest that NANOG has oncogenic properties, such as increasing the migration and invasion capabilities of cancer cells, and that this is achieved through its roles in the formation and maintenance of CSCs.[27]

C-MYC is an oncogene localized to chromosome 8. It plays important roles in many processes, including the regulation of the cell cycle, proliferation, metabolic reprogramming, and cellular survival in cancer cells. Recent studies have revealed that C-MYC induces dedifferentiation through the downregulation of lineage-specific transcription factors. *C-MYC* downregulates *GATA3* and *ESR1* (the master regulator genes of cell differentiation) by binding to their cis-regulatory elements. Hence, oncogenic and epigenetic reprogramming induced by C-MYC protein leads cells to acquire CSC-like properties.[28]

The present study demonstrated that the expression of *NANOG* and *C-MYC* increased significantly in resistant PC-3 cell lines to which paclitaxel had been applied (Fig. 2). Moreover, compared to parental cells, an increase in sphere formation abilities (Fig. 3) and wound healing properties (Fig. 4) was detected in PC-3-R cells. Many studies have investigated the effects of various chemotherapeutics on stem cell characteristics in different types of cancers. For example, Martins-Neves et al. applied increasing concentrations of doxorubicin, cisplatin and methotrexate to osteosarcoma cell lines and evaluated the expression of pluripotency related markers (*KLF4, NANOG, SOX2, OCT4*). They reported that *KLF4, NANOG* and *SOX2* expressions increased in the cell line to which doxorubicin was applied, that *NANOG, KLF4* and *OCT4* expressions increased in the cell line to which cisplatin was applied, and that the expressions of *KLF4* and *OCT4* had increased in the cell line to which methotrexate was applied.[19] When the findings of the current study are evaluated in the light of those obtained by Martins-Neves et al., the entire body of data suggests that different chemotherapeutics stimulate the expressions of different genes related to stem cell characteristics, thus leading to an increase in the stem-like features in various ways. The majority of the studies suggesting that chemotherapeutics can increase the stem cell-like properties of cancer cells show that NANOG expression increases.[8,19,29,30] The other research has reported that NANOG plays a key role in the regulation of stem cell properties, and that it activates many genes in downstream signaling pathways.[26] Considering all these findings, the increase in NANOG expression, C-MYC expression, sphere formation, and migration capability in paclitaxel-resistant prostate cancer cells (compared to parental cells) observed in the current study suggests that paclitaxel may induce the stem cell-related features of PC-3 prostate cancer cells.

A study by Yoshiyama et al. reported that – in addition to the capability of forming spheres – *NANOG, C-MYC* and *SOX2* expressions increased significantly in zoledronate-resistant non-small cell lung cancer and osteosarcoma cell lines, compared to the parental cell lines.[8] Similarly, Wiechert et al. found that CSC-related properties such as increased *NANOG, SOX2* and *OCT4* expressions, as well as in vivo tumor-forming abilities were induced in ovarian cancer cells that were resistant to cisplatin.[29] Liu et al. also reported that neoadjuvant chemotherapy induced the stem-like characteristics of breast cancer cells in both mice and humans. It has been shown that neoadjuvant chemotherapy caused an increase in monocyte chemoattractant proteins (MCPs), which then resulted in elevated expressions of *NANOG* and *SOX9,* together with an increased sphere-forming capability.[30] Cajigas-Du Ross et al. performed transcriptomic profiling using RNA sequencing in the docetaxel-resistant and parental PC-3 and Du145 prostate cancer cells. Their results indicated that 75% of the top 25 genes that are upregulated in the docetaxel-resistant cells are associated with stem cell characteristics (e.g., *NES, TSPAN8, DPPP, DNAJC12*, and *MYC*).[5] Similarly to the current study, that study was performed on prostate cancer cells (PC-3 and Du145). Moreover, gene expression levels were compared between cells resistant to docetaxel, which is also a taxane (like paclitaxel), and parental cells. In this study, *MYC* was among the top 25 genes to exhibit increased expression, which supports the data of the current study. In light of the aforementioned research, it was observed that some genes related to the stem cell characteristics (such as *NANOG, SOX2, OCT4, C-MYC*, and *ABCG2)* were upregulated in cells resistant to chemotherapeutics. Furthermore, these genes block apoptosis and cause drug resistance. They are also associated with stem cell features such as pluripotency and self-renewal, suggesting a close relationship between the increase in CSC characteristics and drug resistance. Our findings that *NANOG* and *C-MYC* expressions are upregulated in PC-3-R cells support this idea. Additionally, the increased sphere-forming capacity and migration capability of the PC-3-R cells indicate an increase in stem cell properties.

The *ABCG2* is located on chromosome 4 and consists of 16 exons. ABCG2 is a member of the family of ATP binding cassette (ABC) transporters, which pump endogenous and exogenous harmful compounds (such as drugs) out of the cell. Many drugs commonly used in cancer chemotherapy are among the substrates of ABCG2. This gene was first cloned from doxorubicin-resistant MCF-7 breast cancer cells; hence, it is also known as breast cancer resistance protein (BCRP). Increased expression of *ABCG2* is thought to cause both active extracellular removal of chemotherapy agents and resistance to chemotherapy. This gene is also

highly expressed in stem cell subpopulations. ABCG2 is thought to inhibit cell death in stem cell populations, and to maintain stem cell homeostasis under extreme stress. It is also believed to be associated with both the stem cell phenotype and drug resistance.[31]

The CD44 is a single polypeptide chain cell surface receptor that is encoded by the *CD44* gene. The *CD44* gene is located on chromosome 11 and has 19 exons. Alternative splicing of exons 6 to 15 of the *CD44* gene leads to the formation of multiple CD44 isoforms, while their removal produces the standard *CD44* transcript. This protein acts as a receptor for hyaluronan and many other extracellular matrix components. It also acts as a cofactor for various growth factors and cytokines. Therefore, CD44 is thought to be a signaling platform that processes and transfers multiple signals to membrane-associated cytoskeleton proteins or the nucleus, thereby regulating the expression of many genes involved in differentiation, cell migration, proliferation, adhesion, EMT, and survival. For example, many cell surface receptors such as EGFR, TGF-BRI, c-MET, ErbB2, and oncogenic signaling pathways become activated when hyaluronan binds to CD44. Increasing evidence suggests that CD44 is a critically important regulator of CSC properties (e.g., self-renewal, tumor initiation, chemoresistance, and metastasis).[32–34]

There was no significant increase in *ABCG2* and *CD44* expressions in paclitaxel-resistant PC-3 cells in the current study (Fig. 2). The lack of change in *ABCG2* expression is possibly related to the fact that paclitaxel may not be an ABCG2 substrate.[35] Martins-Neves et al. evaluated the expressions of the multidrug resistance transport proteins ABCB1 and ABCG2 in osteosarcoma cell lines to which increasing concentrations of doxorubicin, cisplatin and methotrexate were applied. The expressions of these genes increased in doxorubicin-applied cells, whereas the same effect was not observed in cisplatin-applied and methotrexate-applied cells.[19] Similar to the current study, no increase was observed in *ABCB1* and *ABCG2* expressions in cell lines treated with cisplatin and methotrexate in the study of Martins-Neves et al. This may be because paclitaxel, cisplatin and methotrexate are not the substrates of ABCG2 or ABCB1, or that they are excreted in different ways.

Several studies have reported that CD44-negative cells can transform into CD44-positive cells, or that CD44-negative cells may display stem cell-like characteristics.[36,37] One such a study reported that CD44-negative PC-3 cells spontaneously converted into CD44-high cells expressing a different *CD44* isoform in stem cell medium – which was more invasive and had higher clonogenic and self-renewal potential than *CD44*-high cells expressing the standard isoform.[38] In the present study, there may be an increase in the expression of *CD44* isoforms different from the standard one observed in PC-3-R cells.

The present study evaluated the effects of paclitaxel, a chemotherapeutic from the taxane group, on the stem cell properties of prostate cancer cells, and filled a gap in the literature on this subject. The current study indicated that paclitaxel can cause a heightened sphere-forming and migration capability in prostate cancer cells, in addition to an increased expression of *NANOG* and *C-MYC*. In light of these findings, it was thought that targeting CSCs together with taxanes and the use of therapeutic agents regulating the expression of stem cell phenotype-related genes (such as *NANOG* and *C-MYC*) will minimize treatment failures due to taxane resistance. Pouyafar et al. showed that natural compounds such as resveratrol can increase the mesenchymal endothelial transformation rate and transdifferentiation of CSCs. On the other hand, they can also reduce the resistance of cells to chemotherapeutics by modulating GALNT11 synthesis and autophagy signals.[39] To overcome taxane resistance, natural compounds or different treatment agents that target CSCs could be exploited.

Limitations

The present study has several limitations. First, the expressions of other genes related to stem cell characteristics were not evaluated. Second, the changes in gene expression have not yet been confirmed with western blot analysis. Third, other methods that analyze stem cell populations (e.g., using a flow cytometer to measure aldehyde dehydrogenase activity) were not used.

Conclusions

Repeatedly applying paclitaxel to prostate cancer cell lines is thought to increase the stem cell-like properties of the cells since this is one of the mechanisms causing drug resistance. The combined use of therapies targeting CSCs with classical chemotherapy may help patients overcome drug resistance and thus, may improve their treatment. Future studies evaluating the expressions of different genes related to stem cell characteristics and using additional protein expression analyses and flow cytometry techniques may prove beneficial in supporting these conclusions.

ORCID iDs

Fadime Mutlu Içduygu https://orcid.org/0000-0002-4913-9420
Hale Samli https://orcid.org/0000-0003-4728-0735
Asuman Özgöz https://orcid.org/0000-0003-4018-5807
Buse Vatansever https://orcid.org/0000-0002-2873-3885
Kuyas Hekimler Oztürk https://orcid.org/0000-0002-7075-8875
Egemen Akgün https://orcid.org/0000-0003-1979-419X

References

1. World Cancer Research Fund. Prostate cancer statistics. https://www.wcrf.org/dietandcancer/cancer-trends/prostate-cancer-statistics. Accessed June 12, 2020.
2. Bumbaca B, Li W. Taxane resistance in castration-resistant prostate cancer: Mechanisms and therapeutic strategies. *Acta Pharm Sin B*. 2018;8(4):518–529. doi:10.1016/j.apsb.2018.04.007

3. Kroon J, Kooijman S, Cho NJ, Storm G, Van der Pluijm G. Improving taxane-based chemotherapy in castration-resistant prostate cancer. *Trends Pharmacol Sci*. 2016;37(6):451–462. doi:10.1016/j.tips.2016.03.003
4. Galletti G, Leach BI, Lam L, Tagawa ST. Mechanisms of resistance to systemic therapy in metastatic castration-resistant prostate cancer. *Cancer Treat Rev*. 2017;57:16–27. doi:10.1016/j.ctrv.2017.04.008
5. Cajigas-Du Ross CK, Martinez SR, Woods-Burnham L, et al. RNA sequencing reveals upregulation of a transcriptomic program associated with stemness in metastatic prostate cancer cells selected for taxane resistance. *Oncotarget*. 2018;9(54):30363–30384. doi:10.18632/oncotarget.25744
6. Dong L, Zieren RC, Xue W, De Reijke TM, Pienta KJ. Metastatic prostate cancer remains incurable: Why? *Asian J Urol*. 2019;6(1):26–41. doi:10.1016/j.ajur.2018.11.005
7. Zhang S, Zhang H, Ghia EM, et al. Inhibition of chemotherapy-resistant breast cancer stem cells by a ROR1 specific antibody. *Proc Natl Acad Sci U S A*. 2019;116(4):1370–1377. doi:10.1073/pnas.1816262116
8. Yoshiyama A, Morii T, Ohtsuka K, et al. Development of stemness in cancer cell lines resistant to the anticancer effects of zoledronic acid. *Anticancer Res*. 2016;36(2):625–631. PMID:26851017
9. Najafzadeh B, Asadzadeh Z, Motafakker Azad R, et al. The oncogenic potential of NANOG: An important cancer induction mediator. *J Cell Physiol*. 2021;236(4):2443–2458. doi:10.1002/jcp.30063
10. Zhang HL, Wang P, Lu MZ, Zhang SD, Zheng L. c-Myc maintains the self-renewal and chemoresistance properties of colon cancer stem cells. *Oncol Lett*. 2019;17(5):4487–4493. doi:10.3892/ol.2019.10081
11. Elbadawy M, Usui T, Yamawaki H, Sasaki K. Emerging roles of c-Myc in cancer stem cell-related signaling and resistance to cancer chemotherapy: A potential therapeutic target against colorectal cancer. *Int J Mol Sci*. 2019;20(9):2340. doi:10.3390/ijms20092340
12. Senbanjo LT, AlJohani H, Majumdar S, Chellaiah MA. Characterization of CD44 intracellular domain interaction with RUNX2 in PC3 human prostate cancer cells. *Cell Commun Signal*. 2019;17(1):80. doi:10.1186/s12964-019-0395-6
13. Harris KS, Kerr BA. Prostate cancer stem cell markers drive progression, therapeutic resistance, and bone metastasis. *Stem Cells Int*. 2017;2017:8629234. doi:10.1155/2017/8629234
14. Kerr CL, Hussain A. Regulators of prostate cancer stem cells. *Curr Opin Oncol*. 2014;26(3):328–333. doi:10.1097/CCO.0000000000000080
15. Phi LTH, Sari IN, Yang YG, et al. Cancer stem cells (CSCs) in drug resistance and their therapeutic implications in cancer treatment. *Stem Cells Int*. 2018;2018:5416923. doi:10.1155/2018/5416923
16. Batlle E, Clevers H. Cancer stem cells revisited. *Nat Med*. 2017;23(10):1124–1134. doi:10.1038/nm.4409
17. Marín-Aguilera M, Codony-Servat J, Reig Ò, et al. Epithelial-to-mesenchymal transition mediates docetaxel resistance and high risk of relapse in prostate cancer. *Mol Cancer Ther*. 2014;13(5):1270–1284. doi:10.1158/1535-7163.MCT-13-0775
18. Takebe N, Harris PJ, Warren RQ, Ivy SP. Targeting cancer stem cells by inhibiting Wnt, Notch, and Hedgehog pathways. *Nat Rev Clin Oncol*. 2011;8(2):97–106. doi:10.1038/nrclinonc.2010.196
19. Martins-Neves SR, Paiva-Oliveira DI, Wijers-Koster PM, et al. Chemotherapy induces stemness in osteosarcoma cells through activation of Wnt/β-catenin signaling. *Cancer Lett*. 2016;370(2):286–295. doi:10.1016/j.canlet.2015.11.013
20. Yuan B, Liu Y, Yu X, et al. FOXM1 contributes to taxane resistance by regulating UHRF1-controlled cancer cell stemness. *Cell Death Dis*. 2018;9(5):562. doi:10.1038/s41419-018-0631-9
21. Najafi M, Farhood B, Mortezaee K. Cancer stem cells (CSCs) in cancer progression and therapy. *J Cell Physiol*. 2019;234(6):8381–8395. doi:10.1002/jcp.27740
22. Cao S, Wang Z, Gao X, et al. FOXC1 induces cancer stem cell-like properties through upregulation of betacatenin in NSCLC. *J Exp Clin Cancer Res*. 2018;37(1):220. doi:10.1186/s13046-018-0894-0
23. Hadjimichael C, Chanoumidou K, Papadopoulou N, Arampatzi P, Papamatheakis J, Kretsovali A. Common stemness regulators of embryonic and cancer stem cells. *World J Stem Cells*. 2015;7(9):1150–1184. doi:10.4252/wjsc.v7.i9.1150
24. Ma XL, Sun YF, Wang BL, et al. Sphere-forming culture enriches liver cancer stem cells and reveals Stearoyl-CoA desaturase 1 as a potentialtherapeutic target. *BMC Cancer*. 2019;19(1):760. doi:10.1186/s12885-019-5963-z
25. Zhang W, Sui Y, Ni J, Yang T. Insights into the Nanog gene: A propeller for stemness in primitive stem cells. *Int J Biol Sci*. 2016;12(11):1372–1381. doi:10.7150/ijbs.16349
26. De Kumar B, Parker HJ, Parrish ME, et al. Dynamic regulation of Nanog and stem cell-signaling pathways by Hoxa1 during early neuroectodermal differentiation of ES cells. *Proc Natl Acad Sci U S A*. 2017;114(23):5838–5845. doi:10.1073/pnas.1610612114
27. Zhang J, Chen M, Zhu Y, et al. SPOP promotes Nanog destruction to suppress stem cell traits and prostate cancer progression. *Dev Cell*. 2019;48(3):329–344.e5. doi:10.1016/j.devcel.2018.11.035
28. Yoshida GJ. Emerging roles of Myc in stem cell biology and novel tumor therapies. *J Exp Clin Cancer Res*. 2018;37(1):173. doi:10.1186/s13046-018-0835-y
29. Wiechert A, Saygin C, Thiagarajan PS, et al. Cisplatin induces stemness in ovarian cancer. *Oncotarget*. 2016;7(21):30511–30522. doi:10.18632/oncotarget.8852
30. Liu L, Yang L, Yan W, et al. Chemotherapy induces breast cancer stemness in association with dysregulated monocytosis. *Clin Cancer Res*. 2018;24(10):2370–2382. doi:10.1158/1078-0432.CCR-17-2545
31. Ding XW, Wu JH, Jiang CP. ABCG2: A potential marker of stem cells and novel target in stem cell and cancer therapy. *Life Sci*. 2010;86(17–18):631–637. doi:10.1016/j.lfs.2010.02.012
32. Skandalis SS, Karalis TT, Chatzopoulos A, Karamanos NK. Hyaluronan-CD44 axis orchestrates cancer stem cell functions. *Cell Signal*. 2019;63:109377. doi:10.1016/j.cellsig.2019.109377
33. Xu H, Niu M, Yuan X, Wu K, Liu A. CD44 as a tumor biomarker and therapeutic target. *Exp Hematol Oncol*. 2020;9(1):36. doi:10.1186/s40164-020-00192-0
34. Yan Y, Zuo X, Wei D. Concise review: Emerging role of CD44 in cancer stem cells. A promising biomarker and therapeutic target. *Stem Cells Transl Med*. 2015;4(9):1033–1043. doi:10.5966/sctm.2015-0048
35. Mao Q, Unadkat JD. Role of the breast cancer resistance protein (BCRP/ABCG2) in drug transport: An update. *AAPS J*. 2015;17(1):65–82. doi:10.1208/s12248-014-9668-6
36. Oh SY, Kang HJ, Kim YS, Kim H, Lim YC. CD44-negative cells in head and neck squamous carcinoma also have stemcell like traits. *Eur J Cancer*. 2013;49(1):272–280. doi:10.1016/j.ejca.2012.06.004
37. Qian H, Le Blanc K, Sigvardsson M. Primary mesenchymal stem and progenitor cells from bone marrow lack expression of CD44 protein. *J Biol Chem*. 2012;287(31):25795–25807. doi:10.1074/jbc.M112.339622
38. Di Stefano C, Grazioli P, Fontanella RA, et al. Stem-like and highly invasive prostate cancer cells expressing CD44v8-10 marker originate from CD44-negative cells. *Oncotarget*. 2018;9(56):30905–30918. doi:10.18632/oncotarget.25773
39. Pouyafar A, Rezabakhsh A, Rahbarghazi R, et al. Treatment of cancer stem cells from human colon adenocarcinoma cell line HT-29 with resveratrol and sulindac induced mesenchymal–endothelial transition rate. *Cell Tissue Res*. 2019;376(3):377–388. doi:10.1007/s00441-019-02998-9

Therapeutic role of vanillin receptors in cancer

Katarzyna Rakoczy[1,A,B,D], Wojciech Szlasa[1,C–E], Jolanta Saczko[2,E,F], Julita Kulbacka[2,A,C,E,F]

[1] Students' Research Group, Faculty of Medicine, Wroclaw Medical University, Poland
[2] Department of Molecular and Cellular Biology, Faculty of Pharmacy, Wroclaw Medical University, Poland

A – research concept and design; B – collection and/or assembly of data; C – data analysis and interpretation; D – writing the article; E – critical revision of the article; F – final approval of the article

Advances in Clinical and Experimental Medicine, ISSN 1899–5276 (print), ISSN 2451–2680 (online) *Adv Clin Exp Med*. 2021;30(12):1293–1301

Address for correspondence
Julita Kulbacka
E-mail: Julita.Kulbacka@umed.wroc.pl

Funding sources
This research was financially supported by Statutory Subsidy Funds of the Department of Molecular and Cellular Biology No. SUB.D260.21.095.

Conflict of interest
None declared

Received on April 21, 2021
Reviewed on May 18, 2021
Accepted on June 25, 2021

Published online on October 5, 2021

Abstract

Natural products play significant roles in the development of novel drugs. One of such compounds is vanillin – a natural substance commonly used in food. Anticancer potential of the substance is continually encouraging researchers to conduct further investigations. A rising number of publications describe the role of 4-hydroxy-3-methoxybenzaldehyde (vanillin) in the process of inhibiting tumor growth. Four vanilloid receptors play significant roles in the response of cancer cells to the natural compound. Each of these proteins can be individually affected by vanillin; thus, the substance either leads to inhibition of the cell proliferation or increases the Ca^{2+} level. The TRPV1, a non-selective cation channel permeable to calcium, acts on cancer development and progression. Thus, vanilloid receptors have the potential to become the target for therapeutical research. Moreover, selective inhibitors of the receptor have proved their efficacy in vitro. CK2α is an antiapoptotic, cancer-sustaining protein and, therefore, the inhibitor of apoptosis. Thus, drugs that exhibit allosteric and ATP-competitive inhibition of the protein might be crucial for cancer therapy. CAMK4 is a protein kinase expression associated with a wide array of cancers. Also, MARK4 is another kinase responsible for the stability of microtubules, overexpressed in many cancer types. Studies concerning this protein revealed that microtubule impairment might be a cancer therapy direction.

This review aims to demonstrate the crucial role of described vanilloid receptors in inhibiting the proliferation of cancer cells and to prove the usefulness of using vanillin and its derivatives in the process of drug design.

Key words: vanillin, cancer, TRPV1 protein, CK2α protein, CAMK4 protein

Cite as
Rakoczy K, Szlasa W, Saczko J, Kulbacka J. Therapeutic role of vanillin receptors in cancer. *Adv Clin Exp Med*. 2021;30(12):1293–1301.doi:10.17219/acem/139398

DOI
10.17219/acem/139398

Introduction

Vanilla extract consists of various natural substances. One of its most prominent components is vanillin ($C_8H_8O_3$), a hydrophilic and phenolic aldehyde. The chemical structure of vanillin is comprised of aldehyde, hydroxyl and ether groups located around an aromatic ring. This compound is mostly known for its aromatic flavor and specific odor.[1] Vanillin can be of both synthetic and natural origin. When extracted from the seedpods of *Vanilla planifolia*, the compound remains conjugated with β-D-glucose and initially lacks its taste properties. However, in the course of production, free vanillin is released from the glucoside by hydrolytic enzymes.[2] Vanillin may be synthesized from small molecule natural compounds. Clove oil is the source of eugenol, which, through the oxidation of a vinyl group (attached to the aromatic ring), forms vanillin. In a similar way, vanillin may be synthesized from coniferyl alcohol (from spruce tree lignin) and from ferrulic acid (from rice). Interestingly, the vanillin precursor guaiacol may be found in petroleum.[2] Due to its relatively simple structure, vanillin-like fragments are likely to be found in higher mass molecules. Following metabolism, radiation, heat and decomposition, vanillin may be released. For instance, irradiation of curcumin solution leads to the generation of free vanillin, feruloylmethane and acetone. In addition, vanillin remains one of the products of metabolism of curcumin.[3]

Vanillin has a significant antitumor potential,[4] and its activity may be more valuable than previously considered.[5] The antimutagenic effects of 4-hydroxy-3-methoxybenzaldehyde seem to be due to its influence on cell redox homeostasis and DNA repair pathways. However, not only does vanillin exhibit antimutagenic properties, but it is also considered to be an antimutagen.[6–8] Moreover, it has been shown to have antioxidant,[9,10] antimicrobial,[11] analgesic,[12,13] and anti-erythrocyte-sickling[14] properties. Taking the quintessential properties of the discussed phenolic aldehyde into consideration, the process by which the described organic compound affects certain cells is worth further discussion and warrants closer analysis.

Vanillin receptors overview and their role in carcinogenesis

Vanillin may exert its antitumor potential by targeting membrane and intracellular receptors. The current literature suggests that this compound acts on 4 main proteins (transmembrane channel *TRPV1*) and 3 cytoplasmic peptides – MARK4, CAMK4 and CK2 (Fig. 1).

TRPV1

The *TRPV1* receptor belongs to the transient receptor potential gene superfamily that includes 28 separate genes, grouped into 6 subfamilies: TRPC, TRPV, TRPP,

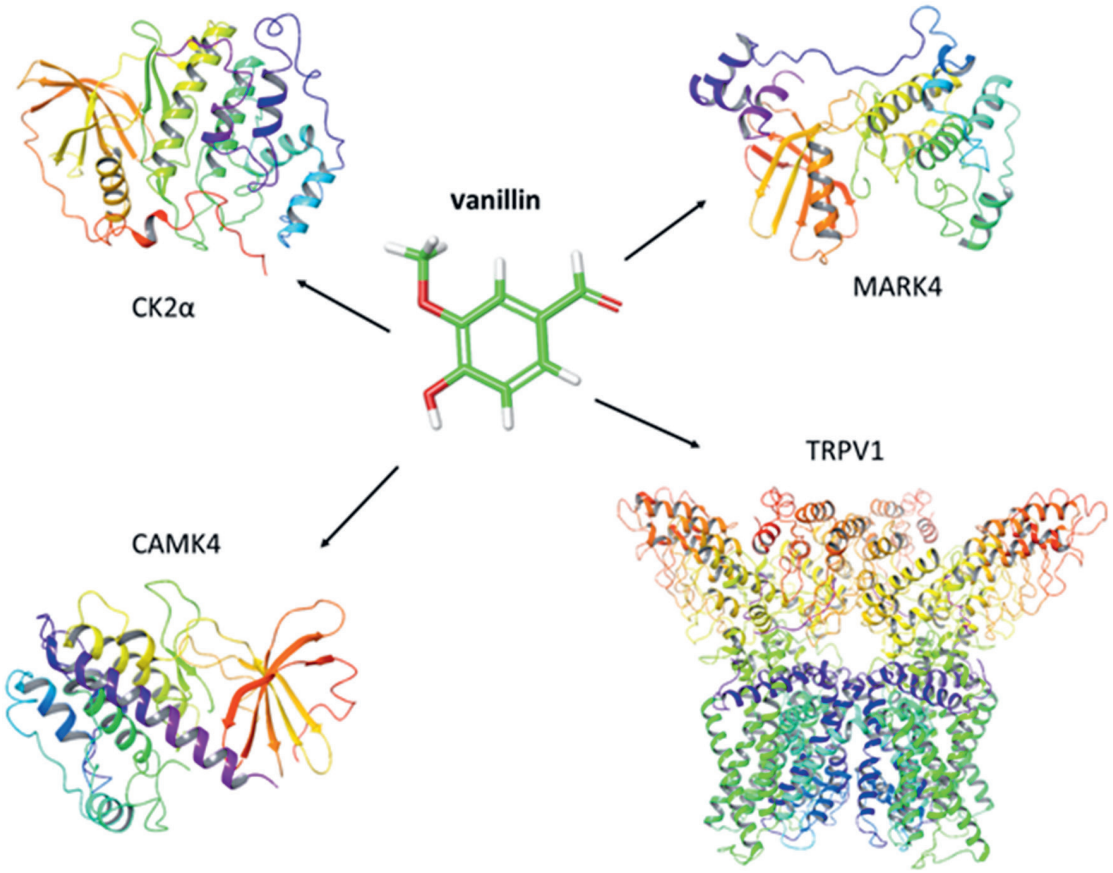

Fig. 1. Four vanilloid receptors play significant roles in the response of cancer cells to the natural compound. Each of the proteins is affected by vanillin in a different way; thus, the substance either leads to an inhibition of cell proliferation or to an increase in Ca^{2+} levels

TRPM, TRPA, and TRPML.[15–17] Each of these genes encode a non-selective cation channel responsible for a variety of functions in the organism.[15,16] These channels function as a molecular gateway, which transforms stimuli of both chemical and physical origins into action potentials. Moreover, these channels are the major transducers for a multitude of biological functions, including vision, taste, olfaction, mechanonsensation, osmosensation, and nociception.[16,18,19] The products encoded by transient receptor potential (TRP) superfamily genes are crucially important sensory receptors, and among the members of the family, there is a group of thermoreceptors,[20] which detect hot (*TRPV1* and *TRPV2*) and cold (*TRPA1*) temperatures – from adverse stimuli to harmless ones (*TRPV3*, *TRPV4* and *TRPM8*).[15,20] However, these channels are activated not only by temperature stimuli, but also by chemical substances like menthol (*TRPM8*), camphor (*TRPV3*), mustard oil (*TRPA1*), wasabi (*TRPA1*), and capsaicin (*TRPV1*).[20–25]

The *TRPV1* is a non-selective cation channel that is permeable to calcium and is gated by noxious heat, vanilloids, extracellular protons, and endocannabinoids.[18,21] This channel is a tetrameric membrane protein that contains 4 indistinguishable subunits gathered around an aqueous pore in the central part of the channel.[26] Each subunit of this multimeric protein consists of 6 transmembrane segments (S1, S2, S3, S4, S5, and S6) with an amphipathic region between the 5th and 6th segment that forms the channel conductive pore (Fig. 2). Glutamic acid docks into the ampiphatic region in a pH-sensitive manner and gates the whole ionic current through the channel.[21] In the cytoplasmic N-terminus of the protein, there are 3 ankyrin domains. These domains present consensus sequences for protein kinases and conciliate the protein-protein model of cytosolic protein interactions. The C-terminus domain includes phosphoinositide calmodulin binding (CAM) domains and phosphorylation sites.[15] In addition, this receptor exhibits the TRP-like motif, which plays the role of an associative domain for the whole receptor to interact with other membrane-bound proteins.[27]

With regard to the involvement of *TRPV1* in cancer, the receptor is now the most important target for the treatment of chronic pain in bone cancer.[28] For this reason, the search for *TRPV1* specific antagonists is becoming a promising direction in drug discovery and development.[29] As a regulator of inflammation and calcium signaling pathways, the *TPRV1* channel can affect the development and progression of cancer.[30] The receptor is also upregulated in various neoplasms, including breast and urothelial cancers,[31] and this relationship may find an application in the therapies targeting tumors.[32] The anticancer potential of *TRPV1* activation arises from an increased permeability of the cell membrane for chemotherapy agents.[33,34] The effects of receptor activation depend on the preliminary sensitization of *TRPV1*. The activation of *TRPV1* in neurons leads to the release of pro-inflammatory substance P and calcitonin-related peptide (CGRP).[35,36] However, the summarized systemic effect of *TRPV1* knockout turned out to be anti-inflammatory.[37] Most of the studies aiming to evaluate the proliferation of cancer cells with the use of selective *TRPV*1 antagonists have shown that the inhibition of the channel is not related to a higher probability of cancer.[38] In addition, a study by Hwang et al. showed that *TRPV1* is not involved in carcinogenesis induced by activation of the Akt pathway.[39]

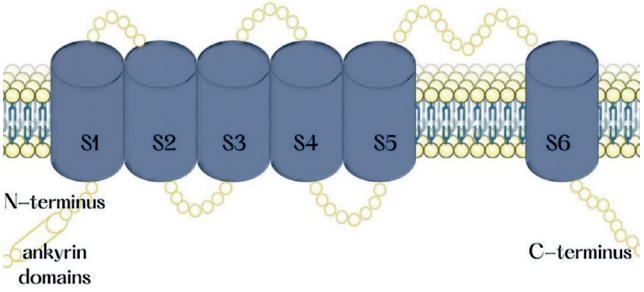

Fig. 2. The *TRPV1* receptor consists of 6 transmembrane segments (S1, S2, S3, S4, S5, and S6) with an amphipathic region between the 5th and 6th segment that forms the channel conductive pore

The other example are vanilloids, which induce *TRPV1*-unrelated apoptosis in oral cancer.[40] Activation of calcium signaling has been widely evaluated for its potential application in the activation of the intrinsic apoptotic pathway in cancer.[41] The assumption is that activation of calcium inflow to the cytoplasm and the mitochondria would result in programmed cell death. However, in the case of *TRPV1*, the effect varies between analyzed cell lines and, curiously, is related to the level of *TRPV1* expression.[31] Namely, breast cancer cell lines (MDA-MB231, MCF7) that express the *TRPV1* channel are not sensitive to the administration of its selective agonist – vanilloids. However, after the transfection with the cDNA of the channel, the sensitivity increases significantly.

The biological effects of *TRPV1* activation may also arise from its interactions with the other transmembrane proteins, especially those from TRP family.[42] In the case of a therapeutic approach, selective inhibitors of *TRPV1* have proven their efficacy in vitro. The application of a *TRPV1* activator simultaneously with standard chemotherapy agents (cisplatin, 5-Fluoruracil, Pirarubicin), leads to a synergistic effect.[43–45] The standalone effect of *TRPV1* activation in thyroid adenocarcinoma cells has been proven effective as well.[46]

CK2α

Although casein kinase II (*CK2*) is not an oncogene, its activity is significant in various types of cancers, especially hematological malignancies.[47–49] The antiapoptotic properties of this kinase are associated with an ability to sustain cancer growth. The CK2α subunit is the anti-apoptotic protein by which vanillin might induce apoptosis in cancer cells through the inhibition of NF-κB

phosphorylation and activation.[50] An interaction between the receptor and 4-hydroxy-3-methoxybenzaldehyde inhibits the kinase function of CK2. A guaiacol functional group interacts with the positively charged region of the CK2α ATP blinding pocket. The potency of the inhibitory activity of vanillin is approximately equivalent to the effects induced by other substances, like feruloyl methane or ferulic aldehyde. The use of vanillin and its derivatives in the design of specific CK2 inhibitors may prove to be very successful.[51] Protein kinase 2 is associated with the increased growth and proliferation of cancer cells.[52] This kinase acts as a potent inhibitor of apoptosis, allowing the cells to proliferate. Moreover, increased expression is related to the level of dysplasia among cancer cells.[53] The CK2 mechanism of action involves activation of the NF-κB pathway by the phosphorylation (and further degradation) of its inhibitor IκB.[54] This kinase is also involved in the induction of drug resistance.[55] In addition, CK2 inhibitors cause the suppression of angiogenesis[56] and the cancer-specific, PTEN-related energetic shift.[57] Various drugs have been tested for allosteric and ATP-competitive inhibition of CK2 in cancer therapy,[58] with the latter including the small molecule inhibitors TBB, DMAT, IQA, CX-4945, and CX-5011.[59] The ATP analogues contain the 2-aminothiazole-derived compounds.[59] Moreover, some CK2 inhibitors have proven efficacious in preclinical studies, like CX4945 for high-risk pediatric leukemias.[47] Aside from the novel chemotherapy agents, curcumin and its degradation products (ferulic acid, vanillin, feruloylmethane and coniferyl aldehyde) turned out to be potent CK2 inhibitors.[51]

CAMK4

Human calcium/calmodulin-dependent protein kinase IV (CAMK4), a member of the Ser/Thr kinase family, is associated with different types of cancer. Vanillin is considered a potential anticancer agent, and therefore its compatibility with the receptor binding pocket of this kinase has been investigated. It has been found that this molecule binds strongly to the active site cavity of CAMK4.[60] As further research has shown, the anticancer potential of vanillin is related to its interaction with the described receptor, successfully inhibiting the proliferation of HepG2 (human hepatocyte carcinoma) and SH-SY5Y neuroblastoma cells.[61] Moreover, vanillin treatment does not only affect tumor proliferation directly, but it also reduces ROS production and mitochondrial membrane depolarization, which eventually leads to the apoptosis in human hepatocyte carcinoma and neuroblastoma cells.[62] Therefore, targeting CAMK4 as a novel therapeutic prospect might result in the common usage of vanillin (a natural chemical molecule) and its derivatives, which could be crucial when it comes to minimizing possible side effects.[62] CAMK4 is also involved in the calmodulin-dependent protein kinase kinase 2 (CAMKK2) signal transduction pathway. Due to its activation of various transcription factors, neuronal communication and immune response, CAMK4 was considered a molecular target for anticancer therapy.[63] Nuclear localization of CAMK4 is associated with the malignant potential of ovarian cancer.[64] It has also been detected in lung and hepatocellular carcinomas.[64] Indeed, hepatic cancer is essentially regulated by the CAMKK2/CAMK4 pathway.[61] The CAMK4 has been examined as a potential target in the case of various malignancies, including hepatocellular carcinoma (HCC), breast cancer, neuroblastoma, prostate cancer, and acute myelogenous leukemia (AML).[65] Vanillin has proven to be efficacious against cancer through binding to CAMK4 in HepG2 and SH-SY5Y cancer cells.[62] Also, ellagic acid and quercetin were shown to inhibit the activity of this kinase.[63] In addition, the natural inhibitor of CAMK4 – miR-129-5p – was found to inhibit MAPK and therefore the proliferation, migration and invasion of hepatic cells.[66]

MARK4

Microtubule affinity-regulating kinase 4 (MARK4) is a Ser/Thr kinase that belongs to the AMPK-like family.[67,68] This kinase regulates the stability of microtubules, and the cell cycle, signaling, differentiation and polarization[69,70]; and its highest expression is observed in kidney, brain and testes.[71,72] Any fluctuations in MARK4 expression can disrupt important cellular pathways, such as mTOR and NF-κB, which may result in countless health disorders.[73,74] For instance, MARK4 has been reported to promote the proliferation of breast cancer cells through the hippo signaling pathway.[74] Vanillin is considered to be a potential inhibitor of MARK4 and future anticancer research might target MARK4 overexpression.[75–77] Therefore, exploring the interaction between MARK4 and vanillin may provide an effective tool to fight cancer.[78] When it comes to the chemical structure and the process of binding, vanillin connects to this protein kinase only by a single hydrogen bond between A135 and the hydroxyl group of vanillin. However, alongside that connection, there is also a π–π bond with Y134.[78] The MARK4 is overexpressed in different types of cancers, and this protein is responsible for the control of cell division in its early stages. This kinase regulates the microtubular system during cell division, and thus could be assigned as a target for novel drugs and naturally derived substances. Several studies have investigated the ability of natural compounds, like vanillin, rutin or rosmarinic acid, to act as inhibitors of MAPK4.[78,79] Also, several novel small molecule drugs have been shown to be potent MAPK4 inhibitors, exhibiting the potential of microtubule impairment for anticancer activity in MCF-7 and HepG2 cells.[80] Dietary polyphenolics, ferulic acid, hesperidin, and gallic acid have also been shown to inhibit MARK4.[78]

Studies examining the use of vanillin to target cancers

The 4-hydroxy-3-methoxybenzaldehyde is considered to be generally non-cytotoxic. However, there is strong evidence confirming that this compound increases the cytotoxicity of cisplatin[81] and mitomycin C,[82] which are DNA-damaging agents. This fact is evidently related to the capability of vanillin to impair DNA double-strand break repair through the inhibition of DNA-PKcs.[81] Even though this organic compound is incapable of directly suppressing the progression of a tumor, it might enhance the efficiency of chemotherapy, as suggested by Marton et al.,[83] who showed that vanillin inhibits angiogenesis in a chorioallantois membrane assay of a chick.[84] Moreover, vanillin suppresses the activation of NF-κB, which is induced by various inflammatory stimuli such as tumor necrosis factor α (TNF-α),[50] trinitrobenzene sulfonic acid[85] and 12-otetradecanoylphorbol-13-acetate.[86] To conclude, even though the intrinsic cytotoxicity of vanillin is low, this organic compound can be used to sensitize cancer cells towards standard chemothrapeutic drugs, which results in the activation of NF-kB,[83] and therefore may increase the effectiveness of these treatments.

In vitro studies concerning vanillin receptors

The administration of 4-hydroxy-3-methoxybenzaldehyde in non-cytotoxic concentrations has shown anticancer potential in in vitro studies on mouse mammary adenocarcinoma 4T1 cells.[87] Both invasion and migration were successfully inhibited by the described organic compound. Furthermore, experiments on human HepG2 cells have confirmed the usefulness of 4-hydroxy-3-methoxybenzaldehyde. Vanillin contributed to suppression of the enzymatic activity of matrix metalloproteinase 9 (MMP-9), induced by 12-O-tetradecanoylphorbol-13-acetate and decreased its mRNA level.[86] The anticancer potential of vanillin was also shown in research on lung A549 carcinoma cells. The migration of these cells induced by hepatocyte growth factor (HGF) was successfully inhibited by vanillin.[87] As demonstrated by these in vitro results, the inhibitory effects of vanillin on the activity of cancer-related proteins make it a very promising potential anticancer agent.

Vanillin is also considered a bio-antimutagen, as it prevents mutagenesis by reducing mutation progress after DNA damage.[88] Studies by Rodrigues de Andrade et al. have shown that the application of 4-hydroxy-3-methoxybenzaldehyde decreases mitomycin C-induced and spontaneous ring X-loss.[89] Even though mitomycin C-induced mutations were not effectively inhibited by vanillin, the proportion of recombination in somatic cells of *Drosophila melanogaster* that were treated with the alkylating agent increased significantly.[90] When applied in combination with ethyl methanesulfonate (EMS), N-methyl-N-nitrosourea (MNU) or bleomycin, 4-hydroxy-3-methoxybenzaldehyde prevented the cellular genotoxicity induced by these chemical substances.[91,92] Furthermore, measurements of DNA repair have shown the impact of vanillin on the repair of lethal damage induced by N-ethyl-N-nitrosourea (ENU) and EMS.[93] Finally, studies on the anti-mutagenic effects of 4-hydroxy-3-methoxybenzaldehyde have shown its inhibitory potential and stimulating effects on detoxification enzymes.[92,93]

In contrast to the research cited above, the following studies were conducted on mammalian ovary fibroblast CHO K-1 cells. Apart from overall antimutagenic effects of 4-hydroxy-3-methoxybenzaldehyde, the influence of the current phase of the cell cycle on these effects was examined. The results showed that vanillin caused significant growth in the incidence of sister chromatid exchange (SCE) induced in cells treated with N-methyl-N′-nitro-N-nitrosoguanidine (MNNG) and methyl methanesulphonate (MMS), EMS and ENU. However, the effects obtained in cells treated with MMC were dependent on the cell cycle and occurred in the S phase.[94] Also, vanillin treatment applied in the G2 phase in these cells decreased the frequency of breakage types of chromosome aberrations caused using X-ray radiation and ultraviolet (UV) light, whereas in phase G1, it suppressed both breakage and exchange types of aberrations induced with X-ray radiation.[95] Even though the experiment was conducted successfully for several mutagens, in cells treated with N-ethyl-N′-nitro-N-nitrosoguanidine (ENNG) and mitomycin (MMC), the usage of vanillin did not produce significant changes. *Cricetulus griseus* lung fibroblast V79 cells have also been used to examine the suppressive properties of 4-hydroxy-3-methoxybenzaldehyde. Vanillin did not only minimize the incidence of 6-thioguanine-resistant mutations generated using ENU, X-ray radiation and UV light,[96] but it also suppressed chromosomal aberrations evoked by hydrogen peroxide.[97,98]

Human colon cancer HCT116 cells have also been used to study the antimutagenic capability of vanillin. The 4-hydroxy-3-methoxybenzaldehyde applied at antimutagenic concentrations caused DNA damage in mismatch-proficient (HCT116 + CHR3), as well as mismatch-deficient (HCT116) cells. In the end, the HCT116 cells treated with vanillin exhibited a change in the expression of 64 genes, mainly related to the DNA damage, oxidative damage, cell growth, and apoptosis.[95] In addition, studies examining the effects of vanillin on DNA damage caused using UV light in human keratinocyte stem cells suggested that the ATM/p53 pathway relates to vanillin-induced protection of the cell.[84]

In vivo studies concerning vanillin receptors

The first in vivo studies testing the anticancerogenic potential of vanillin were conducted in rats. These animal studies involved supplementing the diet with vanillin for

7 days and administering a hepatocarcinogen on the 6th day. Partial hepatectomy, as well as the application of phenobarbital and D-galactosamine, demonstrated antioxidant and inhibitory effects of vanillin on hepatocarcinogenesis initiation.[99] Another study concerning medium-term multiorgan rat carcinogenesis used male F344 rats that were given vanillin in their diet, either from 1 day before and through the exposure to carcinogen, or afterwards. This study showed that 4-hydroxy-3-methoxybenzaldehyde suppressed the carcinogenesis of small intestine cancer and lung cancer, even though only for a week, whereas its effect on colon cancer cells in the initiation phase was strikingly different, and cancer cells progression was observed.[100] Other studies have examined the effects of vanillin in rats with aberrant crypt foci (ACF) induced with azoxymethane.[101] In these studies, the animals were given vanillin at either a low or a high dose, and several parameters, such as ACF density and distribution, as well as gene expression, were monitored. Although orally delivered 4-hydroxy-3-methoxybenzaldehyde did not yield any significant results, vanillin administered through intraperitoneal injection (at the higher concentration) was cancerogenic. However, the expression levels of many parameters were affected by the substance. For instance, the levels of the protooncogenes XRCC2, PMS2, p21, and cyclin B were increased.[101] Both the cancerogenic and anticancerogenic effects of vanillin suggest that further studies are required in the field of vanillin-related changes in DNA.

Clinical trials involving vanillin

To date, several trials examining the use of vanillin in clinical practice have been conducted. Most of these studies have applied this natural compound for the treatment of hypoxic events[102] or apneas[103] in premature infants. In addition, the calming effects of vanilla odor have been tested for the potential induction of analgesia in preterm newborns.[104] The repellent properties of vanillin have also been tested against flies, and thus its potential application for interrupting the transmission of trachoma has been examined.[105] However, no trials have aimed to use vanillin as an anticancer therapy. Although vanillin has never been clinically applied in cancer patients, an extract from vanilla beans has been examined as a supportive/adjuvant therapy for cancer. Vanilla in nutraceuticals (especially flaxseed) has been tested for the prevention of doxorubicin- and trastuzumab-mediated cardiotoxicity.[106] In the future, a registered clinical trial will evaluate its effects on the chemotherapy-induced nausea and vomiting (trial No. NCT04478630). The only study that concerned the standalone anticancer activity of vanilla was conducted on PSA-recurrent prostate cancer.[107] This phase II clinical study revealed a decline in PSA slope after the administration of isoflavones (including vanilla).[108] Although several studies aimed to evaluate the effects of whole food interventions (including vanilla) on mucositis in patients treated for thoracic[109] and head and neck cancers,[110] the studies were terminated early.

Conclusions

Substances of natural origin are effectively used in therapies, as these compounds tend to exhibit significantly less side effects. Even though our knowledge is still very limited, the anticancer potential of a widely accessible organic compound, vanillin, and the multitude of studies examining the role of vanilloid receptors in carcinogenesis, make the prospect of using vanillin and its derivatives in clinical trials very promising. The studies presented in this review reveal the antitumor activity of vanillin and its therapeutic potential in cancer treatment and prevention. The data reviewed above summarize the results of the most important research related to the role of 4-hydroxy-3-methoxybenzaldehyde and its derivatives as effective inhibitors of the pathophysiology of cancer. As it turns out, the described inconspicuous organic compound may be one of the substances that indirectly contributes to the inhibition of the tumor growth and it may become an effective treatment to combat the fatal consequences of carcinogenesis.

ORCID iDs

Katarzyna Rakoczy https://orcid.org/0000-0002-0978-8266
Wojciech Szlasa https://orcid.org/0000-0002-5477-5771
Jolanta Saczko https://orcid.org/0000-0001-5273-5293
Julita Kulbacka https://orcid.org/0000-0001-8272-5440

References

1. Gulsia O. Vanillin: One drug, many cures. *Resonance*. 2020;25(7):981–986. doi:10.1007/s12045-020-1013-z
2. Walton NJ, Mayer MJ, Narbad A. Vanillin. *Phytochemistry*. 2003;63(5):505–515. doi:10.1016/S0031-9422(03)00149-3
3. Sinha AK, Sharma UK, Sharma N. A comprehensive review on vanilla flavor: Extraction, isolation and quantification of vanillin and others constituents. *Int J Food Sci Nutr*. 2008;59(4):299–326. doi:10.1080/09687630701539350
4. Santos Pedroso L, Marino Fávero G, Erzinger Alves de Camargo L, Mara Mainardes R, Maissar Khalil N. Effect of the o-methyl catechols apocynin, curcumin and vanillin on the cytotoxicity activity of tamoxifen. *J Enzyme Inhib Med Chem*. 2013;28(4):734–740. doi:10.3109/14756366.2012.680064
5. Tai A, Sawano T, Yazama F, Ito H. Evaluation of antioxidant activity of vanillin by using multiple antioxidant assays. *Biochim Biophys Acta*. 2011;1810(2):170–177. doi:10.1016/j.bbagen.2010.11.004
6. King AA, Shaughnessy DT, Mure K, et al. Antimutagenicity of cinnamaldehyde and vanillin in human cells: Global gene expression and possible role of DNA damage and repair. *Mutat Res*. 2007;616(1–2):60–69. doi:10.1016/j.mrfmmm.2006.11.022
7. Shaughnessy DT, Setzer RW, DeMarini DM. The antimutagenic effect of vanillin and cinnamaldehyde on spontaneous mutation in Salmonella TA104 is due to a reduction in mutations at GC but not AT sites. *Mutat Res*. 2001;480–481:55–69. doi:10.1016/S0027-5107(01)00169-5
8. Shaughnessy DT, Schaaper RM, Umbach DM, DeMarini DM. Inhibition of spontaneous mutagenesis by vanillin and cinnamaldehyde in *Escherichia coli*: Dependence on recombinational repair. *Mutat Res*. 2006;602(1–2):54–64. doi:10.1016/j.mrfmmm.2006.08.006
9. Kumar SS, Priyadarsini KI, Sainis KB. Inhibition of peroxynitrite–mediated reactions by vanillin. *J Agric Food Chem*. 2004;52(1):139–145. doi:10.1021/jf030319d

10. Chou TH, Ding HY, Hung WJ, Liang CH. Antioxidative characteristics and inhibition of α-melanocyte-stimulating hormone-stimulated melanogenesis of vanillin and vanillic acid from *Origanum vulgare*. *Exp Dermatol*. 2010;19(8):742–750. doi:10.1111/j.1600-0625.2010.01091.x
11. Fitzgerald DJ, Stratford M, Gasson MJ, Ueckert J, Bos A, Narbad A. Mode of antimicrobial of vanillin against *Escherichia coli*, *Lactobacillus plantarum* and *Listeria innocua*. *J Appl Microbiol*. 2004;97(1):104–113. doi:10.1111/j.1365-2672.2004.02275.x
12. Park SH, Sim YB, Choi SM, et al. Antinociceptive profiles and mechanisms of orally administered vanillin in the mice. *Arch Pharm Res*. 2009;32(11):1643–1649. doi:10.1007/s12272-009-2119-8
13. Beaudry F, Ross A, Lema PP, Vachon P. Pharmacokinetics of vanillin and its effects on mechanical hypersensitivity in a rat model of neuropathic pain. *Phyther Res*. 2010;24(4):525–530. doi:10.1002/ptr.2975
14. Abraham DJ, Mehanna AS, Wireko FC, Whitney J, Thomas RP, Orringer EP. Vanillin, a potential agent for the treatment of sickle cell anemia. *Blood*. 1991;77(6):1334–1341. doi:10.1182/blood.v77.6.1334.bloodjournal7761334
15. Clapham DE. TRP channels as cellular sensors. *Nature*. 2003;426(6966):517–524. doi:10.1038/nature02196
16. Montell C, Birnbaumer L, Flockerzi V. The TRP channels, a remarkably functional family. *Cell*. 2002;108(5):595–598. doi:10.1016/S0092-8674(02)00670-0
17. Moran MM, Xu H, Clapham DE. TRP ion channels in the nervous system. *Curr Opin Neurobiol*. 2004;14(3):362–369. doi:10.1016/j.conb.2004.05.003
18. Julius D, Basbaum AI. Molecular mechanisms of nociception. *Nature*. 2001;413(6852):203–210. doi:10.1038/35093019
19. Minke B, Cook B. TRP channel proteins and signal transduction. *Physiol Rev*. 2002;82(2):429–472. doi:10.1152/physrev.00001.2002
20. Montell C. Thermosensation: Hot findings make TRPNs very cool. *Curr Biol*. 2003;13(12):R476–R478. doi:10.1016/S0960-9822(03)00406-8
21. Caterina MJ, Julius D. The vanilloid receptor: A molecular gateway to the pain pathway. *Annu Rev Neurosci*. 2001;24:487–517. doi:10.1146/annurev.neuro.24.1.487
22. Jordt SE, Bautista DM, Chuang H, et al. Mustard oils and cannabinoids excite sensory nerve fibres through the TRP channel ANKTM1. *Nature*. 2004;427(6971):260–265. doi:10.1038/nature02282
23. McKemy DD, Neuhausser WM, Julius D. Identification of a cold receptor reveals a general role for TRP channels in thermosensation. *Nature*. 2002;416(6876):52–58. doi:10.1038/nature719
24. Moqrich A, Hwang SW, Earley TJ, et al. Impaired thermosensation in mice lacking TRPV3, a heat and camphor sensor in the skin. *Science*. 2005;307(5714):1468–1472. doi:10.1126/science.1108609
25. Story GM, Peier AM, Reeve AJ, et al. ANKTM1, a TRP-like channel expressed in nociceptive neurons, is activated by cold temperatures. *Cell*. 2003;112(6):819–829. doi:10.1016/S0092-8674(03)00158-2
26. Smith GD, Gunthorpe MJ, Kelsell RE, et al. TRPV3 is a temperature-sensitive vanilloid receptor-like protein. *Nature*. 2002;418(6894):186–190. doi:10.1038/nature00894
27. García-Sanz N, Fernández-Carvajal A, Morenilla-Palao C, et al. Identification of a tetramerization domain in the C terminus of the vanilloid receptor. *J Neurosci*. 2004;24(23):5307–5314. doi:10.1523/JNEUROSCI.0202-04.2004
28. Ghilardi JR, Röhrich H, Lindsay TH, et al. Selective blockade of the capsaicin receptor TRPV1 attenuates bone cancer pain. *J Neurosci*. 2005;25(12):3126–3131. doi:10.1523/JNEUROSCI.3815-04.2005
29. Messeguer A, Planells-Cases R, Ferrer-Montiel A. Physiology and pharmacology of the vanilloid receptor. *Curr Neuropharmacol*. 2005;4(1):1–15. doi:10.2174/157015906775202995
30. Bujak JK, Kosmala D, Szopa IM, Majchrzak K, Bednarczyk P. Inflammation, cancer and immunity: Implication of TRPV1 channel. *Front Oncol*. 2019;9:1087. doi:10.3389/fonc.2019.01087
31. Pecze L, Jósvay K, Blum W, et al. Activation of endogenous TRPV1 fails to induce overstimulation-based cytotoxicity in breast and prostate cancer cells but not in pain-sensing neurons. *Biochim Biophys Acta*. 2016;1863(8):2054–2064. doi:10.1016/j.bbamcr.2016.05.007
32. Ortega-Guerrero A, Espinosa-Duran JM, Velasco-Medina J. TRPV1 channel as a target for cancer therapy using CNT-based drug delivery systems. *Eur Biophys J*. 2016;45(5):423–433. doi:10.1007/s00249-016-1111-8
33. Hofmann NA, Barth S, Waldeck-Weiermair M, et al. TRPV1 mediates cellular uptake of anandamide and thus promotes endothelial cell proliferation and network-formation. *Biol Open*. 2014;3(12):1164–1172. doi:10.1242/bio.20149571
34. Nabissi M, Morelli MB, Santoni M, Santoni G. Triggering of the TRPV2 channel by cannabidiol sensitizes glioblastoma cells to cytotoxic chemotherapeutic agents. *Carcinogenesis*. 2013;34(1):48–57. doi:10.1093/carcin/bgs328
35. Liddle RA. The role of transient receptor potential vanilloid 1 (TRPV1) channels in pancreatitis. *Biochim Biophys Acta*. 2007;1772(8):869–878. doi:10.1016/j.bbadis.2007.02.012
36. Meng J, Ovsepian SV, Wang J, et al. Activation of TRPV1 mediates calcitonin gene-related peptide release, which excites trigeminal sensory neurons and is attenuated by a retargeted botulinum toxin with anti-nociceptive potential. *J Neurosci*. 2009;29(15):4981–4992. doi:10.1523/JNEUROSCI.5490-08.2009
37. Feng J, Yang P, Mack MR, et al. Sensory TRP channels contribute differentially to skin inflammation and persistent itch. *Nat Commun*. 2017;8(1):980. doi:10.1038/s41467-017-01056-8
38. Park M, Naidoo AA, Burns A, et al. Do TRPV1 antagonists increase the risk for skin tumorigenesis? A collaborative in vitro and in vivo assessment. *Cell Biol Toxicol*. 2018;34(2):143–162. doi:10.1007/s10565-017-9407-8
39. Hwang MK, Bode AM, Byun S, et al. Cocarcinogenic effect of capsaicin involves activation of EGFR signaling but not TRPV1. *Cancer Res*. 2010;70(17):6859–6869. doi:10.1158/0008-5472.CAN-09-4393
40. Gonzales CB, Kirma NB, De La Chapa JJ, et al. Vanilloids induce oral cancer apoptosis independent of TRPV1. *Oral Oncol*. 2014;50(5):437–447. doi:10.1016/j.oraloncology.2013.12.023
41. Kiełbik A, Szlasa W, Michel O, et al. In vitro study of calcium microsecond electroporation of prostate adenocarcinoma cells. *Molecules*. 2020;25(22):5406. doi:10.3390/molecules25225406
42. Staruschenko A, Jeske NA, Akopian AN. Contribution of TRPV1–TRPA1 interaction to the single channel properties of the TRPA1 channel. *J Biol Chem*. 2010;285(20):15167–15177. doi:10.1074/jbc.M110.106153
43. Nur G, Nazıroğlu M, Deveci HA. Synergic prooxidant, apoptotic and TRPV1 channel activator effects of alpha-lipoic acid and cisplatin in MCF-7 breast cancer cells. *J Recept Signal Transduct Res*. 2017;37(6):569–577. doi:10.1080/10799893.2017.1369121
44. Deveci HA, Nazıroğlu M, Nur G. 5-Fluorouracil-induced mitochondrial oxidative cytotoxicity and apoptosis are increased in MCF-7 human breast cancer cells by TRPV1 channel activation but not *Hypericum perforatum* treatment. *Mol Cell Biochem*. 2018;439(1–2):189–198. doi:10.1007/s11010-017-3147-1
45. Zheng L, Chen J, Ma Z, et al. Capsaicin enhances anti-proliferation efficacy of pirarubicin via activating TRPV1 and inhibiting PCNA nuclear translocation in 5637 cells. *Mol Med Rep*. 2016;13(1):881–887. doi:10.3892/mmr.2015.4623
46. Xu S, Zhang L, Cheng X, Yu H, Bao J, Lu R. Capsaicin inhibits the metastasis of human papillary thyroid carcinoma BCPAP cells through the modulation of the TRPV1 channel. *Food Funct*. 2018;9(1):344–354. doi:10.1039/c7fo01295k
47. Gowda C, Soliman M, Kapadia M, Ding Y, Payne K, Dovat S. Casein kinase II (CK2), glycogen synthase kinase-3 (GSK-3) and Ikaros mediated regulation of leukemia. *Adv Biol Regul*. 2017;65:16–25. doi:10.1016/j.jbior.2017.06.001
48. Piazza F, Manni S, Ruzzene M, Pinna LA, Gurrieri C, Semenzato G. Protein kinase CK2 in hematologic malignancies: Reliance on a pivotal cell survival regulator by oncogenic signaling pathways. *Leukemia*. 2012;26(6):1174–1179. doi:10.1038/leu.2011.385
49. Buontempo F, McCubrey JA, Orsini E, et al. Therapeutic targeting of CK2 in acute and chronic leukemias. *Leukemia*. 2018;32(1):1–10. doi:10.1038/leu.2017.301
50. Lirdprapamongkol K, Sakurai H, Suzuki S, et al. Vanillin enhances TRAIL-induced apoptosis in cancer cells through inhibition of NF-κB activation. *In Vivo*. 2010;24(4):501–506. PMID:20668316
51. Cozza G, Zonta F, Dalle Vedove A, et al. Biochemical and cellular mechanism of protein kinase CK2 inhibition by deceptive curcumin. *FEBS J*. 2020;287(9):1850–1864. doi:10.1111/febs.15111
52. Trembley JH, Wang G, Unger G, Slaton J, Ahmed K. CK2: A key player in cancer biology. *Cell Mol Life Sci*. 2009;66(11–12):1858–1867. doi:10.1007/s00018-009-9154-y

53. Faust RA, Niehans G, Gapany M, et al. Subcellular immunolocalization of protein kinase CK2 in normal and carcinoma cells. *Int J Biochem Cell Biol*. 1999;31(9):941–949. doi:10.1016/S1357-2725(99)00050-3
54. Kato T, Delhase M, Hoffmann A, Karin M. CK2 is a C-terminal IκB kinase responsible for NF-κB activation during the UV response. *Mol Cell*. 2003;12(4):829–839. doi:10.1016/S1097-2765(03)00358-7
55. Borgo C, Ruzzene M. Role of protein kinase CK2 in antitumor drug resistance. *J Exp Clin Cancer Res*. 2019;38(1):1–15. doi:10.1186/s13046-019-1292-y
56. Ljubimov AV, Caballero S, Aoki AM, Pinna LA, Grant MB, Castellon R. Involvement of protein kinase CK2 in angiogenesis and retinal neovascularization. *Investig Ophthalmol Vis Sci*. 2004;45(12):4583–4591. doi:10.1167/iovs.04-0686
57. Silva-Pavez E, Tapia J. Protein kinase CK2 in cancer energetics. *Front Oncol*. 2020;10:893. doi:10.3389/fonc.2020.00893
58. Lian H, Su M, Zhu Y, Zhou Y, Soomro SH, Fu H. Protein kinase CK2, a potential therapeutic target in carcinoma management. *Asian Pacific J Cancer Prev*. 2019;20(1):23–32. doi:10.31557/APJCP.2019.20.1.23
59. D'Amore C, Borgo C, Sarno S, Salvi M. Role of CK2 inhibitor CX-4945 in anti-cancer combination therapy: Potential clinical relevance. *Cell Oncol*. 2020;43(6):1003–1016. doi:10.1007/s13402-020-00566-w
60. Beg A, Khan FI, Lobb KA, Islam A, Ahmad F, Hassan MI. High throughput screening, docking, and molecular dynamics studies to identify potential inhibitors of human calcium/calmodulin-dependent protein kinase IV. *J Biomol Struct Dyn*. 2019;37(8):2179–2192. doi:10.1080/07391102.2018.1479310
61. Lin F, Marcelo KL, Rajapakshe K, et al. The CaMKK2/CaMKIV relay is an essential regulator of hepatic cancer. *Hepatology*. 2015;62(2):505–520. doi:10.1002/hep.27832
62. Naz H, Tarique M, Khan P, et al. Evidence of vanillin binding to CAMKIV explains the anti-cancer mechanism in human hepatic carcinoma and neuroblastoma cells. *Mol Cell Biochem*. 2018;438(1–2):35–45. doi:10.1007/s11010-017-3111-0
63. Gupta P, Khan S, Fakhar Z, et al. Identification of potential inhibitors of calcium/calmodulin-dependent protein kinase IV from bioactive phytoconstituents. *Oxid Med Cell Longev*. 2020;8:1–14. doi:10.1155/2020/2094635
64. Takai N, Miyazaki T, Nishida M, Nasu K, Miyakawa I. Ca^{2+}/calmodulin-dependent protein kinase IV expression in epithelial ovarian cancer. *Cancer Lett*. 2002;183(2):185–193. doi:10.1016/S0304-3835(02)00107-6
65. Naz H, Tarique M, Suhail M, et al. Calcium-/calmodulin-dependent protein kinase IV (CAMKIV): A multifunctional enzyme and its role in various cancers. An update. *Curr Mol Biol Rep*. 2020;6(3):139–147. doi:10.1007/s40610-020-00138-9
66. Li Z, Lu J, Zeng G, et al. MiR-129-5p inhibits liver cancer growth by targeting calcium calmodulin-dependent protein kinase IV (CAMK4). *Cell Death Dis*. 2019;10(11):1–14. doi:10.1038/s41419-019-1923-4
67. Heidary Arash E, Shiban A, Song S, Attisano L. MARK4 inhibits Hippo signaling to promote proliferation and migration of breast cancer cells. *EMBO Rep*. 2017;18(3):420–436. doi:10.15252/embr.201642455
68. Sun W, Lee S, Huang X, et al. Attenuation of synaptic toxicity and MARK4/PAR1-mediated Tau phosphorylation by methylene blue for Alzheimer's disease treatment. *Sci Rep*. 2016;6:34784. doi:10.1038/srep34784
69. Rovina D, Fontana L, Monti L, et al. Microtubule-associated protein/microtubule affinity-regulating kinase 4 (MARK4) plays a role in cell cycle progression and cytoskeletal dynamics. *Eur J Cell Biol*. 2014;93(8–9):355–365. doi:10.1016/j.ejcb.2014.07.004
70. Marx A, Nugoor C, Panneerselvam S, Mandelkow E. Structure and function of polarity-inducing kinase family MARK/Par-1 within the branch of AMPK/Snf1-related kinases. *FASEB J*. 2010;24(6):1637–1648. doi:10.1096/fj.09-148064
71. Trinczek B, Brajenovic M, Ebneth A, Drewes G. MARK4 is a novel microtubule-associated proteins/microtubule affinity-regulating kinase that binds to the cellular microtubule network and to centrosomes. *J Biol Chem*. 2004;279(7):5915–5923. doi:10.1074/jbc.M304528200
72. Tang EI, Xiao X, Mruk DD, et al. Microtubule affinity-regulating kinase 4 (MARK4) is a component of the ectoplasmic specialization in the rat testis. *Spermatogenesis*. 2012;2(2):117–126. doi:10.4161/spmg.20724
73. Liu Z, Gan L, Chen Y, et al. Mark4 promotes oxidative stress and inflammation via binding to PPARγ and activating NF-κB pathway in mice adipocytes. *Sci Rep*. 2016;6:21382. doi:10.1038/srep21382
74. Li L, Guan KL. Microtubule-associated protein/microtubule affinity-regulating kinase 4 (MARK4) is a negative regulator of the mammalian target of rapamycin complex 1 (mTORC1). *J Biol Chem*. 2013;288(1):703–708. doi:10.1074/jbc.C112.396903
75. Naz F, Sami N, Naqvi AT, Islam A, Ahmad F, Imtaiyaz Hassan M. Evaluation of human microtubule affinity-regulating kinase 4 inhibitors: Fluorescence binding studies, enzyme, and cell assays. *J Biomol Struct Dyn*. 2017;35(14):3194–3203. doi:10.1080/07391102.2016.1249958
76. Naz F, Sami N, Islam A, Ahmad F, Hassan MI. Ubiquitin-associated domain of MARK4 provides stability at physiological pH. *Int J Biol Macromol*. 2016;93(Pt A):1147–1154. doi:10.1016/j.ijbiomac.2016.09.087
77. Jenardhanan P, Mannu J, Mathur PP. The structural analysis of MARK4 and the exploration of specific inhibitors for the MARK family: A computational approach to obstruct the role of MARK4 in prostate cancer progression. *Mol Biosyst*. 2014;10(7):1845–1868. doi:10.1039/c3mb70591a
78. Khan P, Rahman S, Queen A, et al. Elucidation of dietary polyphenolics as potential inhibitor of microtubule affinity regulating kinase 4: In silico and in vitro studies. *Sci Rep*. 2017;7(1):9470. doi:10.1038/s41598-017-09941-4
79. Anwar S, Shamsi A, Shahbaaz M, et al. Rosmarinic acid exhibits anticancer effects via MARK4 inhibition. *Sci Rep*. 2020;10(1):10300. doi:10.1038/s41598-020-65648-z
80. Voura M, Khan P, Thysiadis S, et al. Probing the inhibition of microtubule affinity regulating kinase 4 by N-substituted acridones. *Sci Rep*. 2019;9(1):1676. doi:10.1038/s41598-018-38217-8
81. Durant S, Karran P. Vanillins: A novel family of DNA-PK inhibitors. *Nucleic Acids Res*. 2003;31(19):5501–5512. doi:10.1093/nar/gkg753
82. Gustafson DL, Franz HR, Ueno AM, Smith CJ, Doolittle DJ, Waldren CA. Vanillin (3-methoxy-4-hydroxybenzaldehyde) inhibits mutation induced by hydrogen peroxide, N-methyl-N-nitrosoguanidine and mitomycin C but not 137Cs-γ-radiation at the CD59 locus in human-hamster hybrid A(L) cells. *Mutagenesis*. 2000;15(3):207–213. doi:10.1093/mutage/15.3.207
83. Marton A, Kúsz E, Kolozsi C, et al. Vanillin analogues o-vanillin and 2,4,6-trihydroxybenzaldehyde inhibit NFκB activation and suppress growth of A375 human melanoma. *Anticancer Res*. 2016;36(11):5743–5750. doi:10.21873/anticanres.11157
84. Lirdprapamongkol K, Kramb JP, Suthiphongchai T, et al. Vanillin suppresses metastatic potential of human cancer cells through PI3K inhibition and decreases angiogenesis in vivo. *J Agric Food Chem*. 2009;57(8):3055–3063. doi:10.1021/jf803366f
85. Wu SL, Chen JC, Li CC, Lo HY, Ho TY, Hsiang CY. Vanillin improves and prevents trinitrobenzene sulfonic acid-induced colitis in mice. *J Pharmacol Exp Ther*. 2009;330(2):370–376. doi:10.1124/jpet.109.152835
86. Liang JA, Wu SL, Lo HY, Hsiang CY, Ho TY. Vanillin inhibits matrix metalloproteinase-9 expression through down-regulation of nuclear factor-κB signaling pathway in human hepatocellular carcinoma cells. *Mol Pharmacol*. 2009;75(1):151–157. doi:10.1124/mol.108.049502
87. Lirdprapamongkol K, Sakurai H, Kawasaki N, et al. Vanillin suppresses in vitro invasion and in vivo metastasis of mouse breast cancer cells. *Eur J Pharm Sci*. 2005;25(1):57–65. doi:10.1016/j.ejps.2005.01.015
88. Kada T, Shimoi K. Desmutagens and bio-antimutagens: Their modes of action. *BioEssays*. 1987;7(3):113–116. doi:10.1002/bies.950070305
89. Rodrigues de Andrade HH, Santos JH, Gimmler-Luz MC, Correa MJF, Lehmann M, Reguly ML. Suppressing effect of vanillin on chromosome aberrations that occur spontaneously or are induced by mitomycin C in the germ cell line of *Drosophila melanogaster*. *Mutat Res*. 1992;279(4):281–287. doi:10.1016/0165-1218(92)90245-U
90. Santos JH, Graf U, Reguly ML, Rodrigues de Andrade HH. The synergistic effects of vanillin on recombination predominate over its antimutagenic action in relation to MMC-induced lesions in somatic cells of *Drosophila melanogaster*. *Mutat Res*. 1999;444(2):355–365. doi:10.1016/S1383-5718(99)00101-1
91. Sinigaglia M, Reguly ML, Rodrigues de Andrade HH. Effect of vanillin on toxicant-induced mutation and mitotic recombination in proliferating somatic cells of *Drosophila melanogaster*. *Environ Mol Mutagen*. 2004;44(5):394–400. doi:10.1002/em.20067
92. Sinigaglia M, Lehmann M, Baumgardt P, et al. Vanillin as a modulator agent in SMART test: Inhibition in the steps that precede N-methyl-N-nitrosourea-, N-ethyl-N-nitrosourea-, ethylmethanesulphonate- and bleomycin-genotoxicity. *Mutat Res*. 2006;607(2):225–230. doi:10.1016/j.mrgentox.2006.04.012

93. Furlanetto MP, Sinigaglia M, do Amaral VS, Dihl RR, Rodrigues de Andrade HH. Effect of vanillin on toxicant-induced lethality in the *Drosophila melanogaster* DNA repair test. *Environ Mol Mutagen*. 2007;48(1):67–70. doi:10.1002/em.20275
94. Sasaki YF, Imanishi H, Ohta T, Shirasu Y. Effects of vanillin on sister-chromatid exchanges and chromosome aberrations induced by mitomycin C in cultured Chinese hamster ovary cells. *Mutat Res*. 1987; 191(3–4):193–200. doi:10.1016/0165-7992(87)90153-9
95. Sasaki YF, Imanishi H, Watanabe M, Ohta T, Shirasu Y. Suppressing effect of antimutagenic flavorings on chromosome aberrations induced by UV-light or X-rays in cultured Chinese hamster cells. *Mutat Res*. 1990;229(1):1–10. doi:10.1016/0027-5107(90)90002-L
96. Imanishi H, Sasaki YF, Matsumoto K, et al. Suppression of 6-TG-resistant mutations in V79 cells and recessive spot formations in mice by vanillin. *Mutat Res*. 1990;243(2):151–158. doi:10.1016/0165-7992(90)90038-L
97. Tamai K, Tezuka H, Kuroda Y. Different modifications by vanillin in cytotoxicity and genetic changes induced by EMS and H_2O_2 in cultured Chinese hamster cells. *Mutat Res*. 1992;268(2):231–237. doi:10.1016/0027-5107(92)90229-U
98. Keshava C, Keshava N, Ong T, Nath J. Protective effect of vanillin on radiation-induced micronuclei and chromosomal aberrations in V79 cells. *Mutat Res*. 1998;397(2):149–159. doi:10.1016/S0027-5107(97)00203-0
99. Tsuda H, Uehara N, Iwahori Y, et al. Chemopreventive effects of β-carotene, α-tocopherol and five naturally occurring antioxidants on initiation of hepatocarcinogenesis by 2-amino-3-methylimidazo[4,5-f]qumoline in the rat. *Jpn J Cancer Res*. 1994;85(12):1214–1219. doi:10.1111/j.1349-7006.1994.tb02932.x
100. Akagi K, Hirose M, Hoshiya T, Mizoguchi Y, Ito N, Shirai T. Modulating effects of ellagic acid, vanillin and quercetin in a rat medium term multi-organ carcinogenesis model. *Cancer Lett*. 1995;94(1):113–121. doi:10.1016/0304-3835(95)03833-I
101. Ho KL, Chong PP, Yazan LS, Ismail M. Vanillin differentially affects azoxymethane-injected rat colon carcinogenesis and gene expression. *J Med Food*. 2012;15(12):1096–1102. doi:10.1089/jmf.2012.2245
102. Praud JP. Effects of vanilla on hypoxic intermittent events in premature infants. ClinicalTrials.gov. Accessed March 19, 2021. https://clinicaltrials.gov/ct2/show/NCT02630147
103. Hospices Civils de Lyon. Odors to insufflate life. ClinicalTrials.gov. Accessed March 19, 2021. https://clinicaltrials.gov/ct2/show/results/NCT02851979
104. Assistance Publique Hopitaux De Marseille. The calming effect of vanilla odor on preterm infant without mother's breast milk feeding. ClinicalTrials.gov. Accessed March 19, 2021. https://clinicaltrials.gov/ct2/show/NCT03626974
105. London School of Hygiene and Tropical Medicine. Testing insect repellents against *Musca sorbens*, the vector of trachoma. ClinicalTrials.gov. Accessed March 19, 2021. https://clinicaltrials.gov/ct2/show/NCT03813069
106. Davinder S. Jassal SBH. Can flaxseed prevent broken hearts in women with breast cancer study? ClinicalTrials.gov. Accessed March 19, 2021. https://clinicaltrials.gov/ct2/show/NCT04632407
107. University of Florida. Isoflavone in prostate-specific antigen recurrent prostate cancer. ClinicalTrials.gov. Accessed March 19, 2021. https://clinicaltrials.gov/ct2/show/NCT00596895
108. Pendleton JM, Tan WW, Anai S, et al. Phase II trial of isoflavone in prostate-specific antigen recurrent prostate cancer after previous local therapy. *BMC Cancer*. 2008;8:132. doi:10.1186/1471-2407-8-132
109. Providence Health & Services. The effects of whole food intervention on mucositis in patients treated for thoracic cancer. Clinical Trials.gov. Accessed March 19, 2021. https://clinicaltrials.gov/ct2/show/NCT02575391
110. Providence Health & Services. The effects of whole food intervention on mucositis in patients treated for head and neck cancer. Clinical Trials.gov. Accessed March 19, 2021. https://clinicaltrials.gov/ct2/show/NCT02575313

Dualistic role of autophagy in cancer progression

Kacper Turek[1,A,B,D], Michał Jarocki[1,A,C,D], Julita Kulbacka[1,E,F], Jolanta Saczko[2,E,F]

[1] Faculty of Medicine, Wroclaw Medical University, Poland
[2] Department of Molecular and Cellular Biology, Faculty of Pharmacy, Wroclaw Medical University, Poland

A – research concept and design; B – collection and/or assembly of data; C – data analysis and interpretation; D – writing the article; E – critical revision of the article; F – final approval of the article

Advances in Clinical and Experimental Medicine, ISSN 1899–5276 (print), ISSN 2451–2680 (online) *Adv Clin Exp Med.* 2021;30(12):1303–1314

Address for correspondence
Julita Kulbacka
E-mail: julita.kulbacka@umed.wroc.pl

Funding sources
This research was financially supported by the Statutory Subsidy Funds of the Department of Molecular and Cellular Biology, Faculty of Pharmacy, Wroclaw Medical University, Poland (grant No. SUB.D.260.21.095).

Conflict of interest
None declared

Received on June 21, 2021
Reviewed on July 16, 2021
Accepted on August 11, 2021

Published online on October 5, 2021

Abstract

This review aims to characterize the dualistic role of autophagy in both the suppression and propagation of carcinogenesis. The process of autophagy is responsible for maintaining the delicate balance between the survival and death of a cell, and in the past years it has been studied profoundly. It has been proven that the role of autophagy in maintaining genomic and structural integrity can lead to the suppression of carcinogenesis in its early stages. However, once carcinogenesis has occurred, the process of autophagy may contribute to the survival of tumor cells and, consequently, lead to tumor progression. Additionally, autophagy can modulate the response of the tumor cells to therapy, leading to radiotherapy and chemotherapy resistance or reduced susceptibility to anticancer drugs that propagate autophagy-related cell death. Although the role and course of autophagy are not yet fully known, the essence of it seems to be within our grasp. We have observed the identification of an increasing number of autophagy-related genes (ATG). Therefore, more research concerning its molecular course and potential applications in cancer treatment and prevention needs to be conducted.

Key words: oncogenes, cancer progression, autophagy, chaperons

Cite as
Turek K, Jarocki M, Kulbacka J, Saczko J. Dualistic role of autophagy in cancer progression. *Adv Clin Exp Med*. 2021;30(12):1303–1314. doi:10.17219/acem/141191

DOI
10.17219/acem/141191

Introduction

Autophagy is considered to be the process responsible for keeping a cell in a state of energetic and material well-being,[1,2] and in the beginning it was studied as such. Over time, researchers started noticing other cellular and molecular processes that are influenced by or dependent on autophagy. The term is derived from Greek, meaning "self-eating" because of the observed digestion of the structures of the cell. As mentioned above, autophagy was thought to be a mechanism cells use during starvation, metabolic stress,[3] and degradation of misfolded proteins,[4] organelles and intracellular pathogens. During years of research, the role of autophagy in cellular senescence and necrosis prevention[5] has been identified, opening up a new field into the possible roles of this process. Researchers have distinguished 3 types of autophagy: microautophagy, macroautophagy and chaperone-mediated autophagy (CMA).[6] All types lead to the common end stage of lysosomal degradation of cellular structures and proteins (Fig. 1). The term microautophagy describes the process of direct invagination of a material meant to be digested by a lysosome. Macroautophagy uses unique structures called autophagosomes which are double-membrane vesicles used to deliver the material into lysosomes. The 2 vesicles fuse to form an autolysosome. In the process of the chaperone-mediated autophagy, chaperones recognize and bind to proteins containing a KFERQ motif. Then, they are translocated across the lysosomal membrane using the LAMP-2A protein, where they are unfolded and degraded.[7,8] Both micro- and macro- autophagy are involved in the degradation of large and small structures, and may be selective or nonselective. Chaperone-mediated autophagy is limited to proteins residing in the cytoplasm and does not apply to larger structures like organelles.

Objectives

This review aims to delineate the dualistic role of autophagy in the suppression and propagation of carcinogenesis. We describe the role of autophagy in maintaining

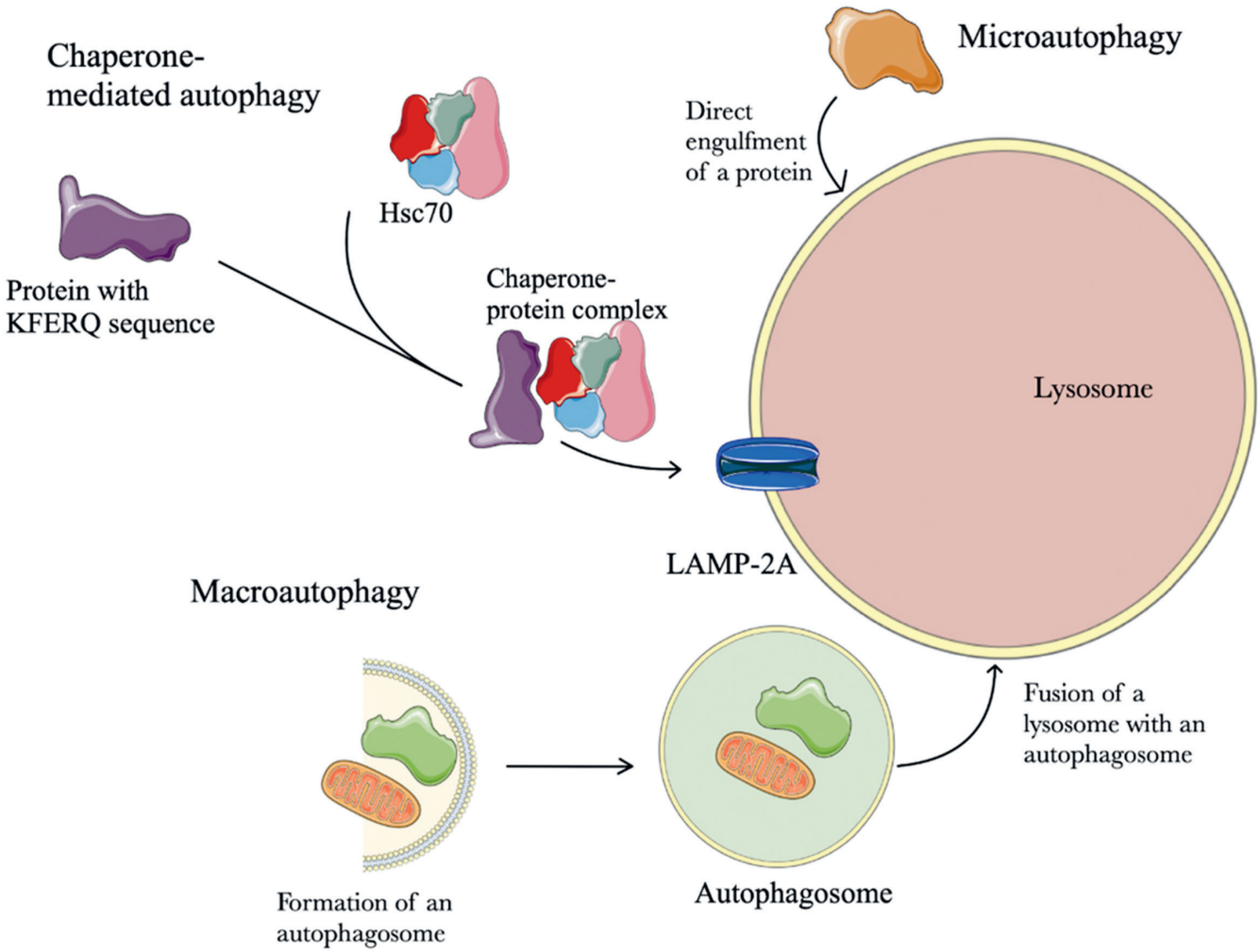

Fig. 1. Types of autophagy. Microautophagy is a process of direct invagination of a material meant to be digested in a lysosome. Macroautophagy uses special structures called autophagosomes to deliver the material into the lysosomes; the 2 vesicles fuse together to form an autolysosome. In the process of chaperone-mediated autophagy, a complex between a protein with a KFERQ motif and a chaperone is recognized and translocated across a lysosomal membrane by the LAMP-2A protein to be unfolded and degraded in the lysosomal environment

the balance between cell survival and death. Based on the available literature, we summarize the role of autophagy in carcinogenesis and the possible modulation of the tumor cell response to therapy.

Methodology

This review was prepared after a literature search was conducted using PubMed, Mendeley, Google, Scopus, Embase, and AccessMedicine. The literature search was limited to articles published between 2001 and 2021, using the following search terms: autophagy regulation, macroautophagy, chaperone-mediated autophagy, autophagosome formation inhibition, autophagy inhibition, and autophagy and treatment.

The complexity of autophagy function

Autophagy, or more specifically the deregulation of it, is considered an essential factor in the development of many types of diseases.[6] The different types of autophagy and its selective and nonselective mechanisms of action result in an astounding diversity of diseases it may play a role in. The list of diseases that deregulated autophagy may be involved in, as a meaningful contributive component, is constantly getting longer.[9] Autophagy occurs on a basal and constitutional level. The role of the basal level has been recently highlighted as a home keeping mechanism for the cell. Different tissues demand various levels of autophagy. Therefore, tissues that do not divide after differentiation, such as neurons and myocytes, are acutely sensitive to the inhibition of autophagy. However, some tissues are less prone to the absence of autophagy. Neurodegenerative disorders are among the most commonly mentioned pathologies proven to be linked to autophagy.[10–12] However, the main focus of this paper is to provide a highly researched description of the relationship between autophagy and cancer. Nowadays, we can state that autophagy plays a noteworthy role in both cellular protection against cancer and the growth of a tumor itself.[3] Autophagy supports tumor growth by promoting the survival of neoplastic cells that have to cope with stressors as a result of their rapid proliferation, such as hypoxia and nutrient starvation. Its protective role is fulfilled by the inhibition of chronic inflammation and necrosis. The more critical roles of autophagy are removing reactive oxygen species (ROS) that emerge from dysfunctional mitochondria, causing intense damage to the cell, preventing cellular oncogene-induced senescence, and maintaining genomic stability.[13] Thus, a conclusion may be drawn that autophagy plays a role in the early stages of tumor progression and even initiation.

The induction and regulation of autophagy

Autophagy consists of 5 main stages: initiation, elongation, maturation, fusion, and degradation. The complex process of initiation has many different triggers. Extensive investigations have been conducted on yeast and have established that nitrogen, carbon and nucleic acids starvation are all activators of autophagy, although some are stronger than others.[14] In yeast, the starvation of compounds essential to cell survival is a strong stimulus to initiate autophagy, as is the same for mammalian cells. The starvation of amino acids and energy, the absence of growth factors, and the accumulation of misfolded proteins, ROS, AMP-activated protein kinase (AMPK) and calcium play a significant role in autophagy induction.[15] Most of the triggers suppress the common pathway mTORC1, referred to as a nutrient-sensing kinase, but some have been proven to activate other signaling routes independent of mTORC1.[16] The presence of a trigger begins the complex process of autophagy (Fig. 2). The process is controlled by over 30 autophagy-related (Atg) proteins.[17] The Atg proteins are essential to control the correct course of autophagy. Numerous Atg genes have been proven to play an important role in tumor suppression. Consequently, decreased levels of many Atg proteins are found in tumor cells.[18] Under "normal" conditions, mTORC1 suppresses autophagy via mTOR-mediated phosphorylation of Atg13 when nutrient levels are sufficient.[19] However, in the presence of a trigger, the mTORC1 pathway is suppressed and the AMPKs (considered the most vital activator of autophagy) pathway allows autophagy to proceed.

The AMPK is the principal energy sensor for a cell and is activated when AMP:ATP and ADP:ATP ratios increase, thereby directly linking the process of autophagy with energy starvation.[20] The AMPK has been proven to have a dualistic role in the induction of autophagy. By suppressing mTORC1, AMPK indirectly induces autophagy, but can also induce phosphorylation ULK1/2 to directly activate the process.[21] The ULK1 is one of 5 orthologs of Atg13 found in yeast. So far, ULK1 and ULK2 have been proven to be involved in the induction of autophagy, and despite slight differences in function and constitution between them, they are often referred to interchangeably. The ULK1/2, Atg13, FIP200, and Atg101 proteins form the so-called ULK1/2 complex.[22] Although the exact course of interaction between these proteins has not been fully elucidated, it has been suggested that ULK1/2 requires both Atg13 and FIP200 for stability and correct function, as both enhance its kinase activity.[23] The role of the ULK1/2 complex seems to be the phosphorylation of 2 proteins: AMBRA1 and ZIPK.[24,25] The effect of these interactions causes the downstream events required for phagophore formation. As shown above, the relationship between mTORC1 and AMPK activity plays a vital role

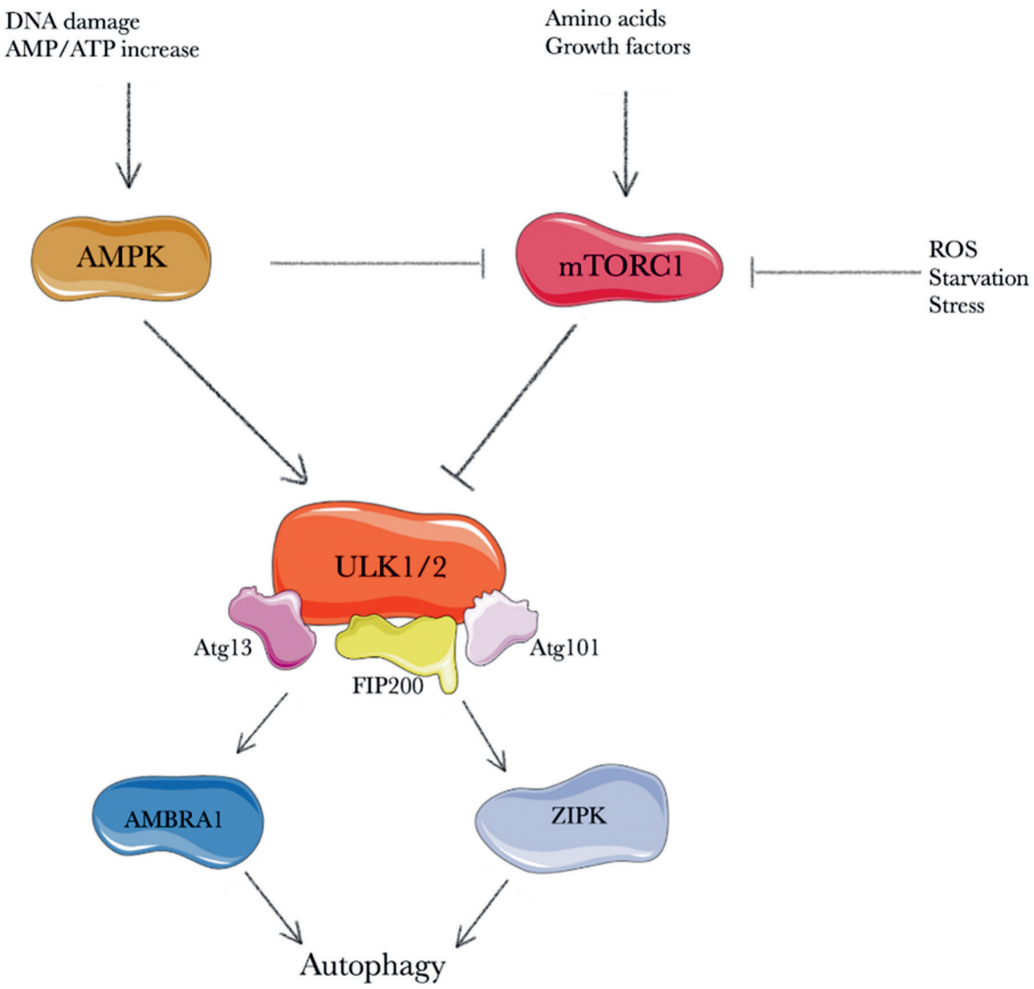

Fig. 2. Schematic representation of the mTORC1-AMPK-ULK1/2 autophagy induction mechanism. The mTORC1 is activated by a growth factor and amino acid rich environment suppressing the ULK1/2 complex (constituting of ULK1/2, Atg13, FIP200, and Atg101 proteins), thereby inhibiting autophagy. When those factors are absent or in low levels, or reactive oxygen species (ROS) and stress condition are present, the autophagy is promoted by inadequate mTORC1 activity. Autophagy is also induced when DNA is damaged or the AMP:ATP ratio rises (directly – by AMPK inducing activity on the ULK1/2 complex, and indirectly – by its suppressing effect on mTORC1). The ULK1/2 complex is responsible for further activation of proteins AMBRA1 and ZIPK, which are essential for the induction of autophagy. This admittedly simplified figure shows the ability of a cell to respond and react to the constantly changing supply and demand of nutrients, as well as act on the damaging effect of stress and ROS

in autophagy induction and suppression. Although these are the most researched regulators of autophagy, they are not the only ones.

The course of macroautophagy

The induction of autophagy allows for the further stages to proceed. After the formation of the phagophore, elongation occurs, resulting in the creation of an autophagosome. Next, the whole structure undergoes maturation. Finally, the fusion of the autophagosome with a lysosome occurs, allowing for the final stage of autophagy to occur – degradation (Fig. 3). The phagophore (also known as the isolation membrane) is a double-membrane structure that is the first traceable structure in autophagosome creation.[26] Unfortunately, after years of research and despite advances in technology, its origins remain unclear. It is believed that a phagophore forms de novo and is distinct among organelles.[27] The current literature has shown phagophores to form close to the endoplasmic reticulum (ER), meaning they could use it as a nucleation site. It has been established that the ULK1/2 complex is responsible for creating a membrane curvature, while other Atg proteins fold it into 2 and detach it from the site of origin.[28] After nucleation, the phagophore grows using other organelle membranes during the elongation stage. The mitochondria, ER and Golgi's complex have been suggested to be involved in the elongation stage.[29] The growing phagophore encloses macromolecules of cytoplasm destined for degradation forming the autophagosome – a double-membrane vesicle.[30] After maturing, the autophagosome fuses with a lysosome and the degradation occurs. During degradation, the contents of the autophagosome are broken down by lysosomal hydrolases.[31]

Importantly, the so-called Beclin-1 protein, a BH3-only domain protein, has a vital role in the nucleation of phagophores and the maturation of the autophagosomes.[32] Beclin-1 consists of 3 domains: Bcl-2-homology-3 (BH3), coiled coil (CCD) and the so-called evolutionary conserved domain (ECD).[33] Together with many cofactors (i.e., Rubicon, AMBRA1, UVRAG, Atg14L), it regulates the lipid kinase Vps-34 and promotes the formation of the Beclin1-Vps34-Vps15 (Vps15 is referred to as p150 by some authors) complex.[34] The Vps-34 is a class III phosphatidylinositol 3-kinase (PI(3)-kinase). Interestingly, it is the only mammalian PI(3)-kinase, as no other PI(3)P producing enzyme has been found. The PI(3)P has been proven to be essential in the course of autophagy.[35] The Beclin1-Vps34-Vps15 structure constitutes the core of other complexes, known

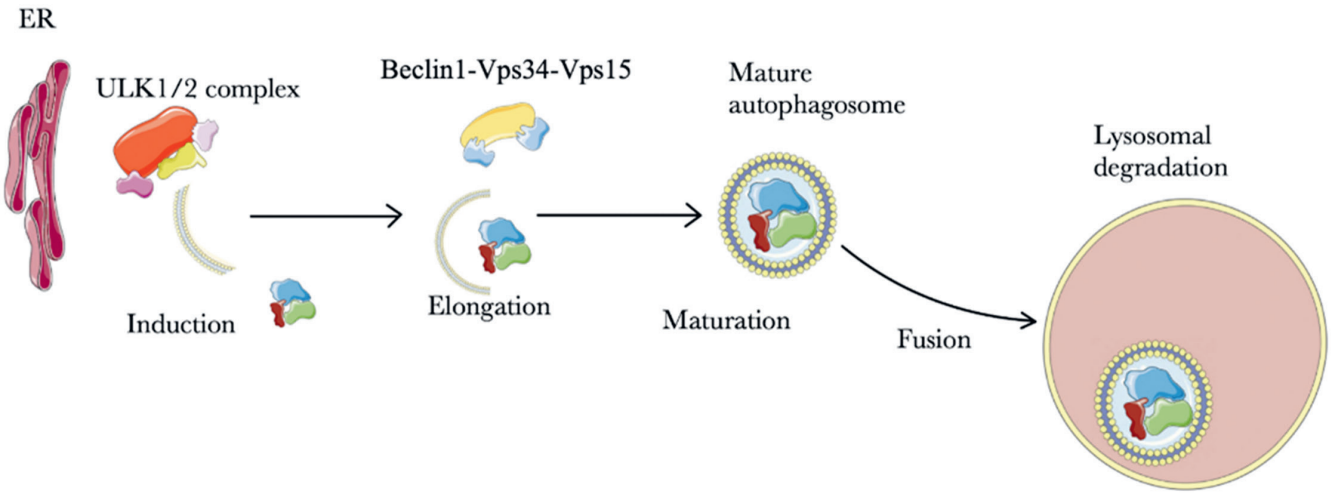

Fig. 3. The course of macroautophagy. Phagophores form in close proximity to the endoplasmic reticulum (ER), which may mean that they use it as a nucleation site. It has been established that the ULK1/2 complex is responsible for creating a membrane curvature, with other autophagy-related (Atg) proteins folding it in 2 and detaching it from its site of origin. The formation of the Beclin1-Vps34-Vps15 complex enables its elongation stage

as PI3KC3 complexes (class III phosphoinositide-3-kinase complexes), which play various roles in the autophagy. The PI3KC3 complex I is formed with Atg14L and has an essential role in autophagosome formation, especially in its early stages (i.e., phagophore formation).[36] This complex is further regulated by other factors, such as AMBRA1, NRBF2 and VMP1.[37] The AMBRA1 is a positive regulator of autophagy and is likely activated by the ULK1/2 complex.[38] In the later stages of autophagy, Atg14L is substituted by UVRAG and the complex II PI3KC3 is formed.[39] This complex has been found to have a role in autophagosome formation and maturation. The 3rd complex, involving core proteins and UVRAG, also contains Rubicon.[40] Although its role has not been well-defined, it has been reported to negatively regulate autophagy via autophagosome maturation suppression.[41] It is important for further research to focus on the complex interactions between these proteins, as some of these compounds are known for their ability to modulate PI3KC3 complexes and, therefore, be used in cancer therapy with hopes of suppressing autophagy in tumor cells.

One of the Beclin-1 domain names is derived from its ability to bind to Bcl-2 proteins. The Bcl-2 is a large family of proteins known for their role in apoptosis and autophagy regulation.[42] It has been established that under "normal" circumstances Bcl-2 binds to Beclin-1, inhibiting its ability to interact with Vps34.[43] But once autophagy propagating conditions occur, Bcl-2 dissociates from Beclin-1, allowing autophagy to proceed. Other members of the Bcl-2 family can interact with Beclin-1 as well, such as Bcl-XL, Bcl-w and Mcl-1.[44] This suggests that the interaction between Beclin-1 and any given Bcl-2 family protein may influence autophagy differently. Furthermore, the Bcl-2 family directly links autophagy and apoptosis.[45] Additionally, short periods of nutrient deprivation stimulate the dissociation of the Beclin-1-Bcl-2 complex propagating autophagy. With a prolonged exposure to these conditions, the Bax-Bcl-2 complex dissociates and propagates apoptosis.[46] It is important to note that BH3-mimetic molecules can disrupt the Beclin-1-Bcl-2 bond stimulating autophagy in cells in the correct clinical situation. Aside from autophagy, those molecules can also induce apoptotic death in cancer cells through their effect on the Bax-Bcl-2 complex.[47]

CMA role in cancer biology

Chaperone-mediated autophagy in non-transformed cells has been proven to be a cancer-preventive process; it acts through degrading proteins of oncogenic activity and facilitating cell death.[48] A decrease in CMA with age has been described.[49] The intensity of CMA increases in most neoplastic cell lines as do the levels of a component of CMA, namely lysosome-associated membrane protein 2 (LAMP2A).[50] Inhibition of CMA in cancer cells reduces their tumorigenicity, cell survival and metastatic potential.[50] The pro-oncogenic effect of elevated levels of CMA components is dependent on the tumor type and stage. The function of CMA as a protein quality inspector explains the increased tumor cell survival and resistance to the conditions of their microenvironment.[51] Moreover, CMA has been proven to be capable of degrading specific proteins that are responsible for antiproliferative effects (Rho-related GTP-binding protein RhoE),[51] in addition to tumor suppressor proteins (REF, MST1)[52] and pro-apoptotic proteins such as PUMA (BBC3- Bcl-2 binding component 3).[53] A high affinity of CMA for enzymes involved in the glycolytic cycle has also been described.[54] Degradation of these enzymes leads to the accumulation of glycolysis intermediates that promote proliferation. The inhibition of CMA causes oxidative stress, apoptosis and higher susceptibility to chemotherapeutics. Thus, CMA inhibition is considered a possible future cancer therapy.[48]

Relation between autophagy and cancer

The role of autophagy in cancer is a double-edged sword. Under physiological conditions and a functional autophagy apparatus, a cell exposed to unfavorable factors (mentioned above) can recover. For instance, a cell is exposed to ROS and the damaged proteins emerge. Autophagy activates to adequately degrade the damaged proteins and organelles, averting potential carcinogenesis. On the other hand, when autophagy is impaired and the cellular response is inadequate, damaged proteins and organelles accumulate, and further oxidative stress results in DNA damage and genome instability. Many cells undergo apoptosis or necrosis when the damage is fatal, but others may mutate unfavorably. The effect of these mutations may result in chronic inflammation, compensatory proliferation to replace lost cells, and tumor initiation. In this instance, before carcinogenesis occurs, autophagy, as a protective mechanism, mitigates the damage done through various factors and prevents a tumor-initiating environment from occurring. The opposite happens once carcinogenesis has begun. Defective autophagy, in this instance, can lead to a better response of cancer cells to treatment, hypoxia and, in some cases, cancer cells death and tumor atrophy. This is because cancer cells are considered to be more autophagy-dependent than noncancerous cells. It is especially applicable to cancer cells within the central part of tumors, as this environment is notorious for nutrient deficiencies and oxygen deprivation. Additionally, these cells have higher bioenergetic and biosynthetic needs due to their high proliferation rates. It has been proven that autophagy in the central cells is significantly more intense, compared to those in the tumor periphery. In this case, autophagy might be seen as a mechanism that allows for the survival and even proliferation in highly unfavorable conditions, leading to further growth, invasion and propagation of metastases (Fig. 4).

By promoting the survival of cancer cells, autophagy also influences future phases of tumor development. The initial steps of metastasis require signals promoting migration and invasion. Many types of cells, such as inflammatory cells, can provide such signals.[55] Various inflammatory cells infiltrate the tumor reacting to necrosis, commonly seen in solid tumors, and produce different effects on the tumor. Natural killer (NK) cells and cytotoxic T lymphocytes generally have anti-metastatic influence, while macrophages in the tumor environment usually correlate with a poor clinical prognosis.[56] By promoting the survival of tumor cells under metabolic stress and hypoxic conditions, autophagy reduces tumor cells necrosis and tumor infiltration through pro-metastatic mediators, such as macrophages. Therefore, in the early stages of metastasis, autophagy may act as a suppressor of metastasis, necrosis, and consequently tumor infiltration by inflammatory cells. However, in the later stages

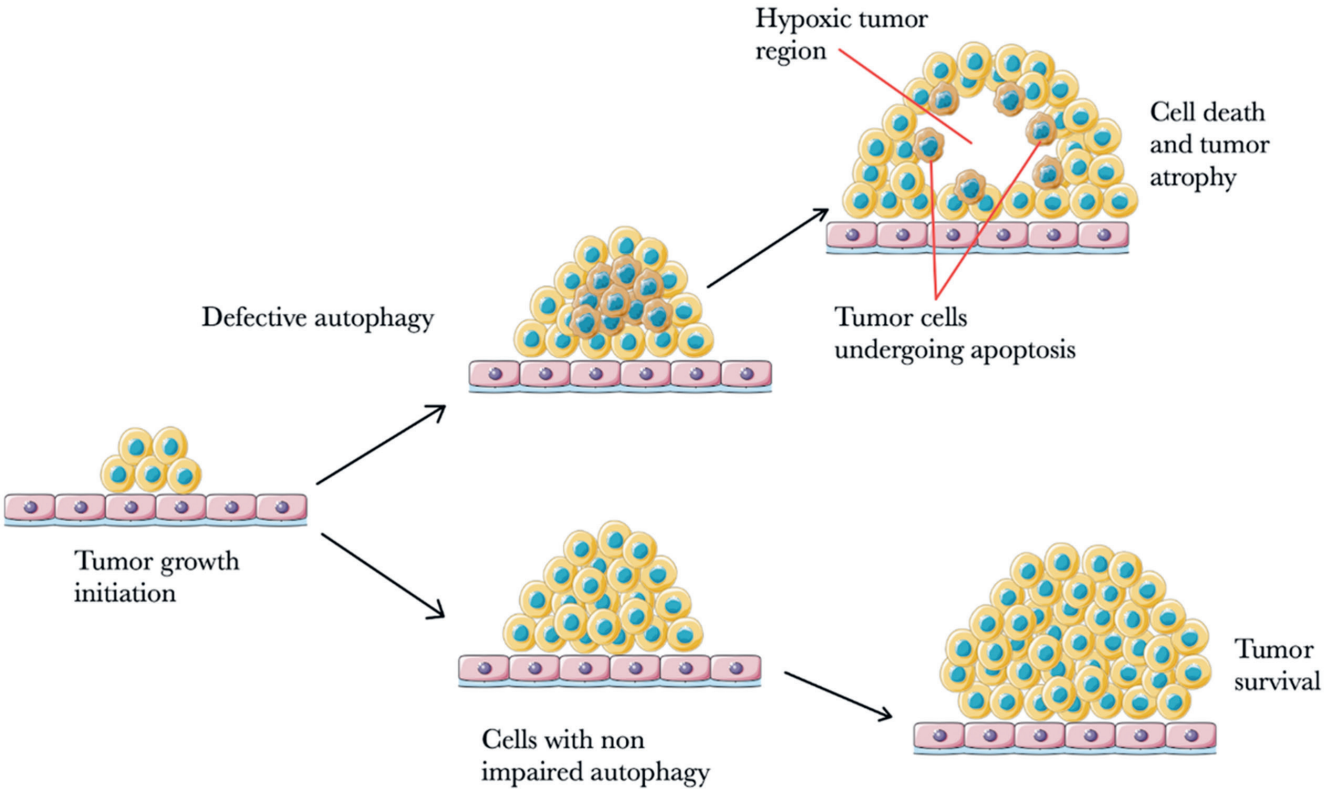

Fig. 4. The growth of an aggressive tumor in conditions of supporting autophagy and a defect in the process. Autophagy is crucial for the cell in the hypoxic regions of a tumor, promoting neoplastic cell survival. Defects of autophagy result in lower resistance to harsh conditions within the tumor microenvironment and accumulation of reactive oxygen species (ROS) and defective mitochondria, hence preventing proliferation and consequently, cell death

Table 1. The consequences of functional and impaired autophagy in different cancer stages

Cancer development stage	Autophagy functional	Autophagy impaired
Initiation	Autophagy allows cells damaged by various factors to recover, potentially preventing genetic alterations	Inadequate cellular response to damaging factors may lead to genome instability and mutations
Promotion	Tumor cells grow and multiply in unfavorable, oxygen-deprived, and nutrient-insufficient conditions	Tumor cells have decreased tolerance to hypoxia, in some cases tumor atrophy
Early progression	Reduced tumor cells necrosis and inflammation, delayed tumor infiltration by inflammatory cells	Quicker necrosis, tumor inflammation and infiltration
Metastases	The survival of anoikis, adaptation to various new environments in secondary organs	Metastatic tumor cell dormancy
Treatment	Weaker response to treatment, chemo- and radioresistance	Better response to treatment

of metastasis, metastatic cells enter the circulation, and autophagy is a factor that allows them to overcome anoikis.[57] In normal cells, the detachment from the extracellular matrix (ECM) propagates apoptosis, termed anoikis. Autophagy has been proven to have a role in anoikis resistance, as the knockdown of Atg proteins enhances cell death after ECM detachment.[58] Therefore, autophagy is a factor facilitating the survival and dissemination of metastatic cells. The final step in the metastasis cascade is the colonization of a distant organ within the host. As the environment in secondary organs differs from the primary site of the tumor, metastatic cells must adapt to the new conditions.[59] For example, metastatic cells that invade the lungs encounter an oxygen-rich environment and must adapt to the increased oxidative toxicity. As stated above, autophagy is the mechanism that allows for the survival and further development of cancer cells. Some studies have also proven that when metastatic cells are unable to adapt to the new environmental conditions, they may enter into a dormant state.[60] Thus, during different stages of cancer development, the impairment or stimulation of autophagy can be beneficial, and the clinical application of both autophagy inhibitors and stimulants may be an answer to the therapeutic challenges of cancer treatment (Table 1).

Cancer cachexia and autophagy processes

Cachexia is a syndrome caused by many factors that are often observed in oncological patients but can occur in a spectrum of non-oncological chronic diseases.[61] We do understand the causes of cachexia to some extent – chronic systemic catabolism and inflammation are described as the 2 main components of this process, although its etiology may differ in various tumor types.[62] It is usually associated with the progressive loss of lean body mass (with or without fatty tissue) through the involuntary degradation of skeletal muscle. Cachexia can result in impaired functionality of the human body displayed as immune system malfunction, nausea, asthenia, anorexia, energy imbalance, and neuroendocrine changes.[63] Cancer cachexia affects

Table 2. Autophagy-related drugs and their potential application in cancer treatment

Drug	Mechanism of action	Clinical stage/FDA approval	Potential application in
SBI-0206965	ULK inhibitor	preclinical studies	neuroblastoma, clear cell renal carcinoma, NSCLC
Verteporfin	autophagosome formation inhibitor	phase 1/2	glioblastoma/recurrent glioblastoma
Chloroquine with taxane	lysosome inhibitor	phase 2	breast cancer
Bafilomycin A1	lysosome inhibitor	preclinical studies	hepatocellular carcinoma, pancreatic cancer, colon cancer
Everolimus	mTOR inhibitor	phase 1	prostate cancer
Temisirolimus	mTOR inhibitor	approved by FDA	renal cell carcinoma
Ridaforolimus	mTOR inhibitor	phase 3	metastatic soft-tissue sarcomas
PX-866	PI3K inhibitor	phase 2	prostate cancer
NVP-BEZ235	PI3K/mTOR inhibitor	phase 1	breast cancer
GDC-0980	PI3K/mTOR inhibitor	phase 1	non-Hodgkin's lymphoma
SAR405	PIK3C3 inhibitor	preclinical studies	renal cell carcinoma
Spautin-1	PI3KC3 inhibitor	preclinical studies	chronic myeloid leukemia
Gossypol	BH3 mimetic	phase 2	adult glioblastoma, adult gliosarcoma
ABT-737	BH3 mimetic	preclinical studies	thyroid carcinoma

FDA – The United States Food and Drug Administration; NSCLC – non-small-cell lung carcinoma.

50% of all cancer patients in the early stages of the disease and 80% as the disease advances,[64] making it a concerning challenge for medicine. Cachexia can affect the entire organism by reducing the quality of life, tolerance, response to treatment, and consequently, survival. Inflammatory factors described in cancer cachexia are eicosanoids,[65] tumor necrosis factor, interferon, interleukin-6 (IL-6), and IL-1β.[66] Chronic inflammatory processes can lead to increased fatty acid content within the blood.[67] Pettersen et al. found that IL-6 secreted by tumor cells stimulates autophagy in myotubes when complexed with soluble IL-6 receptors.[68] Poor prognosis has also been described in lung cancer patients with elevated IL-6 levels.[68] Systemic chronic inflammation, characteristic in cancer cachexia, is a result of immune cell infiltration of the tumor microenvironment and constant stimulation of the immune system by cancer. Systemic inflammation increases the demand for nutrients and energy through catabolic upregulation. Selective autophagy is a process induced by various forms of stress – ROS and adenosine diphosphate (ADP) accumulation, hypoxia and inflammation. It ensures a continuous supply of energy and nutrients for a tumor as a functional adaptive cellular response. Penna et al. demonstrated that muscle atrophy occurring in cancer cachexia is associated with an augmented autophagy rate by studying markers of the process – Beclin-1 (autophagy induction marker), LC3B conversion (autophagosome levels) and p62/SQSTM1 (substrate sequestration).[69] Another study, looking at the association between weight loss and autophagy-accelerated bioactivity, showed no link in a heterogeneous group of oncological patients. However, a different study focusing on lung cancer patients indicated that autophagy-induced activity and weight loss was a characteristic in men only and was responsible for a worse prognosis.[70]

Oncogenes and tumor suppressors involved in autophagy

Years of studies on oncogenesis and autophagy identified shared genes in both processes.[71] Today we know that both oncogenes and tumor suppressor genes play a part in autophagy. An oncogene, *AKT1*, has been identified as an inhibitor of autophagy via mTOR activation.[72] Mutations in the *Ras* gene are common in several types of aggressive cancers and also play a crucial role in autophagy.[73] The *Ras* gene is a known upstream inhibitor of mTOR. On the other hand, PI3K inhibits autophagy via *AKT1* activation and is responsible for the gain-of-function mutations seen in tumor cells.[71,72] The *Bcl-2* gene is known for its anti-apoptotic characteristics and inhibition of Beclin-1,[73] a crucial protein in the initial stages of macroautophagy. Beclin-1 is also considered a tumor suppressor gene that is commonly deleted in breast, ovarian and prostate cancers.[73] The *NF1* is a suppressor often mutated in von Recklinghausen's disease and juvenile myelomonocytic leukemia, and can relieve Ras-mediated inhibition of autophagy.[73] The *TSC1* and *TSC2* genes are mutated in tuberous sclerosis and indirectly inhibit the PI3K-AKT1-mTOR pathway.[74] Another tumor suppressor gene, *RAB7A*, is known for its rearrangement in leukemias, deletion in solid tumors and involvement in autophagosomal maturation.[75] The *DAPK1*, yet another suppressor gene silenced in various tumors, relieves the inhibition of autophagy mediated by Bcl-2/Bcl-XL.[76] The *PTEN* gene is downregulated in ovarian cancer and stops autophagy inhibition mediated by PI3K-AKT1.[72] These examples highlight the fact that autophagy and carcinogenesis have a lot in common.

Treatment opportunities

The research on autophagy has brought to light new cancer treatment possibilities.[77] Thanks to the dualistic role of autophagy in cancer initiation and progression, there are many areas we can target to capitalize on the effect of autophagy in order to suit clinical treatment. Considering that autophagy has an important role in tumor suppression, we can try to modulate and enhance it in patients with an increased risk of developing cancers (Table 2). On the other hand, once carcinogenesis has occurred, the inhibition of autophagy in cancer cells can be very beneficial. The 3rd potential application of our knowledge regarding autophagy is in modulating it to increase the susceptibility of a tumor to radio- and chemotherapy.[78,79]

ULK inhibitors

The ULK proteins have a vital and comparatively well-researched role in autophagy induction and have been one of the main focuses of numerous studies. Many compounds involved in the inhibition of ULK kinase activity have been identified: compound 6, MRT68921, MRT67307, SBI-0206965, ULK100, and ULK101.[77] The most researched compound is SBI-0206965. It has been proven to reduce the growth and induce apoptosis in some neuroblastoma cell lines, and sensitize one line to treatment. Furthermore, it suppresses non-small cell lung cancer (NSCLC) cell growth, enhances its susceptibility to cisplatin, and even induces apoptosis in clear cell renal carcinoma (i.e., by blocking autophagy).[80,81] Some studies have also indicated its utility in the potential treatment of myeloid leukemia FLT3-ITD.[82]

Autophagosome formation inhibition

Since autophagosome formation is an essential stage in macroautophagy, there have been studies to find a compound that suppresses it. Verteporfin disrupts autophagosome formation and other pathways in autophagy.[83] Research has shown that verteporfin sensitizes osteosarcoma cells to cytotoxic drugs.[84]

Lysosomes inhibitors

Lysosome function in autophagy prompted studies on chloroquine (CQ) and its analog hydroxychloroquine. Both substances are known for their use in malaria treatment and rheumatoid diseases, and their application in cancer therapy seems to be the next step. It is known that they can inhibit autophagy by directly interacting with lysosomes. As weak bases, they diffuse into the lysosome and undergo protonation to cause overall alkalization of the lysosome lumen. This creates an unfavorable environment for lysosomal enzymes and impairs their function. A protonated CQ cannot then diffuse out of the lysosome as it loses its ability to transverse cell membranes.[85] Chloroquine also inhibits the fusion of the lysosome with the autophagosome.[86] Importantly, those effects did not go unnoticed and CQ has already entered clinical trials in combination with taxane and taxane-like drugs to evaluate the response of breast cancer cells to this drug combination.[87] The challenge of long-term use of CQ and its derivatives is their well-known toxicity, which highly depends on the dose and duration of treatment. The most common side effects are retinopathy and cardiotoxicity.[88,89]

Another drug with similar effects on lysosomes is bafilomycin A1 (BafA1). It also alkalizes the lumen of lysosomes through a different mechanism than CQ. The BafA1 targets the vacuolar-type H^+-ATPase, a transmembrane proton pump responsible for acidifying the lysosome.[90] Similarly to CQ and its derivatives, it also inhibits the autophagosome-lysosome fusion and impairs TORC1 signaling. Thus, many researchers speculate about BafA1 future use in cancer treatments.[91]

mTOR inhibitors

The name of mTORC1 derived from the fact that it is a target of rapamycin.[92] Rapamycin is a macrolide compound known for its role in transplant surgery (administered to prevent transplant rejection) and coronary stent coating. Additionally, studies have shown, that it might be considered an anti-aging drug (e.g., it extended the lifespan of mice in some studies).[93] These effects are mainly due to its inhibition of mTOR proteins and consequently, autophagy activation. Many researchers have suggested that rapamycin could be used to slow down most (if not all) age-related diseases in humans, including some cancers.[94] Because mTOR activity is commonly upregulated in cancer, its inhibitors have significant promise in cancer therapy.[95] Therefore, rapamycin and its derivatives (known as rapalogs) such as temsirolimus, everolimus and ridaforolimus are undergoing clinical trials to evaluate their potential use in cancer treatment. Temsirolimus has already been approved by the The United States Food and Drug Administration (FDA) in 2007 for use in advanced renal cell carcinoma (RCC) treatment.

PI3K inhibitors

The critical role of PI3K in autophagy inspired the research into compounds able to block its function.[96] Several molecules have been found, such as 3-methyladenine (3-MA), LY294002, wortmannin, and its analog PX-866 (Oncothyreon). Clinical trials have been conducted using PX-866 on patients with advanced prostate cancer, although only modest single-agent activity has been reported. However, more research concerning the activity of PX-866 combined with other drugs needs to be conducted.[97] Additionally, the compounds able to inhibit both PI3K and mTOR, such as NVP-BEZ235 and GDC-0980, have entered clinical trials evaluating their potential use in cancer therapy.

PI3KC3 complex inhibitors

Since PI3KC3 complexes consist of various proteins, there are a few ways to block their activity. The SAR405 is a selective Vps34 inhibitor that affects late autophagosome-lysosome interaction and prevents autophagy.[98] Furthermore, the available research has shown that SAR405 combined with everolimus (mTOR inhibitor) to produce strong antiproliferative effects on renal tumor cells.[99] The potential drawback of SAR405 administration is that PI3KC3 is also involved in endosomal trafficking and therefore, can negatively affect cellular secretion.

Spautin-1 is a compound that impairs PI3KC3 by a different approach. It inhibits autophagy by enhancing the degradation of Beclin-1 and thus, prevents the formation of the PI3KC3 complex.[100] Shao et al. reported promising results with its potential application in overcoming resistance to imatinib mesylate-induced autophagy in chronic myeloid leukemia.[101] Not only does it show proapoptotic properties, but it also potentiates the efficacy of imatinib mesylate in chronic myeloid leukemia cells.

BH3 mimetics

The theory behind administering BH3 mimetics is to stimulate autophagy in cells by liberating Beclin-1 from Bcl-2.[102] Stimulating this interaction can be beneficial also because of the possibility of inducing apoptotic cell death by negating the anti-apoptotic effects of the Bcl-2-Bax complex. Gossypol is a polyphenolic aldehyde that works as a pan-Bcl-2 inhibitor.[103] Clinical trials have been conducted in patients with glioblastoma and despite some adverse events (including cardiac and gastrointestinal disorders), the results are promising.[104] Another BH3-mimetic drug, ABT-737 has been tested on various thyroid carcinoma cell lines and has been proven to cause apoptotic cell death and a synergistic effect with chemotherapeutic drugs.[105] Furthermore, there is an analog of ABT-737 that can be administered orally, ABT-236. Although the clinical application for our constantly evolving knowledge about autophagy is within our grasp, there is still a magnitude of research that needs to be conducted.

Conclusions

From many years of studies, we have learned a lot about autophagy and its role in the pathogenesis of certain diseases. As far as our understanding of the molecular pathways of autophagy is concerned, their relation to cancer seems to be more profound and sophisticated than initially anticipated. We know that it is a housekeeping mechanism of a cell that decreases chances of neoplastic transformation, but after malignant transformation, it supports the proliferation and prosperity of cancer cells. Confirming autophagy as a mechanism that promotes tumor growth, provides us with the knowledge to develop new treatment options for oncologic patients and brings hope to the idea of curing cancer.

ORCID iDs

Kacper Turek https://orcid.org/0000-0001-6551-8079
Michał Jarocki https://orcid.org/0000-0001-8394-6018
Julita Kulbacka https://orcid.org/0000-0001-8272-5440
Jolanta Saczko https://orcid.org/0000-0001-5273-5293

References

1. Levine B, Klionsky DJ. Development by self-digestion: Molecular mechanisms and biological functions of autophagy. *Dev Cell*. 2004; 6(4):463–477. doi:10.1016/s1534-5807(04)00099-1
2. Mizushima N. Autophagy: Process and function. *Genes Dev*. 2007; 21(22):2861–2873. doi:10.1101/gad.1599207
3. Mathew R, Karantza-Wadsworth V, White E. Role of autophagy in cancer. *Nat Rev Cancer*. 2007;7(12):961–967. doi:10.1038/nrc2254
4. Williams A, Jahreiss L, Sarkar S, et al. Aggregate-prone proteins are cleared from the cytosol by autophagy: Therapeutic implications. *Curr Top Dev Biol*. 2006;76:89–101. doi:10.1016/S0070-2153(06)76003-3
5. Degenhardt K, Mathew R, Beaudoin B, et al. Autophagy promotes tumor cell survival and restricts necrosis, inflammation, and tumorigenesis. *Cancer Cell*. 2006;10(1):51–64. doi:10.1016/j.ccr.2006.06.001
6. Mizushima N, Levine B, Cuervo AM, Klionsky DJ. Autophagy fights disease through cellular self-digestion. *Nature*. 2008;451(7182): 1069–1075. doi:10.1038/nature06639
7. Massey AC, Zhang C, Cuervo AM. Chaperone-mediated autophagy in aging and disease. *Curr Top Dev Biol*. 2006;73:205–235. doi:10.1016/S0070-2153(05)73007-6
8. Saftig P, Beertsen W, Eskelinen EL. LAMP-2: A control step for phagosome and autophagosome maturation. *Autophagy*. 2008;4(4):510–512. doi:10.4161/auto.5724
9. Levine B, Kroemer G. Autophagy in the pathogenesis of disease. *Cell*. 2008;132(1):27–42. doi:10.1016/j.cell.2007.12.018
10. Komatsu M, Waguri S, Chiba T, et al. Loss of autophagy in the central nervous system causes neurodegeneration in mice. *Nature*. 2006; 441(7095):880–884. doi:10.1038/nature04723
11. Martinez-Vicente M, Cuervo AM. Autophagy and neurodegeneration: When the cleaning crew goes on strike. *Lancet Neurol*. 2007;6(4): 352–361. doi:10.1016/S1474-4422(07)70076-5
12. Shibata M, Lu T, Furuya T, et al. Regulation of intracellular accumulation of mutant Huntingtin by Beclin 1. *J Biol Chem*. 2006;281(20): 14474–14485. doi:10.1074/jbc.M600364200
13. Nelson DA, Tan TT, Rabson AB, Anderson D, Degenhardt K, White E. Hypoxia and defective apoptosis drive genomic instability and tumorigenesis. *Genes Dev*. 2004;18(17):2095–2107. doi:10.1101/gad.1204904
14. Reggiori F, Klionsky DJ. Autophagic processes in yeast: Mechanism, machinery and regulation. *Genetics*. 2013;194(2):341–361. doi:10.1534/genetics.112.149013
15. Wang L, Ye X, Zhao T. The physiological roles of autophagy in the mammalian life cycle. *Biol Rev Camb Philos Soc*. 2019;94(2):503–516. doi:10.1111/brv.12464
16. Sabatini DM. Twenty-five years of mTOR: Uncovering the link from nutrients to growth. *Proc Natl Acad Sci U S A*. 2017;114(45):11818–11825. doi:10.1073/pnas.1716173114
17. Nishimura T, Tooze SA. Emerging roles of ATG proteins and membrane lipids in autophagosome formation. *Cell Discov*. 2020;6(1):32. doi:10.1038/s41421-020-0161-3
18. Li X, He S, Ma B. Autophagy and autophagy-related proteins in cancer. *Mol Cancer*. 2020;19(1):12. doi:10.1186/s12943-020-1138-4
19. Puente C, Hendrickson RC, Jiang X. Nutrient-regulated phosphorylation of ATG13 inhibits starvation-induced autophagy. *J Biol Chem*. 2016;291(11):6026–6035. doi:10.1074/jbc.M115.689646
20. Hardie DG. AMP-activated/SNF1 protein kinases: Conserved guardians of cellular energy. *Nat Rev Mol Cell Biol*. 2007;8(10):774–785. doi:10.1038/nrm2249
21. Hardie DG. AMPK and autophagy get connected. *EMBO J*. 2011;30(4): 634–635. doi:10.1038/emboj.2011.12
22. Mizushima N. The role of the Atg1/ULK1 complex in autophagy regulation. *Curr Opin Cell Biol*. 2010;22(2):132–139. doi:10.1016/j.ceb.2009.12.004
23. Ganley IG, Lam DH, Wang J, Ding X, Chen S, Jiang X. ULK1.ATG13.FIP200 complex mediates mTOR signaling and is essential for autophagy. *J Biol Chem*. 2009;284(18):12297–12305. doi:10.1074/jbc.M900573200
24. Di Bartolomeo S, Corazzari M, Nazio F, et al. The dynamic interaction of AMBRA1 with the dynein motor complex regulates mammalian autophagy. *J Cell Biol*. 2010;191(1):155–168. doi:10.1083/jcb.201002100
25. Alers S, Löffler AS, Wesselborg S, Stork B. Role of AMPK-mTOR-Ulk1/2 in the regulation of autophagy: Cross talk, shortcuts, and feedbacks. *Mol Cell Biol*. 2012;32(1):2–11. doi:10.1128/MCB.06159-11
26. Juhasz G, Neufeld TP. Autophagy: A forty-year search for a missing membrane source. *PLoS Biol*. 2006;4(2):e36. doi:10.1371/journal.pbio.0040036
27. Schütter M, Graef M. Localized de novo phospholipid synthesis drives autophagosome biogenesis. *Autophagy*. 2020;16(4):770–771. doi:10.1080/15548627.2020.1725379
28. Hurley JH, Young LN. Mechanisms of autophagy initiation. *Annu Rev Biochem*. 2017;86:225–244. doi:10.1146/annurev-biochem-061516-044820
29. Perrotta I. The origin of the autophagosomal membrane in human atherosclerotic plaque: A preliminary ultrastructural study. *Ultrastruct Pathol*. 2017;41(5):327–334. doi:10.1080/01913123.2017.1349853
30. Graef M. Recent advances in the understanding of autophagosome biogenesis. *F1000Res*. 2020;9:F1000. doi:10.12688/f1000research.22111.1
31. Stefaniak S, Wojtyla Ł, Pietrowska-Borek M, Borek S. Completing autophagy: Formation and degradation of the autophagic body and metabolite salvage in plants. *Int J Mol Sci*. 2020;21(6):2205. doi:10.3390/ijms21062205
32. Oberstein A, Jeffrey PD, Shi Y. Crystal structure of the Bcl-XL-Beclin 1 peptide complex: Beclin 1 is a novel BH3-only protein. *J Biol Chem*. 2007;282(17):13123–13132. doi:10.1074/jbc.M700492200
33. Kang R, Zeh HJ, Lotze MT, Tang D. The Beclin 1 network regulates autophagy and apoptosis. *Cell Death Differ*. 2011;18(4):571–580. doi:10.1038/cdd.2010.191
34. Kihara A, Kabeya Y, Ohsumi Y, Yoshimori T. Beclin-phosphatidylinositol 3-kinase complex functions at the trans-Golgi network. *EMBO Rep*. 2001;2(4):330–335. doi:10.1093/embo-reports/kve061
35. Nascimbeni AC, Codogno P, Morel E. Phosphatidylinositol-3-phosphate in the regulation of autophagy membrane dynamics. *FEBS J*. 2017;284(9):1267–1278. doi:10.1111/febs.13987
36. Matsunaga K, Morita E, Saitoh T, et al. Autophagy requires endoplasmic reticulum targeting of the PI3-kinase complex via Atg14L. *J Cell Biol*. 2010;190(4):511–521. doi:10.1083/jcb.200911141
37. Zhong Y, Morris DH, Jin L, et al. Nrbf2 protein suppresses autophagy by modulating Atg14L protein-containing Beclin 1-Vps34 complex architecture and reducing intracellular phosphatidylinositol-3 phosphate levels. *J Biol Chem*. 2014;289(38):26021–26037. doi:10.1074/jbc.M114.561134
38. Cianfanelli V, Nazio F, Cecconi F. Connecting autophagy: AMBRA1 and its network of regulation. *Mol Cell Oncol*. 2015;2(1):e970059. doi:10.4161/23723548.2014.970059
39. Liang C, Lee J, Inn K, et al. Beclin1-binding UVRAG targets the class C Vps complex to coordinate autophagosome maturation and endocytic trafficking. *Nat Cell Biol*. 2008;10(7):776–787. doi:10.1038/ncb1740
40. Sun Q, Zhang J, Fan W, et al. The RUN domain of rubicon is important for hVps34 binding, lipid kinase inhibition, and autophagy suppression. *J Biol Chem*. 2011;286(1):185–191. doi:10.1074/jbc.M110.126425

41. Tabata K, Matsunaga K, Sakane A, Sasaki T, Noda T, Yoshimori T. Rubicon and PLEKHM1 negatively regulate the endocytic/autophagic pathway via a novel Rab7-binding domain. *Mol Biol Cell*. 2010;21(23): 4162–4172. doi:10.1091/mbc.E10-06-0495
42. Hatok J, Racay P. Bcl-2 family proteins: Master regulators of cell survival. *Biomol Concepts*. 2016;7(4):259–270. doi:10.1515/bmc-2016-0015
43. Pattingre S, Tassa A, Qu X, et al. Bcl-2 antiapoptotic proteins inhibit Beclin 1-dependent autophagy. *Cell*. 2005;122(6):927–939. doi:10.1016/j.cell.2005.07.002
44. Erlich S, Mizrachy L, Segev O, et al. Differential interactions between Beclin 1 and Bcl-2 family members. *Autophagy*. 2007;3(6):561–568. doi:10.4161/auto.4713
45. Marquez RT, Xu L. Bcl-2:Beclin 1 complex: Multiple, mechanisms regulating autophagy/apoptosis toggle switch. *Am J Cancer Res*. 2012;2(2): 214–221. PMID:22485198
46. Wei Y, Sinha S, Levine B. Dual role of JNK1-mediated phosphorylation of Bcl-2 in autophagy and apoptosis regulation. *Autophagy*. 2008;4(7):949–951. doi:10.4161/auto.6788
47. Campbell KJ, Tait SWG. Targeting BCL-2 regulated apoptosis in cancer. *Open Biol*. 2018;8(5):180002. doi:10.1098/rsob.180002
48. Kaushik S, Cuervo AM. The coming of age of chaperone-mediated autophagy. *Nat Rev Mol Cell Biol*. 2018;19(6):365–381. doi:10.1038/s41580-018-0001-6
49. Kiffin R, Kaushik S, Zeng M, et al. Altered dynamics of the lysosomal receptor for chaperone-mediated autophagy with age. *J Cell Sci*. 2007;120(Pt 5):782–791. doi:10.1242/jcs.001073
50. Kon M, Kiffin R, Koga H, et al. Chaperone-mediated autophagy is required for tumor growth. *Sci Transl Med*. 2011;3(109):109ra117. doi:10.1126/scitranslmed.3003182
51. Zhou J, Yang J, Fan X, et al. Chaperone-mediated autophagy regulates proliferation by targeting RND3 in gastric cancer. *Autophagy*. 2016;12(3):515–528. doi:10.1080/15548627.2015.1136770
52. Li L, Fang R, Liu B, et al. Deacetylation of tumor-suppressor MST1 in Hippo pathway induces its degradation through HBXIP-elevated HDAC6 in promotion of breast cancer growth. *Oncogene*. 2016;35(31): 4048–4057. doi:10.1038/onc.2015.476
53. Xie W, Zhang L, Jiao H, et al. Chaperone-mediated autophagy prevents apoptosis by degrading BBC3/PUMA. *Autophagy*. 2015;11(9): 1623–1635. doi:10.1080/15548627.2015.1075688
54. Lv L, Li D, Zhao D, et al. Acetylation targets the M2 isoform of pyruvate kinase for degradation through chaperone-mediated autophagy and promotes tumor growth. *Mol Cell*. 2011;42(6):719–730. doi:10.1016/j.molcel.2011.04.025
55. Zhao H, Wu L, Yan G, et al. Inflammation and tumor progression: Signaling pathways and targeted intervention. *Signal Transduct Target Ther*. 2021;6(1):263. doi:10.1038/s41392-021-00658-5
56. Coussens LM, Werb Z. Inflammation and cancer. *Nature*. 2002; 420(6917):860–867. doi:10.1038/nature01322
57. Dower CM, Wills CA, Frisch SM, Wang HG. Mechanisms and context underlying the role of autophagy in cancer metastasis. *Autophagy*. 2018;14(7):1110–1128. doi:10.1080/15548627.2018.1450020
58. Douma S, Van Laar T, Zevenhoven J, Meuwissen R, Van Garderen E, Peeper DS. Suppression of anoikis and induction of metastasis by the neurotrophic receptor TrkB. *Nature*. 2004;430(7003):1034–1039. doi:10.1038/nature02765
59. Schild T, Low V, Blenis J, Gomes AP. Unique metabolic adaptations dictate distal organ-specific metastatic colonization. *Cancer Cell*. 2018;33(3):347–354. doi:10.1016/j.ccell.2018.02.001
60. Chavez-Dominguez R, Perez-Medina M, Lopez-Gonzalez JS, Galicia-Velasco M, Aguilar-Cazares D. The double-edge sword of autophagy in cancer: From tumor suppression to pro-tumor activity. *Front Oncol*. 2020;10:578418. doi:10.3389/fonc.2020.578418
61. Fearon K, Strasser F, Anker SD, et al. Definition and classification of cancer cachexia: An international consensus. *Lancet Oncol*. 2011; 12(5):489–495. doi:10.1016/S1470-2045(10)70218-7
62. Baracos VE, Martin L, Korc M, Guttridge DC, Fearon KCH. Cancer-associated cachexia. *Nat Rev Dis Primers*. 2018;4(1):17105. doi:10.1038/nrdp.2017.105
63. Seelaender M, Laviano A, Busquets S, Püschel GP, Margaria T, Batista ML. Inflammation in cachexia. *Mediators Inflamm*. 2015;2015:536954. doi:10.1155/2015/536954
64. Gonçalves R de C, Freire PP, Coletti D, Seelaender M. Tumor microenvironment autophagic processes and cachexia: The missing link? *Front Oncol*. 2021;10:617109. doi:10.3389/fonc.2020.617109
65. Vaughan VC, Martin P, Lewandowski PA. Cancer cachexia: Impact, mechanisms and emerging treatments. *J Cachexia Sarcopenia Muscle*. 2013;4(2):95–109. doi:10.1007/s13539-012-0087-1
66. Tisdale MJ. Mechanisms of cancer cachexia. *Physiol Rev*. 2009;89(2): 381–410. doi:10.1152/physrev.00016.2008
67. Flueck JL. Body composition in swiss elite wheelchair athletes. *Front Nutr*. 2020;7:1. doi:10.3389/fnut.2020.00001
68. Pettersen K, Andersen S, Degen S, et al. Cancer cachexia associates with a systemic autophagy-inducing activity mimicked by cancer cell-derived IL-6 trans-signaling. *Sci Rep*. 2017;7(1):2046. doi:10.1038/s41598-017-02088-2
69. Penna F, Costamagna D, Pin F, et al. Autophagic degradation contributes to muscle wasting in cancer cachexia. *Am J Pathol*. 2013;182(4): 1367–1378. doi:10.1016/j.ajpath.2012.12.023
70. Cosper PF, Leinwand LA. Cancer causes cardiac atrophy and autophagy in a sexually dimorphic manner. *Cancer Res*. 2011;71(5):1710–1720. doi:10.1158/0008-5472.CAN-10-3145
71. Ávalos Y, Canales J, Bravo-Sagua R, Criollo A, Lavandero S, Quest AFG. Tumor suppression and promotion by autophagy. *Biomed Res Int*. 2014;2014:603980. doi:10.1155/2014/603980
72. Cully M, You H, Levine AJ, Mak TW. Beyond PTEN mutations: The PI3K pathway as an integrator of multiple inputs during tumorigenesis. *Nat Rev Cancer*. 2006;6(3):184–192. doi:10.1038/nrc1819
73. Levine B, Sinha SC, Kroemer G. Bcl-2 family members: Dual regulators of apoptosis and autophagy. *Autophagy*. 2008;4(5):600–606. doi:10.4161/auto.6260
74. Schwartz RA, Fernández G, Kotulska K, Jóźwiak S. Tuberous sclerosis complex: Advances in diagnosis, genetics, and management. *J Am Acad Dermatol*. 2007;57(2):189–202. doi:10.1016/j.jaad.2007.05.004
75. Edinger AL, Cinalli RM, Thompson CB. Rab7 prevents growth factor-independent survival by inhibiting cell-autonomous nutrient transporter expression. *Dev Cell*. 2003;5(4):571–582. doi:10.1016/S1534-5807(03)00291-0
76. Harrison B, Kraus M, Burch L, et al. DAPK-1 binding to a linear peptide motif in MAP1B stimulates autophagy and membrane blebbing. *J Biol Chem*. 2008;283(15):9999–10014. doi:10.1074/jbc.M706040200
77. Pérez-Hernández M, Arias A, Martínez-García D, Pérez-Tomás R, Quesada R, Soto-Cerrato V. Targeting autophagy for cancer treatment and tumor chemosensitization. *Cancers (Basel)*. 2019;11(10):1599. doi:10.3390/cancers11101599
78. Tam SY, Wu VWC, Law HKW. Influence of autophagy on the efficacy of radiotherapy. *Radiat Oncol*. 2017;12(1):57. doi:10.1186/s13014-017-0795-y
79. Sui X, Chen R, Wang Z, et al. Autophagy and chemotherapy resistance: A promising therapeutic target for cancer treatment. *Cell Death Dis*. 2013;4(10):e838. doi:10.1038/cddis.2013.350
80. Tang F, Hu P, Yang Z, et al. SBI0206965, a novel inhibitor of Ulk1, suppresses non-small cell lung cancer cell growth by modulating both autophagy and apoptosis pathways. *Oncol Rep*. 2017;37(6):3449–3458. doi:10.3892/or.2017.5635
81. Lu J, Zhu L, Zheng LP, et al. Overexpression of ULK1 represents a potential diagnostic marker for clear cell renal carcinoma and the antitumor effects of SBI-0206965. *EBioMedicine*. 2018;34:85–93. doi:10.1016/j.ebiom.2018.07.034
82. Hwang DY, Eom JI, Jang JE, et al. ULK1 inhibition as a targeted therapeutic strategy for FLT3-ITD-mutated acute myeloid leukemia. *J Exp Clin Cancer Res*. 2020;39(1):85. doi:10.1186/s13046-020-01580-4
83. Donohue E, Tovey A, Vogl AW, et al. Inhibition of autophagosome formation by the benzoporphyrin derivative verteporfin. *J Biol Chem*. 2011;286(9):7290–7300. doi:10.1074/jbc.M110.139915
84. Saini H, Sharma H, Mukherjee S, Chowdhury S, Chowdhury R. Verteporfin disrupts multiple steps of autophagy and regulates p53 to sensitize osteosarcoma cells. *Cancer Cell Int*. 2021;21(1):52. doi:10.1186/s12935-020-01720-y
85. Browning DJ. Pharmacology of chloroquine and hydroxychloroquine. In: Browning DJ, ed. *Hydroxychloroquine and Chloroquine Retinopathy*. New York, USA: Springer; 2014:35–63.
86. Mauthe M, Orhon I, Rocchi C, et al. Chloroquine inhibits autophagic flux by decreasing autophagosome-lysosome fusion. *Autophagy*. 2018;14(8):1435–1455. doi:10.1080/15548627.2018.1474314
87. Sparano JA. Taxanes for breast cancer: An evidence-based review of randomized phase II and phase III trials. *Clin Breast Cancer*. 2000; 1(1):32. doi:10.3816/cbc.2000.n.002

88. Oluleye TS, Babalola Y, Ijaduola M. Chloroquine retinopathy: Pattern of presentation in Ibadan, Sub-Sahara Africa. *Eye (Lond)*. 2016;30(1): 64–67. doi:10.1038/eye.2015.185
89. Chatre C, Roubille F, Vernhet H, Jorgensen C, Pers YM. Cardiac complications attributed to chloroquine and hydroxychloroquine: A systematic review of the literature. *Drug Saf*. 2018;41(10):919–931. doi:10.1007/s40264-018-0689-4
90. Fedele AO, Proud CG. Chloroquine and bafilomycin A mimic lysosomal storage disorders and impair mTORC1 signalling. *Biosci Rep*. 2020;40(4):BSR20200905. doi:10.1042/BSR20200905
91. Mauvezin C, Nagy P, Juhász G, Neufeld TP. Autophagosome-lysosome fusion is independent of V-ATPase-mediated acidification. *Nat Commun*. 2015;6(1):7007. doi:10.1038/ncomms8007
92. Lamming DW. Inhibition of the mechanistic target of rapamycin (mTOR): Rapamycin and beyond. *Cold Spring Harb Perspect Med*. 2016;6(5):a025924. doi:10.1101/cshperspect.a025924
93. Lamming DW, Ye L, Katajisto P, et al. Rapamycin-induced insulin resistance is mediated by mTORC2 loss and uncoupled from longevity. *Science*. 2012;335(6076):1638–1643. doi:10.1126/science.1215135
94. Blagosklonny MV. Rapamycin for longevity: Opinion article. *Aging (Albany NY)*. 2019;11(19):8048–8067. doi:10.18632/aging.102355
95. Ballou LM, Lin RZ. Rapamycin and mTOR kinase inhibitors. *J Chem Biol*. 2008;1(1–4):27–36. doi:10.1007/s12154-008-0003-5
96. McNamara CR, Degterev A. Small-molecule inhibitors of the PI3K signaling network. *Future Med Chem*. 2011;3(5):549–565. doi:10.4155/fmc.11.12
97. Hotte SJ, Chi KN, Joshua AM, et al. A phase II study of PX-866 in patients with recurrent or metastatic castration-resistant prostate cancer: Canadian cancer trials group study IND205. *Clin Genitourin Cancer*. 2019;17(3):201–208.e1. doi:10.1016/j.clgc.2019.03.005
98. Ronan B, Flamand O, Vescovi L, et al. A highly potent and selective Vps34 inhibitor alters vesicle trafficking and autophagy. *Nat Chem Biol*. 2014;10(12):1013–1019. doi:10.1038/nchembio.1681
99. Pasquier B. SAR405, a PIK3C3/VPS34 inhibitor that prevents autophagy and synergizes with MTOR inhibition in tumor cells. *Autophagy*. 2015;11(4):725–726. doi:10.1080/15548627.2015.1033601
100. Liu J, Xia H, Kim M, et al. Beclin1 controls the levels of p53 by regulating the deubiquitination activity of USP10 and USP13. *Cell*. 2011; 147(1):223–234. doi:10.1016/j.cell.2011.08.037
101. Shao S, Li S, Qin Y, et al. Spautin-1, a novel autophagy inhibitor, enhances imatinib-induced apoptosis in chronic myeloid leukemia. *Int J Oncol*. 2014;44(5):1661–1668. doi:10.3892/ijo.2014.2313
102. Maiuri MC, Criollo A, Tasdemir E, et al. BH3-only proteins and BH3 mimetics induce autophagy by competitively disrupting the interaction between Beclin 1 and Bcl-2/Bcl-XL. *Autophagy*. 2007;3(4):374–376. doi:10.4161/auto.4237
103. Vogler M, Weber K, Dinsdale D, et al. Different forms of cell death induced by putative BCL2 inhibitors. *Cell Death Differ*. 2009;16(7): 1030–1039. doi:10.1038/cdd.2009.48
104. Voss V, Senft C, Lang V, et al. The pan-Bcl-2 inhibitor (-)-gossypol triggers autophagic cell death in malignant glioma. *Mol Cancer Res*. 2010;8(7):1002–1016. doi:10.1158/1541-7786.MCR-09-0562
105. Broecker-Preuss M, Becher-Boveleth N, Müller S, Mann K. The BH3 mimetic drug ABT-737 induces apoptosis and acts synergistically with chemotherapeutic drugs in thyroid carcinoma cells. *Cancer Cell Int*. 2016;16(1):27. doi:10.1186/s12935-016-0303-8

The influence of comorbidities on mortality in bronchiectasis: A prospective, observational study

Adam Nowiński[A–F], Katarzyna Stachyra[A–F], Maria Szybińska[A–F], Michał Bednarek[A–F], Robert Pływaczewski[A–F], Paweł Śliwiński[A–F]

2nd Department of Respiratory Medicine, Institute of Tuberculosis and Lung Diseases, Warszawa, Poland

A – research concept and design; B – collection and/or assembly of data; C – data analysis and interpretation; D – writing the article; E – critical revision of the article; F – final approval of the article

Advances in Clinical and Experimental Medicine, ISSN 1899–5276 (print), ISSN 2451–2680 (online) *Adv Clin Exp Med*. 2021;30(12):1315–1321

Address for correspondence
Adam Nowiński
E-mail: a.nowinski@igichp.edu.pl

Funding sources
None declared

Conflict of interest
None declared

Received on August 25, 2021
Reviewed on October 18, 2021
Accepted on November 23, 2021

Published online on December 17, 2021

Abstract

Background. Bronchiectasis is a progressive chronic disease associated with an increased risk of mortality.

Objectives. To identify the prevalence of comorbidities in patients with bronchiectasis and the impact of these comorbidities on mortality.

Materials and methods. A cohort of 93 patients with computed tomography (CT)-confirmed bronchiectasis admitted consecutively to a tertiary teaching hospital was observed over a period of 5 years. All patients were carefully observed for comorbidities and mortality.

Results. A total of 43 men (46.2%) and 50 women (53.8%) with a median age of 66.0 years (interquartile range (IQR) 59.7–74.0 years), and a median of 3 comorbidities at baseline (IQR 1–5) were observed. The mortality rate during the observation period was 16%. The median number of comorbidities was significantly higher in the group of non-survivors (5 (IQR 3–5.75)) compared with survivors (3 (IQR 1–4); $p = 0.0100$). The burden of comorbidities was associated with an increased hazard of death: having 4 or more comorbidities was associated with an increased risk of death compared to patients with 2 or 3 coexisting illnesses (hazard ratio (HR) = 1.35 (95% confidence interval (95% CI) [0.41, 4.41]); $p = 0.0494$). The Bronchiectasis Aetiology Comorbidity Index (BACI) was a significant predictor of death in patients with severe bronchiectasis.

Conclusions. We found a significant number of comorbidities in patients with bronchiectasis. In these patients, the comorbidity burden has an impact on mortality. The BACI is a useful tool for the clinical assessment of patients with severe bronchiectasis.

Key words: survival, bronchiectasis, comorbidities, mortality

Cite as
Nowiński A, Stachyra K, Szybińska M, Bednarek M, Pływaczewski R, Śliwiński P. The influence of comorbidities on mortality in bronchiectasis: A prospective, observational study. *Adv Clin Exp Med*. 2021;30(12):1315–1321. doi:10.17219/acem/144200

DOI
10.17219/acem/144200

Background

Bronchiectasis is a progressive chronic disease associated with an increased risk of mortality. In recent years, several prospective studies assessing the survival of patients with non-cystic fibrosis (CF) bronchiectasis have been conducted. A Turkish study found a 16.3% mortality rate during 4 years of follow-up.[1] In the UK, the mortality rate was 29.7% during 13 years of follow-up,[2] and a single-center study in Belgium found a mortality rate of 20.4% after 5.18 years of follow-up.[3]

Subsequently, multicenter studies assessing factors affecting mortality allowed for the preparation of complex tools that help in estimating the risk of death. The FACED (FEV1, age, *Psedomonas aeruginosa* colonisation, radiological extension, and dyspnoea) score[4] and the Bronchiectasis Severity Index (BSI)[5] were thus generated, and they have proven to be clinically helpful in assessing the individual risk of death. Recently, the attention has also been directed to the impact of another factor that significantly affects the prognosis of bronchiectasis patients: comorbidities. The occurrence of cardiovascular disease (CVD),[6] infections or kidney diseases,[7] and rheumatological diseases[8] increase the mortality of patients with bronchiectasis.

The multiple comorbidities that are frequent in bronchiectasis patients and can negatively affect survival, prompted McDonnell et al. to develop the Bronchiectasis Aetiology Comorbidity Index (BACI), a new tool prepared to assess the individual risk of mortality.[9]

However, studies assessing the impact of comorbidities on the mortality of bronchiectasis patients are still scarce. Further research is needed, particularly regarding the validation of existing clinical prediction scores in independent prospective studies.

Objectives

In this observational study, our aim was to identify the prevalence of comorbidities in patients with bronchiectasis and the impact of these comorbidities on mortality.

Materials and methods

This study was performed in the tertiary teaching hospital. We designed an observational, prospective study involving a Polish center specialized in the treatment of patients with non-CF bronchiectasis. During the five-year study (2015–2019), 100 consecutive patients aged ≥18 years with a confirmed diagnosis of non-CF bronchiectasis were enrolled.

Before being included in the study, all study participants signed a consent to participate in the study. The study protocol was reviewed and approved by the research ethics committee of the Institute of Tuberculosis and Lung Diseases in Warszawa, Poland. All procedures involving human participants and the written consent submitted by participants followed the scientific ethical standards of the 1964 Declaration of Helsinki and its later amendments.

All patients were assessed according to the current guidelines of the British Thoracic Society (BTS) and the European Respiratory Society (ERS). The diagnosis of bronchiectasis was based on high-resolution computed tomography (HRCT) scans performed prior to the study.[10] Patients with CF were not included. All participants were carefully examined for comorbidities. Comorbidity was defined as a disease coexisting with the primary disease of interest, as suggested by Sin et al.[11] Diagnoses were made by a group of respiratory and internal medicine specialists and were established following the current relevant international guidelines. Diseases that resolved completely during the hospital stay were excluded from the assessment. The list of diagnoses for each patient, including comorbidities, was recorded in an electronic database.

The diseases were counted and grouped into typical comorbidity groups, as proposed by Charlson et al. investigating comorbidities in respiratory medicine.[12]

The BACI was calculated as proposed by McDonnell et al.[9] For the assessment of comorbidities, all physicians were free to review the patients' medical files and to order any additional tests, including radiology and biochemistry tests.

Statistical analyses

Results are expressed as a median quartile range, as numbers, and as relative frequency (n, %). Dichotomous variables were compared using the χ^2 test. The Kolmogorov–Smirnov test was used to check the normality of variable distribution. As the presented data did not meet the assumptions for the parametric tests, the Mann–Whitney U test was used to test the differences between the dichotomous groups, and the Kruskal–Wallis test was used to compare more than 2 groups. Survival analysis was performed with the Kaplan–Meier estimate. The log-rank test with post hoc Bonferroni correction was used for comparisons of the survival curves. Results were considered to be statistically significant at $p < 0.05$. The Strengthening The Reporting of OBservational Studies in Epidemiology (STROBE) recommendations for observational studies were followed during protocol preparation.[13] All statistical calculations were performed with MedCalc software v. 19.1.6 (MedCalc, Ostend, Belgium).

Results

Characteristics of the group and comorbidities

Initially, 100 unselected consecutive patients with confirmed non-CF bronchiectasis were enrolled in the study.

From this group, 7 patients were excluded due to a lack of proper written consent, being lost to follow-up, or due to the withdrawal of consent during the observation period. Mortality was evaluated in the remaining patients at the end of the five-year follow-up period. The final assessment included a group of 93 patients: 43 men (46.2%) and 50 women (53.8%) with a median age of 66.0 (59.7–74.0) years.

Table 1. Characteristics of the study group. The data are reported as median with interquartile range (IQR) or number with prevalence

Demographics	Cohort (n = 93)
Age [years]	66.0 (59.7–74.0)
Female sex, n (%)	50 (53.8)
BMI [kg/m^2]	25.9 (21.9–29.6)
Ex-smokers, n (%)	47 (50.5)
Current smokers, n (%)	15 (16.1)
Never smokers, n (%)	31 (33.3)
Etiology	
ABPA, n (%)	1 (1.1)
Alpha1 antitrypsin deficiency, n (%)	1 (1.1)
Asthma, n (%)	2 (2.2)
COPD, n (%)	6 (6.5)
Idiopathic, n (%)	56 (60.2)
IgG subclass deficiency, n (%)	1 (1.1)
Mounier–Kuhn syndrome, n (%)	1 (1.1)
Nontuberculous mycobacteria, n (%)	2 (2.2)
Postinfective, n (%)	11 (11.8)
Post-tuberculous, n (%)	9 (9.7)
Primary ciliary dyskinesia, n (%)	1 (1.1)
Yellow nail syndrome, n (%)	2 (2.2)
BSI score risk class	
Mild, n (%)	28 (30.1)
Moderate, n (%)	28 (30.1)
Severe, n (%)	37 (39.8)
Clinical status	
Sputum volume [mL/day]	10 (10–20)
MRC dyspnea score [points]	2 (1–2)
Exacerbations not requiring secondary care in the previous year, n	1 (0–2)
At least 1 hospitalization in the previous year, n (%)	46 (49.5)
Functional status	
FEV_1, % predicted	79.8 (53.7–98.6)
Microbiology	
P. aeruginosa infection, n (%)	12 (12.9)
Comorbidity burden	
Number of comorbidities at baseline, n	3 (1–5)
Number of comorbidities range, n	0–8

BMI – body mass index; COPD – chronic obstructive pulmonary disease; TB – tuberculosis; ABPA – allergic bronchopulmonary aspergillosis; BSI – bronchiectasis severity index; MRC – Medical Research Council; FEV_1 – forced expiratory volume in 1 s; *P. aeruginosa* – *Pseudomonas aeruginosa*; IgG – immunoglobulin G.

Table 2. Most prevalent comorbidities in the study group

Comorbidity	Number of patients	Prevalence (%)
Cardiovascular diseases	61	65.5
COPD	48	51.6
Hypertension	32	34.4
Asthma	25	26.9
Obesity	22	23.6
Coronary heart disease	18	19.4
Diabetes	16	17.2
Cancer/neoplasm	12	12.9
Congestive heart failure	12	12.9
Chronic respiratory failure	11	11.8
Osteoporosis	9	9.7
Tuberculosis in anamnesis	9	9.7
Chronic atrial fibrillation	8	8.6
Pulmonary hypertension	7	7.5
Anxiety/depression	7	7.5
Anemia	5	5.4
Chronic renal disease	4	4.3
Liver cirrhosis	3	3.2
Other arrhythmia	2	2.2
Aortic aneurysm	1	1.1
Sarcoidosis	1	1.1

COPD – chronic obstructive pulmonary disease.

The anthropometric data and comorbidities of the patients are shown in Table 1 and Table 2, respectively.

The group consisted predominantly of middle-aged Caucasians with a median forced expiratory volume in 1 s (FEV_1%) predicted of 79.8% (53.7–98.6%). The 3 BSI groups were evenly represented: 28 (30.1%) patients displayed mild bronchiectasis, 28 (30.1%) had moderate symptoms and 37 patients (39.8%) had severe symptoms. Bronchiectasis was considered idiopathic in most of the patients (60.2%), but it was classified as post-tuberculosis bronchiectasis in 9.7% of patients. Other, less common causes of bronchiectasis were identified in the remaining patients.

Half of the patients required hospital treatment in the previous year. Twelve patients (12.9%) were chronically colonized with *Pseudomonas aeruginosa*. The median number of comorbidities at baseline in the whole group was 3 (interquartile range (IQR) 1–5).

Mortality

The total observation period in our group was 50 months, but because patients were enrolled consecutively in the study, the median follow-up period for the whole group was 31.0 (IQR 18.5–42.0) months. During the observation period, 15 patients died (16.1%). The median survival period in non-survivors was 14.0 (IQR 5.2–23.0) months, with a range of 2.0–46.0 months. The median follow-up

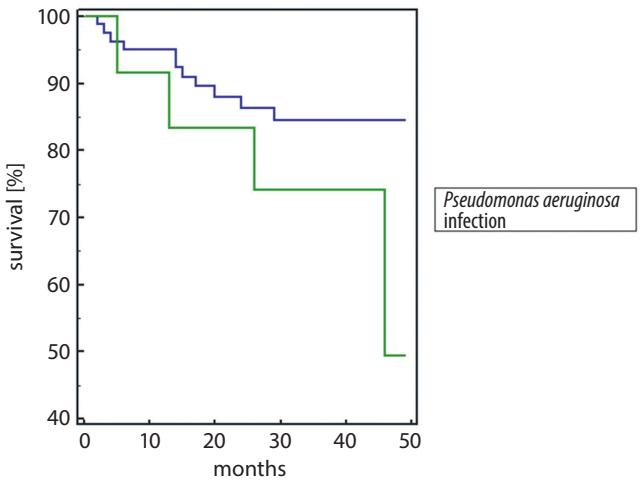

Fig. 1. Kaplan–Meier survival curves demonstrating the survival of patients with non-cystic fibrosis bronchiectasis, with and without *Pseudomonas aeruginosa* infection

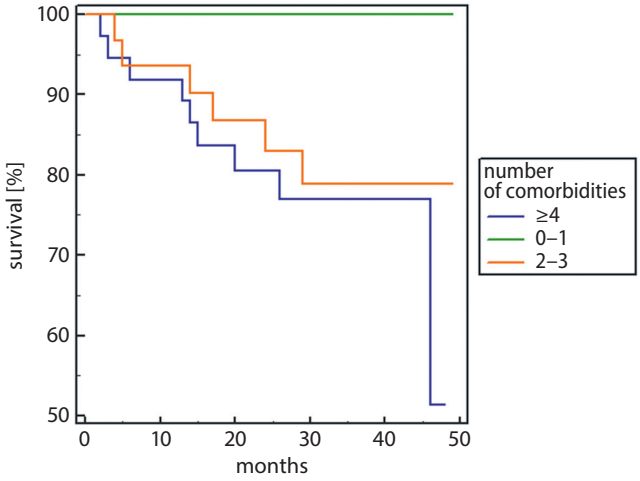

Fig. 2. Kaplan–Meier survival curve showing the survival rates of bronchiectasis patients with different number of comorbidities

for the survivors was 33.0 (IQR 23.0–43.0) months, with a range of 2.0–49.0 months.

The Kaplan–Meier survival curves for the whole group are shown in Fig. 1. The survival curves of patients colonized with *P. aeruginosa* and those not colonized are shown separately because the colonization by *P. aeruginosa* is known to affect the survival.

The number of patients who tested positive for *P. aeruginosa* was small (n = 12, 12.9%), and the comparison of survival curves between infected and non-infected patients showed that the difference was not statistically significant (p = 0.1586, log-rank test, χ^2 = 1.9878). The hazard ratio (HR) for death in the group with *P. aeruginosa* infection was 2.86 (95% confidence interval (95% CI) [0.66, 12.35]) when compared with the group without *P. aeruginosa* infections.

The median number of comorbidities was significantly higher in the group of non-survivors (5 (IQR 3–5.75)) than in the group of survivors (3 (IQR 1–4); p = 0.0100, Mann–Whitney U test, U = 341.5).

Although the total number of deaths was relatively low, and therefore comparisons are difficult, the burden of comorbidities was associated with an increased hazard of death. Having 4 or more comorbidities was associated with an increased risk of death (HR = 1.35 (95% CI [0.41, 4.41])) compared with patients with 2 or 3 coexisting illnesses (p = 0.0494; for HR test, Fig. 2).

BSI and BACI scores

The comparison of the patients' survival curves, grouped according to the BSI score risk classes did not show statistically significant differences between the groups (p = 0.9682, log-rank test, χ^2 = 0.0645). During the observation period, 15 patients died. In this group of non-survivors, 4 patients had a BSI score in the range of 0–4 points, 4 patients in the range of 5–8 points and 7 patients had a score over 9 points. The death HR for patients with a BSI score in the range of 0–4 points was similar to that of patients with a BSI score of more than 9 points (HR = 1.16 (95% CI [0.34, 3.91]); p = 0.9176; for HR test (Fig. 3)).

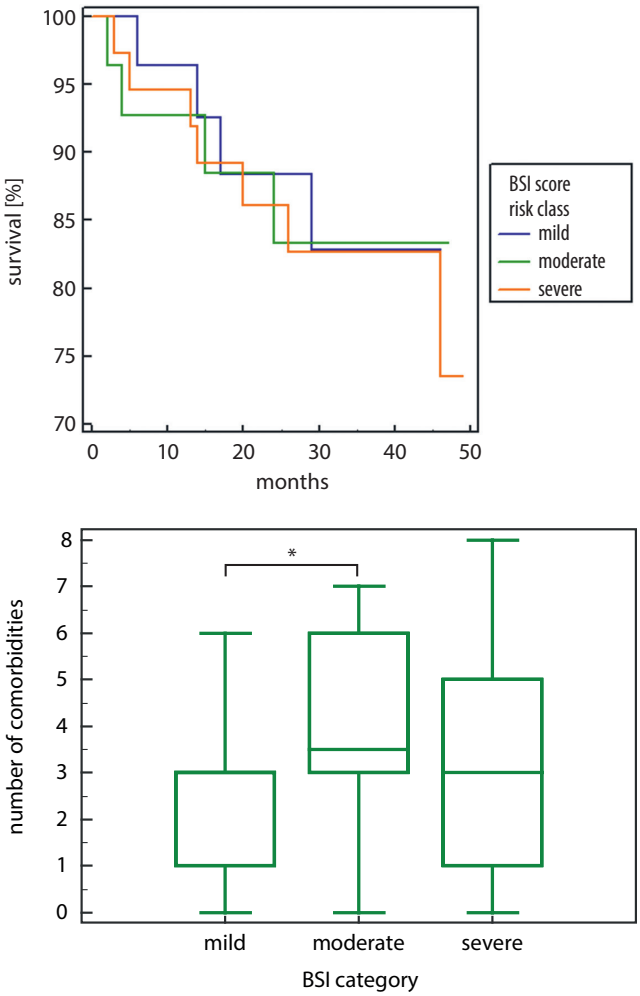

Fig. 3. A. Kaplan–Meier survival curves showing the probability of survival in bronchiectasis patients grouped according to the Bronchiectasis Severity Index (BSI) risk classes; B. The number of comorbidities against the Bronchiectasis Severity Index (BSI) risk classes. The asterisk indicates a statistically significant difference between the groups joined by the line

A significant, although moderate relationship was observed between the median number of comorbidities and the BSI score. Patients with a BSI score in the "moderate" category had a statistically significantly higher number of comorbidities than patients with a BSI score in the "mild" category (p = 0.0367, Kruskal–Wallis test) (Fig. 3, Supplementary Table 1).

The BACI index classes were analyzed across the survival data. While a high risk BACI score suggested an increased risk of death, this parameter did not reach statistical significance while considering the whole study group (HR = 1.69 (95% CI [0.24, 11.62]); p = 0.4352 for HR test). However, when the analysis of the BACI index classes was conducted in the group of patients with the most severe bronchiectasis symptoms (BSI severe class), the BACI was found to be a significant predictor of death (HR = 7.5 (95% CI [1.57, 36.29]); p = 0.0433 for HR test) (Fig. 4).

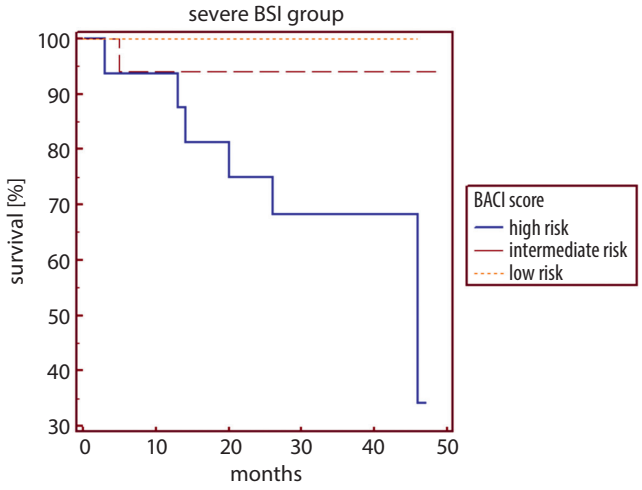

Fig. 4. Kaplan–Meier survival curve showing patient survival against the Bronchiectasis Aetiology Comorbidity Index (BACI) risk classes in the group of patients with severe Bronchiectasis Severity Index (BSI)

Discussion

The 1st and main finding from this single-center longitudinal prospective study was the impact of the comorbidity burden on mortality in non-CF bronchiectasis. The 2nd finding was the usefulness of the BACI in the prognosis assessment of bronchiectasis patients, which agrees with the previous observations from a multicenter trial.[9] The 3rd finding was the usefulness of a simple counting of comorbidities in the prediction of the five-year mortality risk in bronchiectasis patients.

Mortality in bronchiectasis

In our study, we found a 16% mortality rate over a 50-month follow-up period. These results are consistent with other studies. Onen at al. found that 16.3% of patients died during an observation period of 44.6 months. The survival rates they observed at 1, 2, 3, and 4 years were 97%, 89%, 76%, and 58%, respectively.[1] Loebinger et al. reported survival rates of 91% at 4 years, 83.5% at 8.8 years and 68.3% at 12.3 years.[2]

In a multicenter study by Chalmers et al., there were 62 deaths in over 4 years (10.2%) in a cohort of 608 patients. In another multicenter study, the overall mortality after 1, 2, 3, and 5 years of follow-up was 3.7%, 4.8%, 8.6%, and 12.4%, respectively.[5]

Our study was a single-center observational study. Therefore, before assessing our results in the context of mortality, we should evaluate whether our study group is similar to other described groups. Our group of patients is comparable to the abovementioned cohorts in terms of age, sex distribution, the etiology of bronchiectasis, and the functional respiratory parameters, such as FEV_1% predicted. Numerous observational studies have reported that colonization with *P. aeruginosa* significantly affects the prognosis of bronchiectasis patients by increasing the mortality rate.[9,14] In our study, 12.9% of patients were colonized with *P. aeruginosa*, which is a slightly smaller percentage compared to other analyzed cohorts. For example, Chalmers et al. and Pasteur et al. reported a 20–40% prevalence of *P. aeruginosa* in UK cohorts.[5,15] We observed a possible effect of colonization by *P. aeruginosa*. However, the difference in survival rates between the colonized and non-colonized groups was not statistically significant. One reason for this could be the small size of the study group. Another possible explanation is the low percentage of colonized patients in our group, which could be due to geographical differences in the distribution of the microorganism.[16]

The number and type of comorbidities

We found a significant number of comorbidities in the study group, with a significantly higher number in the group of non-survivors than in the group of survivors. This observation is consistent with the study by McDonnell et al.,[9] who reported that even a simple count of the number of comorbidities has some importance in estimating the risk of death in bronchiectasis patients. Moreover, we found that the risk of death increased significantly with the number of comorbidities: patients with 4 or more comorbidities had a 35% higher risk of death than patients with 2 or 3 comorbidities.

The number and type of comorbidities in our group of patients is consistent with those described by other research groups. The most frequent comorbidity in our patients was the CVD. It occurred in 65% of patients, which is similar to the previous observations by other research groups.[17,18] By analogy with chronic obstructive pulmonary disease (COPD), another important bronchial disease, the chronic inflammation in bronchiectasis could result in an increased risk of the CVD through the "spillover" of inflammatory factors from the bronchial tree into the bloodstream.[19]

In our study, a significant percentage of patients with bronchiectasis were also diagnosed with COPD (51.6%).

There is an ongoing discussion regarding the relationship between COPD and bronchiectasis,[20,21] and statistical analyses sometimes give divergent results. In our study, the reason for the frequent coexistence of bronchiectasis and COPD may be local Polish conditions, which are linked to the socioeconomic factors. In Poland, diagnosing COPD allows doctors to prescribe cheaper drugs with better reimbursement for patients, thereby prompting doctors to diagnose COPD more often in patients with bronchiectasis.

The incidence of other comorbidities does not differ significantly from the observations of other researchers, both in retrospective and prospective studies.[5,9]

Outcome prediction tools – BSI and BACI

We did not find any statistically significant relationship between the severity of bronchiectasis assessed with the BSI and an increased risk of death. Others have reported the BSI to be a good parameter to estimate the risk of death in bronchiectasis patients, but the analysis of the Kaplan–Meier curves in our study did not confirm these results. This may be due to the small size of our study group and the relatively low number of deaths we observed. It may also be a confirmation of the important role that comorbidities play in the increasing the risk of death in bronchiectasis patients. This observation seems to be confirmed by the BACI scale analysis.

Despite our small group size, we found that patients with severe bronchiectasis and high BACI classes had an increased risk of death compared to the patients with a severe BSI assessment but a lower number and severity of comorbidities. In our opinion, this confirms the usefulness of the BACI in the clinical assessment of patients with bronchiectasis.

Limitations

This study was not designed as an epidemiological study. Therefore, the overall results of bronchiectasis mortality in our group should be assessed in the context of the study setting. Nevertheless, bronchiectasis requires a multidimensional assessment; coexisting illnesses should be carefully treated in all affected patients. New tools, such as the BSI, FACED and BACI, may prove useful for the clinical assessment of bronchiectasis patients.

Conclusions

We found a significant number of comorbidities in patients with bronchiectasis. The comorbidity burden has an impact on mortality in patients with bronchiectasis. The Bronchiectasis Aetiology Comorbidity Index (BACI) is a useful tool for the clinical assessment of patients with severe bronchiectasis.

Supplementary Table 1. Number of comorbidities against severity of bronchiectasis expressed in Bronchiectasis Severity Index (BSI) results (mild, moderate, severe)

A. Kruskal–Wallis test

Data	Number of comorbidities
Factor codes	BSI categories
Sample size	93

B. Descriptive statistics

BSI category	n	Minimum	25th percentile	Median	75th percentile	Maximum
Mild	28	0.0000	1.000	3.000	3.000	6.000
Moderate	28	0.0000	3.000	3.500	6.000	7.000
Severe	37	0.0000	1.000	3.000	5.000	8.000

C. Kruskal–Wallis test

Test statistic	6.4395
Corrected for ties	6.6088
Degrees of freedom (df)	2
Significance level	p = 0.036720

D. Post hoc analysis (Conover)

BSI category	n	Average rank	Different (p < 0.05) from factor No.
Mild	28	37.93	(2)
Moderate	28	56.23	(1)
Severe	37	46.88	–

Supplementary Table 2. Comorbidities summary statistics in the whole group

A. Comorbidities summary

Variable	Comorbidities, n
Sample size	93
Lowest value	0.0000
Highest value	8.0000
Arithmetic mean	3.2043
95% confidence interval (95% CI) for the arithmetic mean	[2.7764, 3.6322]
Median	3.0000
95% CI for the median	[3.0000, 3.0000]
Variance	4.3165
Standard deviation (SD)	2.0776
Relative standard deviation	0.6484 (64.84%)
Standard error of the mean (SEM)	0.2154
Coefficient of skewness	0.2710 (p = 0.2685)
Coefficient of kurtosis	–0.7375 (p = 0.0348)
Kolmogorov–Smirnov test[a] for normal distribution	D = 0.1521 reject normality (p < 0.0001)

[a] Lilliefors significance correction.

B. Distribution of the number of comorbidities

Percentiles	Median number of comorbidities	95% confidence interval (95% CI)
2.5	0.0000	–
5	0.0000	[0.0000, 0.6356]
10	0.8000	[0.0000, 1.0000]
25	1.0000	[1.0000, 2.0000]
75	5.0000	[4.0000, 6.0000]
90	6.0000	[6.0000, 7.0000]
95	6.8500	[6.0000, 8.0000]
97.5	7.1750	–

ORCID iDs

Adam Nowiński https://orcid.org/0000-0002-2910-129X
Katarzyna Stachyra https://orcid.org/0000-0003-1530-8502
Maria Szybińska https://orcid.org/0000-0002-5850-8419
Michał Bednarek https://orcid.org/0000-0002-6761-5830
Robert Pływaczewski https://orcid.org/0000-0003-4429-1041
Paweł Śliwiński https://orcid.org/0000-0002-1195-784X

References

1. Onen ZP, Gulbay BE, Sen E, et al. Analysis of the factors related to mortality in patients with bronchiectasis. *Respir Med*. 2007;101(7):1390–1397. doi:10.1016/j.rmed.2007.02.002
2. Loebinger MR, Wells AU, Hansell DM, et al. Mortality in bronchiectasis: A long-term study assessing the factors influencing survival. *Eur Respir J*. 2009;34(4):843–849. doi:10.1183/09031936.00003709
3. Goeminne PC, Nawrot TS, Ruttens D, Seys S, Dupont LJ. Mortality in non-cystic fibrosis bronchiectasis: A prospective cohort analysis. *Respir Med*. 2014;108(2):287–296. doi:10.1016/j.rmed.2013.12.015
4. Martínez-García MA, De Gracia J, Relat MV, et al. Multidimensional approach to non-cystic fibrosis bronchiectasis: The FACED score. *Eur Respir J*. 2014;43(5):1357–1367. doi:10.1183/09031936.00026313
5. Chalmers JD, Goeminne P, Aliberti S, et al. The bronchiectasis severity index: An international derivation and validation study. *Am J Respir Crit Care Med*. 2014;189(5):576–585. doi:10.1164/rccm.201309-1575OC
6. Gale NS, Bolton CE, Duckers JM, Enright S, Cockcroft JR, Shale DJ. Systemic comorbidities in bronchiectasis. *Chron Respir Dis*. 2012;9(4):231–238. doi:10.1177/1479972312459973
7. Dury S, Colosio C, Etienne I, et al. Bronchiectasis diagnosed after renal transplantation: A retrospective multicenter study. *BMC Pulm Med*. 2015;15(1):141. doi:10.1186/s12890-015-0133-9
8. Puéchal X, Génin E, Bienvenu T, Le Jeunne C, Dusser DJ. Poor survival in rheumatoid arthritis associated with bronchiectasis: A family-based cohort study. *PLoS One*. 2014;9(10):e110066. doi:10.1371/journal.pone.0110066
9. McDonnell MJ, Aliberti S, Goeminne PC, et al. Comorbidities and the risk of mortality in patients with bronchiectasis: An international multicentre cohort study. *Lancet Respir Med*. 2016;4(12):969–979. doi:10.1016/S2213-2600(16)30320-4
10. Pasteur MC, Bilton D, Hill AT; British Thoracic Society Bronchiectasis non-CF Guideline Group. British Thoracic Society guideline for non-CF bronchiectasis. *Thorax*. 2010;65(Suppl 1):i1–i58. doi:10.1136/thx.2010.136119
11. Sin DD, Anthonisen NR, Soriano JB, Agusti AG. Mortality in COPD: Role of comorbidities. *Eur Respir J*. 2006;28(6):1245–1257. doi:10.1183/09031936.00133805
12. Charlson ME, Pompei P, Ales KL, MacKenzie CR. A new method of classifying prognostic comorbidity in longitudinal studies: Development and validation. *J Chronic Dis*. 1987;40(5):373–383. doi:10.1016/0021-9681(87)90171-8
13. von Elm E, Altman DG, Egger M, Pocock SJ, Gøtzsche PC, Vandenbroucke JP. The Strengthening the Reporting of Observational Studies in Epidemiology (STROBE) statement: Guidelines for reporting observational studies. *Lancet*. 2007;370(9596):1453–1457. doi:10.1016/S0140-6736(07)61602-X
14. Finch S, McDonnell MJ, Abo-Leyah H, Aliberti S, Chalmers JD. A comprehensive analysis of the impact of *Pseudomonas aeruginosa* colonization on prognosis in adult bronchiectasis. *Ann Am Thorac Soc*. 2015;12(11):1602–1611. doi:10.1513/AnnalsATS.201506-333OC
15. Pasteur MC, Helliwell SM, Houghton SJ, et al. An investigation into causative factors in patients with bronchiectasis. *Am J Respir Crit Care Med*. 2000;162(4 Pt 1):1277–1284. doi:10.1164/ajrccm.162.4.9906120
16. De Soyza A, Perry A, Hall AJ, et al. Molecular epidemiological analysis suggests cross-infection with *Pseudomonas aeruginosa* is rare in non-cystic fibrosis bronchiectasis. *Eur Respir J*. 2014;43(3):900–903. doi:10.1183/09031936.00167813
17. Huang HY, Chung FT, Lo CY, et al. Etiology and characteristics of patients with bronchiectasis in Taiwan: A cohort study from 2002 to 2016. *BMC Pulm Med*. 2020;20(1):45. doi:10.1186/s12890-020-1080-7
18. Du Q, Jin J, Liu X, Sun Y. Bronchiectasis as a comorbidity of chronic obstructive pulmonary disease: A systematic review and meta-analysis. *PLoS One*. 2016;11(3):e0150532. doi:10.1371/journal.pone.0150532
19. Barnes PJ, Celli BR. Systemic manifestations and comorbidities of COPD. *Eur Respir J*. 2009;33(5):1165–1185. doi:10.1183/09031936.00128008
20. Martinez-Garcia MA, Miravitlles M. Bronchiectasis in COPD patients: More than a comorbidity? *Int J Chron Obstruct Pulmon Dis*. 2017;12:1401–1411. doi:10.2147/COPD.S132961
21. Nowiński A, Korzybski D, Bednarek M, Geremek AG, Puścińska E, Śliwiński P. Does bronchiectasis affect chronic obstructive pulmonary disease comorbidities? *Adv Respir Med*. 2019;87(6):214–220. doi:10.5603/ARM.2019.0059

ST-segment depression in atrioventricular nodal reentrant tachycardia: Preliminary results

Jakub Szymon Mercik[1,A–F], Jadwiga Radziejewska[2,A–F], Katarzyna Pach[3,A–F], Dorota Zyśko[1,A–F], Jacek Gajek[4,A–F]

[1] Department of Emergency Medicine, Wroclaw Medical University, Poland
[2] Klodzko County Hospital, Poland
[3] Students' Scientific Association, Department of Emergency Medical Service, Wroclaw Medical University, Poland
[4] Department of Emergency Medical Service, Wroclaw Medical University, Poland

A – research concept and design; B – collection and/or assembly of data; C – data analysis and interpretation; D – writing the article; E – critical revision of the article; F – final approval of the article

Advances in Clinical and Experimental Medicine, ISSN 1899–5276 (print), ISSN 2451–2680 (online) *Adv Clin Exp Med*. 2021;30(12):1323–1328

Address for correspondence
Jakub Mercik
E-mail: jakub.mercik@wp.pl

Funding sources
This research was financially supported by the Ministry of Health subvention (No. STM.A280.20.107 from the IT Simple system of Wroclaw Medical University).

Conflict of interest
None declared

Received on November 9, 2020
Reviewed on November 26, 2020
Accepted on November 22, 2021

Published online on December 13, 2021

Abstract

Background. The ST-segment is part of the electrocardiogram and physiologically, it forms an isoelectric line. The ST-segment depression is often observed in young, healthy people with paroxysmal tachycardia with narrow QRS complexes. In this group of patients, the 'mysterious tachycardia-induced ST-segment depression', 'subendocardial myocardial ischemia' and other not fully understood terms are used to explain this phenomenon.

Objectives. To assess the presence and possible mechanisms of ST-segment depression during atrioventricular nodal reentrant tachycardia (AVNRT) in patients undergoing radiofrequency (RF) ablation of the underlying arrhythmia.

Materials and methods. The study included 50 patients (35 women and 15 men) aged about 49 years with clinically relevant paroxysmal narrow QRS complex tachycardia. During electrophysiological study (EPS), all patients had measured QRS components – QR, RS and RJ during the tachycardia and during the sinus rhythm. All of the measurements were done in lead V5.

Results. There was a statistically significant difference in cycle length during sinus rhythm and tachycardia (707.0 ±137.8 ms compared to 327.5 ±29.1 ms, $p = 0.000$), the RJ component (0.819 ±0.381 mV compared to 0.878 ±0.376 mV, $p = 0.003$) and the difference RJ-QR (0.081 ±0.083 mV compared to 0.163 ±0.108 mV, $p = 0.000$). The differences in RS and QR components during sinus rhythm and tachycardia did not reach the statistical significance. The difference RJ-QR during tachycardia correlated negatively with tachycardia cycle length ($R = -0.39$, $p = 0.0049$). The tachycardia cycle length correlated positively with the age of the studied patients ($R = 0.28$, $p = 0.043$).

Conclusions. In patients with AVNRT, there is a ST-segment depression during the episodes of tachycardia and the degree of this change is related to tachycardia cycle length. The most probable explanation of the ST-segment depression is the overlap of the QRS complex on the preceded T wave. Some intrinsic properties of individual electrocardiogram (ECG) also influence this phenomenon. The ischemic origin of the presented ST-segment change can be excluded.

Key words: tachycardia, AVNRT, ST-segment depression

Cite as
Mercik JS, Radziejewska J, Pach K, Zyśko D, Gajek J. ST-segment depression in atrioventricular nodal reentrant tachycardia: Preliminary results. *Adv Clin Exp Med*. 2021;30(12):1323–1328. doi:10.17219/acem/144161

DOI
10.17219/acem/144161

Background

The ST-segment is a part of the electrocardiogram located between the QRS complex and the T wave. There are 2 types of ST-segment changes. First ones, depending on repolarization, appear in the absence of depolarization changes of the action potential.[1,2] The causes may include ischemia, myocarditis, drugs and electrolyte disturbances.[3,4] The secondary changes of ST-segment are related to the depolarization phase aberrations. They are present in bundle branch blocks, ventricular pre-excitation and ventricular QRS complexes including pacing. The ST-segment changes constitute part of electrocardiogram (ECG) assessment for myocardial ischemia; therefore, it is important to understand causes leading to the incorrect interpretation and diagnosis.[5,6] The ST-segment changes could be observed in people with paroxysmal narrow QRS complex tachycardia, with no overt evidence of an ischemic heart disease.[7–9]

In the atrioventricular nodal reentrant tachycardia (AVNRT), we are concerned with a retrograde P wave, which occurs within the QRS complex. Our hypothesis is that if the tachycardia is rapid enough, the QRS complex follows the preceded T wave, which in turn changes the reference point by raising the isoelectric baseline. An example of such changes is presented in Fig. 1.

Objectives

The purpose of the study was to assess the presence and possible mechanisms of ST-segment depression during AVNRT in patients undergoing radiofrequency (RF) ablation of the underlying arrhythmia.

Materials and methods

The study included 50 patients (35 females and 15 males) approx. 49 years old, presenting with a clinically relevant paroxysmal tachycardia. In all studied individuals, the electrophysiological testing was performed, the diagnosis of AVNRT was established and the arrhythmia was successfully eliminated through RF ablation. The clinical and demographic characteristics, as well as laboratory tests are presented in Table 1.

Table 1. Clinical, demographic and biochemical characteristics of studied patients

Parameters	Mean/number	SD/%
Age [years]	49.1	14.2
Sex (female)	35	70.0
Hypertension	22	44.0
Diabetes mellitus	8	16.0
Heart failure	1	2.0
Ischemic heart disease	2	4.0
Hemoglobin [g/dL]	14.0	1.4
K+ [mmol/L]	4.4	0.4
Glucose [mg/dL]	101.9	16.5
TSH [mIU/L]	1.644	0.918

SD – standard deviation; TSH – thyroid-stimulating hormone.

During electrophysiological study (EPS), the cycle length of the sinus rhythm and tachycardia, as well as the amplitudes of QRS components – QR, RS and RJ during the tachycardia and during the sinus rhythm with a paper speed of 200 mm/s and an enhancement of ×64–128 were measured. The described measurements of the particular QRS components in an exemplary patient with a pronounced ST-segment depression are depicted in Fig. 2.

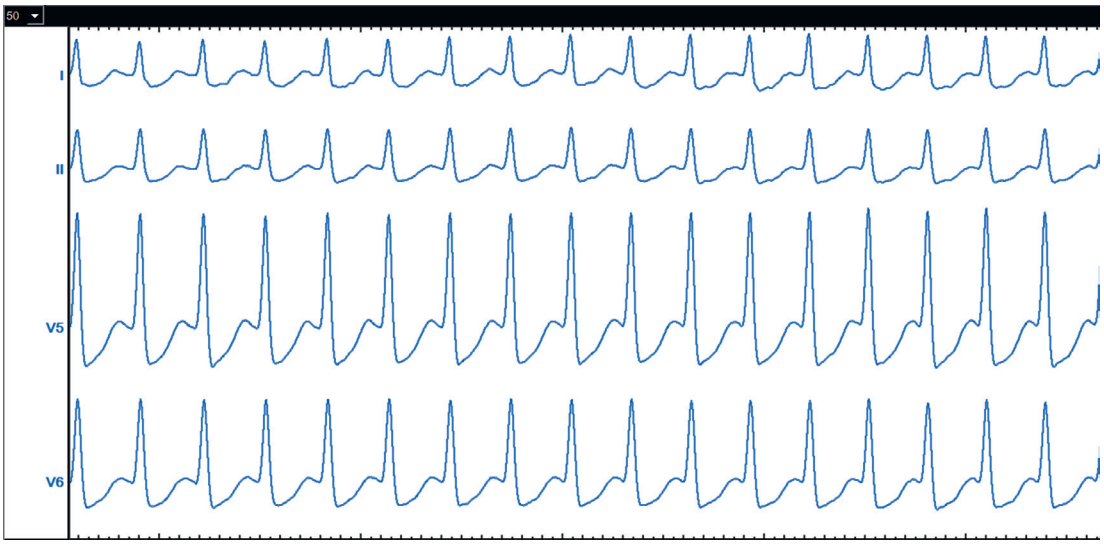

Fig. 1. The example of ST-segment depressions during atrioventricular nodal reentrant tachycardia (AVNRT) in selected electrocardiogram (ECG) leads in 40-year-old male (CL – 279 ms, delta ST in lead V5 – 0.641 mV). Paper speed 50 mm/s

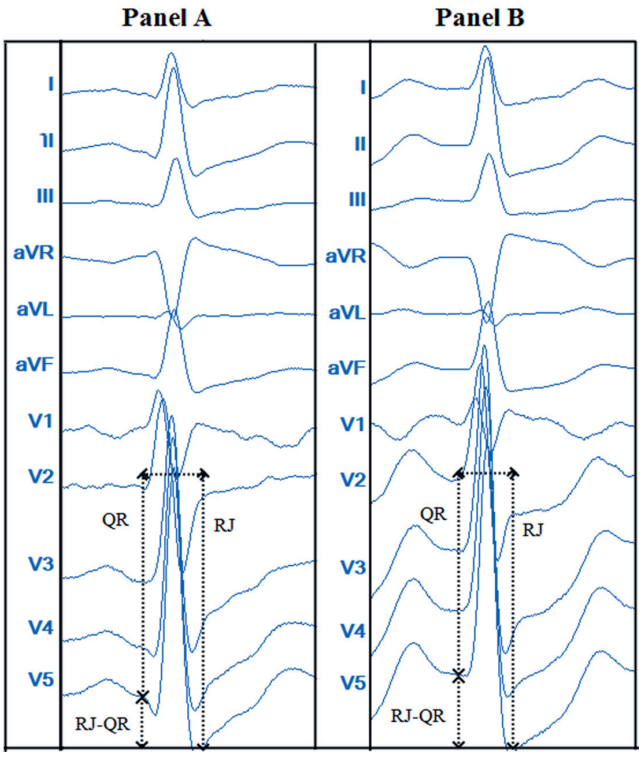

Fig. 2. Measurements of the particular QRS components in an exemplary patient. Panel A: sinus rhythm QR – 1.26 mV, RJ – 1.46 mV, RJ–QR – 0.20 mV; panel B: tachycardia QR – 1.21 mV, RJ – 1.59 mV, RJ–QR – 0.38 mV

Statistical analysis

The statistical analysis was performed using the computer program STATISTICA v. 13.3 (StatSoft Inc., Tulsa, USA). For quantitative variables, basic descriptive statistics were calculated and the compliance of their distributions with the theoretical normal distribution was checked using the Shapiro–Wilk W test. Comparisons were performed with the Wilcoxon signed-rank test for dependent groups. The correlations between the studied parameters were performed using Spearman's rank correlation coefficient. A value of $p < 0.05$ was considered significant.

The study was approved by the local Bioethical Committee at Wroclaw Medical University (approval No. KB 213/2020).

Results

The electrocardiographic measurements in sinus rhythm and tachycardia are presented in Table 2.

The tachycardia-related changes in patients with AVNRT include the elevation of the reference point as indicated by a diminished QR amplitude, as well as by the depression of the J point. This influenced the difference RJ–QR resulting in the ECG ST-segment depression.

The difference RJ–QR during tachycardia negatively correlated with the tachycardia cycle length ($R = -0.39$, $p = 0.0049$). This relationship is depicted in Fig. 3.

Table 2. Electrocardiographic parameters in sinus rhythm and atrioventricular nodal reentrant tachycardia (AVNRT)

Parameters	Sinus rhythm	Tachycardia	p-value
Cycle length [ms]	707.0 ±137.8	327.5 ±29.1	0.000
QR [mV]	0.738 ±0.315	0.715 ±0.289	0.143
RS [mV]	0.982 ±0.385	1.007 ±0.386	0.375
RJ [mV]	0.819 ±0.381	0.878 ±0.376	0.003
RJ–QR [mV]	0.081 ±0.083	0.163 ±0.108	0.000

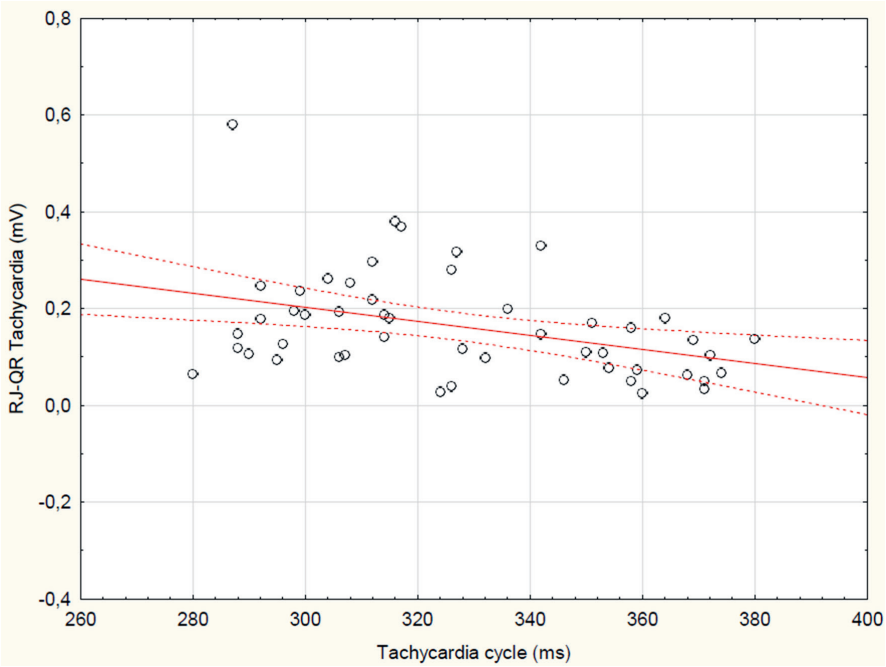

Fig. 3. Negative correlation between the RJ–QR difference during tachycardia and the tachycardia cycle length

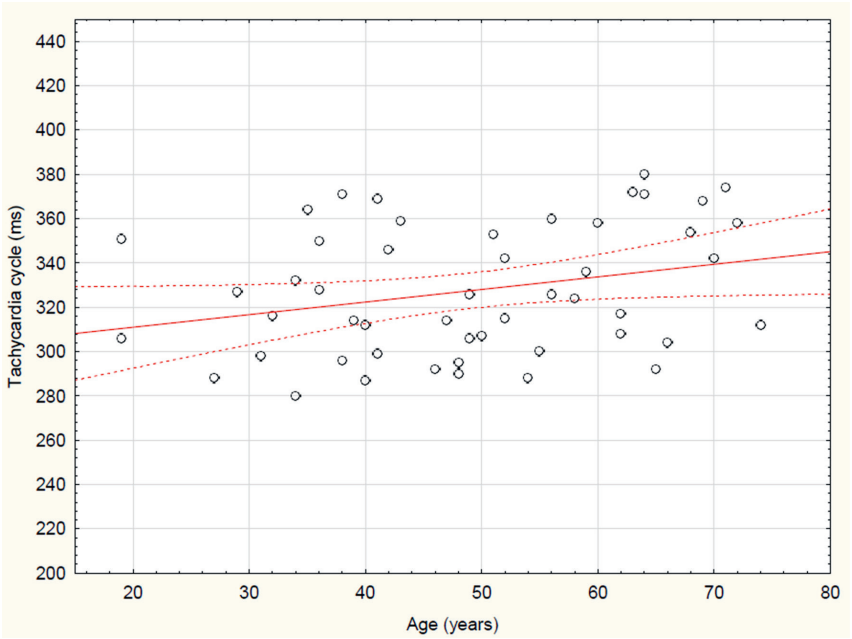

Fig. 4. Positive correlation between the tachycardia cycle length and the age of the studied patients

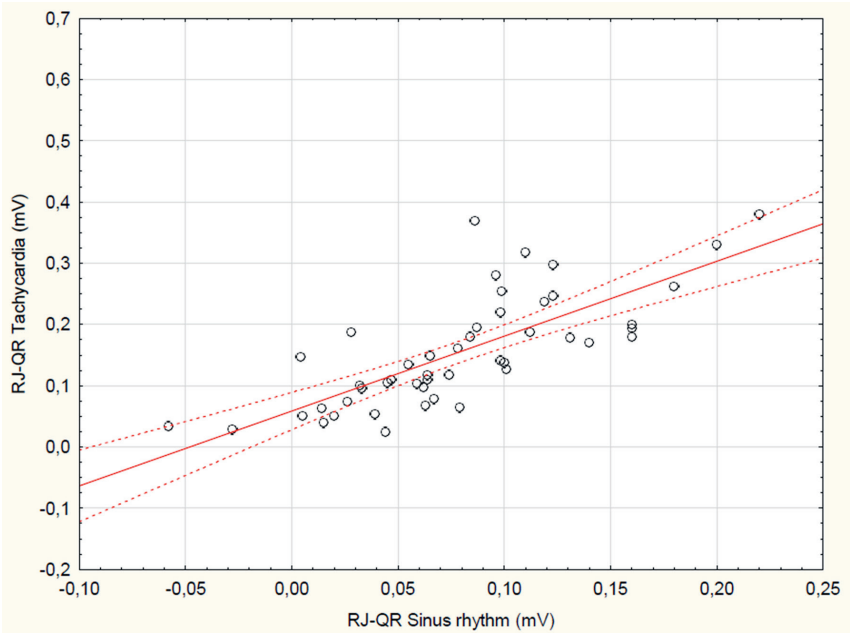

Fig. 5. High positive correlation between RJ–QR in tachycardia and RJ–QR in sinus rhythm

The tachycardia cycle length positively correlated with the age of the studied patients (R = 0.28, p = 0.043), as depicted in Fig. 4.

To examine the individual intrinsic properties of ECG, the correlation between RJ–QR in sinus rhythm and RJ–QR in tachycardia was assessed. Those parameters correlated with each other at high statistical significance (R = 0.8, p = 0.000), as depicted in Fig. 5.

No correlation between the degree of ST-segment changes and the age of the studied subjects was revealed. The gender of the patients did not affect the studied parameters, nor did the laboratory parameters and comorbidities. The age distribution curve of the studied patients was consistent with the Gaussian distribution.

Discussion

In patients with paroxysmal supraventricular tachycardias, the ST-segment depression is a common finding. At first glance, ST-segment depression is an ischemia-related change. Petsas et al. assessed the role and significance of the ST-segment depression in supraventricular tachycardia in terms of the coexistence of a myocardial ischemia, utilizing an exercise test. Fifteen out of 16 subjects with ST-segment depression during supraventricular tachycardia had no changes on tests.[10] In another study, the concentration of troponin I and ST-segment depression were taken as indicators for myocardial damage. Non-invasive examinations (myocardial scintigraphy, exercise

echocardiography and exercise test) and coronary angiography were used for confirmation. The authors concluded that elevated troponin I levels and the ST-segment depression are not significant markers of myocardial damage in patients with paroxysmal tachycardia.[11]

In many studies, the duration of an arrhythmia episode is not associated with an increase in troponins. However, in the case of longer-lasting tachycardia, the instability of the circulation may occur, resulting in troponin release.[12–14]

During the exercise-related sinus tachycardia, there is a gradual QT-interval shortening, which is associated with adrenergic activation. It is not a linear process, but according to the latest research there is a type of hysteresis in which, when accelerating, the heart shortens the QT-interval depending on the heart rate, first slowly, then increasingly faster. After the exertion, the QT-interval lengthens more slowly at first, then it gets faster until it returns to the primary duration. This phenomenon occurs because of the slow responsiveness of QT-interval to changes in the heart rate.[15,16] The patient's gender also constitutes an important aspect that may affect the QT length. It has been proven that women of a given age have a significantly longer corrected QT-interval than men. Additionally, the correlation between the change in the QT-interval and a patient's age was demonstrated. The older the patient is, the shorter the QT-interval gets.[17,18]

The activation of the sympathetic system leads to the acceleration of the heart rate, decrease of the PR interval, the ST-segment depression and, in some cases, to the inversion of the T waves, while the parasympathetic activation slows down the heart rate and elevates the ST-segment.[19] It was also observed in some healthy people. Their baseline ECG was showing slight changes in the ST-segment (<1 mm), often referred to as nonsignificant. This is in line with our results, as the initial J-point depression correlated with depression during tachycardia.

The ST-segment changes could be caused by projection of the retrograde P wave onto the ST-segment, more common in patients with atrioventricular reentrant tachycardia, due to longer ventriculoatrial interval (usually exceeding 100 ms). In AVNRT, the interval is usually below 70 ms, affecting only the QRS complex.[20]

The most probable explanation of the findings

In our study group, the myocardial ischemia was unlikely to occur, due to the short-lasting arrhythmia paroxysms, relatively young age of the subjects and lack of patients' complaints. In AVNRT, the overlapping of retrograde P waves could not be explained. The most probable reason of the ST change is the overlapping of R wave on the preceded T wave with shortening of QT-interval with tachycardia, and something that could be referred to as intrinsic characteristics of ECG. This combination might be explained by our results: a decrease of the amplitude of the QR component concomitantly with an increase of the RJ component, and a strong correlation between initial RJ–QR and tachycardia RJ–QR differences. Those conclusions are further supported by the correlation between the ST-segment depression and the tachycardia cycle length, as well as by the correlation between this last parameter and the age. As the tachycardia gets slower with age while the ST-depression is not related to age, the ST-segment depression in those settings is purely electrocardiographic and not an ischemic one.

Limitations

The study is observational, hence the causality cannot be directly derived from the results. The study group was relatively small. The mechanisms of ST-segment depression could also be different across the age groups. All these factors could have influenced the obtained results. Nevertheless, it does not make our conclusions less important.

Conclusions

1. In patients with AVNRT, the ST-segment is lowered during the episodes of tachycardia, and the degree of this change is related to the tachycardia cycle length.
2. The most probable explanation of the ST-segment depression is the overlapping of the QRS complex on the preceded T wave.
3. Some intrinsic properties of an individual ECG have been observed to be influential in this aspect.

ORCID iDs

Jakub Szymon Mercik https://orcid.org/0000-0002-5627-7071
Jadwiga Radziejewska https://orcid.org/0000-0001-9153-9754
Katarzyna Pach https://orcid.org/0000-0002-3643-9467
Dorota Zyśko https://orcid.org/0000-0001-9190-0052
Jacek Gajek https://orcid.org/0000-0002-0038-1750

References

1. Shapiro E. The first textbook of electrocardiography. Thomas Lewis: Clinical Electrocardiography. *J Am Coll Cardiol*. 1983;1(4):1160–1161. doi:10.1016/s0735-1097(83)80120-x
2. Rautaharju PM, Surawicz B, Gettes LS, et al. AHA/ACCF/HRS recommendations for the standardization and interpretation of the electrocardiogram. *J Am Coll Cardiol*. 2009;53(11):982–991. doi:10.1016/j.jacc.2008.12.014
3. Ghaffar A. Clinical electrocardiography. *Pak J Health*. 1953;3(1):6–12. PMID:13063999.
4. Kenny BJ, Brown KN. *ECG T Wave*. Treasure Island, USA: StatPearls Publishing; 2020.
5. Coppola G, Carità P, Corrado E, et al. ST segment elevations: Always a marker of acute myocardial infarction? *Indian Heart J*. 2013;65(4):412–423. doi:10.1016/j.ihj.2013.06.013
6. Kozłowski D. Method in the chaos: A step-by-step approach to ECG interpretation. *Eur J Transl Clin Med*. 2018;1(1):76–92. doi:10.31373/ejtcm/92255
7. Arya A, Kottkamp H, Piorkowski C, et al. Differentiating atrioventricular nodal reentrant tachycardia from tachycardia via concealed accessory pathway. *Am J Cardiol*. 2005;95(7):875–878. doi:10.1016/j.amjcard.2004.12.020

8. Dorenkamp M, Zabel M, Sticherling C. Role of coronary angiography before radiofrequency ablation in patients presenting with paroxysmal supraventricular tachycardia. *J Cardiovasc Pharmacol Ther*. 2007;12(2):137–144. doi:10.1177/1074248407300775
9. Jastrzębski M. ST-segment depression and elevation during supraventricular tachycardias [in Polish]. *Kardiol Pol*. 2012;70(3):291–293. PMID:22430416.
10. Petsas AA, Anastassiades LC, Antonopoulos AG. Exercise testing for assessment of the significance of ST segment depression observed during episodes of paroxysmal supraventricular tachycardia. *Eur Heart J*. 1990;11(11):974–979. doi:10.1093/oxfordjournals.eurheartj.a059637
11. Bukkapatnam RN, Robinson M, Turnipseed S, Tancredi D, Amsterdam E, Srivatsa UN. Relationship of myocardial ischemia and injury to coronary artery disease in patients with supraventricular tachycardia. *Am J Cardiol*. 2010;106(3):374–377. doi:10.1016/j.amjcard.2010.03.035
12. Ben Yedder N, Roux JF, Paredes FA. Troponin elevation in supraventricular tachycardia: Primary dependence on heart rate. *Can J Cardiol*. 2017;27(1):105–109. doi:10.1016/j.cjca.2010.12.004
13. Miranda RC, Machado MDN, Takakura IT, et al. Elevated troponin levels after prolonged supraventricular tachycardia in patient with normal coronary angiography. *Cardiology*. 2006;106(1):10–13. doi:10.1159/000092449
14. Zellweger MJ, Schaer BA, Cron TA, Pfisterer ME, Osswald S. Elevated troponin levels in the absence of coronary artery disease after supraventricular tachycardia. *Swiss Med Wkly*. 2003;133(31–32):439–441. PMID:14562187.
15. Gravel H, Jacquemet V, Dahdah N, Curnier D. Clinical applications of QT/RR hysteresis assessment: A systematic review. *Ann Noninvasive Electrocardiol*. 2018;23(1):e12514. doi:10.1111/anec.12514
16. Kannankeril PJ, Harris PA, Norris KJ, Warsy I, Smith PD, Roden DM. Rate-independent QT shortening during exercise in healthy subjects: Terminal repolarization does not shorten with exercise. *J Cardiovasc Electrophysiol*. 2008;19(12):1284–1288. doi:10.1111/j.1540-8167.2008.01266.x
17. Królik M, Milnerowicz H. The effect of using estrogens in the light of scientific research. *Adv Clin Exp Med*. 2012;21(4):535–543. PMID:23240460.
18. Pearl W. Effects of gender, age, and heart rate on QT intervals in children. *Pediatr Cardiol*. 1996;17(3):135–136. doi:10.1007/BF02505201
19. Friedman HS. Determinants of the total cosine of the spatial angle between the QRS complex and the T wave (TCRT): Implications for distinguishing primary from secondary T-wave abnormalities. *J Electrocardiol*. 2007;40(1):12–17. doi:10.1016/j.jelectrocard.2006.05.008
20. Rivera S, De La Paz Ricapito M, Conde D, Verdu MB, Roux JF, Paredes FA. The retrograde P-wave theory: Explaining ST segment depression in supraventricular tachycardia by retrograde AV node conduction. *Pacing Clin Electrophysiol*. 2014;37(9):1100–1105. doi:10.1111/pace.12394

Annual Contents

No. 1 (January)

Original papers

Reviews

No. 2 (February)

Original papers

Reviews

No. 3 (March)

Original papers

Reviews

No. 4 (April)

Original papers

Multicenter study

Reviews

No. 5 (May)

Original papers

Reviews

No. 6 (June)

Original papers

Reviews

No. 7 (July)

Editorials

Original papers

Reviews

Research-in-progress

No. 8 (August)

Editorials

Original papers

Reviews

No. 9 (September)

Editorials

Original papers

Research letter

No. 10 (October)

Editorials

Original papers

Reviews

Research letters

No. 11 (November)

Editorials

Original papers

No. 12 (December)

Editorials

Original papers

Reviews

Research letters

Index of Authors